HIGHLIGHTS OF ENPER2019 - EUROPEAN NETWORK FOR PLANT ENDOMEMBRANE RESEARCH MEETING

EDITED BY: Fernando Aniento, Erika Isono, Eugenia Russinova and Enrique Rojo

PUBLISHED IN: Frontiers in Plant Science

frontiers Research Topics

frontiers

ISSN 1664-8714
ISBN 978-2-88971-297-7
DOI 10.3389/978-2-88971-297-7

About Frontiers

Frontiers is more than just an open-access publisher of scholarly articles: it is a pioneering approach to the world of academia, radically improving the way scholarly research is managed. The grand vision of Frontiers is a world where all people have an equal opportunity to seek, share and generate knowledge. Frontiers provides immediate and permanent online open access to all its publications, but this alone is not enough to realize our grand goals.

Frontiers Journal Series

The Frontiers Journal Series is a multi-tier and interdisciplinary set of open-access, online journals, promising a paradigm shift from the current review, selection and dissemination processes in academic publishing. All Frontiers journals are driven by researchers for researchers; therefore, they constitute a service to the scholarly community. At the same time, the Frontiers Journal Series operates on a revolutionary invention, the tiered publishing system, initially addressing specific communities of scholars, and gradually climbing up to broader public understanding, thus serving the interests of the lay society, too.

Dedication to Quality

Each Frontiers article is a landmark of the highest quality, thanks to genuinely collaborative interactions between authors and review editors, who include some of the world's best academicians. Research must be certified by peers before entering a stream of knowledge that may eventually reach the public - and shape society; therefore, Frontiers only applies the most rigorous and unbiased reviews.
Frontiers revolutionizes research publishing by freely delivering the most outstanding research, evaluated with no bias from both the academic and social point of view. By applying the most advanced information technologies, Frontiers is catapulting scholarly publishing into a new generation.

What are Frontiers Research Topics?

Frontiers Research Topics are very popular trademarks of the Frontiers Journals Series: they are collections of at least ten articles, all centered on a particular subject. With their unique mix of varied contributions from Original Research to Review Articles, Frontiers Research Topics unify the most influential researchers, the latest key findings and historical advances in a hot research area! Find out more on how to host your own Frontiers Research Topic or contribute to one as an author by contacting the Frontiers Editorial Office: frontiersin.org/about/contact

HIGHLIGHTS OF ENPER2019 - EUROPEAN NETWORK FOR PLANT ENDOMEMBRANE RESEARCH MEETING

Topic Editors:
Fernando Aniento, University of Valencia, Spain
Erika Isono, University of Konstanz, Germany
Eugenia Russinova, Flanders Institute for Biotechnology, Belgium
Enrique Rojo, National Center of Biotechnology (CSIC), Spain

Citation: Aniento, F., Isono, E., Russinova, E., Rojo, E., eds. (2021). Highlights of ENPER2019 - European Network for Plant Endomembrane Research Meeting. Lausanne: Frontiers Media SA. doi: 10.3389/978-2-88971-297-7

Table of Contents

frontiers in Plant Science

EDITORIAL
published: 09 July 2021
doi: 10.3389/fpls.2021.719367

Editorial: Highlights of ENPER 2019—European Network for Plant Endomembrane Research Meeting

Fernando Aniento [1], Erika Isono [2], Enrique Rojo [3] and Eugenia Russinova [4,5]*

[1] Departamento de Bioquímica y Biología Molecular, Instituto Universitario de Biotecnología i Biomedicina (BIOTECMED), Universitat de València, Valencia, Spain, [2] Department of Biology, University of Konstanz, Konstanz, Germany, [3] Centro Nacional de Biotecnología, Consejo Superior de Investigaciones Científicas, Madrid, Spain, [4] Department of Plant Biotechnology and Bioinformatics, Ghent University, Ghent, Belgium, [5] Center for Plant Systems Biology, Vlaams Instituut voor Biotechnologie, Ghent, Belgium

Keywords: plant endomembranes, ER-golgi trafficking, autophagy, endocytosis, exocytosis, vacuolar trafficking

Editorial on the Research Topic

Highlights of ENPER 2019—European Network for Plant Endomembrane Research Meeting

ENPER (European Network for Plant Endomembrane Research) meeting is the first and oldest international conference of the plant membrane research community specifically devoted to studying plant membrane functions. The ENPER was created in 1996 by Professor David Robinson (University of Heidelberg, Germany), and since then it has been organized every year in different countries, bringing together many different groups working on plant endomembranes from Europe and around the world. A strong emphasis has always been made at the ENPER meetings to give young researchers (PhD students and Post-docs) the opportunity to present their work in front of a highly specialized audience, and this was also the spirit in the last meeting, right before COVID-19 pandemics, which took place in the beautiful city of Valencia (Spain) (**Figure 1**).

The program of the meeting included sessions on different aspects of plant endomembrane trafficking, including "Autophagy," "Endoplasmic reticulum and ER-Golgi trafficking," "Golgi complex and *trans*-Golgi network," "Endocytosis and endosomal transport," "Trafficking and polarity," "Exocytosis and defense," and "Vacuolar trafficking." This Research Topic includes articles from several participants in the meeting and covers different aspects of plant endomembrane trafficking.

Ito and Boutté discuss the subdomain organization of the plant Golgi apparatus focusing on the Golgi entry and exit compartments, the Golgi Entry Core Compartment (GECCO) and the *trans*-Golgi network (TGN), respectively. Both subdomains define distinct protein sorting mechanisms and trafficking pathways. The GECCO may be the plant counterpart of the mammalian endoplasmic reticulum (ER)-Golgi Intermediate Compartments (ERGIC), but in plants, ER-to-GECCO transport is independent from COPII machinery. Whereas, TGN subdomains have been characterized to some extent, the GECCO vesicles have not been isolated yet. GECCO and the first *cis*-Golgi cisternae might be specialized in cargo sorting. Live-cell imaging have demonstrated that TGN can either be associated with the *trans* side of the Golgi apparatus (Golgi-associated TGN/GA-TGN), or can be disassociated and move independently from the Golgi (Golgi-independent TGN/GI-TGN or free TGN). Once formed, TGN is able to further differentiate into other compartments of different composition. The TGN is known to not only receive secretory cargos from the Golgi but also cargos from the endocytic pathway and it is assumed that the TGN is equivalent to the early endosomes (EEs) in plant cells. Trafficking from TGN to late endosomes/multivesicular bodies is thought to partly rely on clathrin-coated vesicles (CCVs) and the SNARE VAMP727. At clathrin/TGN subdomain, the small GTPase RAB-A2a is involved in

OPEN ACCESS

Edited and reviewed by:
Viktor Zarsky,
Charles University, Czechia

****Correspondence:***
Fernando Aniento
fernando.aniento@uv.es

Specialty section:
This article was submitted to Plant Membrane Traffic and Transport, a section of the journal Frontiers in Plant Science

Received: *02 June 2021*
Accepted: *11 June 2021*
Published: *09 July 2021*

Citation:
Aniento F, Isono E, Rojo E and Russinova E (2021) Editorial: Highlights of ENPER 2019—European Network for Plant Endomembrane Research Meeting. Front. Plant Sci. 12:719367. doi: 10.3389/fpls.2021.719367

FIGURE 1 | Logo of ENPER 2019.

endocytic sorting to the plasma membrane through the action of the sphingolipid ceramides whereas at secretory vesicles/TGN, the ECH/YIP4 complex is involved in secretory sorting to the plasma membrane.

Sanchez-Simarro et al. analyzed the function of the two isoforms of beta-COP, one of the subunits of the Coat Protein I (COPI) coatomer complex, involved in the formation of vesicles at the Golgi apparatus, for intra Golgi transport or Golgi-to-ER retrograde transport. Using a loss-of-function approach, the authors show that β-COP is required for plant growth and tolerance to salt (NaCl) stress. In addition, they found that depletion of β-COP caused an increased length of Golgi stacks, which in some cases seemed to be the consequence of lateral fusion between Golgi stacks. This suggests that β-COP function is required for maintaining the structure of the plant Golgi apparatus.

Kaiser and Scheuring discuss the contribution of the plant vacuole to cell elongation. Recent data revealed that the receptor-like kinase FERONIA together with extracellular leucine-rich repeat extensins sense cell wall properties such as loosening and subsequently impact on the intracellular expansion of the vacuole. Therefore, the authors deliberate on the possible connection between cell wall status and vacuolar morphology. In particular, they offer their view on the question whether vacuolar size is dictated by cell size or vice versa.

The conserved exocyst complex plays multiple functions in plant growth, cell wall synthesis, immunity and hormone signaling. In many plant species, there are multiple EXO70 genes and their functional redundancy and specialization has been an important question in understanding the molecular mechanisms of exocyst complex function. The manuscript by Pečenková et al. aims to find any functional redundancy and specialization among selected EXO70 isoforms during plant response to biotic stress. The authors analyse existing transcriptome data with focus on response of individual paralogs to biotic stresses. In addition to data mining, the transcripts of selected EXO70 genes in exo70A1 background were detected to see which other EXO70s compensate for the absence of EXO70A1. The authors then analyse various single mutants, combinations of double mutants, and a triple mutant in their response to pathogens using a root hair growth stimulation assay and a flooding assay. It was revealed that different EXO70 isoforms have both redundant and specialized functions and that different EXO70 mutants have compensatory effects. Especially interesting was the *exo70B1 exo70B2* double mutant and therefore the structure of EXO70B1

and EXO70B2 was modeled to see whether the C-terminal lipid-binding motif might contribute to the diverged function of the two proteins.

In the review article by Schwihla and Korbei, the authors provide a nice and timely overview of the latest knowledge on key steps of endocytic degradation of plasma membrane proteins in plants—from clathrin-mediated endocytosis, adaptor proteins, small GTPases to the ESCRT machinery. The authors also highlight the role of posttranslational modifications in these processes. Similar to what has been reported in other eukaryotes, phosphorylation and ubiquitination are important protein modifications for the correct determination of protein fate. Recent findings suggest that although many basic mechanisms are conserved in the plant endosomal degradation pathway when compared to animals, there are also a significant number of molecular processes relying on plant-specific regulators. Efforts are being made to understand the crosstalk between various intracellular trafficking pathways and the implication of endocytic degradation in plants.

The regulation of autophagy and its physiological function is a topic that fascinates many researchers across the broad field of plant biology. The review from the Boycheva Woltering and Isono summarizes molecules that were reported to affect autophagic activity in plants. These factors include metal ions, sugar, amino acids, radicals to phytohormones and, in most cases, they affect directly or indirectly the activity of the TOR kinase complex enabling the plant to adapt its autophagic activity to the environmental conditions. The authors also discuss interesting differences in ATG8 homologs. In contrast to ATG8a-e, which require processing at the C-terminus by the protease ATG4, ATG8h, and ATG8i have an exposed glycine at the C-terminus and theoretically do not require the activity of ATG4 before it can be conjugated. This seemingly "cleavage-free" ATG8 variants are found in all examined species and are expressed genes in Arabidopsis. Whether and what impact this differences in ATG8 have on their biochemical and biological characteristics is an emerging research question.

Autophagy has been primarily associated with nutrient recycling in plants, however, as recent studies have shown, its physiological implication is broad. The review by Norizuki et al. compares male reproductive process in mammals and plants. Though there are fundamental differences, in both systems, cytosolic contents are removed directly or indirectly by autophagy. In Mosses, an increased number of autophagosomes is observed during spermiogenesis, and defect in the autophagy pathway in *Physcomitrella patens* causes morphological abnormalities of the spermatozoid. In angiosperms, autophagy seems to be dispensable for fertility *per se*, as *atg* mutants in *Arabidopsis* and Maize are fertile. In rice, however, autophagy mutants show decreased fertility. The review cast light on the yet poorly understood molecular regulation of autophagy during developmental processes and provide an excellent overview on the involvement of autophagy in gametogenesis.

True to his undergrad training as an engineer, Daniel Van Damme has a recurrent record of introducing novel technologies for research. On this occasion, his group reports on an elegant method for knocking down gene activity through nanobody-based delocalization of tagged proteins (Winkler et al.). As a proof of concept, they express an anti-GFP nanobody under the control of the PIN2 promoter and target it to the mitochondrial outer membrane. Crossing this construct into a null mutant of the TPLATE complex subunit TML complemented with TML-GFP results in mitochondrial-sequestration of TML-GFP and an ensuing reduction in endocytic fluxes in root epidermal and cortex cells, without affecting root growth or plant viability. These results demonstrate the power of this technology to achieve gene inactivation in a tissue-specific manner, or conditionally if inducible promoters are used, which is particularly relevant for functional studies of essential genes.

Another interesting technology, serial block face scanning electron microscopy (SBF-SEM), is presented in the perspective article from the Stoger lab. This technique allows 3D ultrastructural analysis of large sample volumes and in this report it is used to image developing maize seeds (Arcalís et al.). Their 3D models reveal that endoplasmic reticulum in the endosperm consists primarily of large sheets and that protein bodies bud from central areas of those sheets rather than from zones of higher curvature such as tubules or edges. The use of SBF-SEM is relatively new in plants, and this work is a good example of how it can be used to resolve open questions in plant cell biology.

AUTHOR CONTRIBUTIONS

All authors listed have made a substantial, direct and intellectual contribution to the work, and approved it for publication.

FUNDING

Organization of this meeting was sponsored by Generalitat Valenciana (Grant No. GVAORG2019-029 to FA).

Conflict of Interest: The authors declare that the research was conducted in the absence of any commercial or financial relationships that could be construed as a potential conflict of interest.

frontiers in Plant Science

ORIGINAL RESEARCH
published: 15 April 2020
doi: 10.3389/fpls.2020.00430

Loss of *Arabidopsis* β-*COP* Function Affects Golgi Structure, Plant Growth and Tolerance to Salt Stress

*Judit Sánchez-Simarro, César Bernat-Silvestre, Fátima Gimeno-Ferrer, Pilar Selvi-Martínez, Javier Montero-Pau, Fernando Aniento and María Jesús Marcote**

Departamento de Bioquímica y Biología Molecular, Estructura de Recerca Interdisciplinar en Biotecnología i Biomedicina (ERI BIOTECMED), Facultat de Farmàcia, Universitat de València, Valencia, Spain

The early secretory pathway involves bidirectional transport between the endoplasmic reticulum (ER) and the Golgi apparatus and is mediated by coat protein complex I (COPI)-coated and coat protein complex II (COPII)-coated vesicles. COPII vesicles are involved in ER to Golgi transport meanwhile COPI vesicles mediate intra-Golgi transport and retrograde transport from the Golgi apparatus to the ER. The key component of COPI vesicles is the coatomer complex, that is composed of seven subunits (α/β/β'/γ/δ/ε/ζ). In *Arabidopsis* two genes coding for the β-COP subunit have been identified, which are the result of recent tandem duplication. Here we have used a loss-of-function approach to study the function of β-COP. The results we have obtained suggest that β-COP is required for plant growth and salt tolerance. In addition, β-COP function seems to be required for maintaining the structure of the Golgi apparatus.

Keywords: β-COP, coat protein I (COPI), coat protein II (COPII), Golgi apparatus, plant growth, salt stress, *Arabidopsis*

OPEN ACCESS

Edited by:
Christian Luschnig, University of Natural Resources and Life Sciences Vienna, Austria

Reviewed by:
Caiji Gao, South China Normal University, China
Giovanni Stefano, Michigan State University, United States

***Correspondence:**
María Jesús Marcote
mariajesus.marcote@uv.es

Specialty section:
This article was submitted to Plant Traffic and Transport, a section of the journal Frontiers in Plant Science

Received: *27 December 2019*
Accepted: *24 March 2020*
Published: *15 April 2020*

Citation:
Sánchez-Simarro J, Bernat-Silvestre C, Gimeno-Ferrer F, Selvi-Martínez P, Montero-Pau J, Aniento F and Marcote MJ (2020) Loss of Arabidopsis β-COP Function Affects Golgi Structure, Plant Growth and Tolerance to Salt Stress. Front. Plant Sci. 11:430. doi: 10.3389/fpls.2020.00430

INTRODUCTION

The early secretory pathway involves bidirectional transport between the endoplasmic reticulum (ER) and the Golgi apparatus and is mediated by coat protein complex I (COPI)-coated and coat protein complex II (COPII)-coated vesicles. COPII vesicles are involved in ER to Golgi transport and their formation requires the sequential recruitment of five cytosolic components, the small GTPase SAR1 and the heterodimers SEC23/24 and SEC13/31 (Chung et al., 2016). COPI vesicles are involved in transport between Golgi cisternae (although its directionality is still a matter of debate) as well as in retrograde transport from the *cis*-Golgi to the ER. The basic component of the COPI coat is a complex (coatomer) composed of seven subunits (α/β/β'/γ/δ/ε/ζ) which are recruited *en bloc* from the cytosol onto Golgi membranes. The coatomer complex can be conceptually grouped into two subcomplexes, the B- (α/β'/ε) and F-subcomplex (β/δ/γ/ζ). The B-subcomplex has been proposed to function as the outer layer and the F-subcomplex as the inner layer of the COPI vesicle coat (Jackson, 2014). However, recent structural studies suggest that the COPI structure does not fit with the previously proposed model where the inner F-subcomplex is responsible of cargo selection while the outer B-subcomplex is responsible of membrane deformation, by analogy to coats based on clathrin/adaptor complexes (Dodonova et al., 2015). Following recruitment by the small GTPase ARF1, in its GTP-bound conformation, and cargo, COPI polymerizes on the membrane surface in such a way that COPI coat assembly depends on both membrane and cargo binding.

However, much has yet to be learned about the specific functions played by the different subunits of the coatomer complex.

Genes encoding the components of the COPI machinery have been identified in plants (Robinson et al., 2007; Gao et al., 2014; Ahn et al., 2015; Woo et al., 2015). In *Arabidopsis*, all coatomer subunits (except γ- and δ-COP) have more than one isoform, in contrast to yeast, that contains only one isoform for every subunit, and mammals, which contain 2 isoforms of the γ- and ζ-COP subunits but only one for the others. In mammals and *Arabidopsis*, it has been proposed that different isoforms may be part of alternative coatomer complexes with different localization and perhaps different functions (Wegmann et al., 2004; Donohoe et al., 2007; Moelleken et al., 2007; Popoff et al., 2011; Gao et al., 2014). However, it has been recently reported that all of the isoforms of the mammalian COPI coat produce COPI-coated vesicles with strikingly similar protein compositions (Adolf et al., 2019).

The function of different plant COPI subunits has been studied by loss of function approaches. In *Nicotiana benthamiana* and tobacco BY-2 cells, depletion of β', γ-, and δ-COP subunits suggest that the COPI complex is involved in Golgi maintenance and cell-plate formation, and that its prolonged depletion induces programmed cell death (Ahn et al., 2015). In *Arabidopsis*, knockout (KO) T-DNA mutants of the two α-COP subunit isoforms have been characterized. While the α*1-cop* mutant resembled wild type plants under standard growth conditions, the α*2-cop* mutant had defects in growth and the morphology of the Golgi apparatus was altered. A transcriptomic analysis of the α*2-cop* mutant showed upregulation of plant cell wall and endomembrane system genes, such as the COPII component *SEC31A* (Gimeno-Ferrer et al., 2017). Finally, knockdown of *Arabidopsis* ε-COP subunit isoforms has been reported to cause severe morphological changes in the Golgi apparatus and mislocalization of endomembrane proteins (EMPs) containing the KXD/E COPI interaction motif (Woo et al., 2015). In this manuscript, the function of the β-COP subunit has been studied for the first time in plants. We have found that loss of function of *Arabidopsis* β-COP affects Golgi structure, plant growth and tolerance to salt stress.

MATERIALS AND METHODS

Plant Material and Stress Treatments

Arabidopsis thaliana ecotype Col-0 was used as wild type. The loss-of-function mutants β*1-cop* (SALK_002734) and β*2-cop* (SALK_017975C) were from the Salk Institute Genomic Analysis Laboratory[1] and were obtained from the Nottingham Arabidopsis Stock Centre. *A. thaliana* plants were grown in growth chambers as previously described (Ortiz-Masia et al., 2007). To study whether salt tolerance was affected in the β-COP mutants, seeds of wild type (Col-0) and mutants were sown on Murashige and Skoog (MS) plates containing 100–150 mM NaCl. Plates were transferred to a controlled growth chamber after cold treatment in the dark for 3 days at 4°C. After 12 days, the rates of cotyledon greening were scored. To study mannitol (250–300 mM) and ABA (0.3–0.6 μM) tolerance the same protocol was used. Seeds harvested from Col-0 and mutant plants grown under the same conditions and at the same time were used. In some experiments, seeds of wild type (Col-0) and β-COP mutants were sown on MS plates without salt and grown for 4 days before being transferred to MS plates containing 160 mM NaCl. Three days after transplantation, the rates of cotyledon greening were scored.

[1]http://signal.salk.edu/cgi-bin/tdnaexpress

Electrolyte Leakage (EL)

Electrolyte leakage assays were performed as described previously (Jiang et al., 2017). Seeds of wild type (Col-0) and β-COP mutants were sown on MS plates without salt and grown for 4 days before being transferred to MS plates containing 135 mM NaCl. One day after transplanting, the seedlings were washed 3 times with deionized water to remove surface-adherent electrolytes and transferred to 50 mL tubes containing 25 mL of deionized water. Electrical conductivity (EC) was then measured as S_o. The seedlings were gently shaken for 90 min, and the resulting EC was measured as S_1. Then, the samples were autoclaved to release all electrolytes, cooled down and the final EC was measured as S_2. Electrolyte leakage was measured as follows: EL = $(S_1\text{-}S_o)/(S_2\text{-}S_o) \times 100$ (%).

Mutant Characterization

Mutant lines in a Col-0 background containing a T-DNA insertion (T-DNA mutants) were characterized by PCR. To obtain the amiRNA mutant, the β1/β2-directed amiRNA construct CSHL_0125A8 (Open Biosystems) was purchased from ABRC. Transformation of *Arabidopsis* with this construct was conducted according to the floral dip method (Clough and Bent, 1998). 10 transgenic plants containing the amiRNA construct were selected on half-strength MS medium containing appropriate antibiotics. All lines except one (line 5) showed a dwarf phenotype and gave a reduced number of seeds and only seeds from 5 lines could be collected. Transgenic lines 3, 5, and 10 that segregate 3:1 for antibiotic resistance were selected in the T2 generation. In lines 5 and 10, the T3 homozygous generation was used to characterize silencing by RT–qPCR as below. No T3 homozygous line with seeds was obtained from line 3 and T2 seedlings were used to characterize silencing. T2 and T3 lines were also characterized by PCR. The primers used for genotyping all mutants are included in **Supplementary Table S1**.

Reverse Transcription Quantitative PCR (RT-qPCR)

Total RNA was extracted from seedlings using NucleoSpin RNA plant kit (Macherey-Nagel) and 3 μg of the RNA solution were reverse transcribed using the maxima first strand cDNA synthesis kit for quantitative RT-PCR (Fermentas) according to the manufacturer's instructions. Quantitative PCR (qPCR) was performed by using a StepOne Plus machine (Applied Biosystems) with SYBR Premix Ex Taq TM (Tli RNaseH Plus) (Takara) according to the manufacturer's protocol. Each reaction was performed in triplicate with 100 ng of the first-strand cDNA and 0.3 μM of primers for all the genes and 0.9 μM for *SEC31A* in

a total volume of 20 μL. The specificity of the PCR amplification was confirmed with a heat dissociation curve (from 60 to 95°C). Relative mRNA abundance was calculated using the comparative Ct method according to Pfaffl (2004). Primers used for qPCR are listed in **Supplementary Table S2**.

Isolation and Transformation of *Arabidopsis* Protoplasts

To obtain mesophyll protoplasts from *Arabidopsis* plants, the Tape-Arabidopsis Sandwich method was used, as described previously (Wu et al., 2009). Protoplasts were isolated from 4-week-old *Arabidopsis* rosette leaves of wild type and mutant plants. For transient expression, we used the polyethylene glycol (PEG) transformation method, as described previously (Yoo et al., 2007). Plasmids encoding marker proteins used were: ManI–GFP (Nebenführ et al., 1999) and calnexin-RFP (Künzl et al., 2016).

Transient Transformation of *A. thaliana* Seedlings by Vacuum Infiltration

This protocol was adapted from the protocol described by Marion et al. (2008). For preparation of the *Agrobacterium* cultures used for agroinfiltration, the desired *Agrobacterium* (GV3101:pMP90 strain) was inoculated into 2.5 mL of Luria-Bertani (LB) growth medium containing the appropriate antibiotics. This pre-culture was grown overnight at 28°C in a shaking incubator and next day, 30 mL of LB containing the appropriate antibiotics were inoculated with 0.3 mL of the pre-culture and this culture was grown overnight. Once the *Agrobacterium* culture reached an OD around 2.2, cells were pelleted and resuspended with 2 mL of liquid MS medium. The suspension OD was measured again and the *Agrobacterium* suspension was diluted with the infiltration buffer (MS with 0.005% Silwet L-77® and 200 μM acetosyringone) to have an OD of 2. Infiltration was performed by covering the 4–5 days old seedlings grown on MS 35 × 10 mm Petri dishes (4–6 dishes) with the *Agrobacterium* solution and by applying vacuum (300 mbar) with the help of a manometer twice for 1 min. Excess infiltration medium was subsequently removed and the plates were transferred to a culture room for 3 days. Healthy seedlings were selected and the cotyledons were analyzed by the abaxial side on the confocal microscope. Markers expressed using this system were ManI-YFP (Madison and Nebenführ, 2011), TIP1.1-GFP (Gattolin et al., 2011), and GFP-AGP4 (Martinière et al., 2012).

Confocal Microscopy

Imaging was performed using an Olympus FV1000 confocal microscope[2] with a 60× water lens. Fluorescence signals for GFP (488 nm/496–518 nm), YFP (514 nm/529–550 nm) and RFP (543 nm/593–636 nm) were detected. Sequential scanning was used to avoid any interference between fluorescence channels. Post-acquisition image processing was performed using the FV10-ASW 4.2 Viewer®.

[2]http://www.olympus.com/

Transmission Electron Microscopy (TEM)

For electron microscopy, seedlings were grown on MS medium containing 1% agar, and the seedlings were harvested after 4 days. Chemical fixation of cotyledons was performed according to Osterrieder et al. (2010). Ultrathin (70 nm) sections were cut on a Microtome Leica UC6, stained with uranyl acetate and lead citrate and observed with a JEM-1010 (JEOL) transmission electron microscope. Post-acquisition image processing and quantification of the Golgi apparatus size was performed using ImageJ (v1.45) (Abramoff et al., 2004).

Statistical Analysis

Differences in stress responses among β*1-cop*, β*2-cop*, and *amiR-*β*1/*β*2-cop* mutants compared to Col-0 were tested using a two sample *t*-test with unequal variances using Microsoft Excel 2013. For the analysis of Golgi length, data were analyzed using the software R, version 3.4.2 (Vienna, Austria). The lengths were compared using the Wilcoxon test; prior to this, the data were assessed for normality using the Shapiro–Wilk test.

Genetic Variability of β-COP Genes

Number of copies of β-COP genes in different embriophyta genomes was obtained from EnsemblPlants[3] (Vilella et al., 2009). Additionally, protein and coding sequences and number of synonymous (Ks) and non-synonymous (Ka) values for all orthologs were obtained from Ensembl database using their REST API. Moreover, *A. thaliana* sequences for all genes classified as paralogs were also obtained. Paralogs located at a physical distance of less than 2.5 Kb were naively identified as tandem duplications. Evolutionary distances among pair of paralogs and orthologs were estimated as transversion rates on fourfold degenerate synonymous sites (4DTv). The 4DTv was calculated using an in house Python script after aligning each pair of coding sequences using MACSE v.2.03 (Ranwez et al., 2011). Correction for multiple substitutions was applied (Tang et al., 2008). The maximum likelihood phylogenetic tree of the gene was inferred using IQTREE (Nguyen et al., 2015) from protein sequences. Best amino acid substitution model was JTT + I model selected based on the Bayesian information criterion (BIC). Branch support was obtained by bootstrap using an ultrafast method (Minh et al., 2013).

Genetic diversity of *A. thaliana* β-COP genes (at4g31480, at4g31490) was explored using the collection of single-nucleotide polymorphisms (SNPs) from the 1001 genomes database (1001 Genomes Consortium, 2016) which includes information for 1135 accessions. VCF files annotated using SNPEff were filtered to keep only SNPs with a moderate (e.g., non-synonymous amino acid substitution) or high impact changes (e.g., frameshifts or premature stop codons). In the case of non-synonymous substitutions putative effect was predicted using SNAP2 (Hecht et al., 2015), which takes into account both evolutionary information and structural features to assign a potential effect of changes. Nucleotide diversity (π) for each β-COP gene was calculated using custom Python scripts following VariScan implementation (Hutter et al., 2006); evolutionary distance

[3]http://plants.ensembl.org/

between both genes was assessed using 4DTv. Additionally, nucleotide diversity was also calculated for a random sample of 5000 genes and genes classified as tandem duplications and 4DTv among tandemly duplicated genes.

RESULTS

Arabidopsis β-*COP* Genes

Two β-COP genes, β*1-COP* (At4g31480), and β*2-COP* (At4g31490) have been identified in *Arabidopsis*. They show high nucleotide and protein sequence identity (91 and 99%, respectively), identical number and position of introns (**Figure 1A**), and they exist in a tandem arrangement. Embryophytes tend to present at least two paralogs of β-COP genes, and in approximately 50% of species two copies are found (**Figure 1B**). Moreover, in 7 out of 72 plant species (*A. thaliana, Brassica napus, Leersia perrieri, Musa acuminata, Prunus persica, Tricicum aestivium,* and *Triticum dicoccoides*), at least two of the β-COP paralogs were found adjacent, likely being the result of tandem duplications, with an average distance among tandemly duplicated genes of 1.7 Kb (range from 71 to 4963 bp). The distribution of evolutionary distances measured as fourfold degenerate transversions (4DTv) among paralogs within species (**Supplementary Figure S1A**) suggests that evolutionary dynamics of paralogs is diverse, with some paralogs being the result of ancient duplications (4DTv > 0.5), while others seem to be the result of recent duplications (4DTv < 0.01). In the case of *A. thaliana*, both genes are the result of a recent tandem duplication (**Supplementary Figure S1B**) (Tiley et al., 2016). The genotyping of the 1135 *A. thaliana* accessions (1001 Genomes Consortium, 2016) resulted in 195 SNPs in β*1-COP* and 172 in β*2-COP*. Nucleotide diversity was 0.059 for β*1-COP* and 0.041 for β*2-COP,* which is in the average range of nucleotide diversity of either other *A. thaliana* genes or tandemly duplicated genes (**Figure 1C**). However, despite having a similar nucleotide diversity, the Ka/Ks ratio between both paralogs showed that both copies are under purifying selection (Ka/Ks = 0.06). Both copies tend to be more conserved than other *A. thaliana* tandemly duplicated paralogs (**Figure 1D**). These results could suggest the functional relevance of having two redundant gene copies. None of the SNPs resulted in a nonsense or frameshift mutation, and only 25 SNPs in β*1-COP* and 13 in β*2-COP* were non-synonymous changes. Of them, six and two, respectively, were classified as potentially having a deleterious effect. Interestingly, none of the accessions showed deleterious mutations in both genes simultaneously.

Characterization of β*1-cop* and β*2-cop* Mutants

To investigate the function of the two isoforms (β1-COP and β2-COP) of the β-COP subunit in *Arabidopsis*, T-DNA insertion mutants were identified and analyzed. These mutants were from the Salk collection and correspond to stock numbers SALK_002724 (β*1-cop* mutant) and SALK_017975C (β*2-cop*

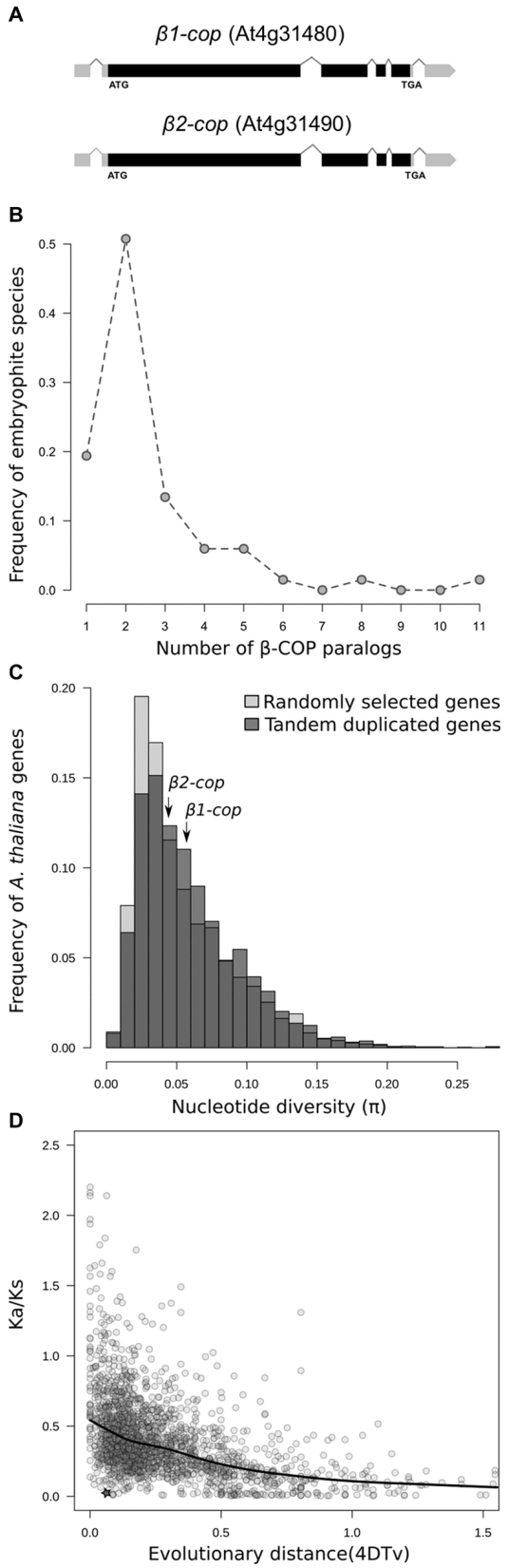

FIGURE 1 | Continued

FIGURE 1 | Genetic variability of β-COP genes. **(A)** Diagram of β*1-COP* and β*2-COP* genes. Black boxes represent coding regions and gray boxes represent 5′ UTR and 3′ UTR regions. **(B)** Number of β-COP paralogs among embryophyte species. **(C)** Histogram of the nucleotide diversity of 5000 randomly selected genes (light gray) and tandem duplicated genes (dark gray) in *A. thaliana.* Nucleotide diversity for β*1-COP* and β*2-COP* genes is marked with arrows. **(D)** Relationship between 4DTv distance and Ka/Ks ratio of pairs of tandemly duplicated genes in *A. thaliana*. Comparison between β*1-COP* and β*2-COP* is marked with a star. Line shows the local regression obtained by LOESS smoothing.

mutant) (**Figure 2A**). RT-PCR analysis confirmed that β*1-cop* and β*2-cop* mutants lacked the β*1-COP* and the β*2-COP* transcripts, respectively, and therefore, they can be considered loss-of-function mutants (**Figures 2B,C**). We next analyzed the expression levels of β*1-COP* and β*2-COP* in the β*1-cop* and β*2-cop* mutants. As shown in **Figures 2B,C**, β*1-cop* mutant showed around a 20% increase in the expression levels of β*2-COP* and β*2-cop* mutant showed around a 30% increase in the expression levels of β*1-COP*. Therefore, both genes seemed to be transcriptionally active as both β*1-COP* and β*2-COP* transcripts are detected and it is possible that loss of function of one isoform induces the expression of the other isoform. To investigate the relative expression of the two β-*COP* genes, we used the public available RNAseq expression database (Zimmermann et al., 2004) (GENEVESTIGATOR)[4]. As shown in **Figure 2D**, the expression pattern of β*1-COP* and β*2-COP* genes is similar, being higher the mRNA levels of β*1-COP*.

Neither β*1-cop* nor β*2-cop* mutants showed any phenotypic alteration under standard growth conditions (**Figure 2E**). We have previously shown that a mutant affecting 4 members of the p24 family, which are involved in COPI vesicle formation, showed enhanced sensitivity to salt stress (Pastor-Cantizano et al., 2018). Therefore, we tested whether β*1-cop* and β*2-cop* mutants were also sensitive to salt stress. To this end, seeds from wild type (Col-0), β*1-cop* and β*2-cop* mutants were sown in the presence of NaCl. As depicted in **Figure 3A**, both mutants were hypersensitive to salt stress, as shown by a drastic cotyledon greening reduction in the presence of 100-150 mM NaCl. To further investigate the salt sensitive phenotype, wild type, β*1-cop* and β*2-cop* mutants were first grown in normal growth medium and then transferred to plates containing 160 mM NaCl. As shown in **Figure 3B**, salt treatment caused a drastic reduction in cotyledon greening of β*1-cop* and β*2-cop* mutants, which confirms their sensitivity to salt stress. Finally, we also tested the effect of salt stress on ion leakage. As shown in **Figure 3C**, ion leakage was significantly increased in both β*1-cop* and β*2-cop* mutants in the presence of NaCl, which may reflect damage to cellular membranes in the mutants upon salt treatment. Since some salinity responses are regulated by abscisic acid (ABA) (Zhu, 2016), β*1-cop* and β*2-cop* mutants were also sown in the presence of ABA. However, similar sensitivity to ABA was detected in the mutants and wild type (**Figure 3D**). β-*cop* mutants were also treated with mannitol to test osmotic stress tolerance. **Figure 3E** shows that none of the mutants were hypersensitive to mannitol, suggesting that the NaCl sensitivity observed in the mutants is not due to osmotic stress.

AmiR-β*1*/β*2-cop* Plants Display a Dwarf Phenotype and Enhanced Sensitivity to Salt Stress

To further investigate the function of the two isoforms of β-COP, we decided to knock down the expression of both genes. Since both genes are in tandem in chromosome 4, it was not possible to generate the double KO mutant. In order to simultaneously silence both β-*COP* genes, we used the artificial microRNA (amiRNA) CSHL_0125A8 (Open Biosystems). The amiRNA that we here called *amiR*-β*1*/β*2-COP* is targeted to a common region at the middle of the first exon of both β-*COP* genes. *A. thaliana* transgenic lines were generated by transformation with *amiR*-β*1*/β*2-COP*. A total of 10 independent lines (lines 1–10) were selected. All lines except one (line 5) showed a dwarf phenotype and gave a reduced number of seeds. The expression levels of both β*1-COP* and β*2-COP* genes were analyzed in three of these lines (lines 3, 5, and 10) by RT-qPCR. A reduction of both β-*COP* transcript levels was observed in the *amiRb1*/β*2-cop-3* and *amiR*-β*1*/β*2-cop-10* lines but not in *amiR*-β*1*/β*2-cop-5* (line 5) compared to the expression of wild type (Col-0) seedlings (**Figure 4A**). In contrast to the normal growth of β*1-cop* and β*2-cop* mutants, the *amiR*-β*1*/β*2-cop-3 and amiR*-β*1*/β*2-cop-10* plants exhibited a dwarf phenotype with reduced rosette leaf size and plant height (**Figure 4B**). Interestingly, the amiR-β*1*/β*2-cop-5*, which had no reduction in the expression levels of β*1-* and β*2-COP*, did not show any phenotypic alteration (**Figure 4B**), suggesting that the dwarf phenotype of the *amiR*-β*1*/β*2-cop-3 and amiR*-β*1*/β*2-cop-10* plants is a consequence of the reduced expression levels of β-COP. For the following experiments the *amiR*-β*1*/β*2-cop-10* line was used.

We next investigated whether the *amiR*-β*1*/β*2-cop-10* mutant had enhanced sensitivity to salt stress, as the single KO mutants. As shown in **Figure 5**, the *amiR*-β*1*/β*2-cop-10* mutant was also hypersensitive to salt stress, either by sowing the seeds directly in NaCl-containing medium (**Figure 5A**) or else by growing the seeds in normal growth medium before transfer to salt-containing plates (**Figure 5B**). We also found that the *amiR*-β*1*/β*2-cop-10* mutant had an increased ion leakage in the presence of salt, compared to wild-type plants (**Figure 5C**), as it was the case with the single β*1-cop* and β*2-cop* mutants.

AmiR-β*1*/β*2-cop* Plants Show an Alteration in the Structure of the Golgi Apparatus

As COPI vesicles have a main role in intra-Golgi transport and in retrograde transport from the *cis*-Golgi to the ER, we examined whether depletion of the β-COP subunit had an effect on the morphology of the Golgi apparatus. For this purpose, we first used transient expression experiments in *Arabidopsis* protoplasts, using a marker of the *cis* side of the Golgi apparatus, Mannosidase I–GFP (Nebenführ et al., 1999). ManI–GFP showed the typical punctate pattern characteristic of normal Golgi stacks

[4]www.genevestigator.com

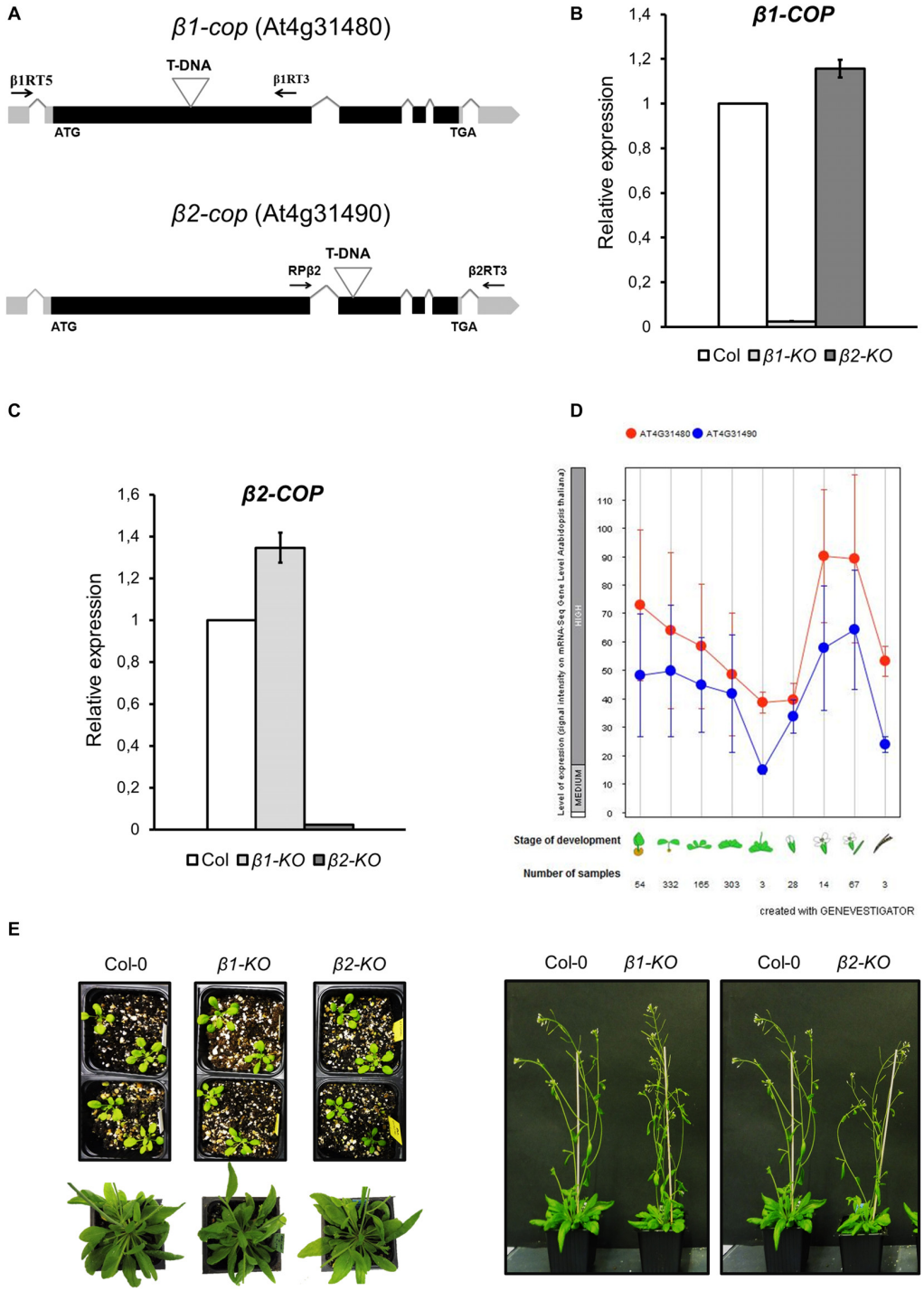

FIGURE 2 | Characterization of β*1-cop* and β*2-cop* mutants. **(A)** Diagram of β*1-COP* and β*2-COP* genes and localization of the T-DNA insertion (triangle) in the mutants. Black boxes represent coding regions and gray boxes represent 5′ UTR and 3′ UTR regions. The positions of β1RT and β1RT3 primers and RPβ2 and β2RT3 primers used to genotype β*1-cop* and β*2-cop* mutants, respectively, are shown by arrows. **(B,C)** RT-qPCR analysis to show the absence of β*1-COP* **(B)** and β*2-COP* **(C)** mRNA in the β*1-cop* and β*2-cop* mutants, respectively. Total RNA was extracted from 4 days seedlings of the mutant and wild type (Col-0). The mRNA was analyzed by RT-qPCR with specific primers and normalized to UBQ10 expression (**Supplementary Table S2**). Results are from three biological samples and three technical replicates. mRNA levels are expressed as relative expression levels and represent fold changes of mutant/wild type. Values represent mean ± s.e.m. of the three biological samples. **(D)** Developmental stage-specific expression patterns of β*1-COP* and β*2-COP*. Seedlings, rosette leaves, floral organs and siliques are sequentially marked from left to right. "HIGH," "MEDIUM," and "LOW" expression were calculated by RNA-seq assay. The number of samples indicates RNA-seq gene expression data collected by GENEVESTIGATOR (www.genevestigator.com). **(E)** β*1-cop* and β*2-cop* mutants did not show any phenotype different from wild type.

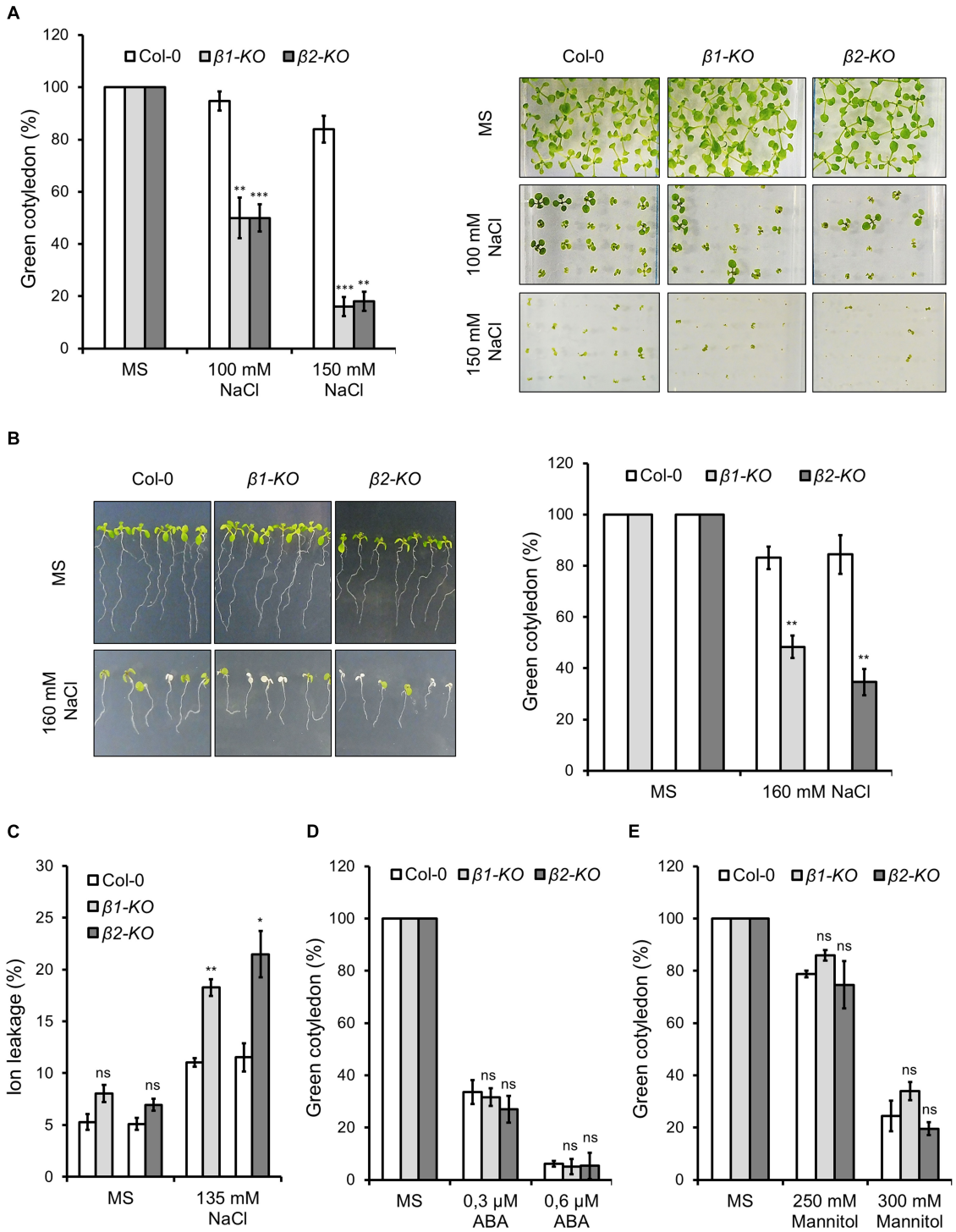

FIGURE 3 | Phenotypic analysis of β*1-cop* and β*2-cop* mutants exposed to salt (NaCl), mannitol and ABA. **(A)** Wild type (Col-0) and β*1-cop* and β*2-cop* seeds were sown on 0.5 × MS as a control and 0.5 × MS supplemented with 100 mM or 150 mM NaCl. Left panel shows the percentage of seedlings with green cotyledons calculated after 12 days and are mean ± s.e.m. (n = 100) of four independent experiments. Right panel shows an image of a representative experiment. **(B)** Seeds of wild type (Col-0) and β-COP mutants were sown on MS plates without salt and grown for 4 days before being transferred to MS plates containing 160 mM NaCl. Three days after transplantation, the percentage of seedlings with green cotyledons was calculated and expressed as mean ± s.e.m. (n = 60) of three independent experiments (right panel). An image of a representative experiment is shown in the left panel. **(C)** Ion leakage of wild type and β-COP mutants one day after transplanting seedlings to MS plates containing 135 mM NaCl. Data show mean ± s.e.m of three independent experiments. **(D,E)** Wild type (Col-0) and β*1-cop* and β*2-cop* seeds were sown on 0.5 × MS or 0.5 × MS supplemented with ABA **(D)** or mannitol **(E)**. Data is the percentage of seedlings with green cotyledons calculated after 12 days and are mean ± s.e.m of three independent experiments (**D:** n = 60; **E:** n = 135). Statistical significance: ns, not significant; *$p < 0.05$; **$p < 0.01$; ***$p < 0.001$.

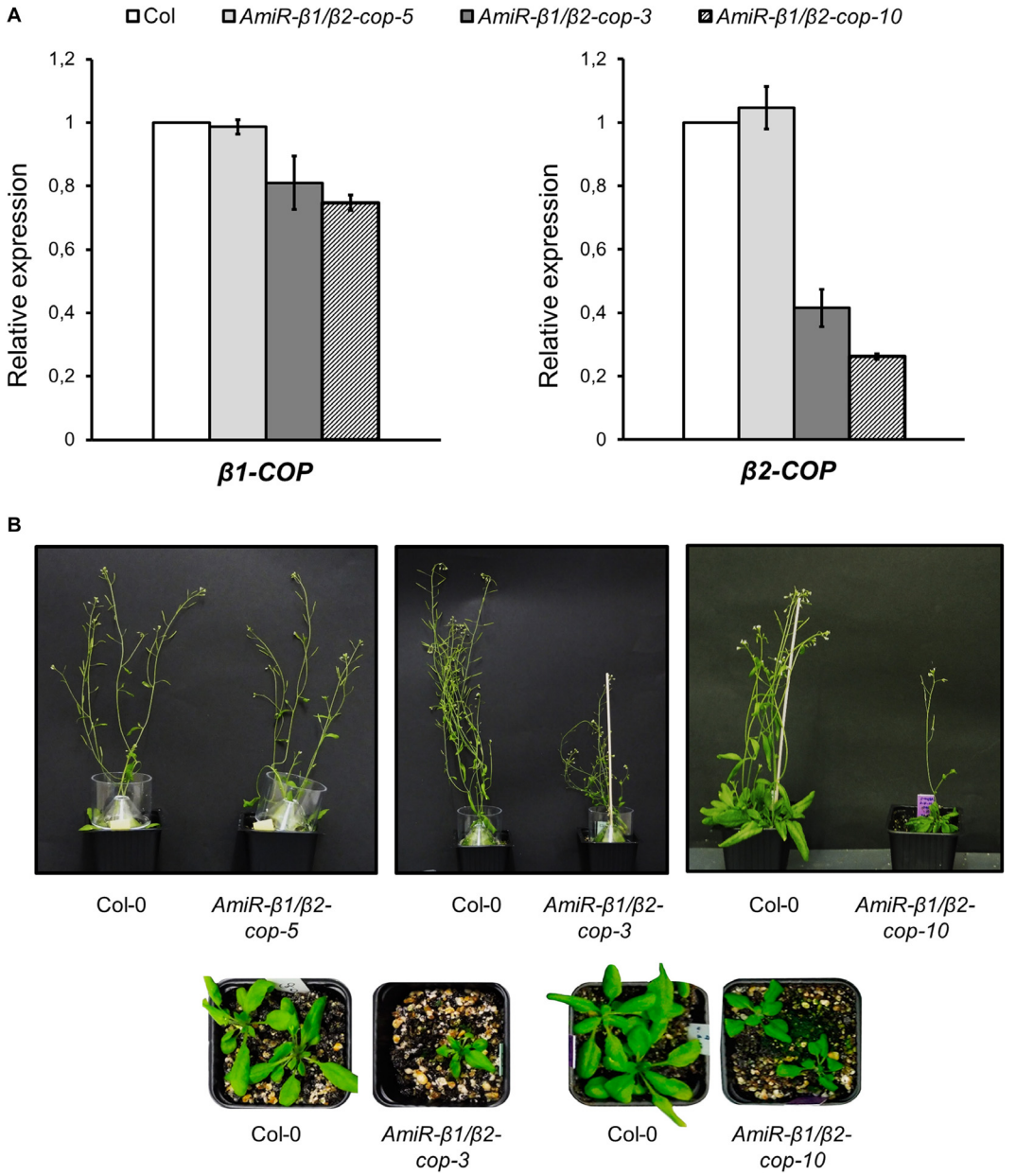

FIGURE 4 | Characterization of *amiR-β1/β2-cop* mutants. **(A)** RT-qPCR analysis to show the silencing of β*1-COP* and β*2-COP* in the *amiR-β1/β2-cop* lines. Total RNA was extracted from 4 days seedlings of the amiRNA lines *amiR-β1/β2-cop-3*, *amiR-β1/β2-cop-5*, *amiR-β1/β2-cop10* and wild type (Col-0). The mRNA was analyzed by RT-qPCR with specific primers and normalized to UBQ10 expression (**Supplementary Table S2**). Results are from three biological samples and three technical replicates. mRNA levels are expressed as relative expression levels and represent fold changes of mutant/wild type. Values represent mean ± s.e.m of the three biological samples. **(B)** Phenotypes of amiRNA lines and wild type (Col-0) plants. Line 5: 36 day-old plants. Line 3: 26 (lower panel) and 50 day-old-plants (upper panel). Line 10: 26 (lower panel) and 36 day-old plants (upper panel).

in protoplasts obtained from wild type plants (**Figure 6A**). However, in one third of the protoplasts from the *amiR-β1/β2-cop* mutant ManI–GFP localized to clusters of punctate structures (**Figures 6B,C**), which suggests an alteration in the organization of the Golgi apparatus in this mutant. To confirm this Golgi phenotype, we also performed transient expression experiments in *Arabidopsis* seedlings, using the same Golgi marker. As shown in **Figures 6E–F**, ManI-YFP was also partially found in clusters of punctate structures in the *amiR-β1/β2-cop* mutant, in contrast to the normal punctate pattern observed in wild-type seedlings (**Figure 6D**). In contrast, no significant change was observed in the localization of other subcellular marker proteins in the *amiR-β1/β2-cop* mutant when compared with wild-type plants, including calnexin-RFP (endoplasmic reticulum)

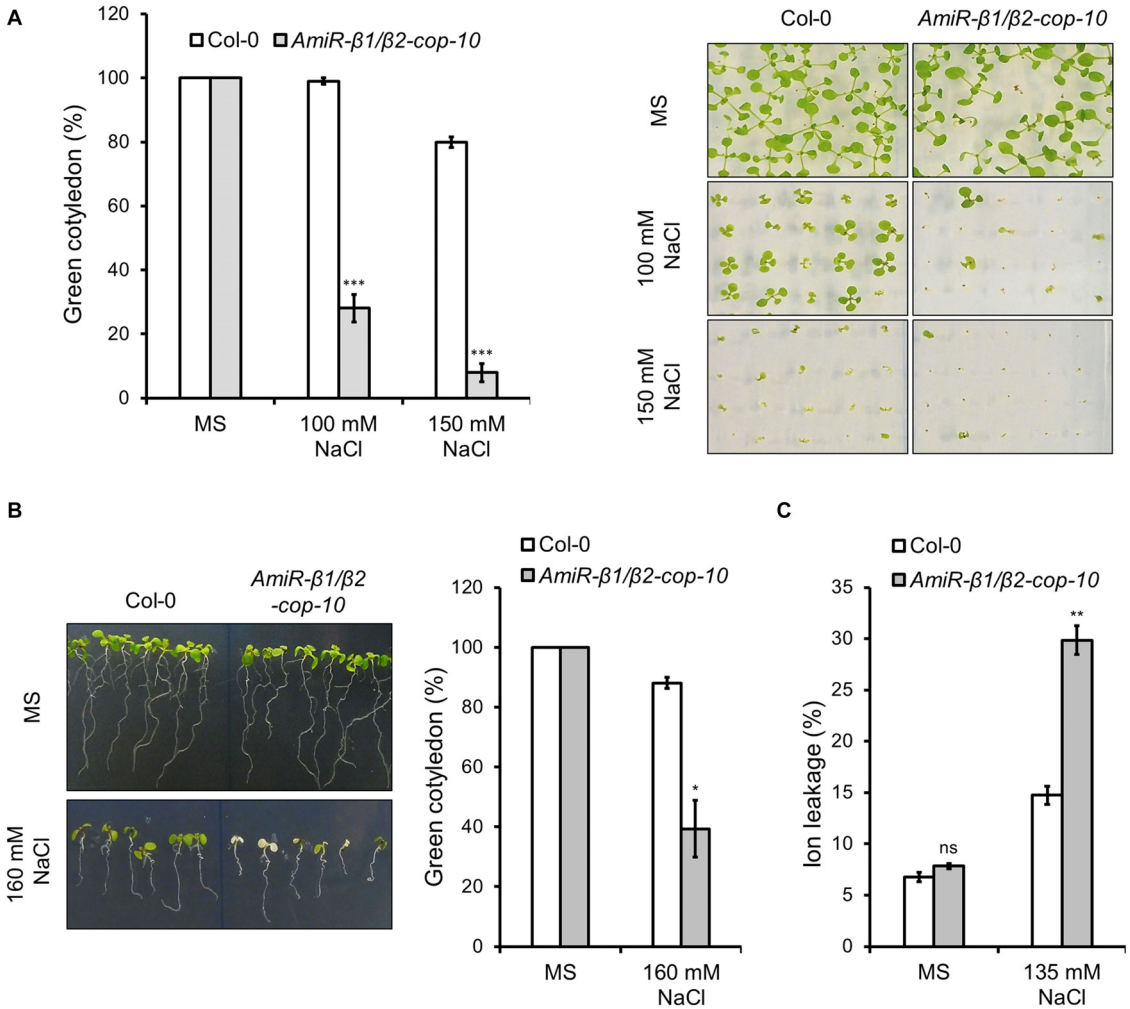

FIGURE 5 | Phenotypic analysis of *amiR-β1/β2-cop* exposed to salt (NaCl). **(A)** Wild type (Col-0) and *amiR-β1/β2-cop* seeds were sown on 0.5 × MS for control conditions and 0.5 × MS supplemented with 100 mM NaCl and 150 mM NaCl in Petri plates. The percentage of seedlings with green cotyledons was calculated after 12 days. Data are mean ± s.e.m. (n = 100) of four independent experiments. **(B)** Seeds of wild type (Col-0) and the *amiR-β1/β2-cop* mutant were sown on MS plates without salt and grown for 4 days before being transferred to MS plates containing 160 mM NaCl. Three days after transplantation, the percentage of seedlings with green cotyledons was calculated and expressed as mean ± s.e.m. (n = 60) of three independent experiments (right panel). An image of a representative experiment is shown in the left panel. **(C)** Ion leakage of wild type and the *amiR-β1/β2-cop* mutant 1 day after transplanting seedlings to MS plates containing 135 mM NaCl. Data show mean ± s.e.m of three independent experiments. Statistical significance: ns, not significant; *p < 0.05; **p < 0.01; ***p < 0.001.

(**Supplementary Figure S2**), as well as two post-Golgi markers, TIP1.1-GFP (tonoplast) and the arabinogalactan protein GFP-AGP4 (plasma membrane) (**Supplementary Figure S3**).

To gain insight into the defects observed in the *amiR-β1/β2-cop* mutant at the ultrastructural level, we performed transmission electron microscopy (TEM) analysis of ultrathin sections of seedlings processed by chemical fixation. As shown in **Figure 7**, the *amiR-β1/β2-cop* mutant showed enlarged Golgi stacks, with a length significantly higher than that observed in wild type cotyledons, although there was no obvious change in the number of cisterna. In some cases, these structures looked as if they were the result of the fusion between two adjacent stacks (**Figure 7E**). Therefore, the *amiR-β1/β2-cop* mutant seems to have an alteration in the structure of the Golgi apparatus.

β-*cop* Mutants Show Increased Expression of *SEC31A*, That Encodes One Subunit of the COPII Coat

SEC31 is a component of the coat protein complex II (COPII) which promotes the formation of transport vesicles from the endoplasmic reticulum (ER). The *Arabidopsis* genome encodes two SEC31 isoforms, SEC31A (At1g18830) and SEC31B (At3g63460) (Chung et al., 2016). We have found previously that a mutant in one of the isoforms of the α-COP subunit of COPI, *α2-cop*, showed a strong up-regulation of *SEC31A*. This up-regulation of *SEC31A* seems to be specific for this particular COPII subunit as the expression other COPII subunit genes did not change. Therefore, we analyzed whether this was also the case for the β-*cop* mutants. As shown in **Figure 8**, both *β1-cop* and

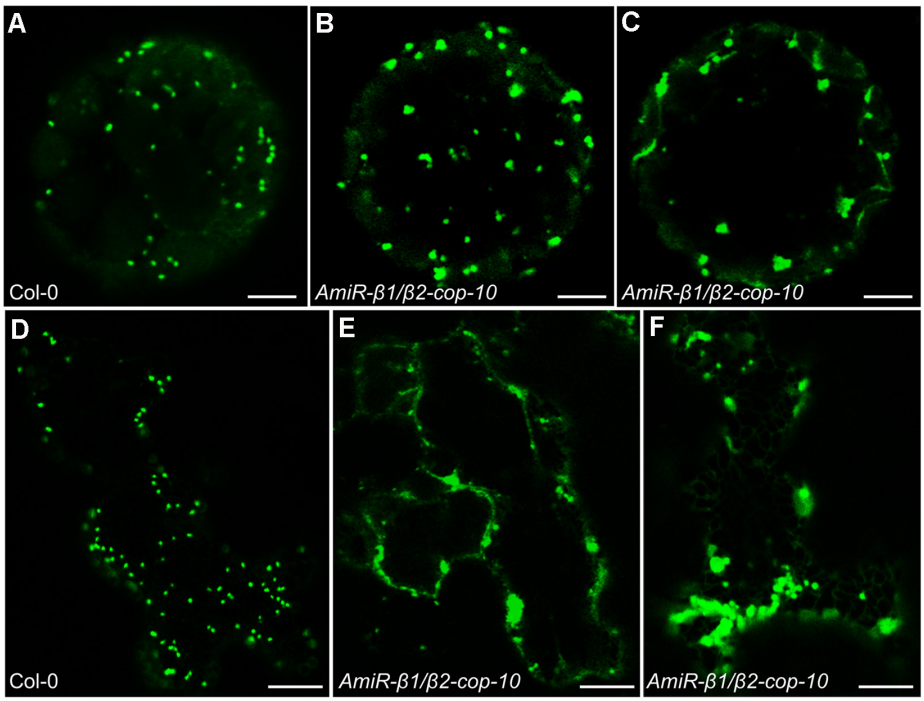

FIGURE 6 | Localization of ManI-GFP in the *amiR-β1/β2-cop* mutant. **(A–C)** Transient gene expression of ManI-GFP in *Arabidopsis* protoplasts obtained from wild type (Col-0) or *amiR-β1/β2-cop* plants grown 4 weeks in soil. Scale bars: 5 μm. **(D–F)** Transient gene expression of ManI-YFP in *Arabidopsis* seedlings of wild type (Col-0) or *amiR-β1/β2-cop*. Scale bars: 10 μm.

β*2-cop* mutants, as well as *amiR-β1/β2-cop-10* showed increased expression of *SEC31A*. In contrast, *SEC31B* was not up regulated in any of the mutants (**Figure 8**).

DISCUSSION

COPI-coated vesicles have been shown to be involved in trafficking within the Golgi and from the Golgi to the ER (Cosson and Letourneur, 1994; Letourneur et al., 1994). COPI is a heptameric protein complex composed of α, β, β', δ, ε, γ, and ζ subunits (Waters et al., 1991) that is recruited onto Golgi membranes in the presence of the small GTP-binding protein ARF1. In this work, depletion of the β-COP subunit has been studied for the first time in plants. Embryophytes tend to present at least two paralogs of β-COP genes, and in *A. thaliana* the two genes coding for β-COP subunits (β*1-COP and* β*2-COP*) are the result of recent tandem duplication. These two genes seem to be evolutionarily conserved and none nonsense or frameshift naturally occurring mutants have been observed. Here we have shown that single null T-DNA insertion mutants of β*1-COP* and β*2-COP* show the same phenotype as wild type plants under standard growth conditions. One possible explanation is that loss of function of one isoform induces the expression of the other isoform, as shown in **Figures 2B,C**, which may be sufficient for normal growth under standard growth conditions, but not to deal with stress conditions. Indeed, both mutants showed enhanced sensitivity to salt stress. Interestingly, *amiR-β1/β2-cop* plants that have reduced levels of both β*1-COP* and β*2-COP* showed defects of growth in addition to enhanced sensitivity to salt stress. According to qPCR analysis, the mRNA levels of β*1-COP* and β*2-COP* were reduced by 20–25% and 60–75%, respectively. The different growth phenotype among the two single null mutants and the *amiR-β1/β2-cop* plants may be explained by the fact that plant amiRNAs have also been shown to have an effect at the translational level (Yu and Pilot, 2014). When grown in the presence of NaCl, the *amiR-β1/β2-cop* mutant was even more sensitive than the single KO mutants. This could be explained, as it has been suggested above, if this mutant has higher β-COP depletion. Unfortunately, the β-COP protein levels could not be tested as we have not found any β-COP antibodies that recognized *Arabidopsis* β-COP. Expression of both isoforms may be important to respond to salt stress, probably to support the trafficking of ion channels or transporters. Indeed, β-COP protein has been shown to regulate the surface expression of several ion channels in mammalian cells (Ryu et al., 2019). In fact, disorders in trafficking of plasma membrane and vacuole Na^+/H^+ antiporters in *Arabidopsis* may cause hypersensitivity to salt stress (Hamaji et al., 2009; Kim and Bassham, 2011; Kim et al., 2017). On the other hand, β-COP mutants also showed a partial mislocalization of mannosidase I, a specific membrane marker for plant *cis*-Golgi (Nebenführ et al., 1999), that is the Soybean ortholog of Arabidopsis α-1, 2-mannosidases MNS1 and MNS2 (Kajiura et al., 2010). These two redundant class I α-mannosidases cleave three α-1,2-mannosyl residues in ER-derived glycoproteins, to generate the substrate

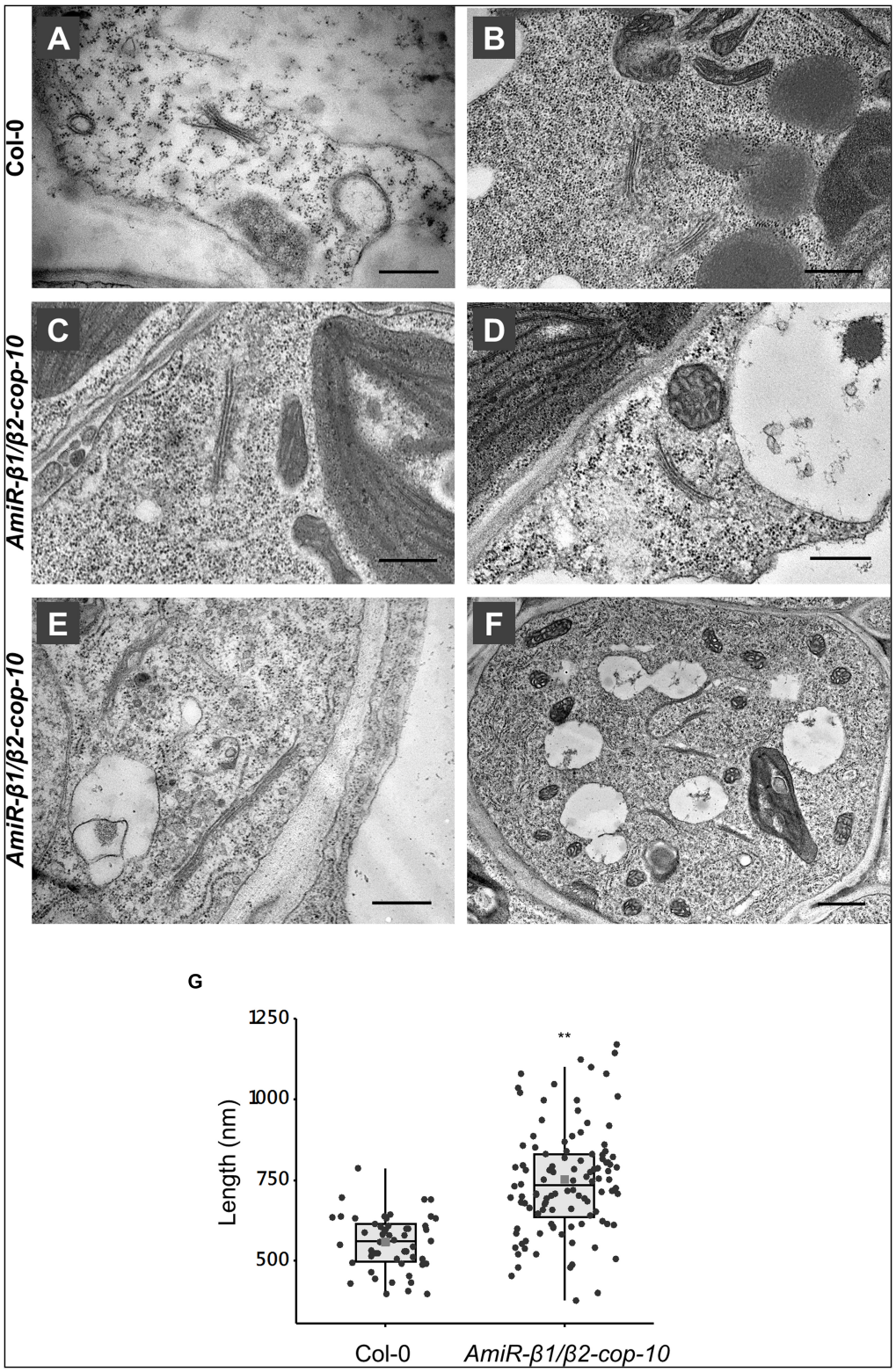

FIGURE 7 | Ultrastructural analysis of the *amiR-β1/β2-cop* mutant. Chemically fixed cotyledon cells from 4-day-old seedlings of wild type (Col-0) **(A,B)** and the *amiR-β1/β2-cop* mutant **(C–F)**. Scale bars: **(A–E)** – 500 nm; **(F)** – 1 mm. **(G)** Quantification of the length of the Golgi apparatus in wild-type (Col-0) cells and in the *amiR-β1/β2-cop* mutant. $n = 52$ (Col-0) and 111 (*amiR-β1/β2-cop*). Golgi length was higher in the *amiR-β1/β2-cop* mutant compared with wild-type (Col-0). Statistical significance: $^{**}p < 0.01$.

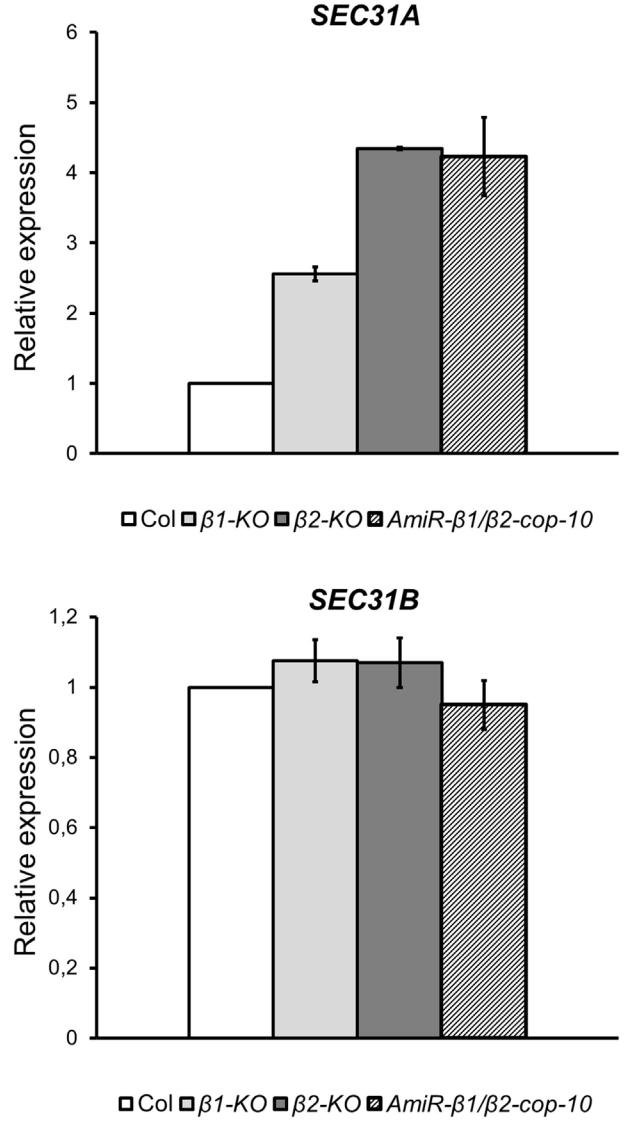

FIGURE 8 | The β*1-cop*, β*2-cop* and *amiR-β1/β2-cop* mutants show upregulation of the COPII subunit SEC31A gene. Expression of *SEC31A* and *SEC31B* was analyzed by RT-qPCR. Total RNA was extracted from 4-day-old seedlings of wild type (Col-0) and the β-*cop* mutants. The mRNA was analyzed by RT-qPCR with specific primers (Gimeno-Ferrer et al., 2017) and normalized to UBIQ10 gene expression (**Supplementary Table S2**). mRNA levels are expressed as relative expression levels and represent fold changes of mutant over wild type. Values represent mean ± s.e.m. of three biological samples.

for the subsequent addition of GlcNAc. Interestingly, it has been described that MNS1/2-mediated mannose trimming of N-glycans is crucial in modulating glycoprotein abundance to withstand salt stress (Liu et al., 2018).

Transient expression experiments in seedlings and protoplasts (using a specific Golgi marker), together with electron microscopy analysis of the *amiR*β*1/*β*2-cop* mutant showed morphological changes of the Golgi apparatus. This indicates that β-COP is important for the maintenance of Golgi structure, as it has been shown for α2-COP, β′-COP, and ε-COP subunits (Ahn et al., 2015; Woo et al., 2015; Gimeno-Ferrer et al., 2017). At the CLSM, Golgi punctae appeared frequently clustered, while at the electron microscope the Golgi apparatus appeared enlarged, with a length significantly higher than that in wild-type plants. It has been previously described that COPI-coated vesicles are essential for Golgi homeostasis. Concerning the β-subunit, knockdown of β-COP in HeLa cells was shown to produce an increase in Golgi volume and a fragmented Golgi (Guo et al., 2008). The apparent volume increase of Golgi markers was proposed to reflect defects in COPI-mediated membrane retrieval from the Golgi to the ER. Indeed, the surface area of Golgi cisternae depends on the ratio of membrane input and output to the Golgi apparatus along different trafficking routes (Sengupta and Linstedt, 2011). In this respect, inhibition of Golgi-to-ER transport by knockdown of Scyl1 (a high affinity-binding partner for COPI coats involved in the regulation of COPI-mediated retrograde trafficking) led to an expanded but intact Golgi in Hela cells (Burman et al., 2010). Therefore, the increased length of Golgi stacks observed in the *amiRb1/*β*2-cop* mutant may be the result of defective membrane recycling from the Golgi apparatus. Alternatively, the defect in β-COP might facilitate membrane fusion between Golgi stacks. The biogenesis of the Golgi ribbon in mammalian cells starts with clustering of Golgi stacks followed by tethering and homotypic fusion of Golgi stacks into a continuous ribbon (Nakamura et al., 2012). Although the plant Golgi apparatus does not form ribbon-like structures (Ito et al., 2014), it is still possible that Golgi stacks may eventually undergo fusion events under certain circumstances, such as COPI depletion. Indeed, Golgi cisternae have been shown to undergo homotypic fusion in *Saccharomyces cerevisiae* (Bhave et al., 2014), although Golgi apparatus in these cells consist in dispersed cisternae in the cytoplasm, without stacks and ribbon structures (Ito et al., 2014). In *Saccharomyces cerevisiae*, depletion of ARF1, which is involved in COPI vesicle formation, also led to Golgi enlargement, which was proposed to be the result of altered dynamics of cisternal maturation (Bhave et al., 2014).

Knockout of the α2-COP isoform of *Arabidopsis* α-COP subunit also caused an alteration in Golgi morphology. However, the Golgi phenotype observed upon α2-COP knockout consisted of a reduced number of cisternae per Golgi stack and many abnormal vesicle clusters around the Golgi remnants (Gimeno-Ferrer et al., 2017). This Golgi phenotype was similar to that obtained upon silencing of ε-COP in *Arabidopsis* and β'-COP in *N. benthamiana* (Ahn et al., 2015; Woo et al., 2015). This is different to the Golgi phenotype obtained upon silencing of β-COP isoforms, which rather produced longer Golgi stacks (this manuscript). This might be related with the fact that β-COP belongs to the F-subcomplex of coatomer, different from the B-subcomplex (including α, β′, and ε-COP subunits), although further work is required to dissect the function of specific COPI subunits in plants.

Finally, all three mutants of β-COP showed induction of the COPII subunit isoform *SEC31A*, but not that of *SEC31B*. This specific induction of *SEC31A* was also observed in the α2-COP mutant (Gimeno-Ferrer et al., 2017) as well as in a quadruple mutant affecting p24 family proteins, which are essential in COPI

vesicle formation (Pastor-Cantizano et al., 2018). Altogether, there seems to be a direct correlation between alterations in COPI function and changes in the expression of the SEC31A subunit of the COPII complex, which is involved in the anterograde ER to Golgi transport.

DATA AVAILABILITY STATEMENT

All datasets generated for this study are included in the article/**Supplementary Material**.

AUTHOR CONTRIBUTIONS

MM and FA: conceptualization, writing – original draft, supervision, project administration, and funding acquisition. JS-S, FG-F, PS-M, JM-P, CB-S, MM, and FA: investigation. MM, JM-P, JS-S, and FA: writing – review and editing.

FUNDING

FA and MM were supported by the Ministerio de Economía y Competitividad (Grant No. BFU2016-76607P) and Generalitat Valenciana (ISIC/2013/004, GVACOMP2014-202). JS-S and CB-S were recipients of a fellowship from the Ministerio de Ciencia, Innovación y Universidades (FPU program).

ACKNOWLEDGMENTS

We thank Francisco Santonja (University of Valencia) for help with statistical analysis. We thank Peter Pimpl (Southern University of Science and Technology, Shenzhen, China) and Lorenzo Frigerio (University of Warwick, United Kingdom) for providing the calnexin-RFP and TIP1.1-GFP constructs. We thank the Salk Institute Genomic Analysis Laboratory for providing the sequence-indexed *Arabidopsis* T-DNA insertion mutants, and the greenhouse, genomic, and microscopy sections of Serveis Centrals de Suport a la Investigació Experimental, University of Valencia (SCSIE).

SUPPLEMENTARY MATERIAL

The Supplementary Material for this article can be found online at: https://www.frontiersin.org/articles/10.3389/fpls.2020.00430/full#supplementary-material

REFERENCES

1001 Genomes Consortium, (2016). 1135 Genomes Reveal the Global Pattern of Polymorphism in *Arabidopsis thaliana*. *Cell* 166, 481–491.

Abramoff, M. D., Magalhães, P. J., and Ram, S. J. (2004). Image processing with Image. *J. Biophot. Int.* 11, 36–42.

Adolf, F., Rhiel, M., Hessling, B., Gao, Q., Hellwig, A., Béthune, J., et al. (2019). Proteomic profiling of mammalian COPII and COPI vesicles. *Cell Rep.* 26, 250–265. doi: 10.1016/j.celrep.2018.12.041

Ahn, H. K., Kang, Y. W., Lim, H. M., Hwang, I., and Pai, H. S. (2015). Physiological functions of the COPI complex in higher plants. *Mol. Cells* 38, 866–875. doi: 10.14348/molcells.2015.0115

Bhave, M., Papanikou, E., Iyer, P., Pandya, K., Jain, B. K., Ganguly, A., et al. (2014). Golgi enlargement in Arf-depleted yeast cells is due to altered dynamics of cisternal maturation. *J. Cell. Sci.* 127, 250–257. doi: 10.1242/jcs.140996

Burman, J. L., Hamlin, J. N., and McPherson, P. S. (2010). Scyl1 regulates Golgi morphology. *PLoS One* 5:e9537. doi: 10.1371/journal.pone.0009537

Chung, K. P., Zeng, Y., and Jiang, L. (2016). COPII Paralogs in plants: functional redundancy or diversity? *Trends Plant Sci.* 21, 758–769. doi: 10.1016/j.tplants.2016.05.010

Clough, S. J., and Bent, A. F. (1998). Floral dip: a simplified method for Agrobacterium-mediated transformation of *Arabidopsis thaliana*. *Plant J.* 16, 735–743. doi: 10.1046/j.1365-313x.1998.00343.x

Cosson, P., and Letourneur, F. (1994). Coatomer interaction with di-lysine endoplasmic reticulum retention motifs. *Science* 263, 1629–1631. doi: 10.1126/science.8128252

Dodonova, S. O., Diestelkoetter-Bachert, P., von Appen, A., Hagen, W. J., Beck, R., Beck, M., et al. (2015). Vesicular transport. A structure of the copi coat and the role of coat proteins in membrane vesicle assembly. *Science* 349, 195–198. doi: 10.1126/science.aab1121

Donohoe, B. S., Kang, B. H., and Staehelin, L. A. (2007). Identification and characterization of COPIa- and COPIb-type vesicle classes associated with plant and algal Golgi. *Proc. Natl. Acad. Sci. U.S.A.* 104, 163–168. doi: 10.1073/pnas.0609818104

Gao, C., Cai, Y., Wang, Y., Kang, B. H., Aniento, F., Robinson, D. G., et al. (2014). Retention mechanisms for ER and Golgi membrane proteins. *Trends Plant Sci.* 19, 508–515. doi: 10.1016/j.tplants.2014.04.004

Gattolin, S., Sorieul, M., and Frigerio, L. (2011). Mapping of tonoplast intrinsic proteins in maturing and germinating *Arabidopsis* seeds reveals dual localization of embryonic TIPs to the tonoplast and plasma membrane. *Mol. Plant.* 4, 180–189. doi: 10.1093/mp/ssq051

Gimeno-Ferrer, F., Pastor-Cantizano, N., Bernat-Silvestre, C., Selvi-Martínez, P., Vera-Sirera, F., Gao, C., et al. (2017). α2-COP is involved in early secretory traffic in *Arabidopsis* and is required for plant growth. *J. Exp. Bot.* 68, 391–401.

Guo, Y., Punj, V., Sengupta, D., and Linstedt, A. D. (2008). Coat-tether interaction in Golgi organization. *Mol. Biol. Cell.* 19, 2830–2843. doi: 10.1091/mbc.e07-12-1236

Hamaji, K., Nagira, M., Yoshida, K., Ohnishi, M., Oda, Y., Uemura, T., et al. (2009). Dynamic aspects of ion accumulation by vesicle traffic under salt stress in Arabidopsis. *Plant Cell Physiol.* 50, 2023–2033. doi: 10.1093/pcp/pcp143

Hecht, M., Bromberg, Y., and Rost, B. (2015). Better prediction of functional effects for sequence variant. *BMC Genomics* 16(Suppl. 8):S1. doi: 10.1186/1471-2164-16-S8-S1

Hutter, S., Vilella, A. J., and Rozas, J. (2006). Genome-wide DNA polymorphism analyses using VariScan. *BMC Bioinformatics* 7:409. doi: 10.1186/1471-2105-7-409

Ito, Y., Uemura, T., and Nakano, A. (2014). Formation and maintenance of the Golgi apparatus in plant cells. *Int. Rev. Cell Mol. Biol.* 310, 221–287. doi: 10.1016/b978-0-12-800180-6.00006-2

Jackson, L. P. (2014). Structure and mechanism of COPI vesicle biogenesis. *Curr. Opin. Cell Biol.* 29, 67–73. doi: 10.1016/j.ceb.2014.04.009

Jiang, B., Shi, Y., Zhang, X., Xin, X., Qi, L., Guo, H., et al. (2017). PIF3 is a negative regulator of the CBF pathway and freezing tolerance in Arabidopsis. *Proc. Natl. Acad. Sci. U.S.A.* 114, E6695–E6702.

Kajiura, H., Koiwa, H., Nakazawa, Y., Okazawa, A., Kobayashi, A., Seki, T., et al. (2010). Two *Arabidopsis thaliana* Golgi alpha-mannosidase I enzymes are responsible for plant N-glycan maturation. *Glycobiology* 20, 235–247. doi: 10.1093/glycob/cwp170

Kim, J. H., Chen, C., and Yun, H. R. (2017). Disorder of trafficking system of plasma membrane and vacuole antiporter proteins causes hypersensitive response to salinity stress in *Arabidopsis thaliana*. *J. Plant Biol.* 60, 380–386. doi: 10.1007/s12374-017-0042-y

Kim, S. J., and Bassham, D. C. (2011). TNO1 is involved in salt tolerance and vacuolar trafficking in *Arabidopsis*. *Plant Physiol.* 156, 514–526. doi: 10.1104/pp.110.168963

Künzl, F., Früholz, S., Fäßler, F., Li, B., and Pimpl, P. (2016). Receptor-mediated sorting of soluble vacuolar proteins ends at the trans-Golgi network/early endosome. *Nat. Plants* 7:16017. doi: 10.1038/nplants.2016.17

Letourneur, F., Gaynor, E. C., Hennecke, S., Démollière, C., Duden, R., Emr, S. D., et al. (1994). Coatomer is essential for retrieval of dilysine-tagged proteins to the endoplasmic reticulum. *Cell* 79, 1199–1207. doi: 10.1016/0092-8674(94)90011-6

Liu, C., Niu, G., Zhang, H., Sun, Y., Sun, S., Yu, F., et al. (2018). Trimming of N-Glycans by the Golgi-Localized α-1,2-Mannosidases, MNS1 and MNS2, Is Crucial for maintaining RSW2 protein abundance during salt stress in *Arabidopsis*. *Mol. Plant* 11, 678–690. doi: 10.1016/j.molp.2018.01.006

Madison, S. L., and Nebenführ, A. (2011). Live-cell imaging of dual-labeled Golgi stacks in tobacco BY-2 cells reveals similar behaviors for different cisternae during movement and brefeldin A treatment. *Mol. Plant* 4, 896–908. doi: 10.1093/mp/ssr067

Marion, J., Bach, L., Bellec, Y., Meyer, C., Gissot, L., and Faure, J. D. (2008). Systematic analysis of protein subcellular localization and interaction using high-throughput transient transformation of *Arabidopsis* seedlings. *Plant J.* 56, 169–179. doi: 10.1111/j.1365-313X.2008.03596.x

Martinière, A., Lavagi, I., Nageswaran, G., Rolfe, D. J., Maneta-Peyret, L., Luu, D.-T., et al. (2012). Cell wall constrains lateral diffusion of plant plasma-membrane proteins. *Proc. Natl. Acad. Sci. U.S.A.* 109, 12805–12810. doi: 10.1073/pnas.1202040109

Minh, B. Q., Nguyen, M. A. T., and von Haeseler, A. (2013). Ultrafast approximation for phylogenetic bootstrap. *Mol. Biol. Evol.* 30, 1188–1195. doi: 10.1093/molbev/mst024

Moelleken, J., Malsam, J., Betts, M. J., Movafeghi, A., Recjmann, I., Meissner, I., et al. (2007). Differential localization of coatomer complex isoforms within the Golgi apparatus. *Proc. Natl. Acad. Sci. U.S.A.* 104, 4425–4430. doi: 10.1073/pnas.0611360104

Nakamura, N., Wei, J. H., and Seemann, J. (2012). Modular organization of the mammalian Golgi apparatus. *Curr. Opin. Cell Biol.* 24, 467–474. doi: 10.1016/j.ceb.2012.05.009

Nebenführ, A., Gallagher, L. A., Dunahay, T. G., Frohlick, J. A., Mazurkiewicz, A. M., Meehl, J. B., et al. (1999). Stop-and-go movements of plant Golgi stacks are mediated by the acto-myosin system. *Plant Physiol.* 121, 1127–1142. doi: 10.1104/pp.121.4.1127

Nguyen, L.-T., Schmidt, H. A., von Haeseler, A., and Minh, B. Q. (2015). IQ-TREE: a fast and effective stochastic algorithm for estimating maximum-likelihood phylogenies. *Mol. Biol. Evol.* 32, 268–274. doi: 10.1093/molbev/msu300

Ortiz-Masia, D., Perez-Amador, M. A., Carbonell, J., and Marcote, M. J. (2007). Diverse stress signals activate the C1 subgroup MAP kinases of *Arabidopsis*. *FEBS Lett.* 581, 1834–1840. doi: 10.1016/j.febslet.2007.03.075

Osterrieder, A., Hummel, E., Carvalho, C. M., and Hawes, C. (2010). Golgi membrane dynamics after induction of a dominant-negative mutant Sar1 GTPase in tobacco. *J. Exp. Bot.* 61, 405–422. doi: 10.1093/jxb/erp315

Pastor-Cantizano, N., Bernat-Silvestre, C., Marcote, M. J., and Aniento, F. (2018). Loss of Arabidopsis p24 function affects ERD2 trafficking and Golgi structure, and activates the unfolded protein response. *J. Cell. Sci.* 131:jcs203802. doi: 10.1242/jcs.203802

Pfaffl, M. W. (2004). "Quantification strategies in real-time PCR," in *A-Z of Quantitative PCR*, ed. S. A. Bustin (La Jolla, CA: International University Line (IUL)), 87–112.

Popoff, V., Adolf, F., Brügger, B., and Wieland, F. (2011). COPI budding within the Golgi stack. *Cold Spring Harb. Perspect. Biol.* 3:a005231. doi: 10.1101/cshperspect.a005231

Ranwez, V., Harispe, S., Delsuc, F., and Douzery, E. J. P. (2011). MACSE: multiple alignment of coding sequences accounting for frameshifts and stop codons. *PLoS One* 6:e22594. doi: 10.1371/journal.pone.00022594

Robinson, D. G., Herranz, M. C., Bubeck, J., Pepperkok, R., and Ritzenthaler, C. (2007). Membrane dynamics in the early secretory pathway. *Crit. Rev. Plant Sci.* 26, 199–225. doi: 10.1080/07352680701495820

Ryu, J., Kim, D. G., Lee, Y. S., Bae, Y., Kim, A., Park, N., et al. (2019). Surface expression of TTYH2 is attenuated by direct interaction with β-COP. *BMB Rep.* 2019, 4311.

Sengupta, D., and Linstedt, A. D. (2011). Control of organelle size: the Golgi complex. *Annu. Rev. Cell. Dev. Biol.* 27, 57–77. doi: 10.1146/annurev-cellbio-100109-104003

Tang, H., Wang, X., Bowers, J. E., Ming, R., Alam, M., and Paterson, A. H. (2008). Unraveling ancient hexaploidy through multiply-aligned angiosperm gene maps. *Genome Res.* 18, 1944–1954. doi: 10.1101/gr.080978.108

Tiley, G. P., Ané, C., and Burleigh, J. G. (2016). Evaluating and characterizing ancient whole-genome duplications in plants with gene count data. *Genome Biol. Evol.* 8, 1023–1037. doi: 10.1093/gbe/evw058

Vilella, A. J., Severin, J., Ureta-Vidal, A., Heng, L., Durbin, R., and Birney, E. (2009). Ensemblcompara genetrees: complete, duplication-aware phylogenetic trees in vertebrates. *Genome Res.* 19, 327–335. doi: 10.1101/gr.073585.107

Waters, M. G., Griff, I. C., and Rothman, J. E. (1991). Proteins involved in vesicular transport and membrane fusion. *Curr. Opin. Cell Biol.* 3, 615–620. doi: 10.1016/0955-0674(91)90031-s

Wegmann, D., Hess, P., Baier, C., Wieland, F. T., and Reinhard, C. (2004). Novel isotypic gamma/zeta subunits reveal three coatomer complexes in mammals. *Mol. Cell. Biol.* 24, 1070–1080. doi: 10.1128/mcb.24.3.1070-1080.2004

Woo, C. H., Gao, C., Yu, P., Tu, L., Meng, Z., Banfield, D. K., et al. (2015). Conserved function of the lysine-based KXD/E motif in Golgi retention for endomembrane proteins among different organisms. *Mol. Biol. Cell* 26, 4280–4293. doi: 10.1091/mbc.e15-06-0361

Wu, F. H., Shen, S. C., Lee, L. Y., Lee, S. H., Chan, M. T., and Lin, C. S. (2009). Tape-arabidopsis sandwich - a simpler arabidopsis protoplast isolation method. *Plant Methods* 5, 16. doi: 10.1186/1746-4811-5-16

Yoo, S.-D., Cho, Y.-H., and Sheen, J. (2007). Arabidopsis mesophyll protoplasts: a versatile cell system for transient gene expression analysis. *Nat. Protoc.* 2, 1565–1572. doi: 10.1038/nprot.2007.199

Yu, S., and Pilot, G. (2014). Testing the efficiency of plant artificial microRNAs by transient expression in *Nicotiana benthamiana* reveals additional action at the translational level. *Front. Plant. Sci.* 5:622. doi: 10.3389/fpls.2014.00622

Zhu, J. K. (2016). Abiotic stress signaling and responses in plants. *Cell* 167, 313–324. doi: 10.1016/j.cell.2016.08.029

Zimmermann, P., Hirsch-Hoffmann, M., Hennig, L., and Gruissem, W. (2004). GENEVESTIGATOR. *Arabidopsis* microarray database and analysis toolbox. *Plant Physiol.* 136, 2621–2632. doi: 10.1104/pp.104.046367

Conflict of Interest: The authors declare that the research was conducted in the absence of any commercial or financial relationships that could be construed as a potential conflict of interest.

frontiers in Plant Science

MINI REVIEW
published: 08 May 2020
doi: 10.3389/fpls.2020.00553

To Lead or to Follow: Contribution of the Plant Vacuole to Cell Growth

*Sabrina Kaiser and David Scheuring**

Plant Pathology, University of Kaiserslautern, Kaiserslautern, Germany

Cell division and cell elongation are fundamental processes for growth. In contrast to animal cells, plant cells are surrounded by rigid walls and therefore loosening of the wall is required during elongation. On the other hand, vacuole size has been shown to correlate with cell size and inhibition of vacuolar expansion limits cell growth. However, the specific role of the vacuole during cell elongation is still not fully resolved. Especially the question whether the vacuole is the leading unit during cellular growth or just passively expands upon water uptake remains to be answered. Here, we review recent findings about the contribution of the vacuole to cell elongation. In addition, we also discuss the connection between cell wall status and vacuolar morphology. In particular, we focus on the question whether vacuolar size is dictated by cell size or *vice versa* and share our personnel view about the sequential steps during cell elongation.

Keywords: vacuole, cell elongation, auxin, cell wall, turgor, cell size, cytoskeleton, actin

OPEN ACCESS

Edited by:
Eugenia Russinova, Ghent University, Belgium

Reviewed by:
Gian Pietro Di Sansebastiano, University of Salento, Italy
Enrique Rojo, National Center of Biotechnology (CSIC), Spain

***Correspondence:**
David Scheuring
scheurin@rhrk.uni-kl.de

Specialty section:
This article was submitted to Plant Traffic and Transport, a section of the journal Frontiers in Plant Science

Received: *28 February 2020*
Accepted: *14 April 2020*
Published: *08 May 2020*

Citation:
Kaiser S and Scheuring D (2020) To Lead or to Follow: Contribution of the Plant Vacuole to Cell Growth. Front. Plant Sci. 11:553. doi: 10.3389/fpls.2020.00553

INTRODUCTION

The plants largest organelle, the vacuole, occupies up to 90% of the cellular volume in vegetative tissues. Although the name *vacuole* originates from the Latin *vacuus* (= vacuum), implying an empty and potentially functionless space, quite the opposite is true. Vacuoles fulfill a plethora of important and diverse functions in plant cells. Among them are the degradation of cellular waste, the storage of ions and proteins, plant defense against pathogens, pH homeostasis and plant growth. The vacuole's prominent size and the finding that individual cells hold turgor pressure up to 5 bar (Zimmermann et al., 1980) established the believe that vacuoles provide the driving force for plant growth. Here, vacuoles were thought to simply drive cell elongation via turgor pressure (Marty, 1999). While there is no doubt that turgor pressure contributes to cell elongation (Cosgrove, 2018), the precise role of the vacuole in this process remains unclear and has not yet been addressed experimentally. However, restricting the vacuole's dimensions has been shown to inhibit cellular elongation and root organ growth (Löfke et al., 2015; Kaiser et al., 2019). Conversely, increasing vacuolar occupancy of the cell is of eminent importance during elongation (Dünser et al., 2019).

Besides the vacuole, the properties of the plant cell wall represent another crucial component for defining cell size and growth rates. Cell wall acidification and subsequent loosening are long known to be a prerequisite for expansion (Cosgrove, 1993), but the interplay with intracellular changes (vacuolar expansion) are less well understood. Only lately substantial progress was made in understanding the signaling and coordination between extracellular and intracellular changes during cell elongation (Dünser et al., 2019).

CELL WALL LOOSENING AS PREREQUISITE FOR CELL ELONGATION

Since plant cells are sheathed by rigid, shape-giving cell walls, cellular extension cannot be explained by vacuolar expansion alone but must, consequently, also include cell wall modifications. Already in the early 70s of the last century, researchers could show that the elongation of stem and coleoptile cells promoted by the phytohormone auxin was coupled to cell wall loosening (Rayle and Cleland, 1970; Hager et al., 1971). This led to the formulation of the so-called *acid growth theory*, primarily proposing a connection of auxin and acidification of the cell exterior, the apoplast. The current understanding of this hypothesis includes the activation of plasma membrane (PM) H^+-ATPases by auxin and subsequent acidification of the apoplast and thus the cell wall. Following this, pH-responsive non-enzymatic proteins from the expansin family (McQueen-Mason et al., 1992) are activated, leading to cell wall loosening via xyloglucan slipping (Cosgrove, 2000). Cell elongation is then achieved by water uptake alongside with the deposition of new wall material.

Not long ago, the acid growth theory has been confirmed in shoots (Fendrych et al., 2016) and roots of the model plant Arabidopsis (Barbez et al., 2017). In the latter, the model was heavily debated, due to the complex role of auxin in plant development and technical limitations in investigating apoplastic pH at cellular resolution. Depending on the concentration and the cell type, auxin promotes and inhibits growth, respectively. In the physiological concentration range, auxin preferentially induces growth in aerial, and inhibits growth in underground tissues (Evans et al., 1994; Dünser and Kleine-Vehn, 2015). However, Barbez and coauthors showed that cell wall acidification induced cellular expansion and that this is preceded by and dependent on auxin signaling (Barbez et al., 2017). Interestingly, increasing total levels of auxin induced a transient alkalinization of the apoplast and reduced cellular elongation. This in turn was dependent on the receptor-like kinase FERONIA (FER) which has been demonstrated to control the elasticity of the cell wall (Höfte, 2015) and functions as a mechano−sensor (Shih et al., 2014).

CONTRIBUTION OF THE VACUOLE TO CELL ELONGATION

It has been shown that auxin does not only affect cell wall loosening but also directly impacts on the vacuole. In the Arabidopsis root meristem, the phytohormone induced smaller and more constricted vacuoles (Löfke et al., 2015). Changes of vacuolar morphology in turn directly affected cell-size control and restricted root growth (Löfke et al., 2015). Since this auxin-induced vacuolar phenotype was accompanied by an increased abundance of soluble N-ethylmaleimide-sensitive-factor attachment receptors (SNAREs), especially VTI11, auxin was hypothesized to impact on homotypic vacuolar fusion events (Löfke et al., 2015). Subsequently, auxin-induced constrictions of the vacuole were demonstrated to be dependent on the actin cytoskeleton (Scheuring et al., 2016). In actin and myosin mutants, auxin-induced changes of vacuolar morphology, cell-size restriction and inhibition of root growth were all largely abolished (Scheuring et al., 2016). In mammalian cells, members of the HOPS (homotypic fusion and protein sorting) complex interact with the actin cytoskeleton (Richardson et al., 2004). This complex mediates homotypic vacuole fusion in plants (Takemoto et al., 2018) and a potential actin interaction here would at least partly explain the actin-dependency of auxin-induced vacuolar changes.

Notably, the tonoplast-localized auxin transporter WALLS ARE THIN1 1 (WAT1) has been identified, facilitating auxin export from the vacuole (Ranocha et al., 2013). Hence, a key role for the vacuole in intracellular auxin homeostasis was suggested. Moreover, WAT1 has been proposed to integrate auxin signaling and secondary cell wall formation of stem fibers in Arabidopsis (Ranocha et al., 2010).

Another layer of complexity is added by the presence of different vacuole types in plants. Dependent on their function, vacuoles are classified into protein storage vacuoles (PSVs), predominantly found in seed tissues, and lytic vacuoles (LVs) which are commonly found in vegetative tissue and are primarily discussed in the present mini-review. For both, PSVs and LVs, independent inhibition of trafficking has been demonstrated (Bolte et al., 2004; Park et al., 2005), and thus separate transport routes were assumed. Furthermore, it has been shown that trafficking to these vacuoles requires different members of SNARE proteins. While VTI12 plays an important role in protein transport to PSVs, trafficking to the LV is mainly dependent on VTI11 (Sanmartín et al., 2007). This could indicate that the auxin induced vacuolar changes seen for LVs accompanied by upregulation of VTI11 (Löfke et al., 2015) are unique for LVs, potentially not impacting on PSVs.

To unravel the morphological changes of the lytic vacuole upon exogenous auxin treatment in detail, the combination of state-of-the-art imaging and staining methods were employed. This allowed 3D modeling and quantitative analysis of different parameters such as vacuolar volume and surface area. Markedly, upon auxin application, most vacuolar subvolumina were still connected and together formed one single interconnected organelle (Scheuring et al., 2015, 2016). Based on the reduced cellular space that (auxin-induced) constricted vacuoles occupy, a space-filling function of the vacuole was proposed. This would allow plant cells to elongate without altering the amount of cytosol, thereby massively reducing energy investment (Scheuring et al., 2016; Krüger and Schumacher, 2018). Accordingly, auxin would limit the intracellular occupancy of the vacuole to restrict cell elongation. This is well in accordance with the observation that the size of plant vacuoles correlates with cell size (Owens and Poole, 1979).

Due to the close proximity of the vacuolar membrane (tonoplast) and actin filaments it has been suggested that there might be a direct physical connection (Kutsuna et al., 2003). In a screen for GFP-fusion proteins labeling actin filaments, the plant-specific Networked (NET) family was identified (Deeks et al., 2012). NET proteins possess an actin-binding domain and are membrane-associated, thus linking actin filaments with different

cell organelles. One specific member, NET4A, has been shown to bind actin and overlaps with the tonoplast (Deeks et al., 2012). Recently, it was shown that NET4A localizes to highly constricted regions of the tonoplast and, together with NET4B, modulates vacuolar occupancy. Overexpression led to a decrease, and loss-of-function to an increase of vacuolar occupancy, respectively (Kaiser et al., 2019). As increased vacuolar volume allows for rapid cellular elongation with relatively little *de novo* production of cytosolic content (Dünser et al., 2019); more compact vacuoles induced by NET4A overexpression might explain the accompanied cell size and root length limitations observed in a NET4A overexpressor line (Kaiser et al., 2019). Furthermore, this finding confirms that cell size and vacuole size are tightly linked and that inhibited cell elongation via restricted vacuolar size does not exclusively depend on auxin. Indeed, additional factors, such as blue light and most of the other described phytohormones are also involved in cell size determination (Halliday et al., 2009; Perrot-Rechenmann, 2010).

Naturally, the observed restrictions of vacuolar expansion led to the question of their function apart from restricting cell size. One explanation could be the requirement of increasing cytosol demands during cell division. In agreement with this, vacuolar volume has been reported to decrease by 80% within cell division, increasing the amount of cytosol required to accommodate the forming phragmoplast and associated cell plate-forming structures (Seguí-Simarro and Staehelin, 2006). In line with this, unequal vacuole partitioning during embryogenesis in the *gravitropism defective 2* (grv2) mutant resulted in daughter cell formation of unequal size (Silady et al., 2008). It was postulated that the presence of an unusually large vacuole in one daughter cell led to misalignment of the phragmoplast, explaining the observed disturbance of cell division in the mutant (Silady et al., 2008).

In contrast to vacuole size restriction during cytokinesis, developing cells of the root meristem display gradually larger vacuoles as cells transit into the elongation zone. Cells leaving meristematic zones extend their original size 10–1,000-fold (Veytsman and Cosgrove, 1998). To fulfill its space-filling function and to avoid high metabolic costs for the generation of large amounts of cytosolic content, the vacuole must dramatically increase its volume (**Figure 1**). Indeed, vacuolar occupancy of the cell increases from around 40% in meristematic cells to more than 85% in cells of the late elongation zone (Dünser et al., 2019). Initially, the osmotic potential in the vacuole must be higher than in the cytosol to enable water uptake, but eventually it must reach equilibrium. The tonoplast (unlike the cell wall) has limited tensile strength and cannot withstand significant differences in pressure without rupturing.

DISCUSSION

Obviously, vacuolar expansion and cell wall loosening both are of eminent importance for cell elongation. Thus, the question arises: How are these processes coordinated and is the vacuole indeed the driving force for cell elongation as proposed previously?

Recent data revealed that the receptor-like kinase FER together with extracellular leucine−rich repeat extensins (LRXs) sense cell wall properties (such as loosening) and subsequently impact on the intracellular expansion of the vacuole (Dünser et al., 2019). This module was proposed to integrate the cell wall status with intracellular growth processes, but it remained unclear how precisely LRX/FER signaling at the cell surface leads to the modulation of vacuolar size. One hypothesis involves several transduction steps to regulate the actin cytoskeleton (Dünser et al., 2019). Since the actin cytoskeleton surrounds the vacuole and contributes to the regulation of vacuolar size (Scheuring et al., 2016), this link could in principle explain how extracellular sensing and intracellular control of vacuolar volume are integrated. In agreement, *lrx* and *fer* mutants display

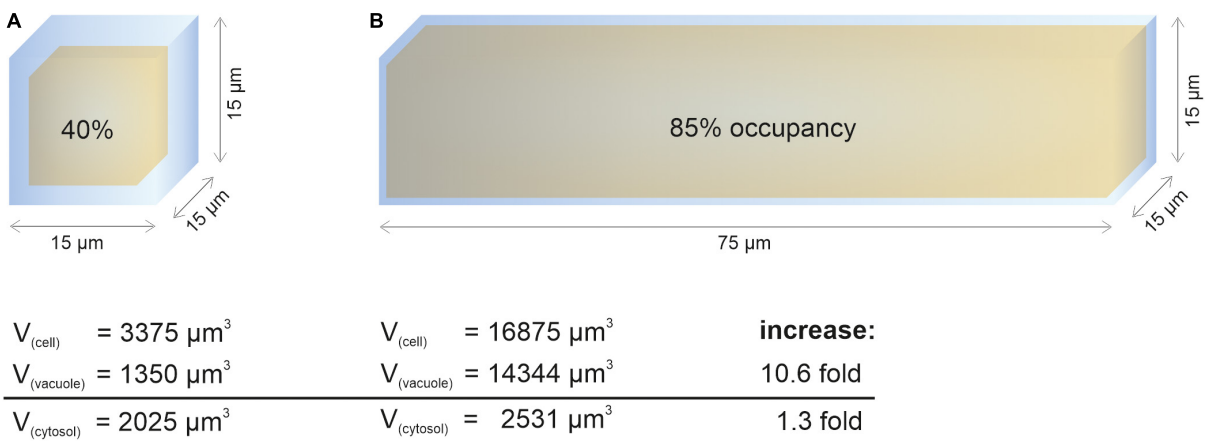

FIGURE 1 | Cytosol homeostasis during cell expansion. The cellular space occupied by the vacuole (occupancy) increases dramatically during elongation, allowing to keep the cytosolic volume relatively constant. For simplification, the geometric body of a cube was used to calculate vacuolar volume (yellow) and cell volume (blue). After subtraction, the remaining space was used to approximate cytosolic volume. Values for vacuolar occupancy were based on Dünser et al. (2019) in this figure. **(A)** Simplified epidermis cell of the late meristem from the Arabidopsis root with the edge length of 15 µm. **(B)** Simplified 5-fold elongated cell from the transition zone. While the vacuolar volume increases more than 10-fold during elongation, the cytosolic volume only increases by factor 1.3.

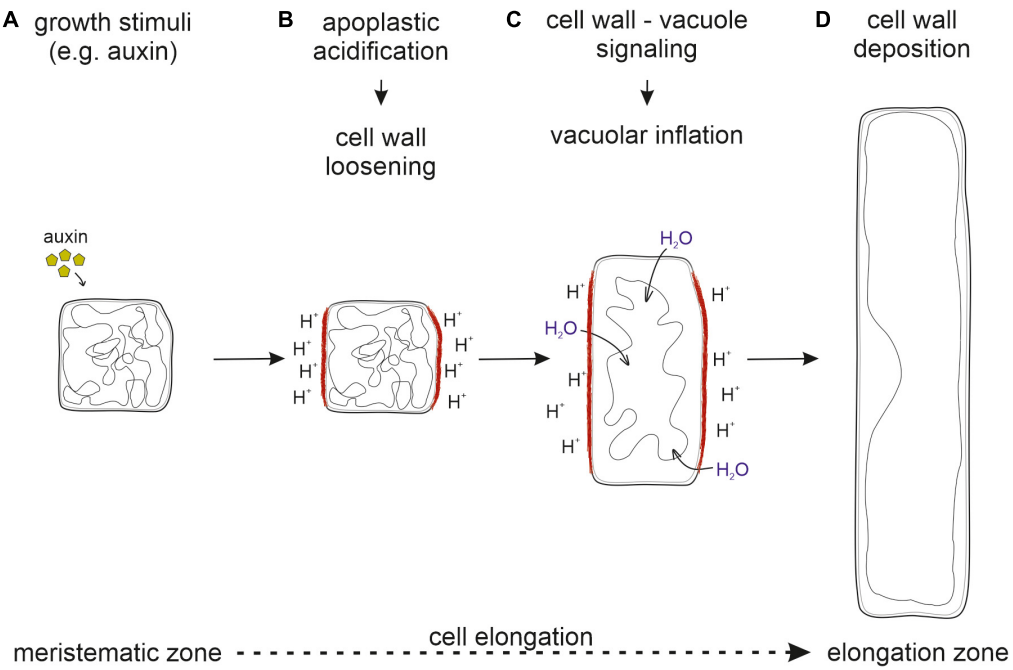

FIGURE 2 | Sequential order of processes necessary for cell elongation. **(A)** Upon perception of growth stimuli, **(B)** the apoplast is acidified and the cell wall loosened. **(C)** The cell wall status is sensed by the FER-LRX module and transmitted into the cell. **(D)** New cell wall material deposition allows for cell elongation. Inhibition at any step prevents proper cell elongation and inhibits growth.

a pronounced enlargement of the vacuolar lumina and a higher vacuolar occupancy of the cell (Dünser et al., 2019). Moreover, these vacuoles are resistant to pharmacological treatments that presumably impact on cell wall properties and normally restrict vacuolar expansion (Dünser et al., 2019). Thus, it is tempting to state that without transmission of the cell wall status, vacuolar changes will not occur. Additionally, in fully elongated cells, the osmotic potential of cytosol and vacuole needs to be equilibrated to prevent membrane rupture. It is conceivable that a high turgor pressure could be build up without the vacuole, albeit with dramatically higher energy investment.

Furthermore, it has been shown that the expression of a specific tonoplast intrinsic protein (γ-TIP), enabling water uptake, is correlated with cell elongation (Ludevid et al., 1992). If the vacuole would be indeed the driving force, one would expect the onset of TIP expression before cell elongation is initiated. In contrast, several TIPs were found to be preferentially expressed in elongating cells but not in the meristematic zone of Arabidopsis roots (Gattolin et al., 2009, 2010). This again questions the vacuole's role in leading cell expansion via increasing turgor pressure.

Taken together, it seems likely that cell wall loosening through apoplastic acidification is the driving force for vacuolar expansion. For this, the cell wall status has to be sensed and external signals must be transmitted into the cell to initiate vacuolar expansion. Only then, the space-filling capacity of the vacuole allows the occupation of the emerging space in expanding cells. This ensures that cytosolic content does not become the growth-limiting factor (**Figure 2**).

Therefore, we believe that vacuolar expansion follows cell wall loosening which marks the onset for cell expansion. Only in concert, both processes jointly grant rapid cell elongation and enable fast plant growth rates. However, the precise relationship between vacuole expansion, cell wall properties and cell elongation is not fully understood and it will be an exciting future task to identify yet unknown players involved in the coordination of this complex and delicate process.

Another important question that needs to be addressed in future research is the source of membrane material to allow for rapid cell elongation. Due to the enormous increase in cell size, not only the vacuole but also the PM requires new membrane material to adapt their surface area. While the endoplasmic reticulum (ER) is the main synthesis site for lipids destined for the PM (Blom et al., 2011) the source for newly synthesized vacuole membrane is not yet unanimously agreed on. During vacuole biogenesis two seemingly opposing models are controversially discussed. One describes the ER as the main membrane source while the second considers small vacuoles (SV), derived through fusion and maturing of multivesicular bodies (MVBs) which in turn originate from the trans-Golgi network (TGN) as membrane carrier (reviewed in Viotti et al., 2013; Krüger and Schumacher, 2018; Cui et al., 2020). Certainly, rearrangement of the convoluted and constricted tonoplast in meristematic cells will provide some excessive membrane material for gradually expanding vacuoles (**Figure 2**), but this seems hardly sufficient for full expansion in elongated cells. Therefore, it must not only shed light upon the relationship

between vacuole expansion and cell wall properties, but also investigated how membrane material is delivered to the PM and the tonoplast during cell elongation. In addition, the spatiotemporal coordination of cell wall loosening and vacuole expansion with growing PM surface area remains to be addressed. Understanding the integration of all these processes and the sequential order of events will provide challenging future research tasks.

AUTHOR CONTRIBUTIONS

SK and DS wrote the manuscript and prepared the figures.

FUNDING

This work was supported by grants to David Scheuring from the German Research Foundation (DFG; SCHE 1836/4-1) and the *BioComp* Research Initiative from the state Rhineland-Palatinate, Germany.

ACKNOWLEDGMENTS

We would like to thank Kai Dünser for critical reading of the manuscript. We apologize to researchers whose work could not be included in this manuscript due to space constraints.

REFERENCES

Barbez, E., Dünser, K., Gaidora, A., Lendl, T., and Busch, W. (2017). Auxin steers root cell expansion via apoplastic pH regulation in *Arabidopsis thaliana*. *Proc. Natl. Acad. Sci. U.S.A.* 114, E4884–E4893. doi: 10.1073/pnas.1613499114

Blom, T., Somerharju, P., and Ikonen, E. (2011). Synthesis and biosynthetic trafficking of membrane lipids. *Cold Spring Harb. Perspect. Biol.* 3:a004713. doi: 10.1101/cshperspect.a004713

Bolte, S., Brown, S., and Satiat-Jeunemaitre, B. (2004). The N-myristoylated Rab-GTPase m-Rabmc is involved in post-Golgi trafficking events to the lytic vacuole in plant cells. *J. Cell Sci.* 117(Pt 6), 943–954. doi: 10.1242/jcs.00920

Cosgrove, D. J. (1993). How do plant cell walls extend? *Plant Physiol.* 102, 1–6. doi: 10.1104/pp.102.1.1

Cosgrove, D. J. (2000). Expansive growth of plant cell walls. *Plant Physiol. Biochem. PPB* 38, 109–124. doi: 10.1016/s0981-9428(00)00164-9

Cosgrove, D. J. (2018). Diffuse growth of plant cell walls. *Plant Physiol.* 176, 16–27. doi: 10.1104/pp.17.01541

Cui, Y., Zhao, Q., Hu, S., and Jiang, L. (2020). Vacuole biogenesis in plants: how many vacuoles, how many models? *Trends Plant Sci*. (in press). doi: 10.1016/j.tplants.2020.01.008

Deeks, M. J., Calcutt, J. R., Ingle, E. K. S., Hawkins, T. J., Chapman, S., Richardson, A. C., et al. (2012). A superfamily of actin-binding proteins at the actin-membrane nexus of higher plants. *Curr. Biol. CB* 22, 1595–1600. doi: 10.1016/j.cub.2012.06.041

Dünser, K., Gupta, S., Herger, A., Feraru, M. I., Ringli, C., and Kleine-Vehn, J. (2019). Extracellular matrix sensing by FERONIA and Leucine-Rich Repeat Extensins controls vacuolar expansion during cellular elongation in *Arabidopsis thaliana*. *EMBO J.* 38:e100353. doi: 10.15252/embj.2018100353

Dünser, K., and Kleine-Vehn, J. (2015). Differential growth regulation in plants—the acid growth balloon theory. *Curr. Opin. Plant Biol.* 28, 55–59. doi: 10.1016/j.pbi.2015.08.009

Evans, M. L., Ishikawa, H., and Estelle, M. A. (1994). Responses of *Arabidopsis* roots to auxin studied with high temporal resolution: comparison of wild type and auxin-response mutants. *Planta* 194, 215–222. doi: 10.1007/BF00196390

Fendrych, M., Leung, J., and Friml, J. (2016). TIR1/AFB-Aux/IAA auxin perception mediates rapid cell wall acidification and growth of *Arabidopsis hypocotyls*. *eLife* 5:e19048. doi: 10.7554/eLife.19048

Gattolin, S., Sorieul, M., and Frigerio, L. (2010). Tonoplast intrinsic proteins and vacuolar identity. *Biochem. Soc. Trans.* 38, 769–773. doi: 10.1042/BST0380769

Gattolin, S., Sorieul, M., Hunter, P. R., Khonsari, R. H., and Frigerio, L. (2009). In vivo imaging of the tonoplast intrinsic protein family in *Arabidopsis* roots. *BMC Plant Biol.* 9:133. doi: 10.1186/1471-2229-9-133

Hager, A., Menzel, H., and Krauss, A. (1971). Versuche und Hypothese zur Primärwirkung des Auxins beim *Streckungswachstum*. *Planta* 100, 47–75. doi: 10.1007/BF00386886

Halliday, K. J., Martínez-García, J. F., and Josse, E.-M. (2009). Integration of light and auxin signaling. *Cold Spring Harb. Perspect. Biol.* 1:a001586.

Höfte, H. (2015). The yin and yang of cell wall integrity control: brassinosteroid and FERONIA signaling. *Plant Cell Physiol.* 56, 224–231. doi: 10.1093/pcp/pcu182

Kaiser, S., Eisa, A., Kleine-Vehn, J., and Scheuring, D. (2019). NET4 modulates the compactness of vacuoles in *Arabidopsis thaliana*. *Int. J. Mol. Sci.* 20:4752. doi: 10.3390/ijms20194752

Krüger, F., and Schumacher, K. (2018). Pumping up the volume - vacuole biogenesis in *Arabidopsis thaliana*. *Semin. Cell Dev. Biol.* 80, 106–112. doi: 10.1016/j.semcdb.2017.07.008

Kutsuna, N., Kumagai, F., Sato, M. H., and Hasezawa, S. (2003). Three-dimensional reconstruction of tubular structure of vacuolar membrane throughout mitosis in living tobacco cells. *Plant Cell Physiol.* 44, 1045–1054. doi: 10.1093/pcp/pcg124

Löfke, C., Dünser, K., Scheuring, D., and Kleine-Vehn, J. (2015). Auxin regulates SNARE-dependent vacuolar morphology restricting cell size. *eLife* 4:e05868. doi: 10.7554/eLife.05868

Ludevid, D., Höfte, H., Himelblau, E., and Chrispeels, M. J. (1992). The expression pattern of the tonoplast intrinsic Protein gamma-TIP in *Arabidopsis thaliana* is correlated with cell enlargement. *Plant Physiol.* 100, 1633–1639. doi: 10.1104/pp.100.4.1633

Marty, F. (1999). Plant vacuoles. *Plant Cell* 11, 587–600. doi: 10.1105/tpc.11.4.587

McQueen-Mason, S., Durachko, D. M., and Cosgrove, D. J. (1992). Two endogenous proteins that induce cell wall extension in plants. *Plant Cell* 4, 1425–1433. doi: 10.1105/tpc.4.11.1425

Owens, T., and Poole, R. J. (1979). Regulation of cytoplasmic and vacuolar volumes by plant cells in suspension culture. *Plant Physiol.* 64, 900–904. doi: 10.1104/pp.64.5.900

Park, M., Lee, D., Lee, G.-J., and Hwang, I. (2005). AtRMR1 functions as a cargo receptor for protein trafficking to the protein storage vacuole. *J. Cell Biol.* 170, 757–767. doi: 10.1083/jcb.200504112

Perrot-Rechenmann, C. (2010). Cellular responses to auxin: division versus expansion. *Cold Spring Harb. Perspect. Biol.* 2:a001446. doi: 10.1101/cshperspect.a001446

Ranocha, P., Denancé, N., Vanholme, R., Freydier, A., Martinez, Y., Hoffmann, L., et al. (2010). Walls are thin 1 (WAT1), an *Arabidopsis* homolog of *Medicago truncatula* NODULIN21, is a tonoplast-localized protein required for secondary wall formation in fibers. *Plant J. Cell Mol. Biol.* 63, 469–483. doi: 10.1111/j.1365-313X.2010.04256.x

Ranocha, P., Dima, O., Nagy, R., Felten, J., Corratgé-Faillie, C., Novák, O., et al. (2013). Arabidopsis WAT1 is a vacuolar auxin transport facilitator required for auxin homoeostasis. *Nat. Commun.* 4:2625. doi: 10.1038/ncomms3625

Rayle, D. L., and Cleland, R. (1970). Enhancement of wall loosening and elongation by Acid solutions. *Plant Physiol.* 46, 250–253. doi: 10.1104/pp.46.2.250

Richardson, S. C. W., Winistorfer, S. C., Poupon, V., Luzio, J. P., and Piper, R. C. (2004). Mammalian late vacuole protein sorting orthologues participate in early endosomal fusion and interact with the cytoskeleton. *Mol. Biol. Cell* 15, 1197–1210. doi: 10.1091/mbc.e03-06-0358

Sanmartín, M., Ordóñez, A., Sohn, E. J., Robert, S., Sánchez-Serrano, J. J., Surpin, M. A., et al. (2007). Divergent functions of VTI12 and VTI11 in trafficking to storage and lytic vacuoles in Arabidopsis. *Proc. Natl. Acad. Sci. U.S.A.* 104, 3645–3650. doi: 10.1073/pnas.0611147104

Scheuring, D., Löfke, C., Krüger, F., Kittelmann, M., Eisa, A., Hughes, L., et al. (2016). Actin-dependent vacuolar occupancy of the cell determines auxin-induced growth repression. *Proc. Natl. Acad. Sci. U.S.A.* 113, 452–457. doi: 10.1073/pnas.1517445113

Scheuring, D., Schöller, M., Kleine-Vehn, J., and Löfke, C. (2015). Vacuolar staining methods in plant cells. *Methods Mol. Biol.* 1242, 83–92. doi: 10.1007/978-1-4939-1902-4_8

Seguí-Simarro, J. M., and Staehelin, L. A. (2006). Cell cycle-dependent changes in Golgi stacks, vacuoles, clathrin-coated vesicles and multivesicular bodies in meristematic cells of Arabidopsis thaliana: a quantitative and spatial analysis. *Planta* 223, 223–236. doi: 10.1007/s00425-005-0082-2

Shih, H.-W., Miller, N. D., Dai, C., Spalding, E. P., and Monshausen, G. B. (2014). The receptor-like kinase FERONIA is required for mechanical signal transduction in Arabidopsis seedlings. *Curr. Biol. CB* 24, 1887–1892. doi: 10.1016/j.cub.2014.06.064

Silady, R. A., Ehrhardt, D. W., Jackson, K., Faulkner, C., Oparka, K., and Somerville, C. R. (2008). The GRV2/RME-8 protein of *Arabidopsis* functions in the late endocytic pathway and is required for vacuolar membrane flow. *Plant J. Cell Mol. Biol.* 53, 29–41. doi: 10.1111/j.1365-313X.2007.03314.x

Takemoto, K., Ebine, K., Askani, J. C., Krüger, F., Gonzalez, Z. A., Ito, E., et al. (2018). Distinct sets of tethering complexes. SNARE complexes, and Rab GTPases mediate membrane fusion at the vacuole in *Arabidopsis*. *Proc. Natl. Acad. Sci. U.S.A.* 115, E2457–E2466. doi: 10.1073/pnas.1717839115

Veytsman, B. A., and Cosgrove, D. J. (1998). A model of cell wall expansion based on thermodynamics of polymer networks. *Biophys. J.* 75, 2240–2250. doi: 10.1016/S0006-3495(98)77668-4

Viotti, C., Krüger, F., Krebs, M., Neubert, C., Fink, F., Lupanga, U., et al. (2013). The endoplasmic reticulum is the main membrane source for biogenesis of the lytic vacuole in *Arabidopsis*. *Plant cell* 25, 3434–3449. doi: 10.1105/tpc.113.114827

Zimmermann, U., Hüsken, D., and Schulze, E. D. (1980). Direct turgor pressure measurements in individual leaf cells of *Tradescantia virginiana*. *Planta* 149, 445–453. doi: 10.1007/BF00385746

Conflict of Interest: The authors declare that the research was conducted in the absence of any commercial or financial relationships that could be construed as a potential conflict of interest.

frontiers in Plant Science

REVIEW
published: 21 May 2020
doi: 10.3389/fpls.2020.00680

The Beginning of the End: Initial Steps in the Degradation of Plasma Membrane Proteins

*Maximilian Schwihla and Barbara Korbei**

Department of Applied Genetics and Cell Biology, Institute of Molecular Plant Biology, University of Natural Resources and Life Sciences, Vienna, Vienna, Austria

The plasma membrane (PM), as border between the inside and the outside of a cell, is densely packed with proteins involved in the sensing and transmission of internal and external stimuli, as well as transport processes and is therefore vital for plant development as well as quick and accurate responses to the environment. It is consequently not surprising that several regulatory pathways participate in the tight regulation of the spatiotemporal control of PM proteins. Ubiquitination of PM proteins plays a key role in directing their entry into the endo-lysosomal system, serving as a signal for triggering endocytosis and further sorting for degradation. Nevertheless, a uniting picture of the different roles of the respective types of ubiquitination in the consecutive steps of down-regulation of membrane proteins is still missing. The *trans*-Golgi network (TGN), which acts as an early endosome (EE) in plants receives the endocytosed cargo, and here the decision is made to either recycled back to the PM or further delivered to the vacuole for degradation. A multi-complex machinery, the endosomal sorting complex required for transport (ESCRT), concentrates ubiquitinated proteins and ushers them into the intraluminal vesicles of multi-vesicular bodies (MVBs). Several ESCRTs have ubiquitin binding subunits, which anchor and guide the cargos through the endocytic degradation route. Basic enzymes and the mode of action in the early degradation steps of PM proteins are conserved in eukaryotes, yet many plant unique components exist, which are often essential in this pathway. Thus, deciphering the initial steps in the degradation of ubiquitinated PM proteins, which is the major focus of this review, will greatly contribute to the larger question of how plants mange to fine-tune their responses to their environment.

Keywords: ubiquitin, ESCRT (endosomal sorting complex required for transport), CME, plasma membrane protein, degradation

OPEN ACCESS

Edited by:
Erika Isono,
University of Konstanz, Germany

Reviewed by:
Masa H. Sato,
Kyoto Prefectural University, Japan
Swen Schellmann,
Universität zu Köln, Germany

***Correspondence:**
Barbara Korbei
barbara.korbei@boku.ac.at

Specialty section:
This article was submitted to Plant Traffic and Transport, a section of the journal Frontiers in Plant Science

Received: *28 February 2020*
Accepted: *30 April 2020*
Published: *21 May 2020*

Citation:
Schwihla M and Korbei B (2020) The Beginning of the End: Initial Steps in the Degradation of Plasma Membrane Proteins. Front. Plant Sci. 11:680. doi: 10.3389/fpls.2020.00680

ENDOSOMAL SYSTEM OF PLANTS

In eukaryotes, next to transcriptional control, the regulation of protein abundance and localization at membranes is achieved by a complex system of internal membranes, the endomembrane system. This transports proteins to their site of action and provides spatial organization by compartmentalizing distinct cellular activities. Organelles of the endomembrane system are linked by branched and often bidirectional trafficking routes. The endomembrane system consists of two

complimentary trafficking pathways, where the endocytic pathway is a major set of trafficking routes with sorting, recycling, and degradative functions while the secretory pathway exports proteins from the ER via the Golgi apparatus to the *trans*-Golgi network (TGN), where they are sorted for delivery to the plasma membrane (PM), to endosomes, or directly to lysosomes/vacuoles (see **Figure 1**; reviewed in Bassham et al., 2008; Frigerio and Hawes, 2008; Robinson et al., 2008; Richter et al., 2009; Viotti et al., 2010; Korbei and Luschnig, 2013; Paez Valencia et al., 2016).

In mammalian cells, the endocytic pathway includes early, recycling and late endosomes, while in yeast and plants, the TGN also serves as early endosome (EE) and recycling endosome, reflecting the ancestral organization of the endomembrane system (Dettmer et al., 2006; Lam et al., 2007; Day et al., 2018). Thus, the TGN/EE is a major sorting hub, which exists close to the *trans*-Golgi face, but also as a Golgi-independent compartment (Viotti et al., 2010; Kang et al., 2011). Here the two trafficking routes meet, sorting and recycling material to or from the Golgi, the PM and the lytic pathway (**Figure 1**) (Viotti et al., 2010).

ENDOCYTOSIS

Through an essential process termed endocytosis, cells internalize regions of the PM and apoplast into small endocytic vesicles, to remove PM-localized proteins, lipids, and nutrients from the cell surface (Henne et al., 2010). This mechanism is vital not only for basic cellular functions but also for growth, development and to be able to respond quickly and accurately to stimuli. During constitutive endocytosis, components are removed from the cell surface in the absence of any stimulus, while during ligand-induced endocytosis, specific proteins are internalized from the PM in response to a stimulus (Traub, 2009; Ekanayake et al., 2019). Endocytosis can be either dependent on clathrin or independent of it (Robinson, 2015; Sandvig et al., 2018). The coat protein clathrin, was first identified as being the major protein making up the lattice-like coat around vesicles in pig brains (Pearse, 1976) and in plants in soyabeans (Mersey et al., 1985). It builds a coat around the endocytosed vesicle to form a clathrin coated vesicle (CCV), which can form both at the PM and the TGN/EE in plants (Robinson and Pimpl, 2013; Rosquete et al., 2018).

Clathrin self-assembles into a three-legged triskelia composed of three clathrin heavy chains (CHCs) and three clathrin light chains (CLCs), that interact with the heavy chains (Chen et al., 2011; Robinson, 2015). The *Arabidopsis* genome contains two *CHC* genes, namely *CHC1* and *CHC2*, which are ∼90% identical and are functionally partially redundant (Kitakura et al., 2011). Their respective single mutants, however, show different phenotypes, where *chc2* plants display abnormal embryo and seedling development, but *chc1* mutants show no obvious phenotypes (Kitakura et al., 2011). The overexpression of a dominant-negative *C*-terminal hub of CHC competes with the unimpaired CHC for CLC binding and thus interferes with endocytosis of several integral membrane proteins, as well as the uptake of the endocytic tracer FM4-64 (Kitakura et al., 2011), highlighting clathrin-mediated endocytosis (CME) as predominant route for endocytosis in plant. Furthermore, a novel chemical inhibitor was shown to disrupt endocytosis by binding to CHC, which then fails to be assembled into coat structures (Dejonghe et al., 2019). The three *CLC* genes (*CLC1* to *CLC3*) show a partial functional redundancy, where the *clc1* plants show pollen lethality, but *clc2* and *clc3* single mutants are viable but with shorter roots and longer hypocotyls. The *clc2*/*clc3* double mutant is impaired in CME and displays strong developmental defects especially in auxin signaling (Wang et al., 2013; Yu Q. et al., 2016). GFP-tagged CLC2 localizes to the TGN, endosomes, and dynamic foci at the PM (Konopka et al., 2008; Ito et al., 2012).

Clathrin-Mediated Endocytosis

Clathrin-mediated endocytosis is the most prominent endocytic pathway in plants and animals (McMahon and Boucrot, 2011) but was demonstrated only fairly recently in plants (Dhonukshe et al., 2007). It thus also represents a major mechanism for regulating signaling, plant immunity and the global responses, as many important PM proteins are established cargos for the CME pathway (Dhonukshe et al., 2007; Barberon et al., 2011; Di Rubbo et al., 2013; Mbengue et al., 2016; Yoshinari et al., 2016). Nevertheless, detailed descriptions of the events that make up CME in plants are still often based on the more advanced studies of CME in animal and yeast systems (reviewed in McMahon and Boucrot, 2011), although pronounced differences exist. Actin in plant CME for example is not present or required during CCV formation on the PM, but is critical for the early post-endocytic trafficking (Narasimhan et al., 2020).

Five Steps of Clathrin-Mediated Endocytosis

Clathrin-mediated endocytosis is a complex process that can be divided into five steps: nucleation, the packaging of cargo into the vesicle, clathrin coat assembly, the release of the mature vesicle from the PM or membrane scission, and uncoating including the fusing of the vesicle with endosomes (**Figure 2**) (McMahon and Boucrot, 2011). It starts with nucleation site foci at the PM called clathrin coated pits (CCPs), which eventually mature and bud off to form CCVs. These are uncoated and fuse with the TGN/EE, where the cargo is further sorted, either for recycling or degradation. The biogenesis of plant CCVs requires the functions of the clathrin core components, adaptors, linking clathrin to cargos and the PM, as well as accessory components, required for scission and uncoating events (**Figure 2**) (Chen et al., 2011; Korbei and Luschnig, 2013; Paez Valencia et al., 2016; Reynolds et al., 2018; Ekanayake et al., 2019).

Nucleation

Nucleation, or the budding of a vesicle, starts by the bending of the PM toward the cytoplasm and the formation of a membrane invagination called CCP (**Figure 2**). As clathrin does not interact directly with membranes or cargos, the formation of the CCP begins with the recruitment of adaptors proteins. These, interact with specific lipids on membranes as well as sorting motifs on cargo proteins and then bring clathrin to the initiation site at the PM (**Figure 2**). Thus, the starting point of CME depends on

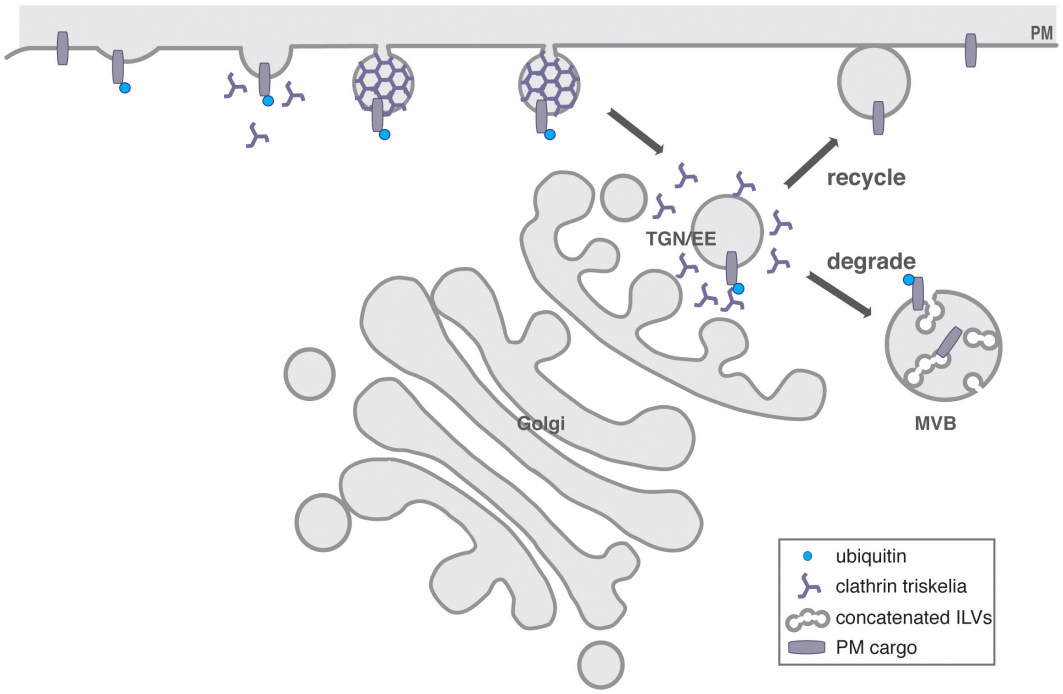

FIGURE 1 | General overview of the endosomal system of plants. CME drives endocytosed cargo delivery from the PM to the TGN, which acts as an EE in plants. Here, the decision is made to either recycle the PM proteins and transport them back to the PM, or to send them for their degradation in the vacuole via the concatenated ILVs of MVBs.

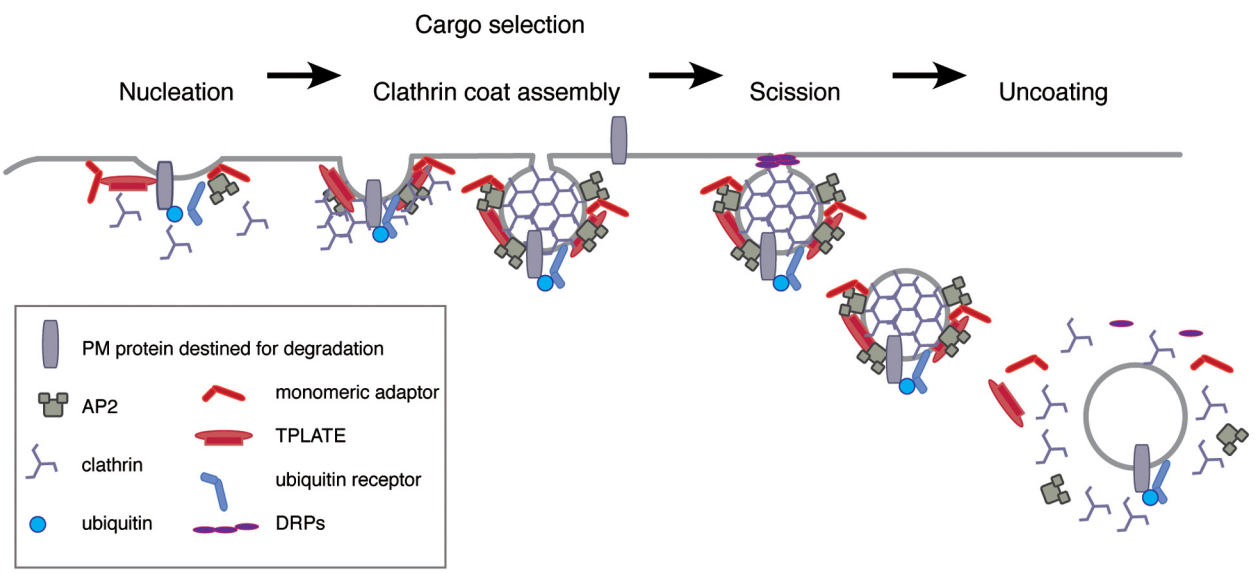

FIGURE 2 | Five-steps of CME. At the PM, extracellular material is internalized by multiple means, including CME. Initiation of CME starts with the enrichment of cargo at nucleation site foci called CCP, which employs various adaptor complexes like TPLATE and AP-2 complexes but also monomeric adaptors. The selection of cargo might require association with thus far uncharacterized cargo-specific adaptor proteins. Adaptor-association is a prerequisite for the subsequent events of clathrin recruitment and coat assembly during the later stages of CCV formation. Mature CCVs are then cleaved from the PM ("scission") by means of DRPs, thereby initiating the endocytic sorting of cargo-loaded CCVs. Before being able to fuse with the TGN/EE, the resulting CCVs undergo uncoating.

lipids, cargos, and adaptor proteins, which provides specificity, determining which cargo is selected and the subcellular compartment for subsequent trafficking. Adaptors therefore consist of multiple domains and motifs that provide a platform for interactions. In monomeric adaptors, these functions are contained within the same protein, while multiple subunits

need to come together in multimeric adaptors (McMahon and Boucrot, 2011; Reider and Wendland, 2011; Cocucci et al., 2012; Paez Valencia et al., 2016; Reynolds et al., 2018).

In mammalian cells, nucleation is started by the binding of a complex composed of the adaptor protein-2 (AP-2) complex and 1–2 clathrin triskelia. This already preassembled complex is recruited to the PM by the membrane lipid phosphatidylinositol-4,5-bisphosphate [PtdIns(4,5)P_2] (Cocucci et al., 2012). Following AP-2 and clathrin recruitment, monomeric adaptor proteins associate with and stabilize the curvature of the budding vesicle and clathrin coat (McMahon and Boucrot, 2011; Cocucci et al., 2012). These including the E/ANTH (epsin/AP180 *N*-terminal homology) domain proteins epsin and AP180, the EGFR pathway substrate 15 (Eps15) proteins as well as muniscin proteins like the FCH domain only (FCHo) proteins and intersectins (Cocucci et al., 2012). The E/ANTH domain is a conserved module for introducing curvature to the bound membranes, which binds phospholipids and proteins responsible for targeting of these proteins to specific compartments (Legendre-Guillemin et al., 2004). Initiation stages may involve the formation of a putative nucleation modules, which include FCHo, Eps15, and intersectins (Henne et al., 2010; Hollopeter et al., 2014) and define the sites on the PM where vesicles will bud (Mayers et al., 2013). However, adaptors might not be crucial for membrane bending in all CME events, as protein crowding at PM foci may be enough to bend the membranes (Dannhauser and Ungewickell, 2012).

Packaging of the Cargo

Regulation of PM protein abundance is based on the ability of the CME machinery, specifically the adaptors, to recognize proteins to be internalized through their specific motifs in their cytosolic domains and package them into the endocytic vesicles. There can be more than one sorting signal in the same cargo protein, participating in cargo recognition. These signals can be present in the protein sequence or structure, or can occur through covalent posttranslational modifications (Traub, 2009).

Clathrin Coat Assembly

The clathrin coat is assembled as soon as cargo is selected and bound by the AP-2, the plant-specific TPLATE complex, or by other cargo-specific adaptor proteins (Chen et al., 2011; Zhang et al., 2015; Reynolds et al., 2018). Clathrin triskelia are recruited directly from the cytosol, where they assemble into a regularly shaped lattice around the forming vesicle (McMahon and Boucrot, 2011). In mammals, polymerization of clathrin results in stabilization of curvature and displacement of some of the monomeric adaptor proteins and curvature effectors, such as Eps15 and epsin, to the edge of the forming vesicle (Tebar et al., 1996). Whether a similar mechanism exists in plants still needs to be determined.

Membrane Scission and Vesicle Release

The molecular scission that mechanically constricts the neck between the CCV and the PM is mediated by dynamins and dynamin-related proteins (DRPs). DRPs are large GTPases, that control membrane scission and tubulation (McMahon and Boucrot, 2011). Plants have six types of DRP families, of which the plant-specific DRP1 family and the DRP2 family, which is the most similar to metazoan dynamins, are involved in clathrin-mediated trafficking and CME (Bednarek and Backues, 2010; Fujimoto and Tsutsumi, 2014). A dominant-negative variant the dynamin related protein DRP1A inhibited endocytosis of the boron efflux transporter BORON TRANSPORTER 1 (BOR1) and altered its polar localization and vacuolar trafficking (Yoshinari et al., 2016).

In animals, Src homology-3 (SH3) domain containing proteins bind dynamin and recruit them to CCPs (Ringstad et al., 1997). In plants the TPLATE complex contains two subunits with SH3 domains, which have been shown to interact with members of the DRP2 and DRP1 families (Gadeyne et al., 2014). Furthermore, the SH3 domain containing protein-2 (SH3P2), which contains a BAR domain that induces vesicle tubulation, forms a complex with a DRP1, affecting its accumulation at the cell plate (Ahn et al., 2017). Whether such an interaction between SH3P2 and DRP1 could also have a significance for CME remains to be resolved.

Vesicle Uncoating

Shedding the coat of the vesicles allows components of the CME machinery to be recycled for further rounds of endocytosis and frees the vesicles for fusion with TGN/EE (Chen et al., 2011; Zhang et al., 2015; Reynolds et al., 2018). While in mammals and yeast, this happens immediately after scission events, the coat of plant CCVs appears to be retained and the components are only gradually discarded on their path to the TGN/EEs (Narasimhan et al., 2020).

In non-plant systems, the ATP−dependent dissociation of clathrin from CCV requires uncoating factors, which are the molecular chaperone heat shock cognate 70 (HSC70) and cofactor proteins like auxilin (Eisenberg and Greene, 2007). In plants, the auxilin-related protein-1 (AUXILIN-LIKE1) stimulates vesicle uncoating in the presence of HSC70 and interacts with SH3P1 and clathrin (Lam et al., 2001). AUXILIN-LIKE1 and 2 possible function in CME as they are part of a complex with clathrin, the ANTH domain protein CAP1, as well as SH3P2 and overexpression of both AUXILIN-LIKE1 and 2 leads to inhibition of endocytosis, most likely by preventing clathrin recruitment to endocytic pits. Nevertheless, they are not essential for endocytosis or development, implying that uncoating in plants may work differently (Adamowski et al., 2018).

Adaptor Proteins in Plants

Multimeric Adaptors

Two types of multimeric adaptors exist in plant endocytosis, the evolutionarily conserved AP complexes and the plant (and some ameba)-specific TPLATE complex (**Figure 2**) (Zhang et al., 2015).

Adaptor protein complexes

There are five hetero-tetrameric AP complexes in *Arabidopsis thaliana*, which are involved in post-Golgi and endosomal vesicular trafficking and each (except for the *At*AP-5;

Hirst et al., 2011) is composed of four subunits: two large, one medium, and one small (Chen et al., 2011; Hirst et al., 2011; Zhang et al., 2015). The AP-2 complex functions in CME (Bashline et al., 2013; Di Rubbo et al., 2013; Kim S. Y. et al., 2013), where it binds clathrin, cargo proteins and PtdIns(4,5)P_2 at the PM (Honing et al., 2005; Fan et al., 2013). The PM association of CHC as well as the endocytic trafficking of the auxin efflux facilitators PIN1 (PIN-FORMED 1) and PIN2 is sensitive to PtdIns(4,5)P_2 production, indicative of its involvement in CME (Ischebeck et al., 2013). Plants impaired in AP-2 subunits showed generally altered endocytosis, in particular of the PINs, brassinosteroid receptor BRASSINOSTEROID INSENSITIVE 1 (BRI1) and the borate efflux transporter BOR1 and exhibited pleiotrophic defects in plant growth and development (Di Rubbo et al., 2013; Fan et al., 2013; Kim S. Y. et al., 2013; Yoshinari et al., 2019). AP-2-dependent endocytosis maintains the polar localization of BOR1 under low-boron conditions, whereas the boron-induced vacuolar sorting of BOR1 is mediated through an AP-2-independent endocytic pathway (Yoshinari et al., 2019). Nevertheless, while the AP-2 complex is essential for early embryonic development in mammals (Mitsunari et al., 2005), *Arabidopsis* mutants of individual AP-2 subunits remain viable (Bashline et al., 2013; Fan et al., 2013; Kim S. Y. et al., 2013).

The TPLATE complex

Nucleation for CME may be different in plants, as they have retained an additional ancestral adaptor complex, the TPLATE complex. This essential component in the early CME events consists of eight core subunits (TPLATE, TASH3, LOLITA, TWD40-1, TWD40-2, TML, AtEH1, and AtEH2) (Gadeyne et al., 2014) and assembles at nucleation sites at the PM preceding AP-2 or at alternative unique sites to AP-2 and subunits of TPLATE complex recruit or stabilize AP-2 at the PM (Gadeyne et al., 2014; Wang et al., 2016). Thus, the TPLATE complex functions as an early multimeric adaptor complex in CME with overlapping, but also distinct, functions compared to the AP-2 complex (Zhang et al., 2015).

The TPLATE complex interacts with both the heavy and the light chain of clathrin, the AP-2, proteins containing the ANTH domain and DRPs and is indispensable for plant development (Van Damme et al., 2006; Gadeyne et al., 2014; Zhang et al., 2015). Several TPLATE subunits contain conserved domains like the SH3 domain in TASH3, the EPS15 homology (EH) domain in AtEH1 and AtEH2, and the μ-homology domain of the AP-2 complex in TML. These are domains, which are generally involved in membrane interactions, cargo recognition, and binding and recruitment of accessory proteins, which are also present in the mammalian Eps15, intersectin, and muniscins. Thus, the TPLATE complex shows functional similarities to the nucleation modules in mammalian system and could function as CME nucleation complex (**Figure 2**) (Gadeyne et al., 2014; Zhang et al., 2015). The presence of specific domains in the TPLATE complex members suggests a common ancestral origin with proteins in other eukaryotes involved in membrane trafficking or a nucleation/adaptor complex (Gadeyne et al., 2014; Hirst et al., 2014). The TML subunit for example could have evolved into the muniscin protein family (Hirst et al., 2014), where a prominent member is the mammalian FCHo protein, which acts as nucleation point for CME (Henne et al., 2010; Cocucci et al., 2012).

Monomeric Adaptor Proteins

Additionally, plants have several monomeric adaptor proteins, these also help link the cargo and membrane lipids to clathrin and multimeric adaptor complexes and thereby play a crucial role in the initiation of CCPs (**Figure 2**) (Paez Valencia et al., 2016). A large number of E/ANTH-domain proteins are found in the *Arabidopsis* genome (Zouhar and Sauer, 2014) and of the six plant proteins with an ENTH domain, two have been functionally characterized. EPSIN1, functions in AP-1-dependent post-Golgi trafficking events (Song et al., 2006) and EPSIN2/EPSINR2, binds PtdIn(3)P and a subunit of the AP-3 complex as well as the AP-2 complex, albeit to a lesser degree, and might localize in the endomembrane system from the TGN to the multi-vesicular bodies (MVBs) (Lee et al., 2007).

The ANTH domain family is larger in *Arabidopsis* and the monomeric adaptor AP180 was the first ANTH domain protein to be characterized. AP180, which gives the domain its name ANTH, interacts with a subunit of the plant AP-2 complex, promotes the assembly of clathrin in CME and regulates CCV size (Barth and Holstein, 2004). For another three ANTH proteins, ECA1, ECA2, and ECA4, it was suggested that they function as adaptors of CCV formation at the cell plate and the PM (Song et al., 2012). AP180 and ECA2, were shown to have a strong affinity to PtdIns(4,5)P_2 and phosphatic acid and play an important role in CME (Kaneda et al., 2019). ECA4 plays a crucial role in recycling cargos from the TGN/EE to the PM (Nguyen et al., 2018) and, like the other ANTH domain protein CAP1, interacts with TML, one of the core components of the TPLATE complex (Gadeyne et al., 2014). CAP1 furthermore is found in a complex, which might function in CME together with clathrin, SH3P2 as well as auxilin-like proteins (Adamowski et al., 2018).

Further monomeric adaptors include the EH domain containing proteins, of which there are five in *A. thaliana* (Miliaras and Wendland, 2004). The *N*-terminal EH domain containing proteins AtEH1 and AtEH2, are part of the TPLATE complex and have recently been shown to interact with actin, like their yeast homologs, localizing to ER-PM contact sites, where they regulate the formation of autophagosomes (Wang P. et al., 2019). There are two *C*-terminal EHD proteins in *Arabidopsis*. Knockdown of AtEHD1 delayed and overexpression of AtEHD2 inhibited endocytosis, however, detailed mechanisms have not been characterized (Bar et al., 2008). A *Zea mays* homolog ZmEHD1 was shown to physically interact with an AP-2 subunit at the PM and in the mutant, endocytosis was drastically reduced and ZmPIN1 localization altered (Wang Y. et al., 2019).

Endocytic Sorting Signals in Plants

Linear Motifs

In animals, the AP-2 recognizes, the di-leucine and the tyrosine (YXXΦ) based sorting motif, (where Y is tyrosine, X is any amino acid, and Φ is a bulky hydrophobic residue) (Traub and Bonifacino, 2013). Both motifs have been identified in plant PM proteins, but only the tyrosine-motifs have so far

been linked to endocytosis (Geldner and Robatzek, 2008). The YXXΦ motif is important for the internalization of several PM proteins. For the PIN auxin efflux facilitators, mutation of the tyrosine motif resulted in a loss of binding of PIN1 to AP-2 subunits and thus reduction of its endocytosis (Sancho-Andres et al., 2016) and for PIN2 also a reduction in its internalization and the mutant construct failed to fully rescue the *pin2* phenotype (Kleine-Vehn et al., 2011). The mutation of the tyrosine motif in the tomato pathogen-related receptor-like protein *Lycopersicon esculentum* ETHYLENE-INDUCING XYLANASE RECEPTOR (LeEIX2) abolished internalization of the receptor in response to EIX application and thus its ability to induce the hypersensitive response (Ron and Avni, 2004). BOR1 contains three tyrosine motifs of in its cytoplasmic domain, which are essential to maintain the proper polar distribution of the boron exporter (Takano et al., 2010). Mutants lacking medium (μ)- or small (σ)-subunits of the AP-2 complex, showed altered polar localization and constitutive endocytosis of BOR1 under low-boron conditions. Nevertheless, association of the AP-2 complex with BOR1, was independent of YXXΦ sorting motifs, and the rapid internalization/vacuolar sorting of BOR1 was not affected in these mutants (Yoshinari et al., 2019).

The tyrosine kinase inhibitor Tyrphostin A23 (TyrA23) is a drug that inhibits the interaction between the tyrosine motif of the cargo and subunits of the AP-2 (Banbury et al., 2003) and is commonly used to interfere with endocytosis in plants (Dhonukshe et al., 2007). Care has to be taken though, as TyrA23, might also inhibit CME due to its protonophore activity, which leads to acidification of the cytoplasm. This undermines its use as a specific inhibitor of cargo recognition by the AP-2 adaptor complex (Dejonghe et al., 2016).

Phosphorylation

The posttranslational modification phosphorylation has been documented as a cue for endocytosis, where it functions in regulating signal recognition (Bonifacino and Traub, 2003). It has a central regulatory function in the endocytosis of PM proteins in plants. Phosphorylation receptor-like-kinase (RLK) LYSIN MOTIF-CONTAINING RLK5 (LYK5) by the CHITIN ELICITOR RECEPTOR KINASE1 (CERK1) is induced by the fungal polysaccharide chitin, and triggers its internalization (Erwig et al., 2017). A point mutation in a potential phosphorylation site of the pathogen-related receptor FLAGELLIN-SENSING 2 (FLS2), decreases the receptor internalization, thus indicating that phosphorylation of FLS2 is required for its endocytosis (Robatzek et al., 2006; Mbengue et al., 2016). Direct metal binding to a histidine-rich stretch of the PM localized IRON-REGULATED TRANSPORTER 1 (IRT1), triggers its phosphorylation and facilitates the subsequent recruitment of the IRT1 degradation factor (IDF) E3 ligase IDF1. Thus, phosphorylation seems to be a prior requirement for ubiquitination, and both are needed for efficient endosomal sorting of IRT1 (Dubeaux et al., 2018). For the boric acid importer NODULIN 26-LIKE INTRINSIC PROTEIN5;1 (NIP5;1), phosphorylation enhanced AP-2-dependent CME and mediates the strong polar localization (Wang H. J. et al., 2017). The phosphorylation states of the auxin efflux facilitators, the PINs, governs their polar distribution to apical and basal PM domains (Adamowski and Friml, 2015), whether the endocytosis of PINs is modulated directly by phosphorylation remain unclear though (Luschnig and Vert, 2014).

Ubiquitination

The post-translation modification of PM proteins by ubiquitin serves as a signal for triggering their endocytosis and consequent sorting for degradation into intraluminal vesicles (ILVs) of MVBs. It thus plays a key role in directing the entry of PM proteins into the endosomal system (**Figure 3**) (Clague et al., 2012; Piper et al., 2014; Dubeaux and Vert, 2017). The enzymes and the mode of action of ubiquitination are conserved in eukaryotes and have been shown to play an important role in most aspects of plant development (Vierstra, 2012; Callis, 2014).

Ubiquitination is catalyzed by a series of consecutively acting enzymes: the ubiquitin activating enzyme (E1), the ubiquitin conjugating enzyme (E2), and the ubiquitin ligase (E3), which generate the formation of an isopeptide bond between the free amine of a lysine residue on the target protein and the *C*-terminus of ubiquitin (MacGurn et al., 2012). More than 1,500 ubiquitin-protein ligases are actively participating in this process, making ubiquitin conjugation an extraordinarily complex process in plants (Hua and Vierstra, 2011). Substrates can be mono-ubiquitinated, multiple mono-ubiquitinated, or decorated with ubiquitin chains. These chains result from linkage of one ubiquitin to the *N*-terminus or an internal lysine residue (K6, 11, 27, 29, 33, 48, and 63) of another ubiquitin moiety (Husnjak and Dikic, 2012; Romero-Barrios and Vert, 2018). Thus different types of chains, which can be linear or branched, can

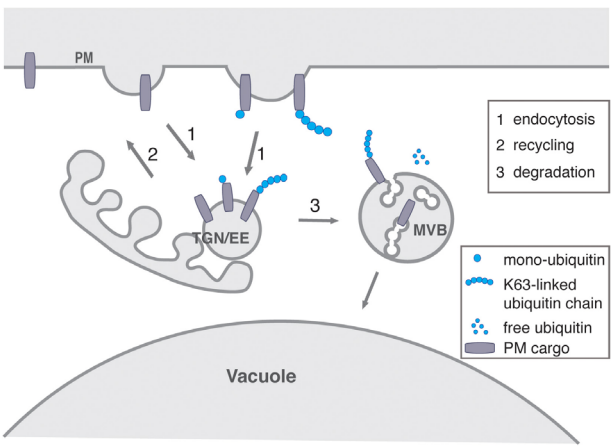

FIGURE 3 | The role of ubiquitin in endocytosis and degradation. Continuous PM protein sorting from the PM to the TGN/EE occur regardless of its ubiquitination status (1) Alternatively, PM protein mono-ubiquination might promote endocytosis of the PM proteins to EE/TGN (1), whereas deubiquitination could favor recycling (2) back to the PM. K63-linked polyubiquitination of PM proteins might promote endocytic sorting from the PM to EE/TGN (1). Alternatively, the PM proteins could be subject to K63-linked polyubiquitination at endosomes and in any case polyubiquitination PM proteins would then be sorted via MVBs into the lytic vacuole. This step involves further ESCRT components (3).

be formed, depending on which amino acid residues of the ubiquitin molecule are conjugated (Husnjak and Dikic, 2012). Two common forms are K48- and K63-linked chains, where the structure of the K48-linked di-ubiquitin is relatively compact, while K63-linked di-ubiquitin adopts an open conformation (Tenno et al., 2004; Varadan et al., 2004). K63-linked ubiquitin chains are the second-most abundant form of ubiquitination in plants (Kim D. Y. et al., 2013; Erpapazoglou et al., 2014; Tomanov et al., 2014; Romero-Barrios and Vert, 2018).

The E2/E3 pairing determines substrate specificity and type of chain linkage, although the same E3 may form different linkage types together with other E2s. Thus, the nature of the chain is defined by E2 enzymes (Tomanov et al., 2014; Stewart et al., 2016). *Arabidopsis* PM localized E3 RING DOMAIN LIGASES (RGLG), can form K63-linked chains together with the E2 UBC35, which appears essential for a wide range of developmental processes (Yin et al., 2007). Only recently, a clean knock out of the *Arabidopsis* E2s UBC35/36 unequivocally demonstrated their central roles as drivers of K63 polyubiquitin chain formation, underlining a key role for this type of protein modification (Romero-Barrios et al., 2020). Further studies on E2/E3 pairing, also revealed interactions between UBC35/36 and plant U-box (PUB) E3s (Turek et al., 2018). This large diversity in ubiquitination types is thought to allow specification of the respective roles in the different steps of down-regulation of membrane proteins, yet a unifying picture is still missing (Sigismund et al., 2004; d'Azzo et al., 2005; Lauwers et al., 2009; Komander and Rape, 2012; Dubeaux and Vert, 2017).

Ubiquitin binding domain (UBD)-containing proteins, or ubiquitin receptors, associate non-covalently with ubiquitin and translate the ubiquitin signals into a cellular response (Husnjak and Dikic, 2012). UBDs are typically short amino acid stretches, without a strict consensus sequence, that bind ubiquitin with a low binding affinity (Husnjak and Dikic, 2012). Several studies have added to deciphering the ubiquitome of plant (Saracco et al., 2009; Kim D. Y. et al., 2013; Svozil et al., 2014; Johnson and Vert, 2016; Walton et al., 2016; Aguilar-Hernandez et al., 2017; Romero-Barrios et al., 2020), enabling the cataloging of ubiquitin-modified proteins and building an excellent basis for future studies to understand this essential modification.

Ubiquitin chains can be altered or removed by deubiquitinating enzymes (DUBs) and in *Arabidopsis* there are around 50 putative DUBs that can be subdivided into five families (Isono and Nagel, 2014). Several E3 ligases involved in internalization processes occur in complexes with DUBs, which either remove or trim the ubiquitin signal contributing to its modulation. This enables tightly regulated and localized cycles of ubiquitination and deubiquitination to reverse or reinforce pathways, but also to prevent promiscuous or inappropriate events (**Figure 3**) (Hicke and Dunn, 2003; Urbe et al., 2012; Isono and Nagel, 2014).

Artificially ubiquitinated cargos, carrying in-frame fusions with ubiquitin showed enhanced internalization, providing direct evidence for ubiquitination acting as principal signal for PM protein endocytosis in plants. This was shown for the auxin efflux facilitator PIN2 (Leitner et al., 2012a), the PM H+-ATPase (PMA) (Herberth et al., 2012), a synthetic PM-localized reporter protein (TMD23-RFP) (Scheuring et al., 2012) and the BRI1 receptor kinase (Martins et al., 2015), where the sole presence of ubiquitin on cargo appeared as a sufficient signal for PM protein endocytosis and further sorting to the vacuolar lumen for degradation. Furthermore, immunoprecipitation experiments showed ubiquitination of a range of PM proteins including PIN2 (Abas et al., 2006; Leitner et al., 2012a), FLS2 (Goehre et al., 2008; Lu et al., 2011), the blue light receptor Phot1 (Roberts et al., 2011), IRT1 (Barberon et al., 2011), BOR1 (Kasai et al., 2011), and BRI1 (Martins et al., 2015). Additionally, several regulatory determinants influence endocytosis of ubiquitinated PM proteins, as shown by recent publications (Lu et al., 2011; Martins et al., 2015; Dubeaux et al., 2018; Retzer et al., 2019; Yoshinari et al., 2019).

The ubiquitination pattern for several PM proteins has been analyzed and dissected in depth and its effect on the endosomal trafficking of the PM protein evaluated. The atypical receptor kinase STRUBBELIG (SUB) is ubiquitinated and internalized by CME and transported via the TGN/EE and MVBs to the vacuole for degradation (Gao et al., 2019). FLS2 is K63-linked polyubiquitinated by the E3 ubiquitin ligases PUB12 and PUB13 after sensing of the flagellin peptide flg22 (Lu et al., 2011; Spallek et al., 2013). These E3 ligases also ubiquitinate LYK5 (Liao et al., 2017). FLS2 and CERK are also ubiquitinated and thus targeted for degradation by the bacterial effector AvrPto, thereby adding to the virulence by eliminating these RLK from the cell periphery (Goehre et al., 2008; Gimenez-Ibanez et al., 2009).

Mono-ubiquitination of several lysine residues in the cytosolic loop of IRT1 by the E3 ligase IDF1 (Shin et al., 2013) controls its internalization from the PM to the TGN/EE (Barberon et al., 2011) and a ubiquitination-defective IRT1 variant accumulates to the outer PM domain and is unable to reach the TGN/EE (Barberon et al., 2011). Abundance and localization of IRT1 is not regulated by iron availability (Barberon et al., 2011), but by non-iron metals, where an excess of those triggers the extension of multi mono-ubiquitins into K63-linked ubiquitin chains by the E3 ligase IDF1 and promotes vacuolar targeting of the transporter (Dubeaux et al., 2018; Cointry and Vert, 2019).

Under boron-limiting conditions, BOR1 is localized at the PM in a polar manner toward the stele, but in response to a boron excess, it is mono- or di-ubiquitinated in the *C*-terminal tail, endocytosed and transported to the vacuole for degradation to avoid the toxicity of boron accumulation (Kasai et al., 2011; Yoshinari and Takano, 2017). Substitution of a single lysine with alanine reduced ubiquitination under high boron concentrations but still allowed for endocytosis, although it completely blocked the degradation of BOR1. Thus, ubiquitination is necessary for BOR1 translocation to MVBs and degradation in the vacuole, but not required for the endocytosis of BOR1 (Kasai et al., 2011).

NITROGEN LIMITATION ADAPTION (NLA) is an E3 ligase that polyubiquitinates the high-affinity phosphate transporters (PHT1) (Park et al., 2014) and thus limits their levels at the PM under phosphate-sufficient conditions (Bayle et al., 2011). NLA also ubiquitinates the nitrate transporter NRT1.7 causing its down-regulation at the PM (Liu et al., 2017). BRI1 is post-translationally modified by ubiquitin or K63-linked ubiquitin chains, which promotes BRI1 internalization from the PM by

CME (Di Rubbo et al., 2013) and is essential for its recognition at the TGN/EE for vacuolar targeting (Martins et al., 2015). Multi-monoubiquitination causes internalization of the photoreceptor Phot1 from the cell surface under low blue light, but does not control its degradation (Roberts et al., 2011).

For the auxin efflux facilitator PIN2, a constitutively ubiquitinated version was endocytosed while a lysine deficient allele, *pin2K-R*, was no longer ubiquitinated and failed to be degraded in the vacuole (Leitner et al., 2012a). The in-frame fusion of this lysin deficient allele with ubiquitin, was still constitutively endocytosed but no longer sorted into the vacuolar compartment, strongly suggesting a requirement of K63-linked ubiquitination for efficient vacuolar targeting of PIN2 while mono-ubiquitination signals its endocytosis from the PM (Leitner et al., 2012a,b). In a plant line lacking both RGLG1 and 2, PIN2 ubiquitination was decreased, making it likely that these E3 ligases control PIN ubiquitination. This PIN2 polyubiquitination is dependent on certain stimuli, thus determining stability of PIN2 by influencing the rate of its vacuolar targeting (Leitner et al., 2012a).

Another single-subunit RING-type E3 ubiquitin ligase, RSL1 K63-polyubiquinates the abscisic acid (ABA) receptors PYL4 and PYR1 at the PM, targeting them to the vacuolar degradation pathway (Bueso et al., 2014), this process involves CME and trafficking of the receptors via the endosomal sorting complex required for transport (ESCRT) pathway (Belda-Palazon et al., 2016; Yu F. et al., 2016; Garcia-Leon et al., 2019).

It is evident that ubiquitination is involved in endocytosis and degradation of PM proteins in plants (Dubeaux and Vert, 2017), yet the direct mechanism of how ubiquitinated proteins are sorted into CCVs is still unclear. Interfering with CME by tampering with CHC function causes defect in the endocytosis of prominent PM proteins like the PINs, whose endocytosis is also controlled by ubiquitination (Luschnig and Vert, 2014), but the direct proof that disruption of CME causes accumulation of ubiquitinated cargos at the PM is still missing. In ubiquitin triggered CME, recruitment of ubiquitinated cargos into CCPs requires endocytic adaptor proteins, which contain UBDs. In mammals, monomeric endocytic adaptors proteins such as Eps15 and epsin, which additionally components of the CME machinery (Hawryluk et al., 2006), fulfill this function and collaborate with the ESCRT machinery to further sort cargos for degradation (Haglund and Dikic, 2012; Mayers et al., 2013; Schuh and Audhya, 2014). In contrast, the plant E/ANTH domain proteins, do not contain conserved UBDs, required for the interaction with ubiquitin (Holstein and Oliviusson, 2005; Zouhar and Sauer, 2014), indicating that ubiquitinated proteins are recognized at the PM by other plant-specific accessory adaptors recruiting cargos to the endocytic machinery (**Figure 4**). Endocytosis of the constitutively ubiquitinated PM cargos like PIN2 (Leitner et al., 2012a,b), PMA (Herberth et al., 2012), and BRI1 (Martins et al., 2015) depend on a hydrophobic patch centered around isoleucine 44 of ubiquitin, which is essential for the binding of ubiquitinated cargos by adaptor proteins containing UBDs (Dikic et al., 2009). For ubiquitin versions, where this isoleucine is mutated to an alanine (I44A), constitutive endocytosis of the ubiquitin-chimera is abolished (Leitner et al., 2012a; Korbei et al., 2013). Thus, internalization and degradation of constitutively ubiquitinated cargo involves their recognition proteins with UBDs. TARGET OF MYB1 (TOM1)-LIKE (TOL) proteins and SH3P2, are ubiquitin-binding protein that bind and transfer ubiquitinated proteins to the ESCRT machinery (Korbei et al., 2013; Nagel et al., 2017; Moulinier-Anzola et al., 2020) and might therefore compensate for the function in the endocytic adaptors that recognize ubiquitinated PM cargos and incorporate them into the nascent CCPs (**Figures 2**, **4**).

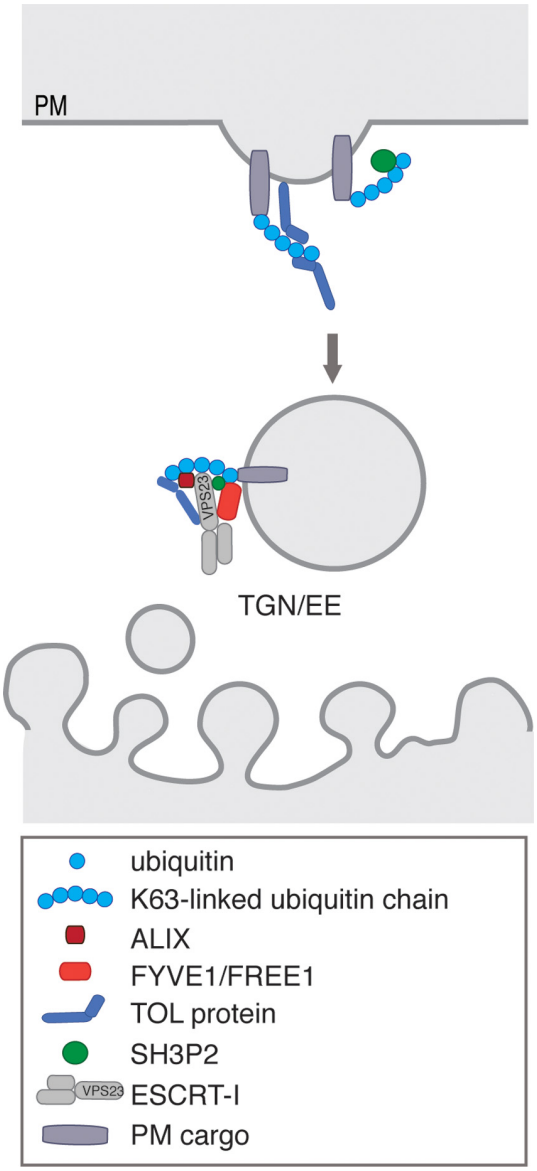

FIGURE 4 | Close up of the endosomal trafficking from the PM toward TGN/EE. TOLs and SH3P2 fulfill ubiquitin recognizing functions at the PM, possibly guiding K63-linked ubiquitinated cargo to the endosomal membrane and interacting with/recruiting ESCRT-I subunits. At the endosomal membrane, the ESCRT-I binding FYVE1/FREE1 and ALIX also shows interaction with ubiquitin. This reveals the complex synergy of several possible ubiquitin receptors in the ESCRT-mediated degradation pathway.

Other Plant Proteins in Clathrin-Mediated Endocytosis

Additional plant proteins play a role in CME, although their precise mechanisms are not known yet. STOMATAL CYTOKINESIS DEFECTIVE (SCD) 1 and 2, colocalize with CLC and co-fractionate with CCV (McMichael et al., 2013). The peripheral protein AT14A-LIKE 1 (AFL1), promotes growth during water stress and drought and localizes to the PM. It colocalizes with AP-2 and CLC and may function in endocytosis by regulating of actin filament organization (Kumar et al., 2015, 2019).

RECYCLING

Once internalized from the cell surface, not all endocytosed membrane proteins are transported for degradation to the vacuole but escape degradation by recycling back to the PM (**Figures 1**, **3**). (Paez Valencia et al., 2016). Recycling could thus enable a faster response to environmental changes without costly investments into *de novo* protein synthesis (Clague and Urbe, 2006). Plants do not possess endosomes specifically dedicated to recycling, but rather utilize the infrastructure provided by the TGN/EE and possibly early stages of the MVBs (Robinson and Neuhaus, 2016). The recycling machinery includes the small GTPases and their regulators as well as the retromer complex, while the ESCRT complex is responsible for transporting PM proteins to their degradation (Rodriguez-Furlan et al., 2019). The function of the retromer has been comprehensively reviewed very recently in (Rodriguez-Furlan et al., 2019).

Small GTPases

Small GTPases are monomeric proteins that bind and hydrolyze GTP to GDP, which in turns requires Guanine nucleotide exchange factors (GEFs) that facilitate GDP-to-GTP exchange. Small GTPases represent master regulators of membrane trafficking, as they activate downstream effectors and are important contributors to organelle identity (Uemura and Ueda, 2014; Fan et al., 2015; Paez Valencia et al., 2016). The small GTPases of the ADP-ribosylation factor (ARF) family function in the recycling of internalized PM proteins. Plants contain eight ARF-GEFs, classified into two subfamilies: the GBF subfamily, which includes the fungal toxin Brefeldin A-sensitive GNOM, and the BIG subfamily (Geldner et al., 2003; Richter et al., 2007). GNOM, localizes to a not well characterized endosomal compartment and acts directly on recycling of cargo (Geldner et al., 2003; Richter et al., 2007). GNOM has also been shown to localize to the Golgi apparatus though and thus plays a role in trafficking from the ER to the Golgi apparatus, allowing to speculate about indirect roles in endosomal recycling, via affecting the integrity of the TGN (Naramoto et al., 2014).

Deubiquitinating Enzymes and the ESCRT Machinery

A summary on the current knowledge an essential determinants for protein recycling is given in: Rodriguez-Furlan et al. (2019). Nevertheless, we would like discuss the effects of the ubiquitination status on protein fate, as proteins trafficking to the vacuole evade degradation by altering their ubiquitin modifications through DUBs (Isono and Nagel, 2014; Dubeaux and Vert, 2017).

Ubiquitination and deubiquitination occur constantly along the endosomal pathway and in mammals, several DUBs interact with ESCRT components to counterbalance the ubiquitination status of PM proteins destined for degradation. These ESCRT-DUBs interactions do not only control receptor fate through altering the ubiquitin code of the cargo at the initial steps, but also by influencing the function of the sorting complex (Clague and Urbe, 2006; Clague et al., 2019). Another important function of ESCRT associated DUBs is the deubiquitination of cargos that are already committed to inclusion into ILVs. Here, the DUBs degradation of alpha 4 (Doa4)/associated molecule with the SH3 domain of STAM (AMSH) in yeast/mammals function in the finals steps of the ESCRT pathway to deubiquitinate the cargo in order to maintain free ubiquitin levels (Clague and Urbe, 2006; Henne et al., 2011; Bissig and Gruenberg, 2014).

In the initial steps of the ESCRT pathway, the non-selective DUB ubiquitin-specific protease 8 (USP8/UBPY) and the stringent K63-linked chain selective DUB AMSH compete for binding to an ESCRT-0 subunit (Clague et al., 2019). The function of USP8 is to deubiquitinate and stabilize the ESCRT-0 complex (Row et al., 2006), while the K63-directed activity of AMSH promotes the deubiquitination and thus recycling of the cargo back to the PM (McCullough et al., 2004). Other reports also claim that AMSH may also directly regulate the function of the endocytic machinery, by altering the ubiquitination status and thus the activity of its components (Sierra et al., 2010). Other DUBs associated with the ESCRT-0 complex affect the ubiquitination status of the subunits, altering the ability of the ESCRT-0 subunits to bind to ubiquitin (Hoeller et al., 2006). USP8 also associates later on with ESCRT components, where it controls the ubiquitination state of one of the ESCRT-III subunits, charged multivesicular body protein (CHMP) 1B. This may promote its assembly into a membrane-associated polymer, which is needed for the budding of ILVs and thus represents a checkpoint for the temporal and spatial assembly of the ESCRT machinery (Crespo-Yanez et al., 2018). DUBs therefore interact with ESCRT components to modulate the ubiquitination status of cargos, or to that of the components of the machinery to control the function of the ESCRT complex and the fate of the ubiquitinated cargo (Wright et al., 2011).

Arabidopsis contains three AMSH-like proteins, where AMSH 1 and 3 associate with subunits of the ESCRT machinery and show a specificity toward K63-linked ubiquitin chains, but can also trim K48 linked chains (Isono et al., 2010). AMSH1 interacts with the ESCRT-III-subunit VPS2.1 are plays a role in autophagic degradation, its knockdown mutant does not have an apparent growth defect (Katsiarimpa et al., 2013). AMSH3 on the other hand is essential for seedling development and proper vacuolar trafficking of both biosynthetic and endocytosed cargo. It also interacts with ESCRT-III subunits VPS2.1 and also VPS24.1. AMSH3 and another ESCRT component, SUPPRESSOR OF K^+ TRANSPORT GROWTH DEFECT 1 (SKD1) compete

for binding to VPS2.1 and this interaction is important for deubiquitination of ubiquitinated membrane substrates prior to their degradation in plants (Katsiarimpa et al., 2011, 2014). AMSH3 is recruited to endosomes through a direct interaction with apoptosis-linked gene-2 interacting protein X (ALIX), a conserved ESCRT-related protein that binds membranes, ubiquitin, and ESCRT components (Kalinowska et al., 2015). Furthermore, AMSH3 associates with SH3P2 and an ESCRT-I subunit on CCV (Nagel et al., 2017). Although AMSH proteins display DUB activity *in vitro*, and ubiquitin-binding proteins like SH3P2 could facilitate the access of DUBs to ubiquitin chains early on in the endocytic pathway, no plant DUB has so far been directly associated with deubiquitination of cargo for recycling (Isono and Nagel, 2014).

DEGRADATIVE SORTING

Proteins that are not recycled back to the PM from the TGN/EE are destined for degradation and proceed further downstream in the endocytic pathway to the vacuole (Paez Valencia et al., 2016; Otegui, 2018). The ESCRT machinery is an evolutionarily conserved, multi-subunit membrane remodeling complex, with the ability to form membrane budding away from the cytosol. It is therefore very different from the machineries involved in the curvature into the cytosol as in the formation of the CCVs and most other vesiculation events (Paez Valencia et al., 2016; Gao et al., 2017; Isono and Kalinowska, 2017). As the endosomal membranes of the TGN/EEs become capable of associating with ESCRT proteins, they start internalizing portions of their limiting membrane into ILVs, and then gradually mature into MVBs, that ultimately fuses with vacuoles, releasing their contents for degradation (Otegui, 2018).

The ESCRT Machinery

The ESCRT machinery plays an essential role in the biogenesis of the MVBs and the sorting of ubiquitinated membrane proteins for degradation (Henne et al., 2011; Paez Valencia et al., 2016; Gao et al., 2017; Isono and Kalinowska, 2017). This starts with cargo recognition and recruitment of the remodeling machinery in a stepwise process, performed by a series of protein complexes termed ESCRT-0 to ESCRT-III and various accessory components, which act in recognition, concentration and sequestering of ubiquitinated cargo into the ILVs and the membrane deforming events essential for this procedure (Henne et al., 2011; Paez Valencia et al., 2016; Gao et al., 2017; Isono and Kalinowska, 2017). The ESCRT-0 complex is required for initial targeting and concentration of ubiquitinated cargo and further recruits the ESCRT-I, to which it passes on the ubiquitinated cargo (Hurley, 2010). The ESCRT-I further recruits the ESCRT-II to endosomes and the presence of both complexes induces the invagination of the limiting membrane toward the endosomal lumen (Hurley, 2010). ESCRT-I and II complexes could also act in parallel to concentrate the ubiquitinated cargo (Hurley, 2008; Hurley and Ren, 2009). The upstream components recruit, activate, and organize the polymerization of ESCRT-III, which does not contain any known UBD. The ubiquitin molecule is removed from the cargo proteins by DUB activity, once the ESCRTs are assembled. In a final step, an AAA ATPase, whose recruitment and activity is mediated by ESCRT-III related proteins, recycles the ESCRT-III back into its monomeric form (Hurley and Hanson, 2010; Schoneberg et al., 2017).

ESCRT-0

The ESCRT-0 complex, which binds and recruits the ESCRT-I, is the made up of two subunits the Vps27/hepatocyte growth factor-regulated tyrosine kinase substrate (HRS) and the Hse1 (Hbp STAM, EAST 1)/signal transducing adaptor molecule (STAM) in yeast/humans (Raiborg and Stenmark, 2009; Henne et al., 2011). It is found at EE and at the PM, although the precise starting point for the interaction of ESCRT-0 with ubiquitin is still under debate (Mayers et al., 2013). It is suggested to preassemble with cargos at the PM at CCPs, where it enhances the efficiency of sorting-events, without affecting the CCVs formation (Mayers et al., 2013). The core structure of the ESCRT-0 complex is made up of two antiparallel intertwined GAT (GGA and TOM1) domains flanked by further α-helical UBDs. This higher order multimeric structure, with its conformational plasticity, allows for recognition of different ubiquitinated cargos and provides a strong ubiquitin-binding platform (Ren and Hurley, 2010; Piper et al., 2014). The ESCRT-0 associates preferentially with K63-linked ubiquitin chains and blocks their binding to proteasomes, thus preventing proteasomal degradation and enhancing lysosomal/vacuolar degradation of cargo proteins (Nathan et al., 2013). Some ESCRT-0 subunits can recruit DUBs, allowing for modulation in the ubiquitination pattern of the cargo as well as of subunits of the machinery (Raiborg and Stenmark, 2009; Wright et al., 2011). The ESCRT-0 interacts with clathrin and this binding to the flat clathrin lattice restricts ESCRT-0 distribution on the endosomes and allows for the clustering of ubiquitinated cargo into microdomains (Schuh and Audhya, 2014). Furthermore, targeting to EEs, is assisted by the Fab 1, YOTB, Vac 1, and EEA1 (FYVE) domains of Vps27/HRS, which, in yeast/mammals binds the EE associated PtdIn(3)P (Hurley, 2010).

While the other ESCRT machinery complexes are ubiquitous in eukaryotes and ancient in origin, the ESCRT-0 appears to be a more recent addition and is as such not present in plants (Winter and Hauser, 2006; Leung et al., 2008). Potential candidates to substitute for this complex involve the TOM1 protein family, which share the same tandem array of *N*-terminal domains, the VHS (Vps27/HRS/Stam) and GAT domain, which are able to bind ubiquitin and potentially membranes (Mosesso et al., 2019). A complex centering around TOM1, functioning either parallel, as in mammals (Wang et al., 2010) or alternatively, as in ameba (Blanc et al., 2009), to the ESCRT-0 complex, has been described. TOM1L1 has also been proposed to package ubiquitinated PM proteins into CCVs (Liu et al., 2009). TOM1 is widely conserved in eukaryotes and from its phylogenetic distribution, it is likely to have been either replaced or perhaps supplemented by ESCRT-0 in opisthokonts (Herman et al., 2011). Additionally, other plant candidates, with similar functional attributes to the ESCRT-0 could also substitute the elusive ESCRT-0 complex in plants (Mosesso et al., 2019).

ESCRT-I

The ESCRT-I complex forms an elongated hetero-tetrameric complex in yeast/mammals, which contains one copy each subunit: Vps23/tumor susceptibility gene-101 (TSG101), VPS28, VPS37, and MVB sorting factor of 12 kDa (MVB12) or the Mvb12-like subunit ubiquitin-associated protein 1 (UBAP1) (Schuh and Audhya, 2014). The Vps23/TSG101 subunit has a UBD at its *N*-terminus, the ubiquitin E2 variant (UEV) domain. This domain has a dual function as it is responsible the binding the ubiquitinated cargo and a subunit of the ESCRT-0, via the P[S/T]AP motif in ESCRT-0 (Bache et al., 2003; Hicke and Dunn, 2003). Furthermore, the VPS28 is responsible for binding of the ESCRT-II via its *C*-terminus (Kostelansky et al., 2007).

Arabidopsis contains two isoforms of each of the ESCRT-I subunits VPS23 (ELC/VPS23A and VPS23B), VPS28 (VPS28-1 and VPS28-2), and VPS37 (VPS37-1 and VPS37-2), but no obvious Mvb12-like proteins (Winter and Hauser, 2006; Leung et al., 2008). VPS23A binds ubiquitin and associates with VPS37 and VPS28 in a putatively intact plant ESCRT-I complex. It participates in trichome development and cell division (Spitzer et al., 2006) and was found to be important in ABA signaling by affecting the subcellular localization and stability of ABA receptors via vacuole-mediated degradation (Yu F. et al., 2016). *vps28-2* and *vps37-1* mutant plants display altered endosomal sorting of the pathogen-related receptor FLS2 and are compromised in pathogen responses, but develop normally otherwise, suggesting functional redundancy with the other VPS28 and VPS37 isoforms (Spallek et al., 2013).

ESCRT-II

The ESCRT-II links the upstream ubiquitin-binding ESCRT complexes to the downstream ESCRT-III complex and is made up of the subunits VPS22, VPS25, and VPS36, which assemble in a Y-shaped 1:2:1 hetero-tetramer (Hurley, 2010). All ESCRT-II subunits are present in single copies in *A. thaliana* (Winter and Hauser, 2006; Leung et al., 2008; Richardson et al., 2011). The *vps22* mutant in rice causes seedling lethality, yet whether endosomal sorting is affected remains to be determined (Zhang et al., 2013). VPS36 binds ubiquitin and forms a putative ESCRT-II with VPS22 and VPS25. It is essential for MVB formation, vacuolar biogenesis and the endosomal sorting of several PM proteins into the vacuole for degradation (Wang S. L. et al., 2017).

ESCRT-III

The ESCRT-III, which does not bind ubiquitinated cargos anymore, is critical for membrane scission during sorting of the cargo into ILVs (Henne et al., 2012). For plant ILVs it was recently shown that they form networks of concatenated vesicles that bud in the lumen of MVBs instead individual vesicles. These concatenated ILVs remain connected by narrow bridges, thus trapping the cargo and the ESCRT-III could act as diffusion barriers to prevent the escape of the cargos destined for degradation (Buono et al., 2017).

Membrane recruitment of the ESCRT-III is initiated by binding to ESCRT-II subunit VPS25 to VPS20, when inactive monomers from the cytosol polymerize into the active ESCRT-III (Hurley, 2010; Schuh and Audhya, 2014). In yeast/animals the core ESCRT-III consists of four small, highly charged subunits, which polymerize into long spiral filaments on highly curved membranes: Vps2p/CHMP2, Vps20p/CHMP6, Vps24p/CHMP3, and Snf7p (Sucrose Non-Fermenting 7)/CHMP4, (Shen et al., 2014). Furthermore, there are three accessory proteins, Did2 (Doa4-independent degradation 2)/CHMP1, Vps60/CHMP5, and increased salt tolerance 1 (IST1). IST1 modulate the activity of the ESCRT-III complex, as well as its association with the Vps4/SKD1 complex (Raiborg and Stenmark, 2009).

The ESCRT-III machinery is conserved in plant cells (Cai et al., 2014) and all core subunits in *Arabidopsis*, have two homologs, except for VPS2, which has three (Winter and Hauser, 2006), however, only VPS2.1 functions as a classical ESCRT subunit and binds the DUB AMSH3 (Katsiarimpa et al., 2011). Transient over-expression of dominant negative core ESCRT-III subunits resulted in defects in vacuolar biogenesis and MVB formation with less ILVs (Cai et al., 2014).

The accessory ESCRT-III related *Arabidopsis* protein CHMP1 interacts with the Vps4/SKD1 complex to regulate MVB biogenesis. The *chmp1a/chmp1b* double-mutants of the two functionally redundant *CHMP1* genes, exhibits embryonic or early seedling lethality and fail to sort PIN1 into ILVs (Spitzer et al., 2009). The maize ortholog supernumerary aleurone layer 1 (SAL1), regulates endosomal sorting and degradation of PM proteins and is therefore necessary for aleurone endosperm differentiation (Shen et al., 2003; Tian et al., 2007). For the *Arabidopsis* homolog of yeast IST1, there are 12 IST1-like proteins (ISTL1–12), however, only ISTL1 has been shown to function in the ESCRT pathway, where it interacts with Lyst-interacting protein 5 (LIP5), SKD1 and CHMP1A and is predicted to regulate MVB biogenesis and sorting of membrane proteins for degradation (Buono et al., 2016).

Vps4/SKD1 and Accessory Proteins

Through ATP hydrolysis, the AAA ATPase Vps4/SKD1, disassembles the ESCRT-III complex, allowing for recycling of the ESCRT III subunits. This step is crucial for the completion of the membrane scission in the formation of ILVs, after which MVBs can fuse with the vacuole/lysosomes, where ILVs are released for degradation (Hurley, 2010; Schuh and Audhya, 2014). Vps4/SKD1 interacts with VPS 20-associated 1 (Vta1)/LIP5, which stabilizes its oligomeric conformation, thus functioning as a positive regulator for its activity (Schuh and Audhya, 2014).

In *Arabidopsis*, there is only one Vps4/SKD1 homolog named SKD1, which localizes to the cytoplasm and MVBs. Its ATPase activity is positively regulated by LIP5 (Haas et al., 2007), and disruption of *SKD1* is lethal, while *lip5* mutants are normal in growth and development. Though LIP5 is not necessary for plant survival, it is essential for normal responses to biotic and abiotic stresses (Haas et al., 2007; Wang et al., 2014, 2015). A SKD1 ortholog from *Zea mays* (ZmSKD1), which is up-regulated by salt or drought stress, interacts with NtLIP5 (LIP5 from *Nicotiana tabacum*) (Xia et al., 2013). PROS (POSITIVE REGULATOR OF SKD1) is a flowering plant-specific ESCRT protein that interacts with SKD1 and increases its ATPase activity *in vitro*.

It is thus, like LIP5, another positive regulator of the SKD1, although the two are structurally different. Silencing of PROS leads to reduced cell expansion and abnormal organ growth (Reyes et al., 2014).

Another ESCRT related protein is the yeast/mammalian bypass of C kinase 1 (BCK1)-like resistance to osmotic shock 1p (Bro1)/ALIX. Both were shown to interact with ESCRT-III, however, only the mammalian ALIX, also interacts with ESCRT-I subunits, therefore having the potential to bridge the ESCRT-I and ESCRT-III complexes (Bissig and Gruenberg, 2014). Loss of Bro1 affects ILV formation, as it regulates the membrane-scission activity of ESCRT-III via binding to Snf7 (Wemmer et al., 2011). Bro1/ALIX bind ubiquitin, specifically K63-linked ubiquitin (Dowlatshahi et al., 2012), suggesting they may function as ubiquitin receptor for protein sorting into MVBs, in addition to ESCRT-0 (Pashkova et al., 2013; Mosesso et al., 2019).

In *Arabidopsis* the conserved ESCRT-related protein ALIX (**Figure 4**), binds membranes, ubiquitin, the ESCRT-I subunit VPS23A and the ESCRT-III subunit SNF7 and is indispensable for the biogenesis of the vacuole and MVB and thus for plant growth and development (Cardona-Lopez et al., 2015; Kalinowska et al., 2015; Shen et al., 2018). ALIX recruits AMSH3 to endosomes through direct interaction (Kalinowska et al., 2015). Furthermore, ALIX, mediates trafficking to the vacuole of PHT1, BRI1 but also ABA receptors, to which ALIX can even bind directly (Cardona-Lopez et al., 2015; Garcia-Leon et al., 2019). ALIX associated with VPS23A and FYVE1/FREE1 to be incorporated into the ESCRT-I complex and thus may also function in bridging ESCRT-I and ESCRT-III complexes in plants (Shen et al., 2016).

Plant-Specific ESCRT Components

In plants, there are several plant unique components with limited protein sequence similarity to the mammalian/yeast ESCRT subunits that interact with known plant ESCRT subunits and help shape and regulate ESCRT-dependent processes.

SH3 Domain Containing Protein-2

The ubiquitin binding protein SH3P2 belongs, together with SH3P1 and SH3P3, to a family of three proteins in *A. thaliana*, with a central BAR domain, acting in membrane curvature generation and present in proteins involved in CME and a *C*-terminal SH3 domain, which functions in protein–protein interactions (Lam et al., 2001; Zhuang et al., 2013). It has been implicated in as vacuolar trafficking of ubiquitinated cargos and has been shown to bind K63-linked ubiquitin, the ESCRT-I subunit VPS23A and the DUB AMSH3. It further localizes to CCV and could thus also function as an ESCRT-0 substitute (**Figure 4**) (Kolb et al., 2015; Nagel et al., 2017; Mosesso et al., 2019). SH3P2 was further shown to interact with CLC1 and found in a complex potentially involved in CME with two putative homologs of the CCV uncoating factor auxilin and the ANTH domain protein CAP1 (Adamowski et al., 2018).

FYVE1/FREE1

An ESCRT-I-related component called FYVE1/FREE1 (FYVE DOMAIN PROTEIN REQUIRED FOR ENDOSOMAL SORTING 1) (**Figure 4**) was identified in *Arabidopsis*, where it localizes to MVBs, binds ubiquitin, PtdIn(3)P, interacts with SH3P2, VPS23A, and VPS23B via its PTAP-like motifs and with SNF7 to be incorporated into the ESCRT-III complex, yet not with the TOLs. It is essential for the formation of ILVs, vacuolar biogenesis, autophagic degradation, seedling development, polar localization of the iron transporter IRT1 and degradation of PM proteins and ABA receptors (Barberon et al., 2014; Gao et al., 2014; Kolb et al., 2015; Belda-Palazon et al., 2016). Additionally, FYVE1/FREE1 has a non-endosomal function in attenuating ABA signaling, where following ABA treatment FYVE1/FREE1 is phosphorylate causing its nuclear import, where it interacts with the ABA-responsive transcription to reduce their binding to the *cis*-regulatory sequences of downstream genes (Li et al., 2019). FYVE1/FREE1 recruitment to the MVBs is regulated by a plant-specific Bro1-domain protein BRAF, which competes with FYVE1/FREE1 in its binding to VPS23A. Thus, BRAF functions as an ESCRT regulator, as its depletion increases FYVE1/FREE1 association with MVB membranes (Shen et al., 2018).

TOM1-Like Proteins

Many eukaryotic groups, do not have ESCRT-0 components and therefore need to rely on other proteins to initially recognize ubiquitinated cargo at the PM (Mosesso et al., 2019). *Arabidopsis* has a family of nine proteins, TOL1-9, with a domain organization similar to the ESCRT-0, demonstrated to be crucial in vacuolar targeting of ubiquitinated PM proteins (Korbei et al., 2013; Yoshinari et al., 2018; Moulinier-Anzola et al., 2020). Members of the TOL protein family, interact with ESCRT-I subunits and bind ubiquitin, with a pronounced substrate preference to K63-linked ubiquitin. This could be caused by the tandemly arranged UBDs in the *N*-terminus of all nine TOL proteins, as mutations of these domains resulted in complete loss of ubiquitin binding. These UBDs, could thus regulate fidelity and kinetics of the sorting of endocytosed ubiquitinated cargo and the TOLs could function as multivalent ubiquitin-binding complexes (**Figure 4**) (Moulinier-Anzola et al., 2020).

Interaction between TOLs and ubiquitinated PM proteins destined for degradation are not clear at present as TOLs were shown to exhibit differences in their subcellular localization, from PM- and EE/TGN-localized TOLs to cytoplasmic ones, indicating they might have activities in different subcellular sites (Moulinier-Anzola et al., 2020). TOL5, with its cytoplasmic localization has been described to function at MVBs, where it co-localizes with BOR1 on its route to the vacuole under high-boron conditions (Yoshinari et al., 2018), while TOL6 functions at the PM in the degradation of PIN2 (Korbei et al., 2013). As only higher order TOL knockouts sufficiently inhibit the down-regulation of PM-localized ubiquitinated proteins (Korbei et al., 2013; Moulinier-Anzola et al., 2020), the TOLs could function in a network in the plant endomembrane system, where they pass on the ubiquitinated cargo, but this of course awaits further assessment (**Figure 4**). TOL ubiquitin receptors are themselves ubiquitinated, which serves as a regulatory signal, influencing their sub-cellular distribution and thus could help to

regulate the efficiency of the degradation of PM localized cargo (Moulinier-Anzola et al., 2020).

Plants have to be able to cope sensitively and accurately to their often times harsh environment and to adapt quickly to immanent changes. The necessity of the sessile plants to fine-tune and control the abundance of their PM proteins to be able to respond quickly and precisely is reflected in high number of plant-specific factors, next to the conserved canonical trafficking machinery, in the ubiquitin-dependent degradation of membrane proteins. Thus, many plant-specific proteins have been shown to be involved in the regulation of endosomal trafficking and endocytosis and some ESCRT subunits have undergone drastic gene expansions. Furthermore, recent publications point to extensive crosstalk of diverse signaling- and trafficking pathways, where specific ESCRT proteins may even fulfill additional roles (Gao et al., 2017; Cui et al., 2018; Vietri et al., 2020). Thus, to thoroughly understand the molecular mechanisms underlying the regulation of ESCRT-dependent degradation of ubiquitinated proteins will be of decisive importance to fully understand plant adaptation processes to a changing environment.

AUTHOR CONTRIBUTIONS

BK wrote the first draft of the manuscript. MS wrote sections of the manuscript. Both authors contributed to manuscript revision, read, and approved the submitted version.

FUNDING

This work has been supported by grants from the Austrian Science Fund (FWF P30850).

ACKNOWLEDGMENTS

We would like to thank Christian Luschnig for critically reading the manuscript. We apologize to those colleagues whose work we were unable to cover due to space restrictions. An adapted version of this article was part of the habilitation thesis submitted by Barbara Korbei in 2019.

REFERENCES

Abas, L., Benjamins, R., Malenica, N., Paciorek, T., Wisniewska, J., Moulinier-Anzola, J. C., et al. (2006). Intracellular trafficking and proteolysis of the *Arabidopsis* auxin-efflux facilitator PIN2 are involved in root gravitropism. *Nat. Cell Biol.* 8, 249–256. doi: 10.1038/ncb1369

Adamowski, M., and Friml, J. (2015). PIN-dependent auxin transport: action, regulation, and evolution. *Plant Cell* 27, 20–32. doi: 10.1105/tpc.114.134874

Adamowski, M., Narasimhan, M., Kania, U., Glanc, M., De Jaeger, G., and Friml, J. (2018). A functional study of AUXILIN-LIKE1 and 2, two putative clathrin uncoating factors in *Arabidopsis*. *Plant Cell* 30, 700–716. doi: 10.1105/tpc.17.00785

Aguilar-Hernandez, V., Kim, D. Y., Stankey, R. J., Scalf, M., Smith, L. M., and Vierstra, R. D. (2017). Mass spectrometric analyses reveal a central role for ubiquitylation in remodeling the *Arabidopsis* proteome during photomorphogenesis. *Mol. Plant* 10, 846–865. doi: 10.1016/j.molp.2017.04.008

Ahn, G., Kim, H., Kim, D. H., Hanh, H., Yoon, Y., Singaram, I., et al. (2017). SH3 domain-containing protein 2 plays a crucial role at the step of membrane tubulation during cell plate formation. *Plant Cell* 29, 1388–1405. doi: 10.1105/tpc.17.00108

Bache, K. G., Raiborg, C., Mehlum, A., and Stenmark, H. (2003). STAM and Hrs are subunits of a multivalent ubiquitin-binding complex on early endosomes. *J. Biol. Chem.* 278, 12513–12521. doi: 10.1074/jbc.M210843200

Banbury, D. N., Oakley, J. D., Sessions, R. B., and Banting, G. (2003). Tyrphostin A23 inhibits internalization of the transferrin receptor by perturbing the interaction between tyrosine motifs and the medium chain subunit of the AP-2 adaptor complex. *J. Biol. Chem.* 278, 12022–12028. doi: 10.1074/jbc.M211966200

Bar, M., Aharon, M., Benjamin, S., Rotblat, B., Horowitz, M., and Avni, A. (2008). AtEHDs, novel *Arabidopsis* EH-domain-containing proteins involved in endocytosis. *Plant J.* 55, 1025–1038. doi: 10.1111/j.1365-313X.2008.03571.x

Barberon, M., Dubeaux, G., Kolb, C., Isono, E., Zelazny, E., and Vert, G. (2014). Polarization of IRON-REGULATED TRANSPORTER 1 (IRT1) to the plant-soil interface plays crucial role in metal homeostasis. *Proc. Natl. Acad. Sci. U.S.A.* 111, 8293–8298. doi: 10.1073/pnas.1402262111

Barberon, M., Zelazny, E., Robert, S., Conejero, G., Curie, C., Friml, J., et al. (2011). Monoubiquitin-dependent endocytosis of the iron-regulated transporter 1 (IRT1) transporter controls iron uptake in plants. *Proc. Natl. Acad. Sci. U.S.A.* 108, E450–E458. doi: 10.1073/pnas.1100659108

Barth, M., and Holstein, S. E. (2004). Identification and functional characterization of *Arabidopsis* AP180, a binding partner of plant alphaC-adaptin. *J. Cell Sci.* 117(Pt 10), 2051–2062. doi: 10.1242/jcs.01062

Bashline, L., Li, S., Anderson, C. T., Lei, L., and Gu, Y. (2013). The endocytosis of cellulose synthase in *Arabidopsis* is dependent on mu2, a clathrin-mediated endocytosis adaptin. *Plant Physiol.* 163, 150–160. doi: 10.1104/pp.113.221234

Bassham, D. C., Brandizzi, F., Otegui, M. S., and Sanderfoot, A. A. (2008). The secretory system of *Arabidopsis*. *Arabidopsis Book* 6:e0116.

Bayle, V., Arrighi, J. F., Creff, A., Nespoulous, C., Vialaret, J., Rossignol, M., et al. (2011). *Arabidopsis thaliana* high-affinity phosphate transporters exhibit multiple levels of posttranslational regulation. *Plant Cell* 23, 1523–1535. doi: 10.1105/tpc.110.081067

Bednarek, S. Y., and Backues, S. K. (2010). Plant dynamin-related protein families DRP1 and DRP2 in plant development. *Biochem. Soc. Trans.* 38, 797–806. doi: 10.1042/Bst0380797

Belda-Palazon, B., Rodriguez, L., Fernandez, M. A., Castillo, M. C., Anderson, E. A., Gao, C., et al. (2016). FYVE1/FREE1 interacts with the PYL4 ABA receptor and mediates its delivery to the vacuolar degradation pathway. *Plant Cell.* 28, 2291–2311. doi: 10.1105/tpc.16.00178

Bissig, C., and Gruenberg, J. (2014). ALIX and the multivesicular endosome: ALIX in wonderland. *Trends Cell Biol.* 24, 19–25. doi: 10.1016/j.tcb.2013.10.009

Blanc, C., Charette, S. J., Mattei, S., Aubry, L., Smith, E. W., Cosson, P., et al. (2009). Dictyostelium Tom1 participates to an ancestral ESCRT-0 complex. *Traffic* 10, 161–171. doi: 10.1111/j.1600-0854.2008.00855.x

Bonifacino, J. S., and Traub, L. M. (2003). Signals for sorting of transmembrane proteins to endosomes and lysosomes. *Annu. Rev. Biochem.* 72, 395–447. doi: 10.1146/annurev.biochem.72.121801.161800

Bueso, E., Rodriguez, L., Lorenzo-Orts, L., Gonzalez-Guzman, M., Sayas, E., Munoz-Bertomeu, J., et al. (2014). The single-subunit RING-type E3 ubiquitin ligase RSL1 targets PYL4 and PYR1 ABA receptors in plasma membrane to modulate abscisic acid signaling. *Plant J.* 80, 1057–1071. doi: 10.1111/tpj.12708

Buono, R. A., Leier, A., Paez-Valencia, J., Pennington, J., Goodman, K., Miller, N., et al. (2017). ESCRT-mediated vesicle concatenation in plant endosomes. *J. Cell Biol.* 216, 2167–2177. doi: 10.1083/jcb.201612040

Buono, R. A., Paez-Valencia, J., Miller, N. D., Goodman, K., Spitzer, C., Spalding, E. P., et al. (2016). Role of SKD1 regulators LIP5 and IST1-LIKE1 in endosomal sorting and plant development. *Plant Physiol.* 171, 251–264. doi: 10.1104/pp.16.00240

Cai, Y., Zhuang, X. H., Gao, C. J., Wang, X. F., and Jiang, L. W. (2014). The *Arabidopsis* endosomal sorting complex required for transport III regulates internal vesicle formation of the prevacuolar compartment and is required for plant development. *Plant Physiol.* 165, 1328–1343. doi: 10.1104/pp.114.238378

Callis, J. (2014). The ubiquitination machinery of the ubiquitin system. *Arabidopsis Book* 12:e0174. doi: 10.1199/tab.0174

Cardona-Lopez, X., Cuyas, L., Marin, E., Rajulu, C., Irigoyen, M. L., Gil, E., et al. (2015). ESCRT-III-associated protein ALIX mediates high-affinity phosphate transporter trafficking to maintain phosphate homeostasis in *Arabidopsis*. *Plant Cell* 27, 2560–2581. doi: 10.1105/tpc.15.00393

Chen, X., Irani, N. G., and Friml, J. (2011). Clathrin-mediated endocytosis: the gateway into plant cells. *Curr. Opin. Plant Biol* 14, 674–682. doi: 10.1016/j.pbi.2011.08.006

Clague, M. J., Liu, H., and Urbe, S. (2012). Governance of endocytic trafficking and signaling by reversible ubiquitylation. *Dev. Cell* 23, 457–467. doi: 10.1016/j.devcel.2012.08.011

Clague, M. J., and Urbe, S. (2006). Endocytosis: the DUB version. *Trends Cell Biol.* 16, 551–559. doi: 10.1016/j.tcb.2006.09.002

Clague, M. J., Urbe, S., and Komander, D. (2019). Breaking the chains: deubiquitylating enzyme specificity begets function. *Nat. Rev. Mol. Cell Biol.* 20, 338–352. doi: 10.1038/s41580-019-0099-1

Cocucci, E., Aguet, F., Boulant, S., and Kirchhausen, T. (2012). The first five seconds in the life of a clathrin-coated pit. *Cell* 150, 495–507. doi: 10.1016/j.cell.2012.05.047

Cointry, V., and Vert, G. (2019). The bifunctional transporter-receptor IRT1 at the heart of metal sensing and signalling. *New Phytol.* 223, 1173–1178. doi: 10.1111/nph.15826

Crespo-Yanez, X., Aguilar-Gurrieri, C., Jacomin, A. C., Journet, A., Mortier, M., Taillebourg, E., et al. (2018). CHMP1B is a target of USP8/UBPY regulated by ubiquitin during endocytosis. *PLoS Genet.* 14:e1007456. doi: 10.1371/journal.pgen.1007456

Cui, Y., He, Y. L., Cao, W. H., Gao, J. Y., and Jiang, L. W. (2018). The multivesicular body and autophagosome pathways in plants. *Front. Plant Sci.* 9:1837. doi: 10.3389/fpls.2018.01837

Dannhauser, P. N., and Ungewickell, E. J. (2012). Reconstitution of clathrin-coated bud and vesicle formation with minimal components. *Nat. Cell Biol.* 14, 634–639. doi: 10.1038/ncb2478

Day, K. J., Casler, J. C., and Glick, B. S. (2018). Budding yeast has a minimal endomembrane system. *Dev. Cell* 44, 56.e4–72.e4. doi: 10.1016/j.devcel.2017.12.014

d'Azzo, A., Bongiovanni, A., and Nastasi, T. (2005). E3 ubiquitin ligases as regulators of membrane protein trafficking and degradation. *Traffic* 6, 429–441. doi: 10.1111/j.1600-0854.2005.00294.x

Dejonghe, W., Kuenen, S., Mylle, E., Vasileva, M., Keech, O., Viotti, C., et al. (2016). Mitochondrial uncouplers inhibit clathrin-mediated endocytosis largely through cytoplasmic acidification. *Nat. Commun.* 7:11710. doi: 10.1038/ncomms11710

Dejonghe, W., Sharma, I., Denoo, B., De Munck, S., Lu, Q., Mishev, K., et al. (2019). Disruption of endocytosis through chemical inhibition of clathrin heavy chain function. *Nat. Chem. Biol.* 15, 641–649. doi: 10.1038/s41589-019-0262-1

Dettmer, J., Hong-Hermesdorf, A., Stierhof, Y. D., and Schumacher, K. (2006). Vacuolar H+-ATPase activity is required for endocytic and secretory trafficking in *Arabidopsis*. *Plant Cell* 18, 715–730. doi: 10.1105/tpc.105.037978

Dhonukshe, P., Aniento, F., Hwang, I., Robinson, D. G., Mravec, J., Stierhof, Y. D., et al. (2007). Clathrin-mediated constitutive endocytosis of PIN auxin efflux carriers in *Arabidopsis*. *Curr. Biol.* 17, 520–527. doi: 10.1016/j.cub.2007.01.052

Di Rubbo, S., Irani, N. G., Kim, S. Y., Xu, Z. Y., Gadeyne, A., Dejonghe, W., et al. (2013). The clathrin adaptor complex AP-2 mediates endocytosis of brassinosteroid insensitive1 in *Arabidopsis*. *Plant Cell* 25, 2986–2997. doi: 10.1105/tpc.113.114058

Dikic, I., Wakatsuki, S., and Walters, K. J. (2009). Ubiquitin-binding domains - from structures to functions. *Nat. Rev. Mol. Cell Biol.* 10, 659–671. doi: 10.1038/nrm2767

Dowlatshahi, D. P., Sandrin, V., Vivona, S., Shaler, T. A., Kaiser, S. E., Melandri, F., et al. (2012). ALIX is a Lys63-specific polyubiquitin binding protein that functions in retrovirus budding. *Dev. Cell* 23, 1247–1254. doi: 10.1016/j.devcel.2012.10.023

Dubeaux, G., Neveu, J., Zelazny, E., and Vert, G. (2018). Metal sensing by the IRT1 transporter-receptor orchestrates its own degradation and plant metal nutrition. *Mol. Cell.* 69, 953.e5–964.e5. doi: 10.1016/j.molcel.2018.02.009

Dubeaux, G., and Vert, G. (2017). Zooming into plant ubiquitin-mediated endocytosis. *Curr. Opin. Plant Biol.* 40, 56–62. doi: 10.1016/j.pbi.2017.07.005

Eisenberg, E., and Greene, L. E. (2007). Multiple roles of auxilin and Hsc70 in clathrin-mediated endocytosis. *Traffic* 8, 640–646. doi: 10.1111/j.1600-0854.2007.00568.x

Ekanayake, G., LaMontagne, E. D., and Heese, A. (2019). Never walk alone: clathrin-coated vesicle (CCV) components in plant immunity. *Annu. Rev. Phytopathol.* 57, 387–409. doi: 10.1146/annurev-phyto-080417-45841

Erpapazoglou, Z., Walker, O., and Haguenauer-Tsapis, R. (2014). Versatile roles of k63-linked ubiquitin chains in trafficking. *Cells* 3, 1027–1088. doi: 10.3390/cells3041027

Erwig, J., Ghareeb, H., Kopischke, M., Hacke, R., Matei, A., Petutschnig, E., et al. (2017). Chitin-induced and CHITIN ELICITOR RECEPTOR KINASE1 (CERK1) phosphorylation-dependent endocytosis of *Arabidopsis thaliana* LYSIN MOTIF-CONTAINING RECEPTOR-LIKE KINASE5 (LYK5). *New Phytol.* 215, 382–396. doi: 10.1111/nph.14592

Fan, L., Hao, H., Xue, Y., Zhang, L., Song, K., Ding, Z., et al. (2013). Dynamic analysis of *Arabidopsis* AP2 sigma subunit reveals a key role in clathrin-mediated endocytosis and plant development. *Development* 140, 3826–3837. doi: 10.1242/dev.095711

Fan, L. S., Li, R. L., Pan, J. W., Ding, Z. J., and Lin, J. X. (2015). Endocytosis and its regulation in plants. *Trends Plant Sci.* 20, 388–397. doi: 10.1016/j.tplants.2015.03.014

Frigerio, L., and Hawes, C. (2008). The endomembrane system: a green perspective. *Traffic* 9:1563. doi: 10.1111/j.1600-0854.2008.00795.x

Fujimoto, M., and Tsutsumi, N. (2014). Dynamin-related proteins in plant post-Golgi traffic. *Front. Plant Sci.* 5:408. doi: 10.3389/fpls.2014.00408

Gadeyne, A., Sanchez-Rodriguez, C., Vanneste, S., Di Rubbo, S., Zauber, H., Vanneste, K., et al. (2014). The TPLATE adaptor complex drives clathrin-mediated endocytosis in plants. *Cell* 156, 691–704. doi: 10.1016/j.cell.2014.01.039

Gao, C., Luo, M., Zhao, Q., Yang, R., Cui, Y., Zeng, Y., et al. (2014). A unique plant ESCRT component, FREE1, regulates multivesicular body protein sorting and plant growth. *Curr. Biol.* 24, 2556–2563. doi: 10.1016/j.cub.2014.09.014

Gao, C., Zhuang, X., Shen, J., and Jiang, L. (2017). Plant ESCRT complexes: moving beyond endosomal sorting. *Trends Plant Sci.* 22, 986–998. doi: 10.1016/j.tplants.2017.08.003

Gao, J., Chaudhary, A., Vaddepalli, P., Nagel, M. K., Isono, E., and Schneitz, K. (2019). The *Arabidopsis* receptor kinase STRUBBELIG undergoes clathrin-dependent endocytosis. *J. Exp. Bot.* 70, 3881–3894. doi: 10.1093/jxb/erz190

Garcia-Leon, M., Cuyas, L., Abd El-Moneim, D., Rodriguez, L., Belda-Palazon, B., Sanchez-Quant, E., et al. (2019). Stomatal aperture and turnover of ABA receptors are regulated by *Arabidopsis* ALIX. *Plant Cell.* 31, 2411–2429. doi: 10.1105/tpc.19.00399

Geldner, N., Anders, N., Wolters, H., Keicher, J., Kornberger, W., Muller, P., et al. (2003). The *Arabidopsis* GNOM ARF-GEF mediates endosomal recycling, auxin transport, and auxin-dependent plant growth. *Cell* 112, 219–230. doi: 10.1016/s0092-8674(03)00003-5

Geldner, N., and Robatzek, S. (2008). Plant receptors go endosomal: a moving view on signal transduction. *Plant Physiol.* 147, 1565–1574. doi: 10.1104/pp.108.120287

Gimenez-Ibanez, S., Hann, D. R., Ntoukakis, V., Petutschnig, E., Lipka, V., and Rathjen, J. P. (2009). AvrPtoB targets the LysM receptor kinase CERK1 to promote bacterial virulence on plants. *Curr. Biol.* 19, 423–429. doi: 10.1016/j.cub.2009.01.054

Goehre, V., Spallek, T., Haeweker, H., Mersmann, S., Mentzel, T., Boller, T., et al. (2008). Plant pattern-recognition receptor FLS2 is directed for degradation by the bacterial ubiquitin ligase AvrPtoB. *Curr. Biol.* 18, 1824–1832. doi: 10.1016/j.cub.2008.10.063

Haas, T. J., Sliwinski, M. K., Martinez, D. E., Preuss, M., Ebine, K., Ueda, T., et al. (2007). The *Arabidopsis* AAA ATPase SKD1 is involved in multivesicular endosome function and interacts with its positive regulator LYST-INTERACTING PROTEIN5. *Plant Cell* 19, 1295–1312. doi: 10.1105/tpc.106.049346

Haglund, K., and Dikic, I. (2012). The role of ubiquitylation in receptor endocytosis and endosomal sorting. *J. Cell Sci.* 125(Pt 2), 265–275. doi: 10.1242/jcs.091280

Hawryluk, M. J., Keyel, P. A., Mishra, S. K., Watkins, S. C., Heuser, J. E., and Traub, L. M. (2006). Epsin 1 is a polyubiquitin-selective clathrin-associated sorting protein. *Traffic* 7, 262–281. doi: 10.1111/j.1600-0854.2006.00383.x

Henne, W. M., Boucrot, E., Meinecke, M., Evergren, E., Vallis, Y., Mittal, R., et al. (2010). FCHo proteins are nucleators of clathrin-mediated endocytosis. *Science* 328, 1281–1284. doi: 10.1126/science.1188462

Henne, W. M., Buchkovich, N. J., and Emr, S. D. (2011). The ESCRT Pathway. *Dev. Cell* 21, 77–91. doi: 10.1016/j.devcel.2011.05.015

Henne, W. M., Buchkovich, N. J., Zhao, Y., and Emr, S. D. (2012). The endosomal sorting complex ESCRT-II mediates the assembly and architecture of ESCRT-III helices. *Cell* 151, 356–371. doi: 10.1016/j.cell.2012.08.039

Herberth, S., Shahriari, M., Bruderek, M., Hessner, F., Muller, B., Hulskamp, M., et al. (2012). Artificial ubiquitylation is sufficient for sorting of a plasma membrane ATPase to the vacuolar lumen of *Arabidopsis* cells. *Planta* 236, 63–77. doi: 10.1007/s00425-012-1587-0

Herman, E. K., Walker, G., van der Giezen, M., and Dacks, J. B. (2011). Multivesicular bodies in the enigmatic amoeboflagellate Breviata anathema and the evolution of ESCRT 0. *J. Cell Sci.* 124(Pt 4), 613–621. doi: 10.1242/jcs.078436

Hicke, L., and Dunn, R. (2003). Regulation of membrane protein transport by ubiquitin and ubiquitin-binding proteins. *Annu. Rev. Cell Dev. Biol.* 19, 141–172. doi: 10.1146/annurev.cellbio.19.110701.154617

Hirst, J., Barlow, L. D., Francisco, G. C., Sahlender, D. A., Seaman, M. N., Dacks, J. B., et al. (2011). The fifth adaptor protein complex. *PLoS Biol.* 9:e1001170. doi: 10.1371/journal.pbio.1001170

Hirst, J., Schlacht, A., Norcott, J. P., Traynor, D., Bloomfield, G., Antrobus, R., et al. (2014). Characterization of TSET, an ancient and widespread membrane trafficking complex. *eLife* 3:e02866. doi: 10.7554/eLife.02866

Hoeller, D., Crosetto, N., Blagoev, B., Raiborg, C., Tikkanen, R., Wagner, S., et al. (2006). Regulation of ubiquitin-binding proteins by monoubiquitination. *Nat. Cell Biol.* 8, 163–169. doi: 10.1038/ncb1354

Hollopeter, G., Lange, J. J., Zhang, Y., Vu, T. N., Gu, M., Ailion, M., et al. (2014). The membrane-associated proteins FCHo and SGIP are allosteric activators of the AP2 clathrin adaptor complex. *eLife* 3:e03648. doi: 10.7554/eLife.03648

Holstein, S. E., and Oliviusson, P. (2005). Sequence analysis of *Arabidopsis thaliana* E/ANTH-domain-containing proteins: membrane tethers of the clathrin-dependent vesicle budding machinery. *Protoplasma* 226, 13–21. doi: 10.1007/s00709-005-0105-7

Honing, S., Ricotta, D., Krauss, M., Spate, K., Spolaore, B., Motley, A., et al. (2005). Phosphatidylinositol-(4,5)-bisphosphate regulates sorting signal recognition by the clathrin-associated adaptor complex AP2. *Mol. Cell.* 18, 519–531. doi: 10.1016/j.molcel.2005.04.019

Hua, Z., and Vierstra, R. D. (2011). The cullin-RING ubiquitin-protein ligases. *Annu. Rev. Plant Biol.* 62, 299–334. doi: 10.1146/annurev-arplant-042809-112256

Hurley, J. H. (2008). ESCRT complexes and the biogenesis of multivesicular bodies. *Curr. Opin. Cell Biol.* 20, 4–11. doi: 10.1016/j.ceb.2007.12.002

Hurley, J. H. (2010). The ESCRT complexes. *Crit. Rev. Biochem. Mol. Biol.* 45, 463–487. doi: 10.3109/10409238.2010.502516

Hurley, J. H., and Hanson, P. I. (2010). Membrane budding and scission by the ESCRT machinery: it's all in the neck. *Nat. Rev. Mol. Cell Biol.* 11, 556–566. doi: 10.1038/nrm2937

Hurley, J. H., and Ren, X. (2009). The circuitry of cargo flux in the ESCRT pathway. *J. Cell Biol.* 185, 185–187. doi: 10.1083/jcb.200903013

Husnjak, K., and Dikic, I. (2012). Ubiquitin-binding proteins: decoders of ubiquitin-mediated cellular functions. *Annu. Rev. Biochem.* 81, 291–322. doi: 10.1146/annurev-biochem-051810-094654

Ischebeck, T., Werner, S., Krishnamoorthy, P., Lerche, J., Meijon, M., Stenzel, I., et al. (2013). Phosphatidylinositol 4,5-bisphosphate influences PIN polarization by controlling clathrin-mediated membrane trafficking in *Arabidopsis*. *Plant Cell* 25, 4894–4911. doi: 10.1105/tpc.113.116582

Isono, E., and Kalinowska, K. (2017). ESCRT-dependent degradation of ubiquitylated plasma membrane proteins in plants. *Curr. Opin. Plant Biol* 40, 49–55. doi: 10.1016/j.pbi.2017.07.003

Isono, E., Katsiarimpa, A., Muller, I. K., Anzenberger, F., Stierhof, Y. D., Geldner, N., et al. (2010). The deubiquitinating enzyme AMSH3 is required for intracellular trafficking and vacuole biogenesis in *Arabidopsis thaliana*. *Plant Cell* 22, 1826–1837. doi: 10.1105/tpc.110.075952

Isono, E., and Nagel, M. K. (2014). Deubiquitylating enzymes and their emerging role in plant biology. *Front. Plant. Sci.* 5:56. doi: 10.3389/fpls.2014.00056

Ito, E., Fujimoto, M., Ebine, K., Uemura, T., Ueda, T., and Nakano, A. (2012). Dynamic behavior of clathrin in *Arabidopsis thaliana* unveiled by live imaging. *Plant J. Cell Mol. Biol.* 69, 204–216. doi: 10.1111/j.1365-313X.2011.04782.x

Johnson, A., and Vert, G. (2016). Unraveling K63 polyubiquitination networks by sensor-based proteomics. *Plant Physiol.* 171, 1808–1820. doi: 10.1104/pp.16.00619

Kalinowska, K., Nagel, M. K., Goodman, K., Cuyas, L., Anzenberger, F., Alkofer, A., et al. (2015). *Arabidopsis* ALIX is required for the endosomal localization of the deubiquitinating enzyme AMSH3. *Proc. Natl. Acad. Sci. U.S.A.* 112, E5543–E5551. doi: 10.1073/pnas.1510516112

Kaneda, M., van Oostende-Triplet, C., Chebli, Y., Testerink, C., Bednarek, S. Y., and Geitmann, A. (2019). Plant AP180 N-terminal homolog proteins are involved in clathrin-dependent endocytosis during pollen tube growth in *Arabidopsis thaliana*. *Plant Cell Physiol.* 60, 1316–1330. doi: 10.1093/pcp/pcz036

Kang, B. H., Nielsen, E., Preuss, M. L., Mastronarde, D., and Staehelin, L. A. (2011). Electron tomography of RabA4b- and PI-4Kbeta1-labeled trans Golgi network compartments in *Arabidopsis*. *Traffic* 12, 313–329. doi: 10.1111/j.1600-0854.2010.01146.x

Kasai, K., Takano, J., Miwa, K., Toyoda, A., and Fujiwara, T. (2011). High boron-induced ubiquitination regulates vacuolar sorting of the BOR1 borate transporter in *Arabidopsis thaliana*. *J. Biol. Chem.* 286, 6175–6183. doi: 10.1074/jbc.M110.184929

Katsiarimpa, A., Anzenberger, F., Schlager, N., Neubert, S., Hauser, M. T., Schwechheimer, C., et al. (2011). The *Arabidopsis* deubiquitinating enzyme AMSH3 interacts with ESCRT-III subunits and regulates their localization. *Plant Cell* 23, 3026–3040. doi: 10.1105/tpc.111.087254

Katsiarimpa, A., Kalinowska, K., Anzenberger, F., Weis, C., Ostertag, M., Tsutsumi, C., et al. (2013). The deubiquitinating enzyme AMSH1 and the ESCRT-III subunit VPS2.1 are required for autophagic degradation in *Arabidopsis*. *Plant Cell* 25, 2236–2252. doi: 10.1105/tpc.113.113399

Katsiarimpa, A., Munoz, A., Kalinowska, K., Uemura, T., Rojo, E., and Isono, E. (2014). The ESCRT-III-interacting deubiquitinating enzyme AMSH3 is essential for degradation of ubiquitinated membrane proteins in *Arabidopsis thaliana*. *Plant Cell Physiol.* 55, 727–736. doi: 10.1093/pcp/pcu019

Kim, D. Y., Scalf, M., Smith, L. M., and Vierstra, R. D. (2013). Advanced proteomic analyses yield a deep catalog of ubiquitylation targets in *Arabidopsis*. *Plant Cell* 25, 1523–1540. doi: 10.1105/tpc.112.108613

Kim, S. Y., Xu, Z. Y., Song, K., Kim, D. H., Kang, H., Reichardt, I., et al. (2013). Adaptor protein complex 2-mediated endocytosis is crucial for male reproductive organ development in *Arabidopsis*. *Plant Cell* 25, 2970–2985. doi: 10.1105/tpc.113.114264

Kitakura, S., Vanneste, S., Robert, S., Lofke, C., Teichmann, T., Tanaka, H., et al. (2011). Clathrin mediates endocytosis and polar distribution of PIN auxin transporters in *Arabidopsis*. *Plant Cell* 23, 1920–1931. doi: 10.1105/tpc.111.083030

Kleine-Vehn, J., Wabnik, K., Martiniere, A., Langowski, L., Willig, K., Naramoto, S., et al. (2011). Recycling, clustering, and endocytosis jointly maintain PIN auxin carrier polarity at the plasma membrane. *Mol. Syst. Biol.* 7:540. doi: 10.1038/msb.2011.72

Kolb, C., Nagel, M. K., Kalinowska, K., Hagmann, J., Ichikawa, M., Anzenberger, F., et al. (2015). FYVE1 is essential for vacuole biogenesis and intracellular trafficking in *Arabidopsis*. *Plant Physiol.* 167, 1361–1373. doi: 10.1104/pp.114.253377

Komander, D., and Rape, M. (2012). The ubiquitin code. *Annu. Rev. Biochem.* 81, 203–229. doi: 10.1146/annurev-biochem-060310-170328

Konopka, C. A., Backues, S. K., and Bednarek, S. Y. (2008). Dynamics of *Arabidopsis* dynamin-related protein 1C and a clathrin light chain at the plasma membrane. *Plant Cell* 20, 1363–1380. doi: 10.1105/tpc.108.059428

Korbei, B., and Luschnig, C. (2013). Plasma membrane protein ubiquitylation and degradation as determinants of positional growth in plants. *J. Integr. Plant Biol.* 55, 809–823. doi: 10.1111/jipb.12059

Korbei, B., Moulinier-Anzola, J., De-Araujo, L., Lucyshyn, D., Retzer, K., Khan, M. A., et al. (2013). *Arabidopsis* TOL proteins act as gatekeepers for vacuolar sorting of PIN2 plasma membrane protein. *Curr. Biol.* 23, 2500–2505. doi: 10.1016/j.cub.2013.10.036

Kostelansky, M. S., Schluter, C., Tam, Y. Y., Lee, S., Ghirlando, R., Beach, B., et al. (2007). Molecular architecture and functional model of the complete yeast ESCRT-I heterotetramer. *Cell* 129, 485–498. doi: 10.1016/j.cell.2007.03.016

Kumar, M. N., Bau, Y. C., Longkumer, T., and Verslues, P. E. (2019). Low Water Potential and At14a-Like1 (AFL1) effects on endocytosis and actin filament organization. *Plant Physiol.* 179, 1594–1607. doi: 10.1104/pp.18.01314

Kumar, M. N., Hsieh, Y. F., and Verslues, P. E. (2015). At14a-Like1 participates in membrane-associated mechanisms promoting growth during drought in *Arabidopsis thaliana*. *Proc. Natl. Acad. Sci. U.S.A.* 112, 10545–10550. doi: 10.1073/pnas.1510140112

Lam, B. C. H., Sage, T. L., Bianchi, F., and Blumwald, E. (2001). Role of SH3 domain-containing proteins in clathrin-mediated vesicle trafficking in *Arabidopsis*. *Plant Cell* 13, 2499–2512. doi: 10.1105/tpc.13.11.2499

Lam, S. K., Siu, C. L., Hillmer, S., Jang, S., An, G., Robinson, D. G., et al. (2007). Rice SCAMP1 defines clathrin-coated, trans-golgi-located tubular-vesicular structures as an early endosome in tobacco BY-2 cells. *Plant Cell* 19, 296–319. doi: 10.1105/tpc.106.045708

Lauwers, E., Jacob, C., and Andre, B. (2009). K63-linked ubiquitin chains as a specific signal for protein sorting into the multivesicular body pathway. *J. Cell Biol.* 185, 493–502. doi: 10.1083/jcb.200810114

Lee, G. J., Kim, H., Kang, H., Jang, M., Lee, D. W., Lee, S., et al. (2007). EpsinR2 interacts with clathrin, adaptor protein-3, AtVTI12, and phosphatidylinositol-3-phosphate. Implications for EpsinR2 function in protein trafficking in plant cells. *Plant Physiol.* 143, 1561–1575. doi: 10.1104/pp.106.095349

Legendre-Guillemin, V., Wasiak, S., Hussain, N. K., Angers, A., and McPherson, P. S. (2004). ENTH/ANTH proteins and clathrin-mediated membrane budding. *J. Cell Sci.* 117(Pt 1), 9–18. doi: 10.1242/jcs.00928

Leitner, J., Petrasek, J., Tomanov, K., Retzer, K., Parezova, M., Korbei, B., et al. (2012a). Lysine63-linked ubiquitylation of PIN2 auxin carrier protein governs hormonally controlled adaptation of *Arabidopsis* root growth. *Proc. Natl. Acad. Sci. U.S.A.* 109, 8322–8327. doi: 10.1073/pnas.1200824109

Leitner, J., Retzer, K., Korbei, B., and Luschnig, C. (2012b). Dynamics in PIN2 auxin carrier ubiquitylation in gravity-responding *Arabidopsis* roots. *Plant Signal. Behav.* 7, 1271–1273. doi: 10.4161/psb.21715

Leung, K. F., Dacks, J. B., and Field, M. C. (2008). Evolution of the multivesicular body ESCRT machinery; retention across the eukaryotic lineage. *Traffic* 9, 1698–1716. doi: 10.1111/j.1600-0854.2008.00797.x

Li, H., Li, Y., Zhao, Q., Li, T., Wei, J., Li, B., et al. (2019). The plant ESCRT component FREE1 shuttles to the nucleus to attenuate abscisic acid signalling. *Nat. Plants* 5, 512–524. doi: 10.1038/s41477-019-0400-5

Liao, D., Cao, Y., Sun, X., Espinoza, C., Nguyen, C. T., Liang, Y., et al. (2017). *Arabidopsis* E3 ubiquitin ligase PLANT U-BOX13 (PUB13) regulates chitin receptor LYSIN MOTIF RECEPTOR KINASE5 (LYK5) protein abundance. *New Phytol.* 214, 1646–1656. doi: 10.1111/nph.14472

Liu, N. S., Loo, L. S., Loh, E., Seet, L. F., and Hong, W. (2009). Participation of Tom1L1 in EGF-stimulated endocytosis of EGF receptor. *EMBO J.* 28, 3485–3499. doi: 10.1038/emboj.2009.282

Liu, W., Sun, Q., Wang, K., Du, Q., and Li, W. X. (2017). Nitrogen Limitation Adaptation (NLA) is involved in source-to-sink remobilization of nitrate by mediating the degradation of NRT1.7 in *Arabidopsis*. *New Phytol.* 214, 734–744. doi: 10.1111/nph.14396

Lu, D., Lin, W., Gao, X., Wu, S., Cheng, C., Avila, J., et al. (2011). Direct ubiquitination of pattern recognition receptor FLS2 attenuates plant innate immunity. *Science* 332, 1439–1442. doi: 10.1126/science.1204903

Luschnig, C., and Vert, G. (2014). The dynamics of plant plasma membrane proteins: PINs and beyond. *Development* 141, 2924–2938. doi: 10.1242/dev.103424

MacGurn, J. A., Hsu, P. C., and Emr, S. D. (2012). Ubiquitin and membrane protein turnover: from cradle to grave. *Annu. Rev. Biochem.* 81, 231–259. doi: 10.1146/annurev-biochem-060210-093619

Martins, S., Dohmann, E. M., Cayrel, A., Johnson, A., Fischer, W., Pojer, F., et al. (2015). Internalization and vacuolar targeting of the brassinosteroid hormone receptor BRI1 are regulated by ubiquitination. *Nat. Commun.* 6:6151. doi: 10.1038/ncomms7151

Mayers, J. R., Wang, L., Pramanik, J., Johnson, A., Sarkeshik, A., Wang, Y., et al. (2013). Regulation of ubiquitin-dependent cargo sorting by multiple endocytic adaptors at the plasma membrane. *Proc. Natl. Acad. Sci. U.S.A.* 110, 11857–11862. doi: 10.1073/pnas.1302918110

Mbengue, M., Bourdais, G., Gervasi, F., Beck, M., Zhou, J., Spallek, T., et al. (2016). Clathrin-dependent endocytosis is required for immunity mediated by pattern recognition receptor kinases. *Proc. Natl. Acad. Sci. U.S.A.* 113, 11034–11039. doi: 10.1073/pnas.1606004113

McCullough, J., Clague, M. J., and Urbe, S. (2004). AMSH is an endosome-associated ubiquitin isopeptidase. *J. Cell Biol.* 166, 487–492. doi: 10.1083/jcb.200401141

McMahon, H. T., and Boucrot, E. (2011). Molecular mechanism and physiological functions of clathrin-mediated endocytosis. *Nat. Rev. Mol. Cell Biol.* 12, 517–533. doi: 10.1038/nrm3151

McMichael, C. M., Reynolds, G. D., Koch, L. M., Wang, C., Jiang, N., Nadeau, J., et al. (2013). Mediation of clathrin-dependent trafficking during cytokinesis and cell expansion by *Arabidopsis* stomatal cytokinesis defective proteins. *Plant Cell* 25, 3910–3925. doi: 10.1105/tpc.113.115162

Mersey, B. G., Griffing, L. R., Rennie, P. J., and Fowke, L. C. (1985). The isolation of coated vesicles from protoplasts of soybean. *Planta* 163, 317–327. doi: 10.1007/BF00395141

Miliaras, N. B., and Wendland, B. (2004). EH proteins: multivalent regulators of endocytosis (and other pathways). *Cell Biochem. Biophys.* 41, 295–318. doi: 10.1385/CBB:41:2:295

Mitsunari, T., Nakatsu, F., Shioda, N., Love, P. E., Grinberg, A., Bonifacino, J. S., et al. (2005). Clathrin adaptor AP-2 is essential for early embryonal development. *Mol. Cell. Biol.* 25, 9318–9323. doi: 10.1128/MCB.25.21.9318-9323.2005

Mosesso, N., Nagel, M. K., and Isono, E. (2019). Ubiquitin recognition in endocytic trafficking - with or without ESCRT-0. *J. Cell Sci.* 132:jcs232868. doi: 10.1242/jcs.232868

Moulinier-Anzola, J., Schwihla, M., De-Araújo, L., Artner, C., Jörg, L., Konstantinova, N., et al. (2020). TOLs function as ubiquitin receptors in the early steps of the ESCRT pathway in higher plants. *Mol. Plant* [Epub ahead of print]. doi: 10.1016/j.molp.2020.02.012

Nagel, M. K., Kalinowska, K., Vogel, K., Reynolds, G. D., Wu, Z., Anzenberger, F., et al. (2017). *Arabidopsis* SH3P2 is an ubiquitin-binding protein that functions together with ESCRT-I and the deubiquitylating enzyme AMSH3. *Proc. Natl. Acad. Sci. U.S.A.* 114, E7197–E7204. doi: 10.1073/pnas.1710866114

Naramoto, S., Otegui, M. S., Kutsuna, N., de Rycke, R., Dainobu, T., Karampelias, M., et al. (2014). Insights into the localization and function of the membrane trafficking regulator GNOM ARF-GEF at the golgi apparatus in *Arabidopsis*. *Plant Cell* 26, 3062–3076. doi: 10.1105/tpc.114.125880

Narasimhan, M., Johnson, A., Prizak, R., Kaufmann, W. A., Tan, S., Casillas-Perez, B., et al. (2020). Evolutionarily unique mechanistic framework of clathrin-mediated endocytosis in plants. *eLife* 9:e52067. doi: 10.7554/eLife.52067

Nathan, J. A., Tae Kim, H., Ting, L., Gygi, S. P., and Goldberg, A. L. (2013). Why do cellular proteins linked to K63-polyubiquitin chains not associate with proteasomes? *EMBO J.* 32, 552–565. doi: 10.1038/emboj.2012.354

Nguyen, H. H., Lee, M. H., Song, K., Ahn, G., Lee, J., and Hwang, I. (2018). The A/ENTH domain-containing protein AtECA4 is an adaptor protein involved in cargo recycling from the trans-golgi network/early endosome to the plasma membrane. *Mol. Plant* 11, 568–583. doi: 10.1016/j.molp.2018.01.001

Otegui, M. S. (2018). ESCRT-mediated sorting and intralumenal vesicle concatenation in plants. *Biochem. Soc. Trans.* 46, 537–545. doi: 10.1042/Bst20170439

Paez Valencia, J., Goodman, K., and Otegui, M. S. (2016). Endocytosis and endosomal trafficking in plants. *Annu. Rev. Plant Biol.* 67, 309–335. doi: 10.1146/annurev-arplant-043015-112242

Park, B. S., Seo, J. S., and Chua, N. H. (2014). NITROGEN LIMITATION ADAPTATION recruits PHOSPHATE2 to target the phosphate transporter PT2 for degradation during the regulation of *Arabidopsis* phosphate homeostasis. *Plant Cell* 26, 454–464. doi: 10.1105/tpc.113.120311

Pashkova, N., Gakhar, L., Winistorfer, S. C., Sunshine, A. B., Rich, M., Dunham, M. J., et al. (2013). The yeast Alix homolog Bro1 functions as a ubiquitin receptor for protein sorting into multivesicular endosomes. *Dev. Cell* 25, 520–533. doi: 10.1016/j.devcel.2013.04.007

Pearse, B. M. (1976). Clathrin: a unique protein associated with intracellular transfer of membrane by coated vesicles. *Proc. Natl. Acad. Sci. U.S.A.* 73, 1255–1259. doi: 10.1073/pnas.73.4.1255

Piper, R. C., Dikic, I., and Lukacs, G. L. (2014). Ubiquitin-dependent sorting in endocytosis. *Cold Spring Harb. Perspect. Biol.* 6:a016808. doi: 10.1101/cshperspect.a016808

Raiborg, C., and Stenmark, H. (2009). The ESCRT machinery in endosomal sorting of ubiquitylated membrane proteins. *Nature* 458, 445–452. doi: 10.1038/nature07961

Reider, A., and Wendland, B. (2011). Endocytic adaptors–social networking at the plasma membrane. *J. Cell Sci.* 124(Pt 10), 1613–1622. doi: 10.1242/jcs.073395

Ren, X., and Hurley, J. H. (2010). VHS domains of ESCRT-0 cooperate in high-avidity binding to polyubiquitinated cargo. *EMBO J.* 29, 1045–1054. doi: 10.1038/emboj.2010.6

Retzer, K., Akhmanova, M., Konstantinova, N., Malinska, K., Leitner, J., Petrasek, J., et al. (2019). Brassinosteroid signaling delimits root gravitropism via sorting of the *Arabidopsis* PIN2 auxin transporter. *Nat. Commun.* 10:5516. doi: 10.1038/s41467-019-13543-1

Reyes, F. C., Buono, R. A., Roschzttardtz, H., Di Rubbo, S., Yeun, L. H., Russinova, E., et al. (2014). A novel endosomal sorting complex required for transport (ESCRT) component in *Arabidopsis thaliana* controls cell expansion and development. *J. Biol. Chem.* 289, 4980–4988. doi: 10.1074/jbc.M113.529685

Reynolds, G. D., Wang, C., Pan, J., and Bednarek, S. Y. (2018). Inroads into internalization: five years of endocytic exploration. *Plant Physiol.* 176, 208–218. doi: 10.1104/pp.17.01117

Richardson, L. G. L., Howard, A. S. M., Khuu, N., Gidda, S. K., McCartney, A., Morphy, B. J., et al. (2011). Protein–protein interaction network and subcellular localization of the *Arabidopsis thaliana* ESCRT machinery. *Front. Plant Sci.* 2:20. doi: 10.3389/fpls.2011.00020

Richter, S., Geldner, N., Schrader, J., Wolters, H., Stierhof, Y. D., Rios, G., et al. (2007). Functional diversification of closely related ARF-GEFs in protein secretion and recycling. *Nature* 448, 488–492. doi: 10.1038/nature05967

Richter, S., Voss, U., and Jurgens, G. (2009). Post-Golgi traffic in plants. *Traffic* 10, 819–828. doi: 10.1111/j.1600-0854.2009.00916.x

Ringstad, N., Nemoto, Y., and DeCamilli, P. (1997). The SH3p4/Sh3p8/SH3p13 protein family: binding partners for synaptojanin and dynamin via a Grb2-like Src homology 3 domain. *Proc. Natl. Acad. Sci. U.S.A.* 94, 8569–8574. doi: 10.1073/pnas.94.16.8569

Robatzek, S., Chinchilla, D., and Boller, T. (2006). Ligand-induced endocytosis of the pattern recognition receptor FLS2 in *Arabidopsis*. *Genes Dev.* 20, 537–542. doi: 10.1101/gad.366506

Roberts, D., Pedmale, U. V., Morrow, J., Sachdev, S., Lechner, E., Tang, X. B., et al. (2011). Modulation of phototropic responsiveness in *Arabidopsis* through ubiquitination of Phototropin 1 by the CUL3-Ring E3 Ubiquitin Ligase CRL3(NPH3). *Plant Cell* 23, 3627–3640. doi: 10.1105/tpc.111.087999

Robinson, D. G., Jiang, L., and Schumacher, K. (2008). The endosomal system of plants: charting new and familiar territories. *Plant Physiol.* 147, 1482–1492. doi: 10.1104/pp.108.120105

Robinson, D. G., and Neuhaus, J. M. (2016). Receptor-mediated sorting of soluble vacuolar proteins: myths, facts, and a new model. *J. Exp. Bot.* 67, 4435–4449. doi: 10.1093/jxb/erw222

Robinson, D. G., and Pimpl, P. (2013). Clathrin and post-Golgi trafficking: a very complicated issue. *Trends Plant Sci.* 19, 134–139. doi: 10.1016/j.tplants.2013.10.008

Robinson, M. S. (2015). Forty years of clathrin-coated vesicles. *Traffic* 16, 1210–1238. doi: 10.1111/tra.12335

Rodriguez-Furlan, C., Minina, E. A., and Hicks, G. R. (2019). Remove, recycle, degrade: regulating plasma membrane protein accumulation. *Plant Cell* 31, 2833–2854. doi: 10.1105/tpc.19.00433

Romero-Barrios, N., Monachello, D., Dolde, U., Wong, A., San Clemente, H., Cayrel, A., et al. (2020). Advanced cataloging of lysine-63 polyubiquitin networks by genomic, interactome, and sensor-based proteomic analyses. *Plant Cell* 32, 123–138. doi: 10.1105/tpc.19.00568

Romero-Barrios, N., and Vert, G. (2018). Proteasome-independent functions of lysine-63 polyubiquitination in plants. *New Phytol.* 217, 995–1011. doi: 10.1111/nph.14915

Ron, M., and Avni, A. (2004). The receptor for the fungal elicitor ethylene-inducing xylanase is a member of a resistance-like gene family in tomato. *Plant Cell* 16, 1604–1615. doi: 10.1105/tpc.022475

Rosquete, M. R., Davis, D. J., and Drakakaki, G. (2018). The plant trans-golgi network: not just a matter of distinction. *Plant Physiol.* 176, 187–198. doi: 10.1104/pp.17.01239

Row, P. E., Prior, I. A., McCullough, J., Clague, M. J., and Urbe, S. (2006). The ubiquitin isopeptidase UBPY regulates endosomal ubiquitin dynamics and is essential for receptor down-regulation. *J. Biol. Chem.* 281, 12618–12624. doi: 10.1074/jbc.M512615200

Sancho-Andres, G., Soriano-Ortega, E., Gao, C., Bernabe-Orts, J. M., Narasimhan, M., Muller, A. O., et al. (2016). Sorting motifs involved in the trafficking and localization of the PIN1 auxin efflux carrier. *Plant Physiol.* 171, 1965–1982. doi: 10.1104/pp.16.00373

Sandvig, K., Kavaliauskiene, S., and Skotland, T. (2018). Clathrin-independent endocytosis: an increasing degree of complexity. *Histochem. Cell Biol.* 150, 107–118. doi: 10.1007/s00418-018-1678-5

Saracco, S. A., Hansson, M., Scalf, M., Walker, J. M., Smith, L. M., and Vierstra, R. D. (2009). Tandem affinity purification and mass spectrometric analysis of ubiquitylated proteins in *Arabidopsis*. *Plant J.* 59, 344–358. doi: 10.1111/j.1365-313X.2009.03862.x

Scheuring, D., Kunzl, F., Viotti, C., Yan, M. S., Jiang, L., Schellmann, S., et al. (2012). Ubiquitin initiates sorting of Golgi and plasma membrane proteins into the vacuolar degradation pathway. *BMC Plant Biol.* 12:164. doi: 10.1186/1471-2229-12-164

Schoneberg, J., Lee, I. H., Iwasa, J. H., and Hurley, J. H. (2017). Reverse-topology membrane scission by the ESCRT proteins. *Nat. Rev. Mol. Cell Biol.* 18, 5–17. doi: 10.1038/nrm.2016.121

Schuh, A. L., and Audhya, A. (2014). The ESCRT machinery: from the plasma membrane to endosomes and back again. *Crit. Rev. Biochem. Mol. Biol.* 49, 242–261. doi: 10.3109/10409238.2014.881777

Shen, B., Li, C., Min, Z., Meeley, R. B., Tarczynski, M. C., and Olsen, O. A. (2003). sal1 determines the number of aleurone cell layers in maize endosperm and encodes a class E vacuolar sorting protein. *Proc. Natl. Acad. Sci. U.S.A.* 100, 6552–6557. doi: 10.1073/pnas.0732023100

Shen, J. B., Gao, C. J., Zhao, Q., Lin, Y. S., Wang, X. F., Zhuang, X. H., et al. (2016). AtBRO1 functions in ESCRT-I complex to regulate multivesicular body protein sorting. *Mol. Plant* 9, 760–763. doi: 10.1016/j.molp.2016.02.005

Shen, J. B., Zhao, Q., Wang, X. F., Gao, C. J., Zhu, Y., Zeng, Y. L., et al. (2018). A plant Bro1 domain protein BRAF regulates multivesicular body biogenesis and membrane protein homeostasis. *Nat. Commun.* 9:3784. doi: 10.1038/s41467-018-05913-y

Shen, Q. T., Schuh, A. L., Zheng, Y., Quinney, K., Wang, L., Hanna, M., et al. (2014). Structural analysis and modeling reveals new mechanisms governing ESCRT-III spiral filament assembly. *J. Cell Biol.* 206, 763–777. doi: 10.1083/jcb.201403108

Shin, L. J., Lo, J. C., Chen, G. H., Callis, J., Fu, H. Y., and Yeh, K. C. (2013). IRT1 DEGRADATION FACTOR1, a RING E3 ubiquitin ligase, regulates the degradation of IRON-REGULATED TRANSPORTER1 in *Arabidopsis*. *Plant Cell* 25, 3039–3051. doi: 10.1105/tpc.113.115212

Sierra, M. I., Wright, M. H., and Nash, P. D. (2010). AMSH interacts with ESCRT-0 to regulate the stability and trafficking of CXCR4. *J. Biol. Chem.* 285, 13990–14004. doi: 10.1074/jbc.M109.061309

Sigismund, S., Polo, S., and Di Fiore, P. P. (2004). Signaling through monoubiquitination. *Curr. Top. Microbiol. Immunol* 286, 149–185. doi: 10.1007/978-3-540-69494-6_6

Song, J., Lee, M. H., Lee, G. J., Yoo, C. M., and Hwang, I. (2006). *Arabidopsis* EPSIN1 plays an important role in vacuolar trafficking of soluble cargo proteins in plant cells via interactions with clathrin, AP-1, VTI11, and VSR1. *Plant Cell* 18, 2258–2274. doi: 10.1105/tpc.105.039123

Song, K., Jang, M., Kim, S. Y., Lee, G., Lee, G. J., Kim, D. H., et al. (2012). An A/ENTH domain-containing protein functions as an adaptor for clathrin-coated vesicles on the growing cell plate in *Arabidopsis* root cells. *Plant Physiol.* 159, 1013–1025. doi: 10.1104/pp.112.199380

Spallek, T., Beck, M., Ben Khaled, S., Salomon, S., Bourdais, G., Schellmann, S., et al. (2013). ESCRT-I mediates FLS2 endosomal sorting and plant immunity. *PLoS Genet.* 9:e1004035. doi: 10.1371/journal.pgen.1004035

Spitzer, C., Reyes, F. C., Buono, R., Sliwinski, M. K., Haas, T. J., and Otegui, M. S. (2009). The ESCRT-related CHMP1A and B proteins mediate multivesicular body sorting of auxin carriers in *Arabidopsis* and are required for plant development. *Plant Cell* 21, 749–766. doi: 10.1105/tpc.108.064865

Spitzer, C., Schellmann, S., Sabovljevic, A., Shahriari, M., Keshavaiah, C., Bechtold, N., et al. (2006). The *Arabidopsis* elch mutant reveals functions of an ESCRT component in cytokinesis. *Development* 133, 4679–4689. doi: 10.1242/dev.02654

Stewart, M. D., Ritterhoff, T., Klevit, R. E., and Brzovic, P. S. (2016). E2 enzymes: more than just middle men. *Cell Res.* 26, 423–440. doi: 10.1038/cr.2016.35

Svozil, J., Hirsch-Hoffmann, M., Dudler, R., Gruissem, W., and Baerenfaller, K. (2014). Protein abundance changes and ubiquitylation targets identified after inhibition of the proteasome with syringolin A. *Mol. Cell. Proteomics* 13, 1523–1536. doi: 10.1074/mcp.M113.036269

Takano, J., Tanaka, M., Toyoda, A., Miwa, K., Kasai, K., Fuji, K., et al. (2010). Polar localization and degradation of *Arabidopsis* boron transporters through distinct trafficking pathways. *Proc. Natl. Acad. Sci. U.S.A.* 107, 5220–5225. doi: 10.1073/pnas.0910744107

Tebar, F., Sorkina, T., Sorkin, A., Ericsson, M., and Kirchhausen, T. (1996). Eps15 is a component of clathrin-coated pits and vesicles and is located at the rim of coated pits. *J. Biol. Chem.* 271, 28727–28730. doi: 10.1074/jbc.271.46.28727

Tenno, T., Fujiwara, K., Tochio, H., Iwai, K., Morita, E. H., Hayashi, H., et al. (2004). Structural basis for distinct roles of Lys63- and Lys48-linked polyubiquitin chains. *Genes Cells* 9, 865–875. doi: 10.1111/j.1365-2443.2004.00780.x

Tian, Q., Olsen, L., Sun, B., Lid, S. E., Brown, R. C., Lemmon, B. E., et al. (2007). Subcellular localization and functional domain studies of DEFECTIVE KERNEL1 in maize and *Arabidopsis* suggest a model for aleurone cell fate specification involving CRINKLY4 and SUPERNUMERARY ALEURONE LAYER1. *Plant Cell* 19, 3127–3145. doi: 10.1105/tpc.106.048868

Tomanov, K., Luschnig, C., and Bachmair, A. (2014). Ubiquitin Lys 63 chains - second-most abundant, but poorly understood in plants. *Front. Plant Sci.* 5:15. doi: 10.3389/fpls.2014.00015

Traub, L. M. (2009). Tickets to ride: selecting cargo for clathrin-regulated internalization. *Nat. Rev. Mol. Cell Biol.* 10, 583–596. doi: 10.1038/nrm2751

Traub, L. M., and Bonifacino, J. S. (2013). Cargo recognition in clathrin-mediated endocytosis. *Cold Spring Harb. Perspect. Biol.* 5:a016790. doi: 10.1101/cshperspect.a016790

Turek, I., Tischer, N., Lassig, R., and Trujillo, M. (2018). Multi-tiered pairing selectivity between E2 ubiquitin-conjugating enzymes and E3 ligases. *J. Biol. Chem.* 293, 16324–16336. doi: 10.1074/jbc.RA118.004226

Uemura, T., and Ueda, T. (2014). Plant vacuolar trafficking driven by RAB and SNARE proteins. *Curr. Opin. Plant. Biol.* 22, 116–121. doi: 10.1016/j.pbi.2014.10.002

Urbe, S., Liu, H., Hayes, S. D., Heride, C., Rigden, D. J., and Clague, M. J. (2012). Systematic survey of deubiquitinase localization identifies USP21 as a regulator of centrosome- and microtubule-associated functions. *Mol. Biol. Cell* 23, 1095–1103. doi: 10.1091/mbc.E11-08-0668

Van Damme, D., Coutuer, S., De Rycke, R., Bouget, F. Y., Inze, D., and Geelen, D. (2006). Somatic cytokinesis and pollen maturation in *Arabidopsis* depend on TPLATE, which has domains similar to coat proteins. *Plant Cell* 18, 3502–3518. doi: 10.1105/tpc.106.040923

Varadan, R., Assfalg, M., Haririnia, A., Raasi, S., Pickart, C., and Fushman, D. (2004). Solution conformation of Lys63-linked di-ubiquitin chain provides clues to functional diversity of polyubiquitin signaling. *J. Biol. Chem.* 279, 7055–7063. doi: 10.1074/jbc.M309184200

Vierstra, R. D. (2012). The expanding universe of ubiquitin and ubiquitin-like modifiers. *Plant Physiol.* 160, 2–14. doi: 10.1104/pp.112.200667

Vietri, M., Radulovic, M., and Stenmark, H. (2020). The many functions of ESCRTs. *Nat. Rev. Mol. Cell Biol.* 21, 25–42. doi: 10.1038/s41580-019-0177-4

Viotti, C., Bubeck, J., Stierhof, Y. D., Krebs, M., Langhans, M., van den Berg, W., et al. (2010). Endocytic and secretory traffic in *Arabidopsis* merge in the trans-Golgi network/early endosome, an independent and highly dynamic organelle. *Plant Cell* 22, 1344–1357. doi: 10.1105/tpc.109.072637

Walton, A., Stes, E., Cybulski, N., Van Bel, M., Inigo, S., Durand, A. N., et al. (2016). It's Time for Some "Site"-seeing: novel tools to monitor the ubiquitin landscape in *Arabidopsis thaliana*. *Plant Cell* 28, 6–16. doi: 10.1105/tpc.15.00878

Wang, C., Hu, T., Yan, X., Meng, T., Wang, Y., Wang, Q., et al. (2016). Differential regulation of clathrin and its adaptor proteins during membrane recruitment for endocytosis. *Plant Physiol.* 171, 215–229. doi: 10.1104/pp.15.01716

Wang, C., Yan, X., Chen, Q., Jiang, N., Fu, W., Ma, B., et al. (2013). Clathrin light chains regulate clathrin-mediated trafficking, auxin signaling, and development in *Arabidopsis*. *Plant Cell* 25, 499–516. doi: 10.1105/tpc.112.108373

Wang, F., Shang, Y. F., Fan, B. F., Yu, J. Q., and Chen, Z. X. (2014). *Arabidopsis* LIP5, a positive regulator of multivesicular body biogenesis, is a critical target of pathogen-responsive MAPK cascade in plant basal defense. *PLoS Pathog.* 10:e1004243. doi: 10.1371/journal.ppat.1004243

Wang, F., Yang, Y., Wang, Z., Zhou, J., Fan, B. F., and Chen, Z. X. (2015). A critical role of lyst-interacting Protein5, a positive regulator of multivesicular body biogenesis, in plant responses to heat and salt stresses. *Plant Physiol.* 169, 497–518. doi: 10.1104/pp.15.00518

Wang, H. J., Hsu, Y. W., Guo, C. L., Jane, W. N., Wang, H., Jiang, L., et al. (2017). VPS36-dependent multivesicular bodies are critical for plasmamembrane protein turnover and vacuolar biogenesis. *Plant Physiol.* 173, 566–581. doi: 10.1104/pp.16.01356

Wang, P., Pleskot, R., Zang, J., Winkler, J., Wang, J., Yperman, K., et al. (2019). Plant AtEH/Pan1 proteins drive autophagosome formation at ER-PM contact sites with actin and endocytic machinery. *Nat. Commun.* 10:5132. doi: 10.1038/s41467-019-12782-6

Wang, S. L., Yoshinari, A., Shimada, T., Hara-Nishimura, I., Mitani-Ueno, N., Ma, J. F., et al. (2017). Polar localization of the NIP5;1 boric acid channel is maintained by endocytosis and facilitates boron transport in *Arabidopsis* roots. *Plant Cell* 29, 824–842. doi: 10.1105/tpc.16.00825

Wang, T., Liu, N. S., Seet, L. F., and Hong, W. (2010). The emerging role of VHS domain-containing Tom1, Tom1L1 and Tom1L2 in membrane trafficking. *Traffic* 11, 1119–1128. doi: 10.1111/j.1600-0854.2010.01098.x

Wang, Y., Liu, W., Wang, H., Du, Q., Fu, Z., Li, W. X., et al. (2019). ZmEHD1 is required for kernel development and vegetative growth through regulating auxin homeostasis. *Plant Physiol.* 182, 1467–1480. doi: 10.1104/pp.19.01336

Wemmer, M., Azmi, I., West, M., Davies, B., Katzmann, D., and Odorizzi, G. (2011). Bro1 binding to Snf7 regulates ESCRT-III membrane scission activity in yeast. *J. Cell Biol.* 192, 295–306. doi: 10.1083/jcb.201007018

Winter, V., and Hauser, M. T. (2006). Exploring the ESCRTing machinery in eukaryotes. *Trends Plant Sci.* 11, 115–123. doi: 10.1016/j.tplants.2006.01.008

Wright, M. H., Berlin, I., and Nash, P. D. (2011). Regulation of endocytic sorting by ESCRT-DUB-mediated deubiquitination. *Cell Biochem. Biophys* 60, 39–46. doi: 10.1007/s12013-011-9181-9

Xia, Z. L., Wei, Y. Y., Sun, K. L., Wu, J. Y., Wang, Y. X., and Wu, K. (2013). The maize AAA-type protein SKD1 confers enhanced salt and drought stress tolerance in transgenic tobacco by interacting with lyst-interacting protein 5. *PLoS One* 8:e69787. doi: 10.1371/journal.pone.0069787

Yin, X. J., Volk, S., Ljung, K., Mehlmer, N., Dolezal, K., Ditengou, F., et al. (2007). Ubiquitin lysine 63 chain-forming ligases regulate apical dominance in *Arabidopsis*. *Plant Cell* 19, 1898–1911. doi: 10.1105/tpc.107.052035

Yoshinari, A., Fujimoto, M., Ueda, T., Inada, N., Naito, S., and Takano, J. (2016). DRP1-dependent endocytosis is essential for polar localization and boron-induced degradation of the borate transporter BOR1 in *Arabidopsis thaliana*. *Plant Cell Physiol.* 57, 1985–2000. doi: 10.1093/pcp/pcw121

Yoshinari, A., Hosokawa, T., Amano, T., Beier, M. P., Kunieda, T., Shimada, T., et al. (2019). Polar localization of the borate exporter BOR1 requires AP2-dependent endocytosis. *Plant Physiol.* 179, 1569–1580. doi: 10.1104/pp.18.01017

Yoshinari, A., Korbei, B., and Takano, J. (2018). TOL proteins mediate vacuolar sorting of the borate transporter BOR1 in *Arabidopsis thaliana*. *Soil Sci. Plant Nutr.* 64, 598–605. doi: 10.1080/00380768.2018.1504322

Yoshinari, A., and Takano, J. (2017). Insights into the mechanisms underlying boron homeostasis in plants. *Front. Plant Sci.* 8:1951. doi: 10.3389/fpls.2017.01951

Yu, F., Lou, L., Tian, M., Li, Q., Ding, Y., Cao, X., et al. (2016). ESCRT-I component VPS23A affects ABA signaling by recognizing ABA receptors for endosomal degradation. *Mol. Plant* 9, 1570–1582. doi: 10.1016/j.molp.2016.11.002

Yu, Q., Zhang, Y., Wang, J., Yan, X., Wang, C., Xu, J., et al. (2016). Clathrin-mediated auxin efflux and maxima regulate hypocotyl hook formation and light-stimulated hook opening in *Arabidopsis*. *Mol. Plant* 9, 101–112. doi: 10.1016/j.molp.2015.09.018

Zhang, X. Q., Hou, P., Zhu, H. T., Li, G. D., Liu, X. G., and Xie, X. M. (2013). Knockout of the VPS22 component of the ESCRT-II complex in rice (*Oryza sativa* L.) causes chalky endosperm and early seedling lethality. *Mol. Biol. Rep.* 40, 3475–3481. doi: 10.1007/s11033-012-2422-1

Zhang, Y., Persson, S., Hirst, J., Robinson, M. S., van Damme, D., and Sanchez-Rodriguez, C. (2015). Change your TPLATE, change your fate: plant CME and beyond. *Trends Plant Sci.* 20, 41–48. doi: 10.1016/j.tplants.2014.09.002

Zhuang, X., Wang, H., Lam, S. K., Gao, C., Wang, X., Cai, Y., et al. (2013). A BAR-domain protein SH3P2, which binds to phosphatidylinositol 3-phosphate and ATG8, regulates autophagosome formation in *Arabidopsis*. *Plant Cell* 25, 4596–4615. doi: 10.1105/tpc.113.118307

Zouhar, J., and Sauer, M. (2014). Helping hands for budding prospects: ENTH/ANTH/VHS accessory proteins in endocytosis, vacuolar transport, and secretion. *Plant Cell* 26, 4232–4244. doi: 10.1105/tpc.114.131680

Conflict of Interest: The authors declare that the research was conducted in the absence of any commercial or financial relationships that could be construed as a potential conflict of interest.

frontiers in Plant Science

PERSPECTIVE
published: 11 June 2020
doi: 10.3389/fpls.2020.00809

3D Electron Microscopy Gives a Clue: Maize Zein Bodies Bud From Central Areas of ER Sheets

*Elsa Arcalís, Ulrike Hörmann-Dietrich, Lukas Zeh and Eva Stoger**

Department of Applied Genetics and Cell Biology, University of Natural Resources and Life Sciences, Vienna, Vienna, Austria

Zeins are the main storage proteins in maize seed endosperm, and the onset of zein synthesis in young seeds challenges the endomembrane system and results in the formation of storage organelles. Even though zeins lack a conventional endoplasmic reticulum (ER) retention signal, they accumulate within the ER and assemble in conspicuous ER-derived protein bodies (PBs) stabilized by disulfide bridge formation and hydrophobic interaction between zein chains. Zein body formation during seed development has been extensively studied, as well as the mechanisms that lead to the initiation of PBs. However, the exact course of the PB formation process and the spatial relationship with the ER remain unclear. The development of serial block face scanning electron microscopy (SBF-SEM) techniques that allow three-dimensional imaging combined with the high resolution of electron microscopy provides new perspectives on the study of the plant endomembrane system. Here, we demonstrate that (i) the ER of maize seeds is mainly formed by massive sheets and (ii) PBs are not budding from tubules or the edge of sheets, but protrude from the entire surface of the ER sheet.

Keywords: electron microscopy, volume electron microscopy, endomembrane system, endoplasmic reticulum, protein bodies, cereal endosperm, maize

OPEN ACCESS

Edited by:
Erika Isono,
University of Konstanz, Germany

Reviewed by:
Xiaohong Zhuang,
The Chinese University of Hong Kong, China
Jean-Marc Neuhaus,
Université de Neuchâtel, Switzerland

***Correspondence:**
Eva Stoger
eva.stoger@boku.ac.at;
eva.stoeger@boku.ac.at

Specialty section:
This article was submitted to Plant Traffic and Transport, a section of the journal Frontiers in Plant Science

Received: *27 March 2020*
Accepted: *19 May 2020*
Published: *11 June 2020*

Citation:
Arcalís E, Hörmann-Dietrich U, Zeh L and Stoger E (2020) 3D Electron Microscopy Gives a Clue: Maize Zein Bodies Bud From Central Areas of ER Sheets. Front. Plant Sci. 11:809. doi: 10.3389/fpls.2020.00809

INTRODUCTION

Cereal seeds are characterized by a high degree of functional specialization for the storage of proteins and energy. For example in maize, 70% of the seed proteome consists of storage proteins (Flint-Garcia et al., 2009). The main storage proteins are zeins, which are divided into four subfamilies termed α-, β-, γ-, and δ-zein. Zein synthesis in the endosperm starts as soon as 10 days after pollination (daps), increases steadily along development and reaches a peak around 25 daps (Woo et al., 2001; Arcalis et al., 2010). To support such a level of protein synthesis, the endoplasmic reticulum (ER) of the endosperm has to be highly active and well developed. Moreover, it needs to be flexible enough to be able to rapidly accommodate the synthesized proteins in newly formed storage organelles (Arcalis et al., 2014). Zeins do not carry a conventional ER retention sequence, but they assemble into aggregates within the ER lumen leading to the formation of protein bodies (PBs), surrounded by a ribosome studded membrane (Lending and Larkins, 1989). The induction of PBs has been extensively studied in maize (Lending and Larkins, 1989; Guo et al., 2013), but also in heterologous systems such as tobacco seeds, in which recombinant zeins from different subfamilies have been expressed (Coleman et al., 1996, 2004; Bagga et al., 1997).

In spite of the abundant literature about PBs, the exact mechanism of their formation is not yet fully understood, and little is known about the morphology and development of the ER in cereal endosperm. Most of the available data are based either on confocal or transmission electron microscopy (TEM). Confocal microscopy is an excellent tool that allows *in vivo* imaging and provides three-dimensional (3D) information. Moreover, the use of fluorescent tags in combination with different γ-zein fragments in leaves has revealed the crucial role of the N-terminal part of 27-kD γ-zein in the initiation of the formation of PBs (Llop-Tous et al., 2010), which is not restricted to specific tissues or organelles (Hofbauer et al., 2014). However, confocal microscopy has a limited resolution. Electron microscopy, on the other hand, offers a high resolution and early studies on PB biogenesis and distribution of zeins within the PBs were mostly based on TEM pictures providing detailed, but only two-dimensional information, at the ultrastructural level (Lending and Larkins, 1989). Modern 3D imaging techniques with nanoscale resolution include serial section TEM or electron tomography. Both techniques offer the possibility to image volumes at ultrastructural level, but the former is technically challenging and the latter is restricted to small volumes (Kittelmann, 2018). The recent development of block face imaging techniques such as serial block face scanning electron microscopy (SBF-SEM) facilitates the 3D study of ultrastructural features by generating large numbers of images aligned in the *z*-axis that allow not only the generation of 3D models but also the rapid screening of a large sample volume (Kittelmann, 2018).

In order to investigate the ultrastructure of the ER and its spatial relationship with nascent PBs and oil bodies in a highly specialized storage tissue, we have generated 3D models based on SBF-SEM of maize endosperm cells at two stages of seed development.

MATERIALS AND METHODS

Plant Material

Experiments were performed in wild-type (WT) maize plants (HiII) grown in soil in a growth chamber with a 13-h photoperiod, 25/22°C day/night temperatures and 70% relative humidity. Seeds were harvested at two different developmental stages, 14 and 21 days after pollination (dap) that correspond to the stages 2 and 3 of maize seed development described in Arcalis et al. (2010).

Sample Preparation for Electron Microscopy

Thin slices of maize seed tissue were cut under the silk hair scar with a razor blade, small tissue pieces of about 1 mm^3 including the aleurone layer were then excised and immediately immersed in fixative solution (2.5% glutaraldehyde and 2% paraformaldehyde in 0.1 M cacodylate buffer, pH 7.4). After several washing steps with cacodylate buffer (0.1 M, pH 7.4), samples were subjected to osmium impregnation by incubation in 2% osmium tetroxide and 0.2% ruthenium red in 0.1 M cacodylate buffer (pH 7.4) for 1 h, followed by 1% (w/v) thiocarbohydrazide (TCH) solution in ultrapure water for 45 min and 2% aqueous osmium tetroxide for an additional hour. TCH acts as a mordant that allows deposition of additional osmium to the original osmium sites. Moreover, it makes the specimen more conductive to electrons, preventing excess surface charging of the sample that leads to poor quality images under the SEM (Tapia et al., 2012 and references therein). In order to improve the contrast of the sample, uranyl acetate (UA) was used in combination with lead aspartate. *En bloc* staining was performed overnight with 2% aqueous UA, followed by Walton's lead aspartate (Walton, 1979) for 30 min. Tissue pieces were thoroughly rinsed after each step, before proceeding to the next. Samples were dehydrated through an ethanol series and prior to resin infiltration, samples were incubated in pure acetone. Dehydrated samples were progressively infiltrated in epoxy resin, embedded in flat molds and polymerized at 60°C during 24 h.

Resin blocks were trimmed in such a way that the aleurone layer was retained in all sections to facilitate orientation within the tissue. Sections with silver interferences were collected on copper grids and observed using a FEI Tecnai G2 transmission electron microscope operating at 160 kV. At least three sections per developmental stage were analyzed.

Serial Block Face Imaging

Tissue blocks with an approximate surface of 3600 μm^2 were fixed with silver conductive epoxy (TED PELLA Inc., United States) on 8–mm SBEM stubs (TED Pella Inc., United States) and hardened for 24 h at 60°C. Subsequently, samples were sputter-coated with a 40–nm gold layer prior to volume imaging in a Volumescope SEM (Thermo Fisher Scientific, United States). Images were collected at 1.78 kV, with a beam current of 100 pA. Pixel size was 5 nm and section thickness 40 nm. The obtained stack of images was scaled to 25% and aligned with ImageJ and the reconstruction of endomembranes was done with Amira software (Thermo Fisher Scientific, United States). At least five different stacks were obtained for each of the time points studied and one representative model of each developmental stage was generated.

RESULTS

Once differentiated, the cereal endosperm consists of four different cell types, including the embryo-surrounding region, transfer cells, the starchy endosperm and the aleurone layer. The aleurone layer covers the entire perimeter of the endosperm except for the transfer cell region (Olsen, 2001). In the case of maize, the aleurone is a monolayer of regular, cuboidal cells, with a thick cell wall and a prominent nucleus (**Figure 1A**). Early in endosperm development, complete cellularization occurs by centripetal growth of the cell layers, toward the center of the endospermal cavity (Olsen, 2001). Subsequently, the final population of endosperm cells is generated via mitotic cell divisions, whereby the endosperm cells adjacent to the aleurone layer (sub-aleurone) are mitotically more active than the inner starchy endosperm cells and retain their mitotic activity until

later during seed development (Sabelli and Larkins, 2009). Thus, a developmental gradient exists within a seed, since the cells in the sub-aleurone are younger than those found in deeper layers of the endosperm (starchy endosperm). The centripetal maturation of the endosperm is revealed in **Figure 1A**, showing a representative cross section comprising aleurone, sub-aleurone and first starchy endosperm cell layers of a maize seed at mid-developmental stage, when the PBs are already formed (Stage 2, Arcalis et al., 2010). Cells in the sub-aleurone are smaller and contain many electron-transparent vacuole-like structures and very few, small starch grains. Only three to four cell layers deeper, in the starchy endosperm, the morphology of the cells is completely different: they are much larger and are at least double the size of the sub-aleurone cells. Moreover, the number of vacuole-like structures in the starchy endosperm is significantly reduced and abundant, large starch grains are observed (**Figure 1A**). In addition, numerous small PBs of around 600 nm in diameter are present, as well as highly electron-dense oil bodies. Large and abundant ER strands, with ribosome-studded membranes are characteristic of these cells (**Figure 1B** and **Supplementary Figure S1**).

In order to investigate the 3D organization of the ER and PBs in starchy endosperm cells in developing maize seeds, SBF-SEM was performed in samples corresponding to two different developmental stages: 14 daps (stage 2) and 21 daps (stage 3). A representative data set was selected for generating a 3D model. **Figure 2A** shows a reconstructed volume of a younger cell (stage 2) of around 2600 μm^3 from different angles, with a resolution of 20 × 20 × 40 nm. The high lateral (*x*, *y*) and axial (*z*) resolution (slice thickness) enabled 3D analysis of specific ER strands from the block face (*xy*) that extended in the depth through the *z* plane, along 14 μm. It is also interesting to note the tangential disposition of the PBs to the ER strands (**Figure 2A**). Although these observations on the planes of the z-stack already give an impression of the 3D structure of the ER and the disposition of the PBs, it is only when those structures are rendered in a model that the architecture of the ER can be properly observed. Thus,

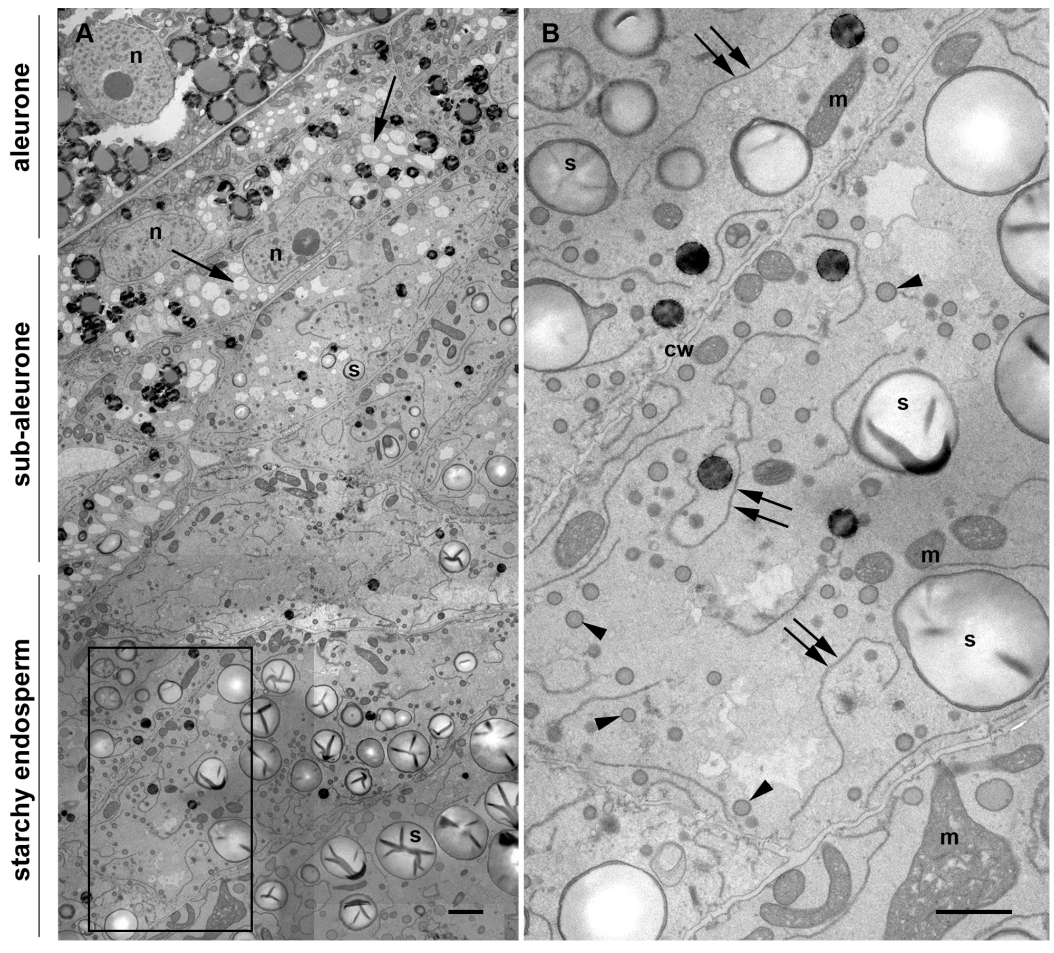

FIGURE 1 | Transmission electron microscopy of a maize seed at mid-developmental stage (14 dap, Stage 2). **(A)** Composed image comprising aleurone, sub-aleurone, and starchy endosperm. The nucleus (n) and the prominent electron transparent vacuole-like structures (arrows), as well as small, scarce starch grains (s) are indicated in the sub-aleurone cells. Large and abundant starch granules (s) are found in the starchy endosperm. **(B)** Enlargement from inset in [**(A)**, framed box], showing starchy endosperm cells with prominent ER strands (double arrows), abundant protein bodies (arrowheads) and starch grains (s). Cell walls (cw), mitochondria (m). Scale bars, 2 μm.

the 3D rendering of the ER membranes (**Figure 2B**) shows that at mid-developmental stage, maize endosperm cells possess massive ER sheets, extending all through the cell, and that the presence of tubules is negligible. Additionally, it can also be observed that the PBs, as well as oil bodies, bud from different z-planes of the entire ER sheets. Moreover, according to these models, oil bodies appear randomly distributed in domains neighboring PBs (**Figures 2C,E** and **Supplementary Video S1**). In later developmental stages, when the zein synthesis reaches its peak, the model is also valid. At 21 dap, the ER-PB network has become much denser. While the number of oil bodies is not significantly higher, PBs are more abundant and larger (**Figures 2D,E**). It is interesting to note that in older seeds, the cisternae are still predominant but are not as large as in younger cells, probably because increasing portions of ER membrane are now forming part of the nascent PBs (**Figures 2D,E**).

DISCUSSION

The ER constitutes the entry point of the secretory pathway and plays a crucial role in the biosynthesis of diverse molecules within the cells. It is the organelle with the largest membrane surface area, consisting of a network of tubules and cisternae. Its morphology depends on the cell specialization and developmental stage (Stefano et al., 2014), and also other parts of the endomembrane system are subject to dynamic remodeling in response to physiological and developmental cues. As observed in **Figure 1**, the changes in the endomembrane system of maize endosperm cells are obvious and occur rapidly, since even adjacent cells show a distinct morphology. Thus, cells immediately under the sub-aleurone contain numerous vacuole-like structures and fewer PBs, whereas the neighboring starchy endosperm cells are characterized by the frequent presence of PBs and remarkably long ER strands. These changes are not exclusively found in maize endosperm, but are a general feature of cereal endosperm cells, in which the synthesis of seed storage proteins is accompanied by their deposition in storage organelles that are formed *de novo* (Arcalis et al., 2014). The apparent expansion of the ER that is accompanied by the appearance of the first PBs could be due to the increasing synthesis of zeins and might be needed to facilitate the formidable task for the synthetic machinery. Another example of ER expansion upon onset of high protein synthesis rates can be found in the B-cells of the mammalian immune system. Upon antigen stimulation, B-type lymphocytes can reach secretion rates of 3000 antibody molecules per second (King and Corley, 1989). In order to accommodate such an enormous protein load, the ER in these cells changes from rudimentary in a steady stage to a well-developed ER network containing the whole chaperon machinery needed for correct protein folding. Under the electron microscope, stimulated B-cells, as well as other highly differentiated secretory cells, like pancreatic exocrine cells, show a highly compacted ER ultrastructure, with rough ER cisternae densely studded with ribosomes (Barlowe, 2010; Kirk et al., 2010). Although maize endosperm cells do not reach the level of protein synthesis typically found in B-cells, parallels can be observed in the ER morphology, indicating that seed storage protein synthesis is enough to shift the balance in favor of sheets. There are different factors that control the rearrangement of the plant ER, including the actin cytoskeleton (Sparkes et al., 2009) and ER-shaping proteins like reticulons. Reticulons are found in areas of the ER with high curvature, e.g., in tubules (Shibata et al., 2008; Zurek et al., 2011), but they also play a role in the stabilization of the edge of ER cisternae (Tolley et al., 2008, 2010). Loss of function of ROOT HAIR DEFECTIVE 3 (RHD3), which participates in the shaping of the plant ER, is lethal, thus indicating that the control of the ER shape is important for the cell (Stefano and Brandizzi, 2018). In order to fully understand the mechanisms controlling ER morphology in endosperm cells, the expression patterns of these different plant ER shapers along endosperm maturation need to be determined and correlated with developmental studies at the submicron level.

It has been an open question whether PB formation and budding occurs preferably in ER areas with high curvature, such as tubules or the edge of the cisternae, or rather in flat areas of sheets. The anecdotic presence of ER tubules in developing maize endosperm cells, together with the fact that ribosomes are less frequently found on the surface of tubules (Shibata et al., 2006, 2010), indicates that a preference for PB formation from sheets is more likely. The use of 3D electron microscopy allowed us to conclude that PBs are formed within ER cisternae and that the entire surface of these cisternae is suitable for budding, without obvious ER domains being dedicated to the formation of PBs. Indeed, we could observe several oil bodies budding from the same ER cisternae in close proximity to PBs, indicating that no specific domains are defined in the ER of maize endosperm cells for the production of proteins or lipids.

Zeins are packed within the ER in spherical protein bodies with a final diameter of around 1 μm. Similar to other cereals like rice, wheat or barley, prolamins packed in PBs do not proceed through the secretory pathway in maize because they are transport incompatible. A goal in this study was to establish whether the majority of zein bodies remain in contact with the ER lumen or become terminal cytosolic organelles. Several previous studies have addressed this question using ectopically induced PBs. Llop-Tous et al. (2010) determined that mature Zera-induced PBs in *Nicotiana benthamiana* leaves remained connected with the ER. By co-expressing a soluble fluorescent protein in the ER (YFP-KDEL), they could observe that after photobleaching, YFP-KDEL diffused rapidly through the ER to reach the periphery of the bleached protein bodies. Similarly, Saberianfar et al. (2016) performed a series of photoconversion experiments on zein bodies also ectopically expressed in *N. benthamiana* leaves. Different to photobleaching, the recovery of fluorescence by newly synthesized protein is minimized when using photoconversion. The irreversible conversion of GFP into DsRed allowed the authors to track the photoconverted GFP within a PB or a group of PBs to neighboring or even distal PBs, providing evidence that PBs communicate with each other through the ER, and therefore the authors concluded that they remain attached to the ER

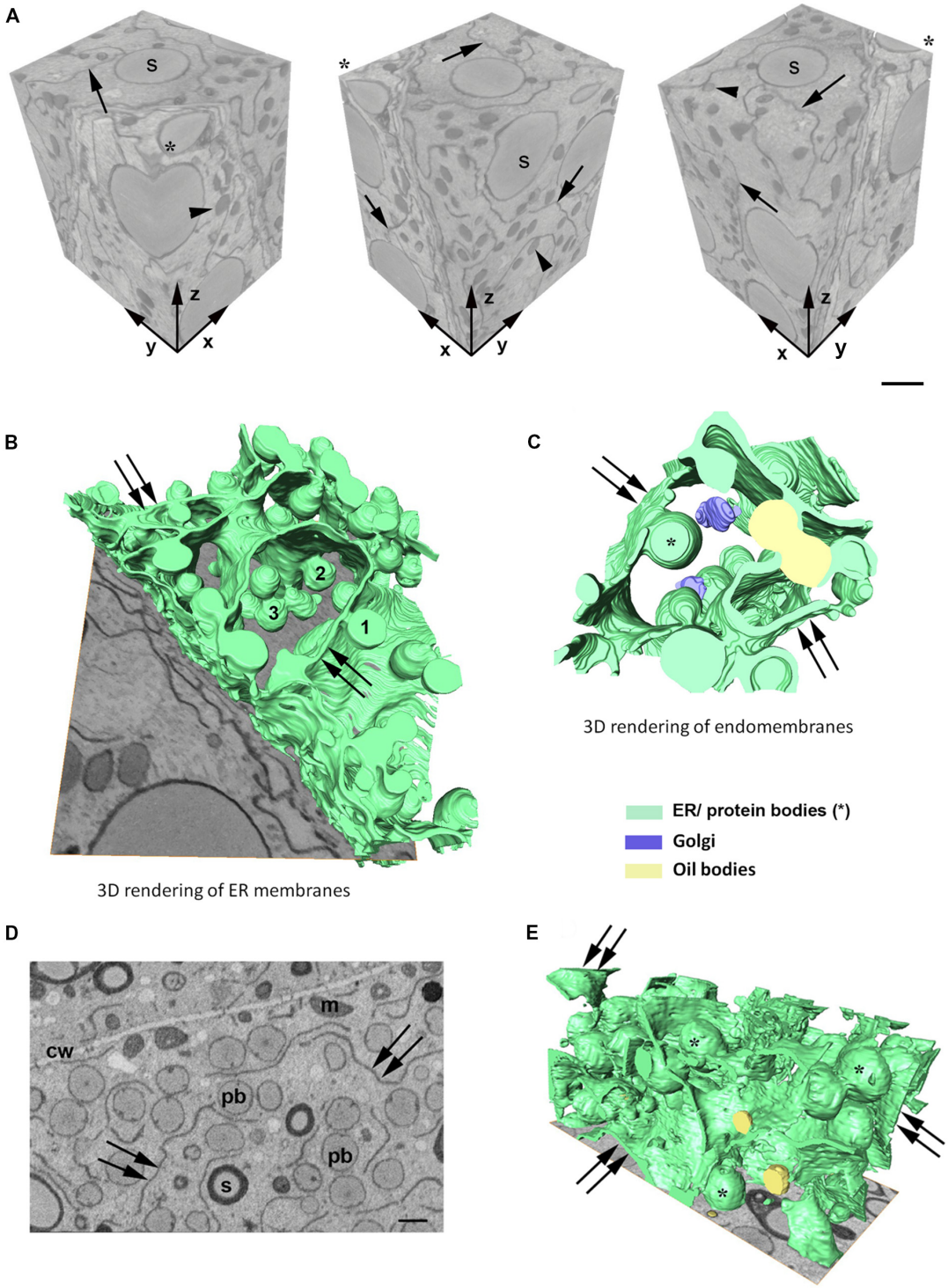

FIGURE 2 | (A) Serial block face imaging of a starchy endosperm cell at mid-developmental stage (14 dap, Stage 2) and cut at 40-nm increments. Reconstructed volume, shown from different angles (asterisk marks the same corner at different positions). Note the high resolution in the *z* axis. Arrows mark the ER and arrowheads the protein bodies. Number of slices: 350, total volume: 2646 μm^3, pixel size 20 × 20 nm. Scale bar, 1 μm. **(B–E)** 3D rendering of membranes in endosperm cells at different developmental stages. **(B,C)** Developmental stage 2 (14 dap). **(D,E)** Developmental stage 3 (21 dap). 3D rendering of ER membranes **(B)** and endomembranes **(C)** in a starchy endosperm cell. Massive ER sheets (double arrows) and abundant protein bodies (1, 2, 3) are budding from different *z*-positions **(B)**. Oil bodies bud from ER sheets (double arrows) neighboring the domains where PBs are formed **(C)**. **(D)** Representative z-stack image showing shorter ER strands (double arrow) and abundant protein bodies (>1 μm, pb). Cell wall (cw), mitochondria (m), starch (s). Scale bar, 1 μm. **(E)** 3D rendering of membranes. Smaller ER sheets (double arrow), protein bodies (*).

(Saberianfar and Menassa, 2017). Based on their observations, the authors postulated a working model of PB formation and development. With our study, we provide information about the native ER-PB network at an ultrastructural level and we combine the high resolution of TEM with 3D modeling, allowing us to confirm that zein bodies are connected with the continuous ER network, not only in heterologous systems, but in the native system, i.e., the maize seed.

In conclusion, our study demonstrates that the development of 3D electron microscopy imaging techniques for ultrastructural volume reconstruction allows to address long-standing questions regarding the spatial relationship of membrane organelles and opens a new and exciting perspective on the endomembrane system of plant cells.

DATA AVAILABILITY STATEMENT

The original contributions presented in the study are included in the article/**Supplementary Material**, further inquiries can be directed to the corresponding author/s.

AUTHOR CONTRIBUTIONS

EA and ES contributed to the conception and design of the study and wrote the manuscript. EA and UH-D designed and carried out the electron microscopy and SBF-SEM experiments. EA and LZ analyzed the data and generated the 3D models. All authors contributed to manuscript revision, read, and approved the submitted version.

FUNDING

The work was supported by the Austrian Science Fund FWF (I1461-B16 and I2823-B25).

ACKNOWLEDGMENTS

The authors thank Dietmar Pum (Department of Nanobiotechnology, BOKU, Vienna) for technical advice and acknowledge the HRSM project NANOBILD for infrastructure support.

SUPPLEMENTARY MATERIAL

The Supplementary Material for this article can be found online at: https://www.frontiersin.org/articles/10.3389/fpls.2020.00809/full#supplementary-material

FIGURE S1 | Transmission Electron Microscopy. Developing endosperm cell at mid-developmental stage. Ribosomes decorate the membrane around the protein body (pb) and also the ER membrane (arrowheads). Protein storage vacuole (PSV), rough endoplasmic reticulum (rER), starch (s). Scale bar, 0.5 μm.

VIDEO S1 | 3D model of ER and protein bodies in young endosperm cells (stage 2).

REFERENCES

Arcalis, E., Ibl, V., Peters, J., Melnik, S., and Stoger, E. (2014). The dynamic behavior of storage organelles in developing cereal seeds and its impact on the production of recombinant proteins. *Front. Plant Sci.* 5:439. doi: 10.3389/fpls.2014.00439

Arcalis, E., Stadlmann, J., Marcel, S., Drakakaki, G., Winter, V., Rodriguez, J., et al. (2010). The changing fate of a secretory glycoprotein in developing maize endosperm. *Plant Physiol.* 153, 693–702. doi: 10.1104/pp.109.152363

Bagga, S., Adams, H. P., Rodriguez, F. D., Kemp, J. D., and Sengupta-Gopalan, C. (1997). Coexpression of the maize delta-zein and beta-zein genes results in stable accumulation of delta-zein in endoplasmic reticulum-derived protein bodies formed by beta-zein. *Plant Cell* 9, 1683–1696. doi: 10.1105/tpc.9.9.1683

Barlowe, C. (2010). ER sheets get roughed up. *Cell* 143, 665–666. doi: 10.1016/j.cell.2010.11.011

Coleman, C. E., Herman, E. M., Takasaki, K., and Larkins, B. A. (1996). The maize gamma-zein sequesters alpha-zein and stabilizes its accumulation in protein bodies of transgenic tobacco endosperm. *Plant Cell* 8, 2335–2345. doi: 10.1105/tpc.8.12.2335

Coleman, C. E., Yoho, P. R., Escobar, S., and Ogawa, M. (2004). The accumulation of alpha-zein in transgenic tobacco endosperm is stabilized by co-expression of beta-zein. *Plant Cell Physiol.* 45, 864–871. doi: 10.1093/pcp/pch104

Flint-Garcia, S. A., Bodnar, A. L., and Scott, M. P. (2009). Wide variability in kernel composition, seed characteristics, and zein profiles among diverse maize inbreds, landraces, and teosinte. *Theor. Appl. Genet.* 119, 1129–1142. doi: 10.1007/s00122-009-1115-1

Guo, X., Yuan, L., Chen, H., Sato, S. J., Clemente, T. E., and Holding, D. R. (2013). Nonredundant function of zeins and their correct stoichiometric ratio drive protein body formation in maize endosperm. *Plant Physiol.* 162, 1359–1369. doi: 10.1104/pp.113.218941

Hofbauer, A., Peters, J., Arcalis, E., Rademacher, T., Lampel, J., Eudes, F., et al. (2014). The induction of recombinant protein bodies in different subcellular compartments reveals a cryptic plastid-targeting signal in the 27-kDa gamma-Zein sequence. *Front. Bioeng. Biotechnol.* 2:67. doi: 10.3389/fbioe.2014.00067

King, L. B., and Corley, R. B. (1989). Characterization of a presecretory phase in B-cell differentiation. *Proc. Natl. Acad. Sci. U.S.A.* 86, 2814–2818. doi: 10.1073/pnas.86.8.2814

Kirk, S. J., Cliff, J. M., Thomas, J. A., and Ward, T. H. (2010). Biogenesis of secretory organelles during B cell differentiation. *J. Leukoc. Biol.* 87, 245–255. doi: 10.1189/jlb.1208774

Kittelmann, M. (2018). 3D Electron Microscopy of the ER. *Methods Mol. Biol.* 1691, 15–21. doi: 10.1007/978-1-4939-7389-7_2

Lending, C. R., and Larkins, B. A. (1989). Changes in the zein composition of protein bodies during maize endosperm development. *Plant Cell* 1, 1011–1023. doi: 10.1105/tpc.1.10.1011

Llop-Tous, I., Madurga, S., Giralt, E., Marzabal, P., Torrent, M., and Ludevid, M. D. (2010). Relevant elements of a maize gamma-zein domain involved in protein body biogenesis. *J. Biol. Chem.* 285, 35633–35644. doi: 10.1074/jbc.M110.116285

Olsen, O. A. (2001). Endosperm development: cellularization and cell fate specification. *Annu. Rev. Plant Physiol. Plant Mol. Biol.* 52, 233–267. doi: 10.1146/annurev.arplant.52.1.233

Sabelli, P. A., and Larkins, B. A. (2009). The development of endosperm in grasses. *Plant Physiol.* 149, 14–26. doi: 10.1104/pp.108.129437

Saberianfar, R., and Menassa, R. (2017). Protein bodies: how the ER deals with high accumulation of recombinant proteins. *Plant Biotechnol. J.* 15, 671–673. doi: 10.1111/pbi.12730

Saberianfar, R., Sattarzadeh, A., Joensuu, J. J., Kohalmi, S. E., and Menassa, R. (2016). Protein bodies in leaves exchange contents through the endoplasmic reticulum. *Front. Plant Sci.* 7:693. doi: 10.3389/fpls.2016.00693

Shibata, Y., Shemesh, T., Prinz, W. A., Palazzo, A. F., Kozlov, M. M., and Rapoport, T. A. (2010). Mechanisms determining the morphology of the peripheral ER. *Cell* 143, 774–788. doi: 10.1016/j.cell.2010.11.007

Shibata, Y., Voeltz, G. K., and Rapoport, T. A. (2006). Rough sheets and smooth tubules. *Cell* 126, 435–439. doi: 10.1016/j.cell.2006.07.019

Shibata, Y., Voss, C., Rist, J. M., Hu, J., Rapoport, T. A., Prinz, W. A., et al. (2008). The reticulon and DP1/Yop1p proteins form immobile oligomers in the tubular endoplasmic reticulum. *J. Biol. Chem.* 283, 18892–18904. doi: 10.1074/jbc.M800986200

Sparkes, I., Runions, J., Hawes, C., and Griffing, L. (2009). Movement and remodeling of the endoplasmic reticulum in nondividing cells of tobacco leaves. *Plant Cell* 21, 3937–3949. doi: 10.1105/tpc.109.072249

Stefano, G., and Brandizzi, F. (2018). Advances in plant ER architecture and dynamics. *Plant Physiol.* 176, 178–186. doi: 10.1104/pp.17.01261

Stefano, G., Renna, L., and Brandizzi, F. (2014). The endoplasmic reticulum exerts control over organelle streaming during cell expansion. *J. Cell Sci.* 127(Pt 5), 947–953. doi: 10.1242/jcs.139907

Tapia, J. C., Kasthuri, N., Hayworth, K. J., Schalek, R., Lichtman, J. W., Smith, S. J., et al. (2012). High-contrast en bloc staining of neuronal tissue for field emission scanning electron microscopy. *Nat. Protoc.* 7, 193–206. doi: 10.1038/nprot.2011.439

Tolley, N., Sparkes, I., Craddock, C. P., Eastmond, P. J., Runions, J., Hawes, C., et al. (2010). Transmembrane domain length is responsible for the ability of a plant reticulon to shape endoplasmic reticulum tubules in vivo. *Plant J.* 64, 411–418. doi: 10.1111/j.1365-313X.2010.04337.x

Tolley, N., Sparkes, I. A., Hunter, P. R., Craddock, C. P., Nuttall, J., Roberts, L. M., et al. (2008). Overexpression of a plant reticulon remodels the lumen of the cortical endoplasmic reticulum but does not perturb protein transport. *Traffic* 9, 94–102. doi: 10.1111/j.1600-0854.2007.00670.x

Walton, J. (1979). Lead aspartate, an en bloc contrast stain particularly useful for ultrastructural enzymology. *J. Histochem. Cytochem.* 27, 1337–1342. doi: 10.1177/27.10.512319

Woo, Y. M., Hu, D. W., Larkins, B. A., and Jung, R. (2001). Genomics analysis of genes expressed in maize endosperm identifies novel seed proteins and clarifies patterns of zein gene expression. *Plant Cell* 13, 2297–2317. doi: 10.1105/tpc.010240

Zurek, N., Sparks, L., and Voeltz, G. (2011). Reticulon short hairpin transmembrane domains are used to shape ER tubules. *Traffic* 12, 28–41. doi: 10.1111/j.1600-0854.2010.01134.x

Conflict of Interest: The authors declare that the research was conducted in the absence of any commercial or financial relationships that could be construed as a potential conflict of interest.

frontiers in Plant Science

CORRECTION
published: 18 August 2020
doi: 10.3389/fpls.2020.01266

Corrigendum: 3D Electron Microscopy Gives a Clue: Maize Zein Bodies Bud From Central Areas of ER Sheets

*Elsa Arcalis, Ulrike Hörmann-Dietrich, Lukas Zeh and Eva Stoger**

Department of Applied Genetics and Cell Biology, University of Natural Resources and Life Sciences, Vienna, Vienna, Austria

OPEN ACCESS

Approved by:
Frontiers Editorial Office, Frontiers Media SA, Switzerland

***Correspondence:**
Eva Stoger
eva.stoeger@boku.ac.at

Specialty section:
This article was submitted to Plant Cell Biology, a section of the journal Frontiers in Plant Science

Received: *17 July 2020*
Accepted: *31 July 2020*
Published: *18 August 2020*

Citation:
Arcalis E, Hörmann-Dietrich U, Zeh L and Stoger E (2020) Corrigendum: 3D Electron Microscopy Gives a Clue: Maize Zein Bodies Bud From Central Areas of ER Sheets. Front. Plant Sci. 11:1266. doi: 10.3389/fpls.2020.01266

Keywords: cereal endosperm, electron microscopy, endomembrane system, endoplasmic reticulum, maize, protein bodies, volume electron microscopy

A Corrigendum on

3D Electron Microscopy Gives a Clue: Maize Zein Bodies Bud From Central Areas of ER Sheets
By Arcalis, E., Hormann-Dietrich, U., Zeh L., and Stoger, E. (2020). Front Plant Sci. 11:809. doi: 10.3389/fpls.2020.00809

MISSING FUNDING

In the original article, we neglected to acknowledge the HRSM project NANOBILD for infrastructure support. The corrected acknowledgment statement appears below:

The authors thank Dietmar Pum (Department of Nanobiotechnology, BOKU, Vienna) for technical advice and acknowledge the HRSM project NANOBILD for infrastructure support.

The authors apologize for this error and state that this does not change the scientific conclusions of the article in any way. The original article has been updated.

frontiers in Plant Science

MINI REVIEW
published: 17 June 2020
doi: 10.3389/fpls.2020.00756

Role of Autophagy in Male Reproductive Processes in Land Plants

*Takuya Norizuki[1,2], Naoki Minamino[2] and Takashi Ueda[2,3]**

[1]Department of Biological Sciences, Graduate School of Science, The University of Tokyo, Tokyo, Japan, [2]Division of Cellular Dynamics, National Institute for Basic Biology, Okazaki, Japan, [3]The Department of Basic Biology, SOKENDAI (The Graduate University for Advanced Studies), Okazaki, Japan

Autophagy is a highly conserved system for degrading and recycling cytoplasmic components. The identification of autophagy-related (*ATG*) genes, required for autophagosome formation, has led to numerous studies using *atg* mutants. These studies have revealed the physiological significance of autophagy in various functions of diverse organisms. In land plants, autophagy is required for higher-order functions such as stress responses and development. Although defective autophagy does not result in any marked defect in the reproductive processes of *Arabidopsis thaliana* under laboratory conditions, several studies have shown that autophagy plays a pivotal role in male reproduction in several land plants. In this review, we aim to summarize information on the role of autophagy in male reproductive processes in land plants.

Keywords: autophagy, male reproductive processes, tapetum, pollen germination, spermiogenesis

OPEN ACCESS

Edited by:
Erika Isono,
University of Konstanz, Germany

Reviewed by:
Kohki Yoshimoto,
Meiji University, Japan
Tamar Avin-Wittenberg,
The Hebrew University of Jerusalem, Israel

***Correspondence:**
Takashi Ueda
tueda@nibb.ac.jp

Specialty section:
This article was submitted to Plant Traffic and Transport, a section of the journal Frontiers in Plant Science

Received: *03 April 2020*
Accepted: *12 May 2020*
Published: *17 June 2020*

Citation:
Norizuki T, Minamino N and Ueda T (2020) Role of Autophagy in Male Reproductive Processes in Land Plants. Front. Plant Sci. 11:756. doi: 10.3389/fpls.2020.00756

INTRODUCTION

Autophagy is a highly conserved system for degrading and recycling cytoplasmic components, including organelles, in the vacuole or lysosome. Among the various modes of autophagy reported thus far, macroautophagy, hereafter referred to as autophagy, has been the most intensively studied. This type of autophagy begins with the formation of a membrane sac called the isolation membrane (also known as the phagophore), which extends, engulfing cytoplasmic components, to form a double membrane-bound autophagosome. The outer membrane of this autophagosome fuses with the vacuolar membrane, releasing the inner membrane-bound autophagic body into the vacuolar lumen, to be degraded by vacuolar hydrolases (**Figure 1A**; Takeshige et al., 1992; Baba et al., 1994). In the 1990s, a gene set required for autophagosome formation, hereafter referred to as core autophagy-related (*ATG*) genes, was identified by forward genetics in *Saccharomyces cerevisiae* (Tsukada and Ohsumi, 1993; Thumm et al., 1994; Harding et al., 1995; Klionsky et al., 2003). The core *ATG* genes encode a group of Atg proteins that form several functional units: the Atg1 complex, the phosphatidylinositol 3-kinase (PI3K) complex, Atg9, the Atg2-Atg18 complex, and two ubiquitin-like conjugation system complexes (Nakatogawa et al., 2009; Mizushima et al., 2011). One of the core Atg proteins, Atg8, is conjugated to phosphatidylethanolamine by the

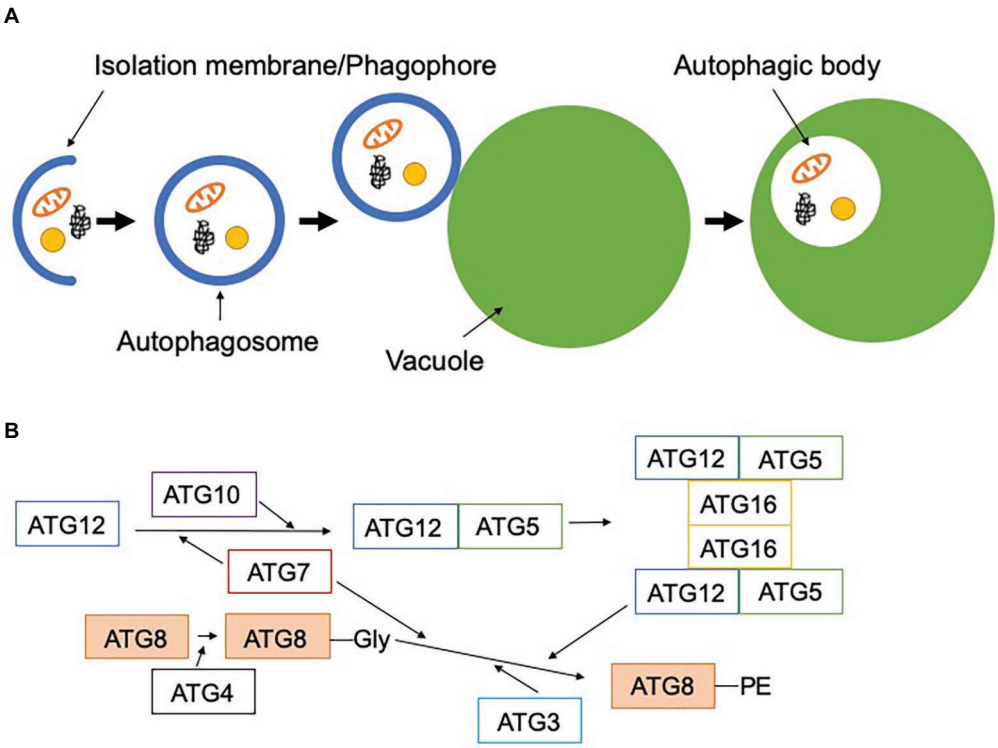

FIGURE 1 | Scheme of macroautophagy. **(A)** Macroautophagy starts with the formation of the isolation membrane (phagophore) in the cytosol. This engulfs cytoplasmic components and forms the double membrane-bound autophagosome. The outer membrane of the autophagosome fuses with the vacuolar membrane to release a single membrane-bound autophagic body into the vacuole. **(B)** Two ubiquitin-like conjugation systems are involved in the lipidation of ATG8. First, ATG12 is conjugated to ATG5 by ATG7 (E1-like) and ATG10 (E2-like), and ATG12-ATG5 forms a complex with ATG16. ATG8 is cleaved by ATG4, resulting in the exposure of glycine at its carboxyl terminus. This processed ATG8 is conjugated to phosphatidylethanolamine by ATG7 (E1-like), ATG3 (E2-like), and the dimeric ATG12-ATG5-ATG16 complex (E3-like). Lipidated ATG8 can be localized to the autophagosomal membrane.

ubiquitin-like conjugation systems (**Figure 1B**; Mizushima et al., 1998, 1999; Kirisako et al., 1999, 2000; Shintani et al., 1999; Ichimura et al., 2000; Hanada et al., 2007). Since lipidated Atg8 localizes to the isolation membrane from the beginning until after completion of autophagosome formation, it is commonly used as an autophagosome marker in various organisms (Kirisako et al., 1999; Kabeya et al., 2000; Yoshimoto et al., 2004). Reverse genetic approaches have unraveled the physiological roles of autophagy in a wide range of biological functions, including metabolic adaptation, intracellular quality control, and development (Mizushima and Komatsu, 2011; Mizushima, 2018).

In land plants (embryophytes), core *ATG* genes are highly conserved, and their functions are shown to be similar to homologs in yeast and mammals (Avin-Wittenberg et al., 2012; Yoshimoto, 2012; Norizuki et al., 2019). Studies of *Arabidopsis thaliana atg* mutants have demonstrated that autophagy is involved in responses to abiotic and biotic stressors such as nutrient starvation and pathogen attacks (Marshall and Vierstra, 2018). Furthermore, recent studies have shown that autophagy plays a critical role in male reproduction in various species including *Oryza sativa*, *Nicotiana tabacum*, *Marchantia polymorpha*, and *Physcomitrella patens* (Kurusu et al., 2014; Minamino et al., 2017; Sanchez-Vera et al., 2017; Zhao et al., 2020). In this review, we will briefly outline male reproduction in angiosperms and bryophytes, then summarize the physiological roles of autophagy in these processes.

MALE REPRODUCTION IN LAND PLANTS

Various organisms reproduce through a sexual process in which haploid male and female gametes fuse with each other to generate diploid zygotes. Male gametes in land plants are roughly classified into two types based on the presence or absence of flagella. In angiosperms and the majority of gymnosperms, male gametes lack a flagellum and are therefore immotile, requiring transportation to egg cells *via* pollen tubes to accomplish fertilization. Conversely, bryophytes, lycophytes, monilophytes, and some gymnosperms such as ginkgoes and cycads utilize motile male gametes called spermatozoids, which are equipped with two or more flagella, for sexual reproduction (Southworth and Cresti, 1997; Renzaglia and Garbary, 2001). In both cases, drastic reorganization of cellular components occurs during male gamete development (Hackenberg and Twell, 2019). In the angiosperm, *A. thaliana*, four haploid microspores are produced by meiosis of a diploid pollen mother

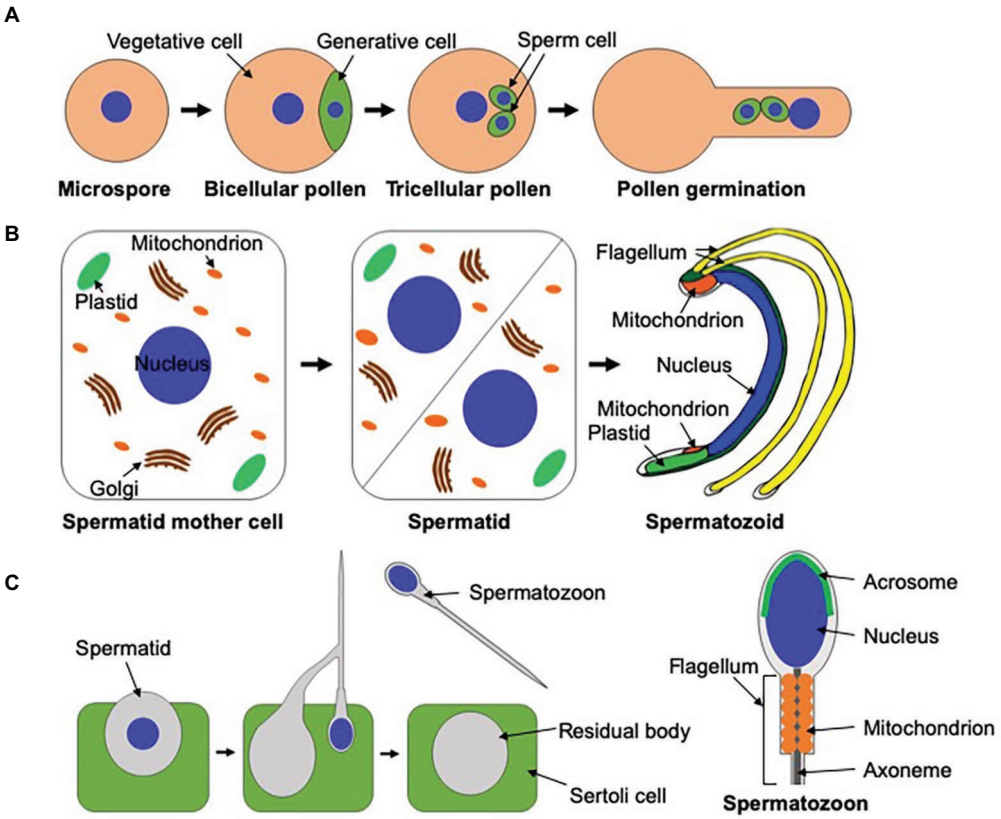

FIGURE 2 | Male gametogenesis in *Arabidopsis thaliana*, *Marchantia polymorpha*, and mammals. **(A)** In *A. thaliana*, microspores generated from meiosis of pollen mother cells undergo asymmetrical cell division to form vegetative and generative cells. Each generative cell divides symmetrically to yield two immotile sperm cells. Once pollen grains are attached to the surface of stigmas, they germinate to produce pollen tubes, which transport male gametes to female gametes. This figure is illustrated based on figures in Berger and Twell (2011) and Hackenberg and Twell (2019). **(B)** In *M. polymorpha*, spermatids are formed by the diagonal cell division of spermatid mother cells. Spermatids undergo a dynamic morphogenetic transformation called spermiogenesis to form spermatozoids. This figure was illustrated based on a figure in Shimamura (2016). **(C)** Dynamic cellular reorganization also takes place during mammalian spermiogenesis. Just before the release of spermatozoa, unnecessary cytoplasmic components are excluded from their cell bodies as the residual body, which is phagocytosed and degraded by the neiboring Sertoli cell.

cell. Each microspore divides asymmetrically to form vegetative and generative cells, and each generative cell undergoes symmetrical division to form two sperm cells (**Figure 2A**; Southworth and Russell, 2001; Berger and Twell, 2011). Once pollen grains are attached to the surface of stigmas, they germinate to produce pollen tubes, which are precisely guided to female gametes to deliver sperm cells (**Figure 2A**; Higashiyama and Takeuchi, 2015; Zheng et al., 2018). Pollen grains are covered by an outer cell wall called the exine, which provides chemical and physical protection against stressors. The tapetum surrounding pollen grains plays a pivotal role in the synthesis of the exine by supplying nutrients and metabolites to pollen grains (Ariizumi and Toriyama, 2011).

In contrast to angiosperms, in which the sporophytic generation is dominant in the life cycle, the gametophytic generation is dominant in bryophytes, and spermatozoids are generated without meiosis. In the liverwort, *M. polymorpha*, spermatids are produced by the diagonal division of spermatid mother cells. Spermatids then differentiate into motile spermatozoids through a dynamic morphological conversion called spermiogenesis. This process includes *de novo* synthesis of the locomotory apparatus, chromatin condensation, nuclear elongation, a decrease in the number of mitochondria, and exclusion of a major part of the cytoplasm (**Figure 2B**). Spermatozoids move toward female gametes in water to accomplish fertilization (Shimamura, 2016). Although the molecular mechanisms of male reproduction in angiosperms are well-documented, molecular mechanisms of spermatozoid formation in basal land plants remain mostly ambiguous (Hackenberg and Twell, 2019).

ROLE OF AUTOPHAGY IN MALE REPRODUCTIVE DEVELOPMENT IN ANGIOSPERMS

Studies of *A. thaliana atg* mutants have not detected a marked effect of *atg* mutations on sexual reproduction under normal experimental conditions, whereas these mutations affect vegetative growth in this species (Doelling et al., 2002; Hanaoka et al., 2002; Marshall and Vierstra, 2018). Mutation in *ATG6* is the only exception; the *atg6* mutant exhibits a defect in pollen

germination (Fujiki et al., 2007; Qin et al., 2007; Harrison-Lowe and Olsen, 2008). However, this defect might not be a result of defective autophagy. In yeast, Atg6 is also known as Vps30 and forms a complex with Vps34 and Vps15 to produce phosphatidylinositol 3-phosphate (PI3P) from phosphatidylinositol (Kihara et al., 2001). Because the *A. thaliana vps15* mutant also exhibits a defect in pollen germination and PI3P is also required for various cellular reactions beyond autophagy, defective pollen germination in the *atg6* mutant could result from a deficiency independent of autophagy (Fujiki et al., 2007; Qin et al., 2007; Harrison-Lowe and Olsen, 2008; Xu et al., 2011; Wang et al., 2012). Thus, *ATG*-dependent autophagy should be dispensable for male reproduction in *A. thaliana*. In addition, *Zea mays atg* mutants are fertile under normal experimental conditions (Li et al., 2015). However, autophagy is indispensable for male reproduction in *O. sativa* (Kurusu et al., 2014). In this species, autophagy is highly activated in the tapetum during microspore development (Kurusu et al., 2014; Hanamata et al., 2019). The tapetum undergoes programmed cell death to supply metabolites and nutrients to developing microspores, which is essential for pollen maturation and pollen tube elongation (Ku et al., 2003; Kawanabe et al., 2006; Li et al., 2006; Zhang et al., 2008). The *atg7* mutant exhibits limited anther dehiscence, and its pollen maturation and germination are severely compromised, resulting in markedly reduced male fertility (Kurusu et al., 2014; Sera et al., 2019). This could be explained by the fact that the *atg7* mutant exhibits defective programmed cell death of the tapetum, which could result in an insufficient supply of metabolites and nutrients to developing microspores (Kurusu et al., 2014). Given that autophagy executes programmed cell death during tracheary element differentiation in *A. thaliana* and embryogenesis in *Picea abies* (Kwon et al., 2010; Minina et al., 2013), autophagy could directly induce programmed cell death in the tapetum of *O. sativa*. Alternatively, autophagy might indirectly affect programmed cell death by regulating the metabolism of phytohormones. The phytohormone gibberellin plays an essential role in the development of tapeta and pollen in *O. sativa* (Chhun et al., 2007; Aya et al., 2009). Gibberellin accumulation is reduced in the anther of the *atg7* mutant, and treatment with active gibberellin (GA_4) fully and partially repairs the defect in pollen maturation and germination, respectively. This suggests that autophagy regulates the development of male reproductive tissues *via* the metabolism of gibberellin to some extent (Kurusu et al., 2017). The different effects of defective autophagy on male fertility between *O. sativa* and *A. thaliana* might result from differences in the structure of the tapetum, lipidic components of pollen grains, or both (Hanamata et al., 2014). Further study will be needed to clarify why autophagy is particularly required during male reproductive processes in *O. sativa*.

Cellular and molecular reorganization during pollen germination and pollen tube elongation also involve autophagy. In addition to the essential role of autophagy in *O. sativa* pollen germination described above (Kurusu et al., 2014), a similar process in *N. tabacum* also requires autophagy (Zhao et al., 2020). In this species, autophagy is highly activated during the initial stage of pollen germination, and autophagosomes accumulate around the germination aperture. *ATG2*, *ATG5*, and *ATG7* RNAi *N. tabacum* lines exhibit reduced rates of pollen germination, and in these lines, unlike in wild-type plants, a convex layer of the cytoplasm containing mitochondria remains at the germination aperture. Furthermore, a mitochondrial marker and the autophagosome marker ATG8 partially colocalize, and cardiolipin, a mitochondria-specific phospholipid, accumulates in the *ATG* RNAi lines. This information suggests that mitochondria are a target of autophagy in *N. tabacum* pollen grains (Zhao et al., 2020). In contrast, *atg* mutants of *A. thaliana* exhibit no detectable abnormality in pollen germination (Zhao et al., 2020). Vacuolar degradation systems other than *ATG*-dependent autophagy might contribute to reorganization of intracellular components during pollen germination in *A. thaliana*; this should be verified in future studies.

ROLE OF AUTOPHAGY DURING BRYOPHYTE SPERMIOGENESIS

The spermatozoids of most bryophytes consist of two flagella and a cell body, which comprises an elongated spiral nucleus, one plastid, two mitochondria, and trace amounts of cytosol (**Figure 2B**; Renzaglia and Garbary, 2001; Shimamura, 2016). Although reorganization of intracellular structures during bryophyte spermiogenesis has been intensively observed by transmission electron microscopy (TEM; Renzaglia and Garbary, 2001), the dynamics of intracellular reorganization remain unclear. The moss, *P. patens*, and the liverwort, *M. polymorpha*, are model plants associated with genetic studies (Rensing et al., 2008; Strotbek et al., 2013; Ishizaki et al., 2016; Bowman et al., 2017). Taking advantage of various organelle markers established in *M. polymorpha* (Kanazawa et al., 2016; Minamino et al., 2018), Minamino et al. (2017) observed the dynamics of organelles during spermiogenesis by confocal microscopy. They found that the size of the vacuole increases during spermiogenesis, and proteins in various organelles, including the plasma membrane, Golgi apparatus, and multivesicular endosomes, are transported to the luminal space of the vacuole during spermiogenesis. These findings indicate that the vacuole plays a major role in the removal and degradation of cellular components, including organelles, during *M. polymorpha* spermiogenesis (Minamino et al., 2017). Multivesicular endosomes and autophagosomes, which are involved in endocytic degradation of membrane proteins and degradation of cytoplasmic components, respectively, are frequently observed in spermatids undergoing spermiogenesis. The number of autophagosomes increases during spermiogenesis, and autophagic body-like structures are observed inside the vacuole, suggesting that autophagy is activated during spermiogenesis. These findings suggest that both autophagy and endocytic degradation play important roles during *M. polymorpha* spermiogenesis.

A critical role of autophagy in spermiogenesis has been identified in *P. patens* (Sanchez-Vera et al., 2017). Autolysosome-like structures are frequently observed in spermatids undergoing spermiogenesis; these may be formed by fusion between autophagosomes and the vacuole. An elevated expression level

of GFP-PpATG8e has also been detected in *P. patens* spermiogenesis, suggesting upregulated autophagy during this process. Furthermore, spermatozoids of the autophagy-defective *atg5* mutant are sterile and possess a wide spectrum of morphological abnormalities such as a larger amount of cytoplasm and an abnormally shaped nucleus. TEM observation has also revealed that the *atg5* mutation impairs decreasing the number of mitochondria and plastids, and flagellar formation during spermiogenesis (Sanchez-Vera et al., 2017). Thus, autophagy plays an important role in male gametogenesis in bryophytes, whose molecular regulatory mechanisms would be interesting targets to study.

MALE REPRODUCTION AND AUTOPHAGY IN THE MAMMALIAN SYSTEM

Mammalian sexual reproduction also utilizes motile male gametes with a flagellum (spermatozoa; **Figure 2C**), whose composition of intracellular structures is different from that of bryophytes. A mammalian spermatozoon possesses a nucleus at its head and a flagellum at the tail, and a mitochondrial helical sheath surrounds the axoneme at the midpiece (**Figure 2C**; Toure et al., 2020). Although the exclusion of the cytoplasm takes place during spermiogenesis in both mammals and bryophytes, their molecular mechanisms must be not the same. Although the residual body released from mammalian spermatids, which contain unnecessary cytoplasmic components, is removed by the phagocytic activity of the neighboring Sertoli cell during mammalian spermiogenesis (O'Donnell et al., 2011), phagocytosis by neighboring cells cannot take place in bryophytes due to the surrounding rigid cell wall (**Figure 2C**). Nevertheless, autophagy also plays indispensable roles during mammalian spermiogenesis. The germ cell-specific *ATG7* knockout in mice results in male sterility, exhibiting multiple defects in spermiogenesis, such as defective biogenesis of the acrosome (Wang et al., 2014). The acrosome, which is not present in the male gametes of plants, is a lysosome-related organelle required for fertilization (**Figure 2C**; Moreno and Alvarado, 2006; Ikawa et al., 2010; Khawar et al., 2019). LC3, which is homologous to yeast Atg8, is localized on the proacrosomal vesicles in an *ATG7*-dependent manner. These proacrosomal vesicles accumulate near the nucleus without fusing with each other in the *atg7* mutant, suggesting that autophagy is required for the biogenesis of the acrosome (Wang et al., 2014). Another marked defect in the mouse *atg7* mutant is the abnormal reorganization of microtubules during spermiogenesis. Irregular cytoskeletal structures are observed in autophagy-defective mouse embryonic fibroblasts (MEFs). PDLIM1, a regulator of cytoskeletons, accumulates in *atg7* MEFs and spermatids, and knockdown of PDLIM1 partially suppresses cytoskeletal defects in *atg7* MEFs. These results suggest that autophagy regulates cytoskeletal organization by degrading PDLIM1 (Shang et al., 2016). The *P. patens atg5* mutant also exhibits defective microtubule organization during flagella formation, which may reflect a similar mechanism of cytoskeletal regulation by autophagy during spermiogenesis. Further investigation to identify targets of autophagy during spermiogenesis would be needed to understand the precise functions of autophagy during plant spermiogenesis.

HOW IS AUTOPHAGY INVOLVED IN PLANT MALE REPRODUCTION?

As described above, autophagy is involved in distinct male reproductive processes in land plants. However, the regulatory networks and precise targets of autophagy remain almost unknown. The first step to address this would be to determine whether autophagic degradation during male reproduction in each plant species is devoted to bulk degradation of the cytoplasm or selective degradation of certain targets. Recent studies have revealed that a wide range of targets, including organelles and proteins, are selectively degraded by autophagy in various organisms, including *A. thaliana* (Marshall and Vierstra, 2018; Johansen and Lamark, 2020). Selective autophagy appears to operate during spermiogenesis in plants because organelles unnecessary for spermatozoids seem to be removed through autophagic degradation (Minamino et al., 2017; Sanchez-Vera et al., 2017). Bryophyte spermatozoids only retain two mitochondria and a plastid in the cell body, potentially resulting from selective removal of unneeded organelles by autophagy. Furthermore, in germinating pollen of *N. tabacum*, mitochondrial markers are colocalized with an autophagosome marker, implying selective autophagic degradation of mitochondria (mitophagy) (Zhao et al., 2020). However, the existence of mitophagy is not firmly demonstrated in plants thus far (Broda et al., 2018) and detailed electron microscopic or super-resolution microscopic observation of phagophores and autophagosomes is needed to be conclusive. Genetic or pharmacological inhibition of autophagic body degradation in the vacuole would also be effective in investigating the targets of autophagic degradation during male reproduction. Another promising approach is to identify proteins that interact with ATG8, since ATG8 is involved in cargo recognition in selective autophagy as well as in the formation and transport of autophagosomes in various organisms (Nakamura and Yoshimori, 2017; Marshall and Vierstra, 2018; Mizushima, 2019; Stephani and Dagdas, 2019; Johansen and Lamark, 2020). Since many land plants possess multiple *ATG8* genes, each of which could play a specialized function (Kellner et al., 2017), it would be also informative to examine whether any of *ATG8* genes are highly and/or specifically expressed during male reproductive development.

Another enigma is how autophagy is regulated during male reproduction in plants. As described above, autophagic activity is highly activated in certain male reproductive processes. Autophagic activity can be regulated at several distinct levels, for example, at the transcriptional and post-transcriptional levels, as reported in *S. cerevisiae* and mammals

(Fullgrabe et al., 2016; Corona Velazquez and Jackson, 2018). In *A. thaliana*, the expression of core *ATG* genes is spatiotemporally regulated, and the transcription factor TGA9 has been shown to positively regulate *ATG8* expression and autophagic activity (Slavikova et al., 2005; Rose et al., 2006; Wang et al., 2019). Post-transcriptional regulation has also been reported in *A. thaliana*, which is exemplified by that the TOR and SnRK1 complexes catalyze phosphorylation of and SINAT proteins mediate ubiquitylation of the ATG1 complex responding to the nutrient status (Chen et al., 2017; Huang et al., 2019; Van Leene et al., 2019; Qi et al., 2020). It would be useful to explore whether these regulations have a role in male reproduction in plants. Transcription factors responsible for the differentiation of male gametes have been identified in various organisms, including *M. polymorpha* (Hackenberg and Twell, 2019; Hisanaga et al., 2019). It would be worthwhile to study whether these transcription factors also regulate autophagic activities in order to understand the genetic regulation of autophagy during male reproduction.

AUTHOR CONTRIBUTIONS

TN and TU drafted the manuscript. NM edited the manuscript.

FUNDING

This study was financially supported by Grants-in-Aid for Scientific Research from the Ministry of Education, Culture, Sports, Science, and Technology of Japan [grant nos. 19H05675, 19H05760, and 18H02470 (to TU)], and a Grant-in-Aid from the Japan Society for the Promotion of Science (JSPS) (to TN, grant no. 19J13751).

REFERENCES

Ariizumi, T., and Toriyama, K. (2011). Genetic regulation of sporopollenin synthesis and pollen exine development. *Annu. Rev. Plant Biol.* 62, 437–460. doi: 10.1146/annurev-arplant-042809-112312

Avin-Wittenberg, T., Honig, A., and Galili, G. (2012). Variations on a theme: plant autophagy in comparison to yeast and mammals. *Protoplasma* 249, 285–299. doi: 10.1007/s00709-011-0296-z

Aya, K., Ueguchi-Tanaka, M., Kondo, M., Hamada, K., Yano, K., Nishimura, M., et al. (2009). Gibberellin modulates anther development in rice via the transcriptional regulation of GAMYB. *Plant Cell* 21, 1453–1472. doi: 10.1105/tpc.108.062935

Baba, M., Takeshige, K., Baba, N., and Ohsumi, Y. (1994). Ultrastructural analysis of the autophagic process in yeast: detection of autophagosomes and their characterization. *J. Cell Biol.* 124, 903–913. doi: 10.1083/jcb.124.6.903

Berger, F., and Twell, D. (2011). Germline specification and function in plants. *Annu. Rev. Plant Biol.* 62, 461–484. doi: 10.1146/annurev-arplant-042110-103824

Bowman, J. L., Kohchi, T., Yamato, K. T., Jenkins, J., Shu, S., Ishizaki, K., et al. (2017). Insights into land plant evolution garnered from the *Marchantia polymorpha* genome. *Cell* 171, 287.e15–304.e15. doi: 10.1016/j.cell.2017.09.030

Broda, M., Millar, A. H., and Van Aken, O. (2018). Mitophagy: a mechanism for plant growth and survival. *Trends Plant Sci.* 23, 434–450. doi: 10.1016/j.tplants.2018.02.010

Chen, L., Su, Z. Z., Huang, L., Xia, F. N., Qi, H., Xie, L. J., et al. (2017). The AMP-activated protein kinase KIN10 is involved in the regulation of autophagy in *Arabidopsis*. *Front. Plant Sci.* 8:1201. doi: 10.3389/fpls.2017.01201

Chhun, T., Aya, K., Asano, K., Yamamoto, E., Morinaka, Y., Watanabe, M., et al. (2007). Gibberellin regulates pollen viability and pollen tube growth in rice. *Plant Cell* 19, 3876–3888. doi: 10.1105/tpc.107.054759

Corona Velazquez, A. F., and Jackson, W. T. (2018). So many roads: the multifaceted regulation of autophagy induction. *Mol. Cell. Biol.* 38, e00303–e00318. doi: 10.1128/MCB.00303-18

Doelling, J. H., Walker, J. M., Friedman, E. M., Thompson, A. R., and Vierstra, R. D. (2002). The APG8/12-activating enzyme APG7 is required for proper nutrient recycling and senescence in *Arabidopsis thaliana*. *J. Biol. Chem.* 277, 33105–33114. doi: 10.1074/jbc.M204630200

Fujiki, Y., Yoshimoto, K., and Ohsumi, Y. (2007). An *Arabidopsis* homolog of yeast ATG6/VPS30 is essential for pollen germination. *Plant Physiol.* 143, 1132–1139. doi: 10.1104/pp.106.093864

Fullgrabe, J., Ghislat, G., Cho, D. H., and Rubinsztein, D. C. (2016). Transcriptional regulation of mammalian autophagy at a glance. *J. Cell Sci.* 129, 3059–3066. doi: 10.1242/jcs.188920

Hackenberg, D., and Twell, D. (2019). The evolution and patterning of male gametophyte development. *Curr. Top. Dev. Biol.* 131, 257–298. doi: 10.1016/bs.ctdb.2018.10.008

Hanada, T., Noda, N. N., Satomi, Y., Ichimura, Y., Fujioka, Y., Takao, T., et al. (2007). The Atg12-Atg5 conjugate has a novel E3-like activity for protein lipidation in autophagy. *J. Biol. Chem.* 282, 37298–37302. doi: 10.1074/jbc.C700195200

Hanamata, S., Kurusu, T., and Kuchitsu, K. (2014). Roles of autophagy in male reproductive development in plants. *Front. Plant Sci.* 5:457. doi: 10.3389/fpls.2014.00457

Hanamata, S., Sawada, J., Toh, B., Ono, S., Ogawa, K., Fukunaga, T., et al. (2019). Monitoring autophagy in rice tapetal cells during pollen maturation. *Plant Biotechnol.* 36, 99–105. doi: 10.5511/plantbiotechnology.19.0417a

Hanaoka, H., Noda, T., Shirano, Y., Kato, T., Hayashi, H., Shibata, D., et al. (2002). Leaf senescence and starvation-induced chlorosis are accelerated by the disruption of an *Arabidopsis* autophagy gene. *Plant Physiol.* 129, 1181–1193. doi: 10.1104/pp.011024

Harding, T. M., Morano, K. A., Scott, S. V., and Klionsky, D. J. (1995). Isolation and characterization of yeast mutants in the cytoplasm to vacuole protein targeting pathway. *J. Cell Biol.* 131, 591–602. doi: 10.1083/jcb.131.3.591

Harrison-Lowe, N. J., and Olsen, L. J. (2008). Autophagy protein 6 (ATG6) is required for pollen germination in *Arabidopsis thaliana*. *Autophagy* 4, 339–348. doi: 10.4161/auto.5629

Higashiyama, T., and Takeuchi, H. (2015). The mechanism and key molecules involved in pollen tube guidance. *Annu. Rev. Plant Biol.* 66, 393–413. doi: 10.1146/annurev-arplant-043014-115635

Hisanaga, T., Yamaoka, S., Kawashima, T., Higo, A., Nakajima, K., Araki, T., et al. (2019). Building new insights in plant gametogenesis from an evolutionary perspective. *Nat. Plants* 5, 663–669. doi: 10.1038/s41477-019-0466-0

Huang, X., Zheng, C., Liu, F., Yang, C., Zheng, P., Lu, X., et al. (2019). Genetic analyses of the *Arabidopsis* ATG1 kinase complex reveal both kinase-dependent and independent autophagic routes during fixed-carbon starvation. *Plant Cell* 31, 2973–2995. doi: 10.1105/tpc.19.00066

Ichimura, Y., Kirisako, T., Takao, T., Satomi, Y., Shimonishi, Y., Ishihara, N., et al. (2000). A ubiquitin-like system mediates protein lipidation. *Nature* 408, 488–492. doi: 10.1038/35044114

Ikawa, M., Inoue, N., Benham, A. M., and Okabe, M. (2010). Fertilization: a sperm's journey to and interaction with the oocyte. *J. Clin. Invest.* 120, 984–994. doi: 10.1172/JCI41585

Ishizaki, K., Nishihama, R., Yamato, K. T., and Kohchi, T. (2016). Molecular genetic tools and techniques for *Marchantia polymorpha* research. *Plant Cell Physiol.* 57, 262–270. doi: 10.1093/pcp/pcv097

Johansen, T., and Lamark, T. (2020). Selective autophagy: ATG8 family proteins, LIR motifs and cargo receptors. *J. Mol. Biol.* 432, 80–103. doi: 10.1016/j.jmb.2019.07.016

Kabeya, Y., Mizushima, N., Ueno, T., Yamamoto, A., Kirisako, T., Noda, T., et al. (2000). LC3, a mammalian homologue of yeast Apg8p, is localized in autophagosome membranes after processing. *EMBO J.* 19, 5720–5728. doi: 10.1093/emboj/19.21.5720

Kanazawa, T., Era, A., Minamino, N., Shikano, Y., Fujimoto, M., Uemura, T., et al. (2016). SNARE molecules in *Marchantia polymorpha*: unique and conserved features of the membrane fusion machinery. *Plant Cell Physiol.* 57, 307–324. doi: 10.1093/pcp/pcv076

Kawanabe, T., Ariizumi, T., Kawai-Yamada, M., Uchimiya, H., and Toriyama, K. (2006). Abolition of the tapetum suicide program ruins microsporogenesis. *Plant Cell Physiol.* 47, 784–787. doi: 10.1093/pcp/pcj039

Kellner, R., De la Concepcion, J. C., Maqbool, A., Kamoun, S., and Dagdas, Y. F. (2017). ATG8 expansion: a driver of selective autophagy diversification? *Trends Plant Sci.* 22, 204–214. doi: 10.1016/j.tplants.2016.11.015

Khawar, M. B., Gao, H., and Li, W. (2019). Mechanism of acrosome biogenesis in mammals. *Front. Cell Dev. Biol.* 7:195. doi: 10.3389/fcell.2019.00195

Kihara, A., Noda, T., Ishihara, N., and Ohsumi, Y. (2001). Two distinct Vps34 phosphatidylinositol 3-kinase complexes function in autophagy and carboxypeptidase Y sorting in *Saccharomyces cerevisiae*. *J. Cell Biol.* 152, 519–530. doi: 10.1083/jcb.152.3.519

Kirisako, T., Baba, M., Ishihara, N., Miyazawa, K., Ohsumi, M., Yoshimori, T., et al. (1999). Formation process of autophagosome is traced with Apg8/Aut7p in yeast. *J. Cell Biol.* 147, 435–446. doi: 10.1083/jcb.147.2.435

Kirisako, T., Ichimura, Y., Okada, H., Kabeya, Y., Mizushima, N., Yoshimori, T., et al. (2000). The reversible modification regulates the membrane-binding state of Apg8/Aut7 essential for autophagy and the cytoplasm to vacuole targeting pathway. *J. Cell Biol.* 151, 263–276. doi: 10.1083/jcb.151.2.263

Klionsky, D. J., Cregg, J. M., Dunn, W. A. Jr., Emr, S. D., Sakai, Y., Sandoval, I. V., et al. (2003). A unified nomenclature for yeast autophagy-related genes. *Dev. Cell* 5, 539–545. doi: 10.1016/S1534-5807(03)00296-X

Ku, S., Yoon, H., Suh, H. S., and Chung, Y. Y. (2003). Male-sterility of thermosensitive genic male-sterile rice is associated with premature programmed cell death of the tapetum. *Planta* 217, 559–565. doi: 10.1007/s00425-003-1030-7

Kurusu, T., Koyano, T., Hanamata, S., Kubo, T., Noguchi, Y., Yagi, C., et al. (2014). OsATG7 is required for autophagy-dependent lipid metabolism in rice postmeiotic anther development. *Autophagy* 10, 878–888. doi: 10.4161/auto.28279

Kurusu, T., Koyano, T., Kitahata, N., Kojima, M., Hanamata, S., Sakakibara, H., et al. (2017). Autophagy-mediated regulation of phytohormone metabolism during rice anther development. *Plant Signal. Behav.* 12:e1365211. doi: 10.1080/15592324.2017.1365211

Kwon, S. I., Cho, H. J., Jung, J. H., Yoshimoto, K., Shirasu, K., and Park, O. K. (2010). The Rab GTPase RabG3b functions in autophagy and contributes to tracheary element differentiation in *Arabidopsis*. *Plant J.* 64, 151–164. doi: 10.1111/j.1365-313X.2010.04315.x

Li, F., Chung, T., Pennington, J. G., Federico, M. L., Kaeppler, H. F., Kaeppler, S. M., et al. (2015). Autophagic recycling plays a central role in maize nitrogen remobilization. *Plant Cell* 27, 1389–1408. doi: 10.1105/tpc.15.00158

Li, N., Zhang, D. S., Liu, H. S., Yin, C. S., Li, X. X., Liang, W. Q., et al. (2006). The rice tapetum degeneration retardation gene is required for tapetum degradation and anther development. *Plant Cell* 18, 2999–3014. doi: 10.1105/tpc.106.044107

Marshall, R. S., and Vierstra, R. D. (2018). Autophagy: the master of bulk and selective recycling. *Annu. Rev. Plant Biol.* 69, 173–208. doi: 10.1146/annurev-arplant-042817-040606

Minamino, N., Kanazawa, T., Era, A., Ebine, K., Nakano, A., and Ueda, T. (2018). RAB GTPases in the basal land plant *Marchantia polymorpha*. *Plant Cell Physiol.* 59, 845–856. doi: 10.1093/pcp/pcy027

Minamino, N., Kanazawa, T., Nishihama, R., Yamato, K. T., Ishizaki, K., Kohchi, T., et al. (2017). Dynamic reorganization of the endomembrane system during spermatogenesis in *Marchantia polymorpha*. *J. Plant Res.* 130, 433–441. doi: 10.1007/s10265-017-0909-5

Minina, E. A., Filonova, L. H., Fukada, K., Savenkov, E. I., Gogvadze, V., Clapham, D., et al. (2013). Autophagy and metacaspase determine the mode of cell death in plants. *J. Cell Biol.* 203, 917–927. doi: 10.1083/jcb.201307082

Mizushima, N. (2018). A brief history of autophagy from cell biology to physiology and disease. *Nat. Cell Biol.* 20, 521–527. doi: 10.1038/s41556-018-0092-5

Mizushima, N. (2019). The ATG conjugation systems in autophagy. *Curr. Opin. Cell Biol.* 63, 1–10. doi: 10.1016/j.ceb.2019.12.001

Mizushima, N., and Komatsu, M. (2011). Autophagy: renovation of cells and tissues. *Cell* 147, 728–741. doi: 10.1016/j.cell.2011.10.026

Mizushima, N., Noda, T., and Ohsumi, Y. (1999). Apg16p is required for the function of the Apg12p-Apg5p conjugate in the yeast autophagy pathway. *EMBO J.* 18, 3888–3896. doi: 10.1093/emboj/18.14.3888

Mizushima, N., Noda, T., Yoshimori, T., Tanaka, Y., Ishii, T., George, M. D., et al. (1998). A protein conjugation system essential for autophagy. *Nature* 395, 395–398. doi: 10.1038/26506

Mizushima, N., Yoshimori, T., and Ohsumi, Y. (2011). The role of Atg proteins in autophagosome formation. *Annu. Rev. Cell Dev. Biol.* 27, 107–132. doi: 10.1146/annurev-cellbio-092910-154005

Moreno, R. D., and Alvarado, C. P. (2006). The mammalian acrosome as a secretory lysosome: new and old evidence. *Mol. Reprod. Dev.* 73, 1430–1434. doi: 10.1002/mrd.20581

Nakamura, S., and Yoshimori, T. (2017). New insights into autophagosome-lysosome fusion. *J. Cell Sci.* 130, 1209–1216. doi: 10.1242/jcs.196352

Nakatogawa, H., Suzuki, K., Kamada, Y., and Ohsumi, Y. (2009). Dynamics and diversity in autophagy mechanisms: lessons from yeast. *Nat. Rev. Mol. Cell Biol.* 10, 458–467. doi: 10.1038/nrm2708

Norizuki, T., Kanazawa, T., Minamino, N., Tsukaya, H., and Ueda, T. (2019). *Marchantia polymorpha*, a new model plant for autophagy studies. *Front. Plant Sci.* 10:935. doi: 10.3389/fpls.2019.00935

O'Donnell, L., Nicholls, P. K., O'Bryan, M. K., McLachlan, R. I., and Stanton, P. G. (2011). Spermiation: the process of sperm release. *Spermatogenesis* 1, 14–35. doi: 10.4161/spmg.1.1.14525

Qi, H., Li, J., Xia, F. N., Chen, J. Y., Lei, X., Han, M. Q., et al. (2020). *Arabidopsis* SINAT proteins control autophagy by mediating ubiquitylation and degradation of ATG13. *Plant Cell* 32, 263–284. doi: 10.1105/tpc.19.00413

Qin, G., Ma, Z., Zhang, L., Xing, S., Hou, X., Deng, J., et al. (2007). *Arabidopsis* AtBECLIN 1/AtAtg6/AtVps30 is essential for pollen germination and plant development. *Cell Res.* 17, 249–263. doi: 10.1038/cr.2007.7

Rensing, S. A., Lang, D., Zimmer, A. D., Terry, A., Salamov, A., Shapiro, H., et al. (2008). The *Physcomitrella* genome reveals evolutionary insights into the conquest of land by plants. *Science* 319, 64–69. doi: 10.1126/science.1150646

Renzaglia, K. S., and Garbary, D. J. (2001). Motile gametes of land plants: diversity, development, and evolution. *Crit. Rev. Plant Sci.* 20, 107–213. doi: 10.1080/20013591099209

Rose, T. L., Bonneau, L., Der, C., Marty-Mazars, D., and Marty, F. (2006). Starvation-induced expression of autophagy-related genes in *Arabidopsis*. *Biol. Cell* 98, 53–67. doi: 10.1042/BC20040516

Sanchez-Vera, V., Kenchappa, C. S., Landberg, K., Bressendorff, S., Schwarzbach, S., Martin, T., et al. (2017). Autophagy is required for gamete differentiation in the moss *Physcomitrella patens*. *Autophagy* 13, 1939–1951. doi: 10.1080/15548627.2017.1366406

Sera, Y., Hanamata, S., Sakamoto, S., Ono, S., Kaneko, K., Mitsui, Y., et al. (2019). Essential roles of autophagy in metabolic regulation in endosperm development during rice seed maturation. *Sci. Rep.* 9:18544. doi: 10.1038/s41598-019-54361-1

Shang, Y., Wang, H., Jia, P., Zhao, H., Liu, C., Liu, W., et al. (2016). Autophagy regulates spermatid differentiation via degradation of PDLIM1. *Autophagy* 12, 1575–1592. doi: 10.1080/15548627.2016.1192750

Shimamura, M. (2016). *Marchantia polymorpha*: taxonomy, phylogeny and morphology of a model system. *Plant Cell Physiol.* 57, 230–256. doi: 10.1093/pcp/pcv192

Shintani, T., Mizushima, N., Ogawa, Y., Matsuura, A., Noda, T., and Ohsumi, Y. (1999). Apg10p, a novel protein-conjugating enzyme essential for autophagy in yeast. *EMBO J.* 18, 5234–5241. doi: 10.1093/emboj/18.19.5234

Slavikova, S., Shy, G., Yao, Y., Glozman, R., Levanony, H., Pietrokovski, S., et al. (2005). The autophagy-associated Atg8 gene family operates both under favourable growth conditions and under starvation stresses in *Arabidopsis* plants. *J. Exp. Bot.* 56, 2839–2849. doi: 10.1093/jxb/eri276

Southworth, D., and Cresti, M. (1997). Comparison of flagellated and nonflagellated sperm in plants. *Am. J. Bot.* 84:1301. doi: 10.2307/2446056

Southworth, D., and Russell, S. (2001). "Male gametogenesis" in *Current trends in the embryology of angiosperms*. eds. S. S. Bhojwani and W.-Y. Soh (Dordrecht: Springer Netherlands), 1–16.

Stephani, M., and Dagdas, Y. (2019). Plant selective autophagy—still an uncharted territory with a lot of hidden gems. *J. Mol. Biol.* 432, 63–79. doi: 10.1016/j.jmb.2019.06.028

Strotbek, C., Krinninger, S., and Frank, W. (2013). The moss *Physcomitrella patens*: methods and tools from cultivation to targeted analysis of gene function. *Int. J. Dev. Biol.* 57, 553–564. doi: 10.1387/ijdb.130189wf

Takeshige, K., Baba, M., Tsuboi, S., Noda, T., and Ohsumi, Y. (1992). Autophagy in yeast demonstrated with proteinase-deficient mutants and conditions for its induction. *J. Cell Biol.* 119, 301–311. doi: 10.1083/jcb.119.2.301

Thumm, M., Egner, R., Koch, B., Schlumpberger, M., Straub, M., Veenhuis, M., et al. (1994). Isolation of autophagocytosis mutants of *Saccharomyces cerevisiae*. *FEBS Lett.* 349, 275–280. doi: 10.1016/0014-5793(94)00672-5

Toure, A., Martinez, G., Kherraf, Z. E., Cazin, C., Beurois, J., Arnoult, C., et al. (2020). The genetic architecture of morphological abnormalities of the sperm tail. *Hum. Genet.* doi: 10.1007/s00439-020-02113-x [Epub ahead of print].

Tsukada, M., and Ohsumi, Y. (1993). Isolation and characterization of autophagy-defective mutants of *Saccharomyces cerevisiae*. *FEBS Lett.* 333, 169–174. doi: 10.1016/0014-5793(93)80398-E

Van Leene, J., Han, C., Gadeyne, A., Eeckhout, D., Matthijs, C., Cannoot, B., et al. (2019). Capturing the phosphorylation and protein interaction landscape of the plant TOR kinase. *Nat. Plants* 5, 316–327. doi: 10.1038/s41477-019-0378-z

Wang, P., Nolan, T. M., Yin, Y., and Bassham, D. C. (2019). Identification of transcription factors that regulate ATG8 expression and autophagy in *Arabidopsis*. *Autophagy* 16, 123–139. doi: 10.1080/15548627.2019.1598753

Wang, H., Wan, H., Li, X., Liu, W., Chen, Q., Wang, Y., et al. (2014). Atg7 is required for acrosome biogenesis during spermatogenesis in mice. *Cell Res.* 24, 852–869. doi: 10.1038/cr.2014.70

Wang, W. Y., Zhang, L., Xing, S., Ma, Z., Liu, J., Gu, H., et al. (2012). *Arabidopsis* AtVPS15 plays essential roles in pollen germination possibly by interacting with AtVPS34. *J. Genet. Genomics* 39, 81–92. doi: 10.1016/j.jgg.2012.01.002

Xu, N., Gao, X. Q., Zhao, X. Y., Zhu, D. Z., Zhou, L. Z., and Zhang, X. S. (2011). *Arabidopsis* AtVPS15 is essential for pollen development and germination through modulating phosphatidylinositol 3-phosphate formation. *Plant Mol. Biol.* 77, 251–260. doi: 10.1007/s11103-011-9806-9

Yoshimoto, K. (2012). Beginning to understand autophagy, an intracellular self-degradation system in plants. *Plant Cell Physiol.* 53, 1355–1365. doi: 10.1093/pcp/pcs099

Yoshimoto, K., Hanaoka, H., Sato, S., Kato, T., Tabata, S., Noda, T., et al. (2004). Processing of ATG8s, ubiquitin-like proteins, and their deconjugation by ATG4s are essential for plant autophagy. *Plant Cell* 16, 2967–2983. doi: 10.1105/tpc.104.025395

Zhang, D. S., Liang, W. Q., Yuan, Z., Li, N., Shi, J., Wang, J., et al. (2008). Tapetum degeneration retardation is critical for aliphatic metabolism and gene regulation during rice pollen development. *Mol. Plant* 1, 599–610. doi: 10.1093/mp/ssn028

Zhao, P., Zhou, X. M., Zhao, L. L., Cheung, A. Y., and Sun, M. X. (2020). Autophagy-mediated compartmental cytoplasmic deletion is essential for tobacco pollen germination and male fertility. *Autophagy* 30, 1–13. doi: 10.1080/15548627.2020.1719722

Zheng, Y. Y., Lin, X. J., Liang, H. M., Wang, F. F., and Chen, L. Y. (2018). The long journey of pollen tube in the pistil. *Int. J. Mol. Sci.* 19:3529. doi: 10.3390/ijms19113529

Conflict of Interest: The authors declare that the research was conducted in the absence of any commercial or financial relationships that could be construed as a potential conflict of interest.

frontiers in Plant Science

ORIGINAL RESEARCH
published: 26 June 2020
doi: 10.3389/fpls.2020.00960

Redundant and Diversified Roles Among Selected *Arabidopsis thaliana* EXO70 Paralogs During Biotic Stress Responses

Tamara Pečenková[1,2], Andrea Potocká[1], Martin Potocký[1,2], Jitka Ortmannová[1], Matěj Drs[1,2], Edita Janková Drdová[1,2], Přemysl Pejchar[1,2], Lukáš Synek[1], Hana Soukupová[1], Viktor Žárský[1,2] and Fatima Cvrčková[2]*

[1] Institute of Experimental Botany, CAS, Prague, Czechia, [2] Department of Experimental Plant Biology, Faculty of Science, Charles University, Prague, Czechia

The heterooctameric vesicle-tethering complex exocyst is important for plant development, growth, and immunity. Multiple paralogs exist for most subunits of this complex; especially the membrane-interacting subunit EXO70 underwent extensive amplification in land plants, suggesting functional specialization. Despite this specialization, most Arabidopsis *exo70* mutants are viable and free of developmental defects, probably as a consequence of redundancy among isoforms. Our *in silico* data-mining and modeling analysis, corroborated by transcriptomic experiments, pinpointed several EXO70 paralogs to be involved in plant biotic interactions. We therefore tested corresponding single and selected double mutant combinations (for paralogs EXO70A1, B1, B2, H1, E1, and F1) in their two biologically distinct responses to *Pseudomonas syringae,* root hair growth stimulation and general plant susceptibility. A shift in defense responses toward either increased or decreased sensitivity was found in several double mutants compared to wild type plants or corresponding single mutants, strongly indicating both additive and compensatory effects of *exo70* mutations. In addition, our experiments confirm the lipid-binding capacity of selected EXO70s, however, without the clear relatedness to predicted C-terminal lipid-binding motifs. Our analysis uncovers that there is less of functional redundancy among isoforms than we could suppose from whole sequence phylogeny and that even paralogs with overlapping expression pattern and similar membrane-binding capacity appear to have exclusive roles in plant development and biotic interactions.

Keywords: exocyst, EXO70, *Arabidopsis thaliana*, redundancy, gene expression, lipid binding, biotic stress, root hairs

OPEN ACCESS

Edited by:
Eugenia Russinova, Ghent University, Belgium

Reviewed by:
Glenn Hicks, University of California, Riverside, United States
Marie-Theres Hauser, University of Natural Resources and Life Sciences Vienna, Austria
Chunhua Was Zhang, Purdue University, United States

****Correspondence:***
Tamara Pečenková
pecenkova@ueb.cas.cz

Specialty section:
This article was submitted to Plant Traffic and Transport, a section of the journal Frontiers in Plant Science

Received: *28 March 2020*
Accepted: *11 June 2020*
Published: *26 June 2020*

Citation:
Pečenková T, Potocká A, Potocký M, Ortmannová J, Drs M, Janková Drdová E, Pejchar P, Synek L, Soukupová H, Žárský V and Cvrčková F (2020) Redundant and Diversified Roles Among Selected Arabidopsis thaliana EXO70 Paralogs During Biotic Stress Responses. Front. Plant Sci. 11:960. doi: 10.3389/fpls.2020.00960

INTRODUCTION

The exocyst complex is evolutionarily conserved across eukaryotes and mutations impairing its function are often lethal, suggesting its important biological role (Koumandou et al., 2007; Martin-Urdiroz et al., 2016). Initial knowledge of the exocyst comes especially from studies in yeast, where this heterooctameric protein complex regulates exocytosis by mediating the physical tethering of secretory vesicles to the target plasma membrane (TerBush et al., 1996; Hsu et al., 2004). A distinct role in the process of tethering has been ascribed to each of the eight exocyst subunits. The SEC10 and SEC15 subunits mediate interaction of the complex with a vesicle *via* Rab GTPases (Roth et al., 1998; Guo et al., 1999). The EXO70 and SEC3 subunits direct the complex to the target membrane through an interaction with membrane phosphatidylinositol 4,5-bisphosphate (PIP2) (Boyd et al., 2004; He et al., 2007; Liu et al., 2007; Pleskot et al., 2015). The SEC6 subunit has been found to provide for an interaction with the SNARE complex but also to form the inner core of the complex with SEC8 (Dubuke et al., 2015; Picco et al., 2017), while subunits EXO84 and SEC5 mediate activation by Ral type GTPases (Moskalenko et al., 2002). The performance of the tethering function also requires an allosteric regulation of the EXO70 by the RHO GTPases (Wu et al., 2010; Rossi et al., 2020).

In land plants, several exocyst subunits underwent gene amplification, allowing formation of alternative complexes with at least partially distinct roles in the growth, development, and biotic interactions. In particular, the EXO70 subunit has evolved into a large gene family that *e.g.* in the genome of the model plant *Arabidopsis thaliana* consists of 23 EXO70 paralogs that can be classified into three subfamilies/clades and further into eight groups A-H (A in subfamily 1, B, C, D, E, F, H in subfamily 2 and G in subfamily 3; Elias et al., 2003; Synek et al., 2006; Chong et al., 2010; Cvrčková et al., 2012; Rawat et al., 2017; Žárský et al., 2020). Thus, the Arabidopsis exocyst can consist of SEC6, SEC8, one of 23 EXO70 isoforms, and one of two isoforms of SEC3, SEC5, SEC10, SEC15, and EXO84 each, resulting in 736 theoretically possible combinations that may act in various endomembrane compartments and plasma membrane domains, cells and tissues, developmental stages, and environmental situations. Even if the number of really occurring variants is substantially lower due to tissue-specific expression of some subunits isoforms, there are still numerous exocyst variants that must be coordinated in space and time to ensure proper functioning of the plant cell and organism (Žárský et al., 2013).

The multiplicity of the plant exocyst complex functions has been well documented. Distinct exocyst variants are involved in auxin transport, root and hypocotyl epidermal cell elongation, cytokinesis, pollen tube growth, seed coat formation, defense against pathogens, xylem differentiation, and leaf trichome development (Cole et al., 2005; Synek et al., 2006; Hála et al., 2008; Kulich et al., 2015; Sekereš et al., 2017; Vukašinović et al., 2017; Janková Drdová et al., 2019). On the subcellular level, exocyst participates in plasma membrane protein recycling, cytokinesis, autophagic targeting to the vacuole, and deposition of cell wall material, especially callose, to the pathogen attack site (Fendrych et al., 2010; Pecenková et al., 2011; Drdová et al., 2013; Žárský et al., 2013; Kulich et al., 2018; rev. in Pečenková et al., 2017b). It is well documented that several versions of the exocyst function simultaneously within the same cell (Sekereš et al., 2017).

As a consequence of the subunits' genes multiplication, especially in the case of EXO70, single gene knock-out mutations are unlikely to have dramatic phenotypes because of anticipated functional redundancy among the numerous paralogous genes, albeit there are a couple of exceptions. Loss of the main housekeeping variant EXO70A1 causes pleiotropic growth and developmental defects and sterility (Synek et al., 2006), and the double *exo70C1exo70C2* mutant cannot be produced due to at least one of these subunits, highly similar in terms of both sequence and gene expression pattern, being necessary for pollen tube tip growth (Synek et al., 2017).

While *A. thaliana* EXO70 isoforms are generally highly conserved, they are more diverged at their N- and C-termini, including a hypothetical lipid/PI(4,5)P2-binding C-terminal motif (Žárský et al., 2009). This variability indicates a possibility that this region contains a clue for the isoforms' functional specificity due to a differential lipid-binding capacity. During the various abiotic and biotic stress reactions, phospholipases are activated affecting the content of phosphatidyl inositol phosphate (PIP) species and phosphatidic acid (PA) that further function as both signaling and protein recruiting components of stress responses (review in Laxalt and Munnik, 2002; Wang, 2004). Therefore, the plant cell's need for multiple EXO70s may reflect the requirement for trafficking toward the target membranes with different lipid composition.

In order to explore the extent of specificity and redundancy among Arabidopsis EXO70 paralogs, we analyzed available transcriptome data with focus on response of individual paralogs to biotic stresses. Based on the expression patterns' overlaps, we generated several double mutants, aiming to achieve phenotypic deviations enhanced in comparison to corresponding single mutants. Indeed, our two approaches exploring the sensitivity to pathogenic bacteria *Pseudomonas* sp., *i.e.* a flooding assay (Ishiga et al., 2011) and a root hair growth stimulation assay (Pečenková et al., 2017a), revealed either aggravation or suppression of defense-related phenotypes for

Abbreviations: 3-SGC, 3-sulfogalactosylceramide; Chol, Cholesterol; CL, Cardiolipin; DAG, Diacylglycerol; dH_2O, Distilled water; EXO70 Exocyst subunit 70 (named according to its ***ca.*** 70 kDa size); HR, Hypersensitive response; LOF, Loss of function; LPA, Lysophosphatidic acid; LPC, Lysophosphocholine; PA, Phosphatidic acid; PC, Phosphatidylcholine; PE, Phosphatidylethanolamine; PG, Phosphatidylglycerol; PI, Phosphatidylinositol; PI(3)P, Phosphatidylinositol (3) phosphate; PI(3,4)P2, Phosphatidylinositol (3,4) bisphosphate; PI(3,5)P2, Phosphatidylinositol (3,5) bisphosphate; PI(3,4,5)P3, Phosphatidylinositol (3,4,5) trisphosphate; PI(4)P, Phosphatidylinositol (4) phosphate; PI(4,5)P2, Phosphatidylinositol (4,5) bisphosphate; PI(5)P, Phosphatidylinositol (5) phosphate; PIP, Phosphoinositides; PS, Phosphatidylserine; S1P, Sphingosine 1-Phosphate; SA, Salicylic acid; SM, Sphingomyelin; TG, Triglyceride; WT, Wild type.

some of the mutants' combinations. For several selected isoforms we also characterized both *in silico* and experimentally their lipid binding affinities, assuming that the lipid-binding capacity may hold one of the keys to functional specificity. Our results are documenting on-going evolutionary specialization of isoforms that may both overlap and compete in their functions.

MATERIALS AND METHODS

Plant Material and Growth Conditions

The following previously published Arabidopsis mutant lines were used in this study: *exo70A1-2* (SALK_135462, Synek et al., 2006), *exo70B1-1* (GABI_114C03, Kulich et al., 2013), *exo70B2-2* (SAIL_339-D07, Pecenková et al., 2011), *exo70E1* (SALK_084145, Redditt et al., 2019; primers for genotyping in **Supplementary Table 1**) *exo70F1* (SALK_036927, Synek et al., 2006), and *exo70H1* (SALK_042456, Pecenková et al., 2011). The following double mutants were generated by crossing: *exo70A1-2exo70B1-2* (further on *exo70A1exo70B1*), *exo70A1-2exo70B2-2* (further on *exo70A1exo70B2*), *exo70B1-1exo70B2-2* (*exo70B1exo70B2*), *exo70B2-2exo70H1* (*exo70B2exo70H1*), and *exo70E1exo70F1*, and the triple mutant *exo70A1-2exo70B2-2exo70H1* (*exo70A1exo70B2exo70H1*). The wild type (WT) Col-0 or out-crossed sister WT lines were used as controls to single and double mutant lines in pathogen sensitivity experiments. Primers used for the genotyping were the same as used in the above-cited original studies.

For seedlings and plants' cultivation, seeds were surface sterilized (3 min in 70% ethanol, 2 × 5 min in 10% commercial bleach, rinsed three times in sterile distilled water) and stratified for 2–3 days at 4°C. Seeds were then germinated and grown on vertical 1/2 × MS agar plates (half-strength Murashige and Skoog salts, Duchefa Biochemie, supplemented with 1% sucrose, vitamin mixture, and 1.6% plant agar, Duchefa Biochemie) at 21°C and 16 h of light per day for seven days.

Gene Expression Analysis

Published microarray transcriptome data were analyzed using the Genevestigator gene expression tool (Hruz et al., 2008). We only included Affymetrix ATH1 Arabidopsis arrays which provide more extended coverage of conditions in comparison to *e.g.* RNASeq. The expression data for each EXO70 isoform gene involved in various developmental stages, anatomic parts, and under different biotic stress conditions were data-mined using Genevestigator tools. For the developmental course of gene expression, average values are presented, typically from several hundreds to 2,000 samples, with exception of siliques and senescent leaves, where the number of samples was less than 100. Expression data from tissues and cell types and from biotic stress treatments are presented as heat maps either as different shades (absolute expression levels in anatomical parts) or in different colors (representing relative expression compared to control; green—downregulation, red—upregulation). The color scales with heat maps are given in log2 ratio values. Hierarchical clustering analysis was performed with Hierarchical Clustering Tool of Genevestigator using Pearson correlation for all or selection of genes for relevant experiments excluding combinations of simultaneous treatments and stresses and experiments which include mutant lines expression data.

Expression data from our own study comparing gene expression in *exo70A1* mutants and isogenic WT seedlings have been obtained and analyzed as reported previously (Hála et al., 2010); the complete data are available as GEO data set GSE18986 (https://www.ncbi.nlm.nih.gov/geo/).

Assay of Bacterial Stimulation of Root Hair Growth

For the root hair growth stimulation assay by pathogenic bacteria, the experiments were performed as described in (Pečenková et al., 2017a). Briefly, inoculation was performed with *P. syringae* pv. *maculicola* ES4326 (Psm) as follows: cultures from freshly inoculated plates (Luria–Bertani medium with 25 mg/l of rifampicin and streptomycin) were used to prepare liquid overnight culture (40 ml; with incubation at 28°C on an orbital shaker at 130 rpm). Bacteria were centrifuged at 1,500 g for 10 min and the pellet was resuspended in sterile distilled water (dH_2O) and diluted to an OD_{600} of 0.3 (10^8 CFU/ml). Approximately 10 µl droplets were applied to cover the root tips within the elongation and differentiation zone. As a mock control, dH_2O was applied in the same manner and, 48 h later, the root hair growth was inspected. Root hair lengths were analyzed using AnalySIS (Soft Imaging System GmbH, Germany) or ImageJ (Schindelin et al., 2015) software. The numerical data obtained (sample sizes for each of the lines are presented in **Supplementary Table 2**) were processed using Microsoft Excel. Experimental values were analyzed in R using Welch's corrected one-way analysis of variance (ANOVA), and the pairwise multiple comparisons were done with Games–Howell *post hoc* test at $P < 0.05$.

Flooding Assay

Flooding assay was performed with modifications according to Ishiga et al. (Ishiga et al., 2011; Kalachova et al., 2019). Briefly, we used P. syringae pv. tomato DC3000 mutant strain hrpH– [Pst hrpH–; donated by Chris Staiger, West Lafayette, USA; (Yuan and He, 1996)] in OD = 0, 05, diluted in water with Silwet (0.0025%), for flooding of 2-week-old plants for 2 *min*. Suspension was decanted from plates and seedlings incubated for 24 *h* on 12/12 *h* (day/night). After the incubation, in order to quantify bacterial populations, plants (three to four seedlings in one sample, three samples for each line, usually two to six replications, for WT line which was used as a reference among experiments 12 replications; **Supplementary Table 2**) were weighted, surface sterilized by 70% ethanol and homogenized. Series of dilutions were plated onto LB with rifampicin (25 µg/ml) and chloramphenicol (34 µg/ml) and left for approximately 30 *h* until the colonies become visible and countable. The number of colonies was always normalized to corresponding seedling weights, usually resulting in the range of 10^5–10^6 CFU/mg fresh weight. To account for experiment-to-experiment

variation, colony forming unit (CFU) values for various mutants in individual experiments were normalized to the CFU of control plants and expressed as a sensitivity fold change; subsequently all data were compared together, using ggplot2 and agricolae packages in R. Kruskal–Wallis and Dunn's *post hoc* tests with the Benjamini–Hochberg correction to test for significant differences at $P < 0.05$.

Bioinformatic Analysis of Lipid Binding Motifs

An alignment of *Arabidopsis thaliana* EXO70 sequences has been generated in our previous phylogenetic study (Cvrčková et al., 2012) and is available there, including a full list of sequences. Paralogs of *A. thaliana* EXO70s found to exhibit significant expression in biotic stress have been visually examined for differences between the two Arabidopsis species in the region corresponding to the putative C-terminal lipid-binding site (Kalachova et al., 2019), as well as for conservation of individual positions, with the aid of the BioEdit visualization tool (Hall, 1999).

Structural Homology Modeling

3D models of near full-length Arabidopsis EXO70B1 (aa 57-618) and EXO70B2 (aa 63-596) were predicted using mouse Exo70 (PDB code 2PFT) and partial Arabidopsis EXO70A1 (PDB code 4RL5) structures as templates, using Modeller 9v8 software (Webb and Sali, 2016). A structure–sequence multiple alignment of 231 EXO70 sequences from multiple eukaryotic lineages was used as a starting point for the prediction. 100 generated models were evaluated with internal Modeller ranking (DOPE-HR, molpdf and Z), and 10 best models were further evaluated using Prosa (Wiederstein and Sippl, 2007) and WhatIf (Hekkelman et al., 2010) algorithms. The best models scored comparable to or even better than the experimental template structures. Electrostatic potential map of the EXO70B1 and EXO70B2 models was calculated using Poisson–Boltzmann equation in the APBS program (Baker et al., 2001). Images were prepared using Pymol and Inkscape software packages (Yuan et al., 2016).

Cloning Procedures

Constructs in the pGEX4T-2 vector encoding C termini of GST-EXO70B1 (GST-EXO70B1-ct) and GST-EXO70B2 (GST : EXO70B2-ct) were cloned from PCR products obtained using primers shown in **Supplementary Table 1**. Full length constructs of EXO70B1, B2, and H1 were cloned into pTNT vectors providing N-terminal fusion with the HA epitope under the control of the SP6 promoter. List of primers used for cloning is shown in **Supplementary Table 1**. Already existing clones (Pecenková et al., 2011; Kulich et al., 2013) were used as templates for PCR.

Bacterial Expression and Purification of Proteins

Constructs in the pGEX4T-2 vector encoding C termini of GST-EXO70B1 (GST-EXO70B1-ct) and GST-EXO70B2 (GST-EXO70B2-ct) were used for the transformation of *Escherichia coli* ArcticExpress (DE3) RIL cells with Codon Plus technology (Stratagene). Bacterial culture was grown in LB medium (200 ml) supplemented with ampicillin (50 mg/l) at 37°C until OD_{600} reached 0.5–0.8, then the protein expression was induced by 1 mM isopropyl β-D-thiogalactoside. Cells were harvested by centrifugation and resuspended in 5 ml of the lysis buffer (25 mM Tris, 250 mM NaCl, 5 mM beta-mercaptoethanol, protease inhibitors cocktail (Roche), pH 8.0). Bacterial cells were disrupted by sonication, and lysates were cleared by centrifugation. Soluble fractions were loaded on a glutathione-agarose column (Sigma). After two washes with 10 ml of the lysis buffer, the GST-EXO70B1-ct and GST-EXO70B2-ct proteins were eluted by 0.25 ml of 1 M Tris-HCl (pH 8.8) supplemented with 30 mM glutathione.

Protein Expression In Vitro

For the expression of full versions of proteins EXO70B1and EXO70B2, the TnT® SP6 High-Yield Wheat Germ Protein Expression System (Promega) was used according to the manufacturer's instructions. Briefly, plasmid DNA with cloned EXO70s genes (2 µg) was mixed with an optimized wheat germ extract containing all the components (tRNA, ribosomes, amino acids, polymerase, and translation initiation, elongation and termination factors) necessary for protein synthesis in a reaction volume of 50 µl and incubated for 60–90 minutes at 25°C. The aliquots of expression reactions were verified by Western blots using anti-HA antibody (Thermo Fisher Scientific). Expressed proteins were used directly for lipid overlay.

Protein–Lipid Binding Assays

Protein–lipid overlay assays with PIP and lipid strips (P-6001 and P-6002 respectively, Echelon Biosciences) were performed according to the manufacturer's instructions. Briefly, strips were first blocked with 3% fatty acid-free BSA in PBS (3 ml, 10 mM phosphate, and 150 mM NaCl, pH 7.4) for 1 h and incubated 2 h at room temperature with blocking buffer containing 0.5 µg/ml for each of GST-EXO70B1-ct, GST-EXO70B2-ct, HA-EXO70B1, and HA-EXO70B2. The strips were washed 3× with 3 ml of PBS with 0.1% Tween. To detect the proteins, an anti-GST (Echelon Biosciences, dilution 1/2000) or anti-HA mouse monoclonal antibody (Thermo Fisher Scientific, dilution 1/1,000 dilution) was used. Subsequently, chemiluminescence detection (ECL, Amersham) of the secondary anti-mouse antibody (Promega) conjugated with horse radish peroxidase was used for identification of positive interactions. The signal was documented using Bio-Rad documentation system.

RESULTS

Gene Expression of EXO70 Paralogs

We first examined to what extent are the evolutionary relationships between EXO70 paralogs mirrored in their gene expression patterns. All but one of the 23 EXO70 isoforms

(except EXO70H6) are covered by the standard Affymetrix ATH1 Arabidopsis arrays. We used Genevestigator (Hruz et al., 2008) to compare the expression of these genes during Arabidopsis development and under varying environmental conditions. Unlike the core exocyst subunits (*e.g.* SEC6 or SEC8) with typically stable expression (Cole et al., 2005), most EXO70 paralogs exhibited low and fluctuating transcript levels during development, and only eight paralogs reached high transcript levels comparable to the core subunits at least at one developmental stage (**Figure 1A**). Only three isoforms, EXO70A1, B1, and D3, maintain stable transcript levels (high in the case of A1 and B1 and intermediate for D3) while EXO70B2, E1, and H7 exhibit varying/variable expression levels. Isoforms G1 and H8 seem to be upregulated in senescent organs and mature siliques, respectively.

The expression of several EXO70 paralogs largely varies across tissues and cell types as reported earlier (Cole et al., 2005; Sekereš et al., 2017; Synek et al., 2017). For example, in the root maturation zone, as well as in root hairs, we found that isoforms EXO70 C1, C2, D1, H1, B2, E1, H7, H2, and F1 are the most abundantly expressed, and a lower level of A1 transcript is present, while D1 and E2 have a transcript level peak in guard cells and B2, H7, and B1 in the leaf mesophyll (**Figure 1B**, **Supplementary Figure 1**).

Further on, we focused on the selection of paralogs which were induced by various biotic stress treatments. There we could observe differential expression depending on the type of biotic stress. The expression patterns and hierarchical clustering of these isoforms, with EXO70A1 included as a reference for comparison, are shown for elicitor and bacterial treatments (**Figure 2**) and also for fungal and oomycete infection (**Supplementary Figure 2**, summarization in **Table 1**). Generally, the most responsive paralogs to elicitor and bacteria treatments are H1, H2, E2, B2, H4, H7, and B1, while to fungal and oomycete treatments B2, E2, and H1. Interestingly, the expression of EXO70B2 correlated with H4 and E1 in elicitor treatments, with B1 upon bacterial infection and with E1, B1, and E2 upon fungal and oomycete treatments. B1 and B2 also appear to correlate with F1 and H7.

In order to examine the ability of other EXO70 isoforms to compensate for loss of EXO70A1, we performed microarray analysis of gene expression in 7 days old light-grown *exo70A1* and WT seedlings using the Arabidopsis ATH1 chip (Hála et al., 2010 and Methods). In general, changes in expression levels of most EXO70 paralogs were rather modest (**Figure 3A**), but some differences were nevertheless observed. While EXO70B1 and H7 remained the most expressed paralogs in both WT and *exo70A1* seedlings, loss of EXO70A1 leads to further increase in relative transcript abundance of H-group paralogs, especially H1and H2, and to a lesser extent also of F1, as well as to a slight drop in relative abundance of E2 (**Figure 3B**). Even though the pollen specific isoform EXO70A2 mRNA levels were in our experiments under the detection limit, recent work by Markovic et al., 2020 indicates the importance of a sporophytic EXO70A2 function of in the *exo70A1* plants. Interestingly, the increase of H1 and H2 in both biotic stresses and in the absence of A1 implies that H1 and H2 might compensate functionally for loss of basal A1 level during pathogen response.

These analyses confirm that only some EXO70 isoforms have high expression levels under normal conditions and that the expression patterns mostly do not follow phylogenetic relatedness. Under the biotic stress conditions, expression of several paralogs from clade 2 is upregulated. Additionally, when the developmentally most important isoform EXO70A1 is missing, the compensatory upregulation is distributed among several clade 2 isoforms.

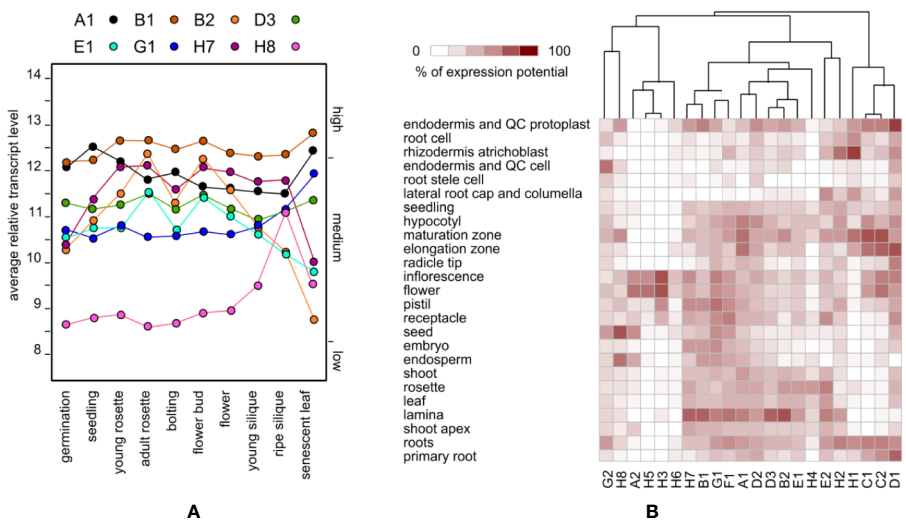

FIGURE 1 | (A) Developmental distribution of expression levels of the eight EXO70 isoforms that exhibit a high transcript level at least at one developmental stage. **(B)** Hierarchical clustering of EXO70 isoforms according to expression levels in a selection of anatomical parts. Gene names are abbreviated (A1 = EXO70A1 *etc.*); for standard locus identifiers see (Cvrčková et al., 2012).

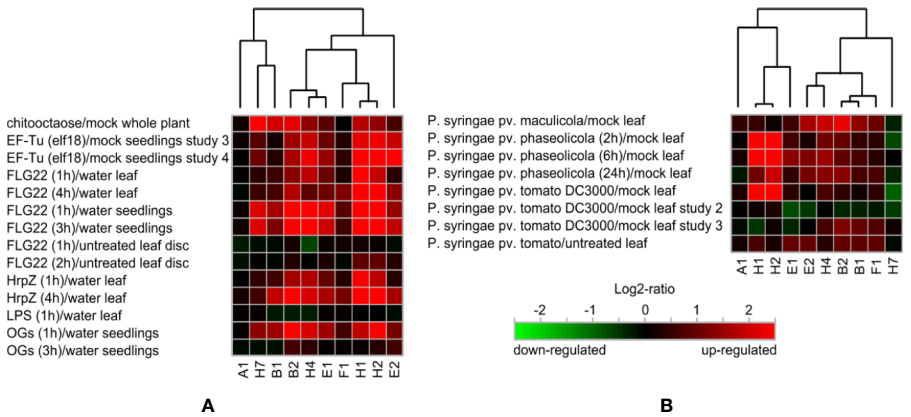

FIGURE 2 | (A) Hierarchical clustering of biotic stress-responsive EXO70 isoforms upon elicitor treatment. **(B)** Hierarchical clustering of EXO70 isoforms according to expression levels upon bacterial treatments. For gene terminology see **Figure 1**.

Defense-Related Phenotypes of Selected Double Mutants

In order to further understand the involvement of multiple paralogs in biotic stress, we decided to perform the assay for seedling root hair growth stimulation by pathogenic bacteria (Pečenková et al., 2017a). For that purpose, we focused on intersection of paralogs expressed in root hairs (**Supplemental Figure 2**) and under the biotic stress (**Figure 2**), mainly EXO70B2, E1, F1, and H1, but also on the developmentally relevant EXO70A1 and EXO70B1. Besides single mutants of theses paralogs, we used also several combinations of double mutants (*exo70A1exo70B1, exo70A1exo70B2*, *exo70B1exo70B2, exo70B2exo70H1,* and *exo70E1exo70F1*) and one triple mutant *exo70A1exo70B2exo70H1* in order to detect the aggravation of defense-related phenotypes as an evidence of the mutual redundancy capacity. No obvious additive developmental or growth phenotypic deviations were observed in any of the double or triple mutant under standard culture conditions. All mutant combinations involving *exo70A1* resembled the previously characterized single *exo70A1* dwarf mutant (Synek et al., 2006), while any mutant carrying *exo70B1* exhibited leaf HR-like lesions as previously reported for the single *exo70B1* and *exo70A1exo70B*1 mutants (Kulich et al., 2013).

We first looked for possible effects of these mutations on the responses elicited by biotic stress by quantifying root hair growth stimulation in single and double mutants after application of pathogenic bacteria *Pseudomonas syringae* pv. *maculicola* (Psm) to root tips (Pečenková et al., 2017a). Root hair response to bacterial challenge involves the perception of bacteria presence, response to pathogenic bacteria, and root hair elongation by tip growth, *i.e.* processes involving the exocyst and possibly specific EXO70 isoforms. Most of the analyzed single mutants exhibited significantly smaller stimulation of root hair growth than WT plants, most prominently double and triple mutants comprising *exo70A1* (**Figures 4A, B**; root hair appearance of selected lines in **Supplemental Figure 3**). Some of the analyzed mutant lines exhibit shorter or longer root hairs than WT plants already in conditions of mock treatment (**Supplementary Figure 3**). To eliminate these effects when focusing specifically on the biotic stress responses, we evaluated the effects of biotic stress by measuring the ratio of bacteria- *versus* mock-treated root hair

TABLE 1 | Summarization of biotic stress-related EXO70 paralog expression upregulation. Genes strongly upregulated (log2 ratio app. >2) in at least one study or experimental setup are shown in bold, moderately upregulated (log2 ratio app. < 2) in standard font.

Treatment		Upregulated clade members				
		EXO70A	**EXO70B**	**EXO70E**	**EXO70F**	**EXO70H**
Elicitors	chitaoctaose		**B1**, **B2**			**H1**, H2, H4, **H7**
	Elf18		**B2**	E1,**E2**		**H1**, **H2**, **H4**
	Flg22		B1, **B2**	E2	F1	**H1**, **H2**, **H4**, **H7**
	HrpZ		B1, **B2**	E1		**H1**, **H2**, H4
	oligogalacturans		B1, **B2**	E1		**H1**, **H2**, **H4**, H7
Bacteria	*Pseudomonas syringae*		B1, **B2**	E1, E2	F1	**H1**, **H2**, **H4**
Non-host fungus	*Blumeria graminis*		B1, B2	E1,**E2**		**H1**, H4, H7
Host fungus	*Alternaria brassicicola*		B1, **B2**	E1		**H1**, **H4**
	Golovinomyces orontii	A1	B1, **B2**	E1,**E2**		**H4**
	Sclerotinia sclerotiorum		B1, **B2**	E1,**E2**		H4, H7
Oomycete	*Hyaloperonospora arabidopsidis*		B1, **B2**	E1,**E2**		
	Phytophthora parasitica		**B1**, **B2**	**E1**	F1	**H1**, **H7**

Genes strongly upregulated (log2 ratio app. > 2) in at least one study or experimental setup are shown in bold, moderately upregulated (1 log2 ratio app. < 2) in standard font.

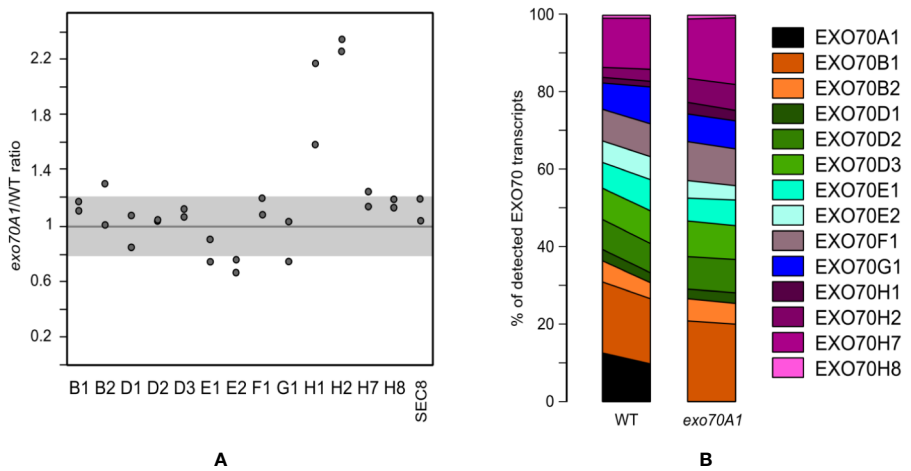

FIGURE 3 | (A) Relative transcript levels of detectable EXO70 isoforms and the SEC8 subunit in *exo70A1* mutant *vs.* WT seedlings (from two replicates). Gray zone represents a less than 20% change in transcript abundance. **(B)** Composition of the EXO70 transcript population in *exo70A1* mutant *vs.* WT seedlings. Two replicates for each genotype are represented by the left and right sides of the corresponding stacked bar graph, respectively. For gene terminology see **Figure 1**.

lengths. Interestingly, in the case of *exoB1exo70B2* mutants we observed the opposite and counterintuitive effect, *i.e.* enhanced root hair growth after bacterial stimulation when compared to the single mutants' responses.

In order to further follow pathogen perception-related defects, we also examined the same set of mutants for their ability to sustain propagation of *Pseudomonas syringae* pv. *tomato* (Pst) after flooding inoculation (Ishiga et al., 2011). A nonvirulent Pst hrpH-strain was used, avoiding thus effector-responsive component of plant defense. All of the tested mutant lines were normalized to their corresponding wild type, allowing thus a comparison of the relative strength of response among different mutants (**Figure 4C**). Again, most of the analyzed mutant lines have significantly compromised resistance toward Pst hrpH−. Surprisingly and contrasting to the situation with single mutants, double mutant combinations *exoB1exo70B2* and *exo70B2exo70H1* seem to sustain the bacterial inoculation to a level comparable to WT. Interestingly, combinations of some mutants (*exo70B1*, *exo70B2* and *exo70H1*) with *exo70A1* increase the susceptibility toward hrpH−, but the triple mutant *exo70A1exo70B2exo70H1* has again sensitivity "corrected" to single *exo70A1* mutant levels.

These results evidence a more complex pattern of functional overlap that includes also the compensatory effect among EXO70 mutations, probably as a consequence of competition of isoforms for the core of the exocyst complex.

Diversity and Preferences of EXO70 Lipid-Binding Domains

To explore the possibility that the phospholipid-binding capacity of EXO70 isoforms C-termini could be a determinant of localization and therefore also functional specificity, we compared the amino acid sequences of the EXO70 protein C-termini containing a predicted membrane-binding site (Žárský et al., 2009; Cvrčková et al., 2012). Several highly conserved motifs among all paralogs were detected (yellow boxes in **Figure 5A**); besides, stretches of basic and acidic residues were found to be conserved as well (blue and red letters, respectively). Combining the data from gene expression and lipid-binding *in silico* analysis, we could pinpoint several candidates for mutations that might have resulted in within-clade diversification of membrane-binding specificities. We focused in particular on EXO70B1 and B2 since they behaved in different manner in our biotic response assays. Indeed, a pair of prolines and a valine replacing basic amino acids in the putative phospholipid-binding motif were found in EXO70B2 but not in EXO70B1; one of the basic amino acid is also not conserved in the H group isoforms. Furthermore, several conserved glutamate/aspartate residues are replaced by an asparagine residue in some of EXO70H isoforms (**Figure 5A**).

In order to further predict a functional role of the amino acid residues that are mutated in EXO70B2 C-terminus, we modeled 3D structures of EXO70B1 and B2 using known EXO70 structures as templates. Importantly, the visualization of electrostatic potential of EXO70B1 C-terminal domain revealed a positively charged pocket containing three lysine residues that are mutated in EXO70B2. While the overall backbone structures of EXO70B1 and B2 are very similar and there is only a small structural difference between predicted EXO70B1 and B2 C-termini (RMSD = 0.306), the three lysines mutated to prolines and valine in EXO70B2 result in significant loss of positive charge (**Figure 5B**). Moreover, the presence of the two other backbone-bending mutations ((L > P and K > P) affects the shape of EXO70B2 C terminus near the putative membrane-binding pocket (**Figure 5B**).

We further assessed how the differences found between the EXO70B1 and B2 C-termini will affect their lipid-binding capacity using an *in vitro* assay. For this purpose, we used qualitative *in vitro* assays of lipid binding profiles employing PIP and membrane lipid strips (thus, the results might not fully

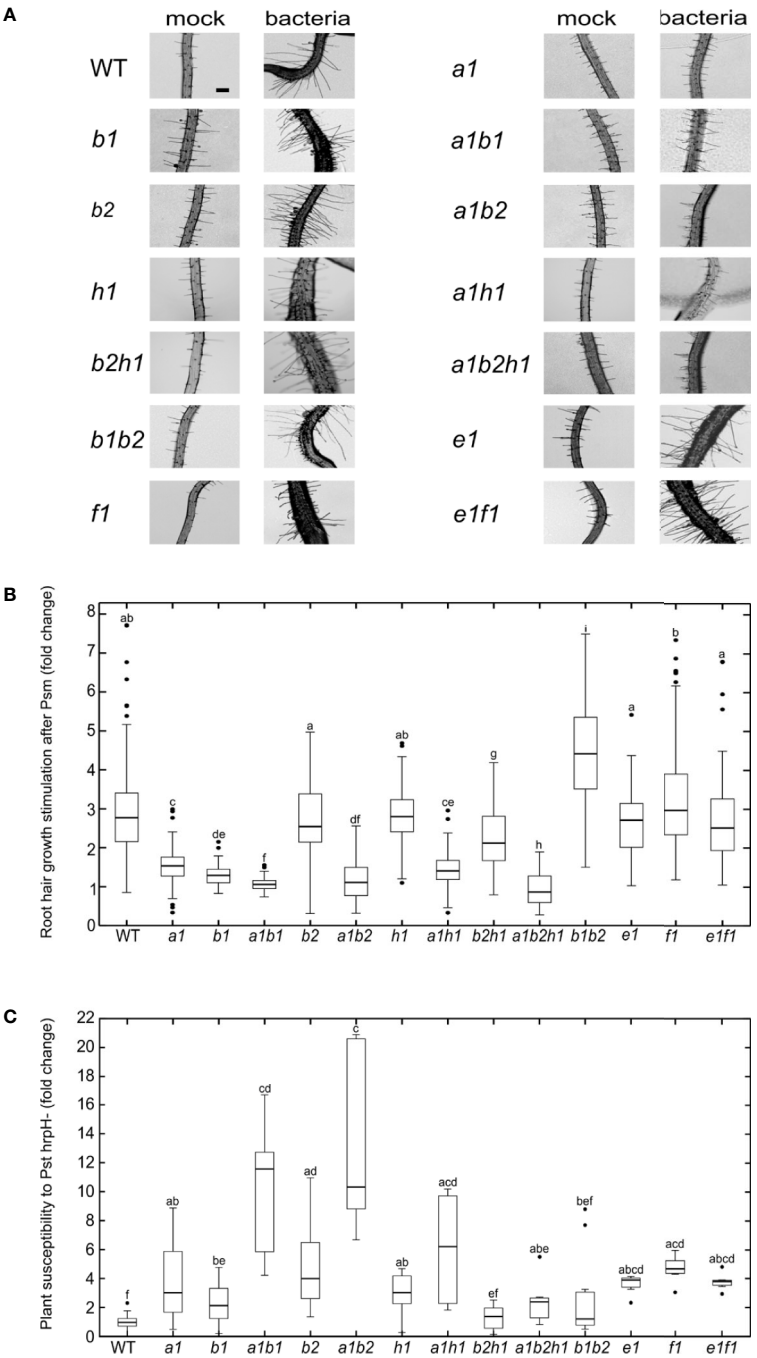

FIGURE 4 | (A) Root hair growth appearance 48 h after mock or *P. syringae* pv. *maculicola* (Psm) treatment for each of analyzed lines (bar = 100 μm). **(B)** Root hair growth stimulation after *P. syringae* pv. *maculicola* (Psm) inoculation. For each of mutant lines root hair length is compared to mock treated control and the difference expressed as a fold change; the mock treated WT root hair size represents fold change 1; error bars—standard deviation, n = 60–407 root hairs; different letters indicate significant differences ($P < 0.05$). **(C)** *P. syringae* pv. *tomato* DC3000 *hrpH*– flooding inoculation. The variation in sensitivity is expressed as a fold change of CFU in comparison to the WT (fold change 1) and is presented for each of analyzed lines; error bars—standard deviation, n = 6–36 samples from three to four pooled seedlings each; different letters indicate significant differences ($P < 0.05$).

correspond to the situation *in vivo*). The C-terminal fragments of EXO70B1 and B2 (aa 431-624 and 415-599, respectively) were expressed in *E. coli* as GST fusions (**Supplementary Figure 4A**). Purified fusion proteins were incubated with different phosphatidylinositol phosphates (PIP) immobilized as spots on membrane strips (**Figure 6**, upper row). Interestingly, despite their amino acid differences in lipid-binding domain, the two EXO70B isoforms appear to bind a similar repertoire of PIP

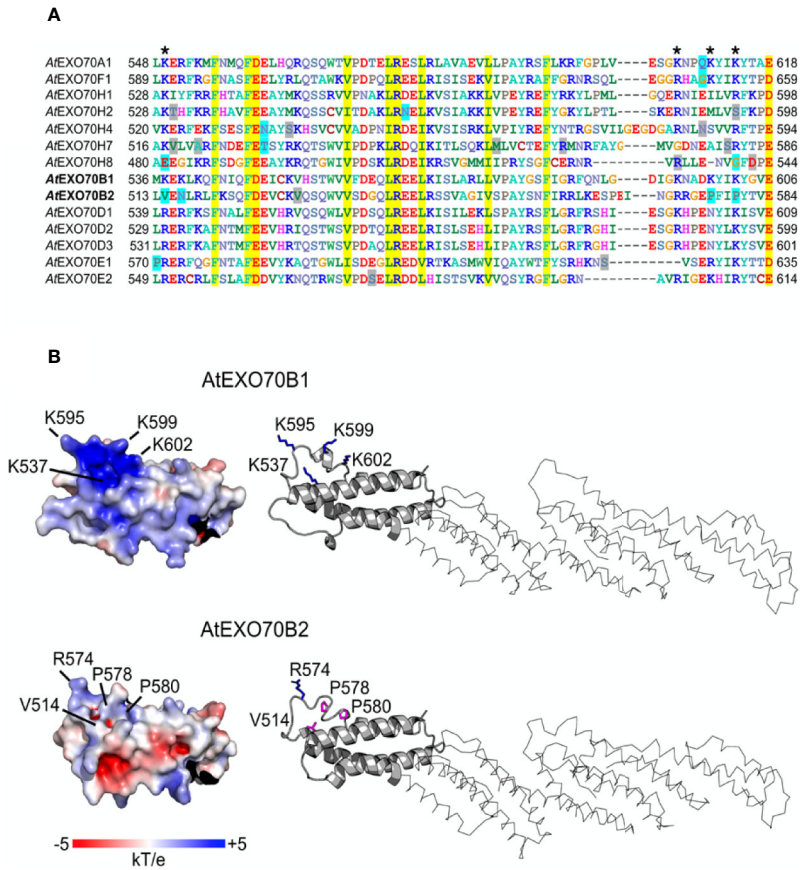

FIGURE 5 | Alignment of predicted lipid-interacting motifs of selected EXO70 paralogs **(A)** and 3D structures of C termini of EXO70B1 and EXO70B2 **(B)**. Residues shown on yellow background are conserved in all isoforms; positions with basic and acidic residues were found to be conserved as well (blue and red letters, respectively); a pair of prolins and valine replacing basic amino acids in the putative binding motif was found in EXO70B2 but not in EXO70B1; several conserved glutamate/aspartate residues are replaced by an asparagine residue in some of EXO70H isoforms (blue boxes; **A)**. The visualization of electrostatic potential of EXO70B1 C-terminal domain revealed positively charged pocket containing three lysine residues that are mutated in EXO70B2, resulting in significant loss of positive charge **(B)**.

species—most strongly PI(3)P and PI(5)P monophosphates. The PIP-strip assays were also performed with full-length HA-tagged EXO70B1 and B2 proteins produced in an *in vitro* translation system, together with the less related isoform EXO70H1 (**Figure 6**, upper row, on the right; **Supplementary Figure 4B**). Similar lipid-binding affinity for all analyzed isoforms was also detected using membrane lipid strips (**Figure 6**, lower row). The full length versions of the tested EXO70s were found to interact weakly also with phosphatidylserine (PS) and phosphatidic acid (PA), unlike their C-terminal fragments, indicating the presence of protein regions outside the C-terminal motif contributing to lipid-binding specificity. Nevertheless, the analyzed proteins do not bind to lipids on strips with the same intensity (*e.g.* for EXO70B1 positive spots are much fainter than in the case of EXO70B2 under the same exposure time; **Supplemental Figure 4B**), at least partially as a consequence of different efficiencies of *in vitro* translation, but possibly also of intrinsic lipid-binding affinities, a matter requesting further alternative quantitative assays.

Despite their diverged lipid-binding domains and distinct roles in the plant cell context, the lipid-binding analysis shows that the EXO70B1 and B2 isoforms could bind the same type of lipids, only slightly different from more distantly related EXO70H1. This suggests that their sequence diversification affects other types of interactions, probably protein–protein, that might result in functional specialization.

DISCUSSION

In this work, we aimed to map and assess some aspects of functional overlap (redundancy) and specialization among Arabidopsis EXO70 isoforms. We are building on the working hypothesis that redundancy can be expected among those paralogs that (i) exhibit the closest evolutionary relationship, (ii) have overlapping expression patterns and lipid affinities, and that (iii) combination of their multiple loss-of-function

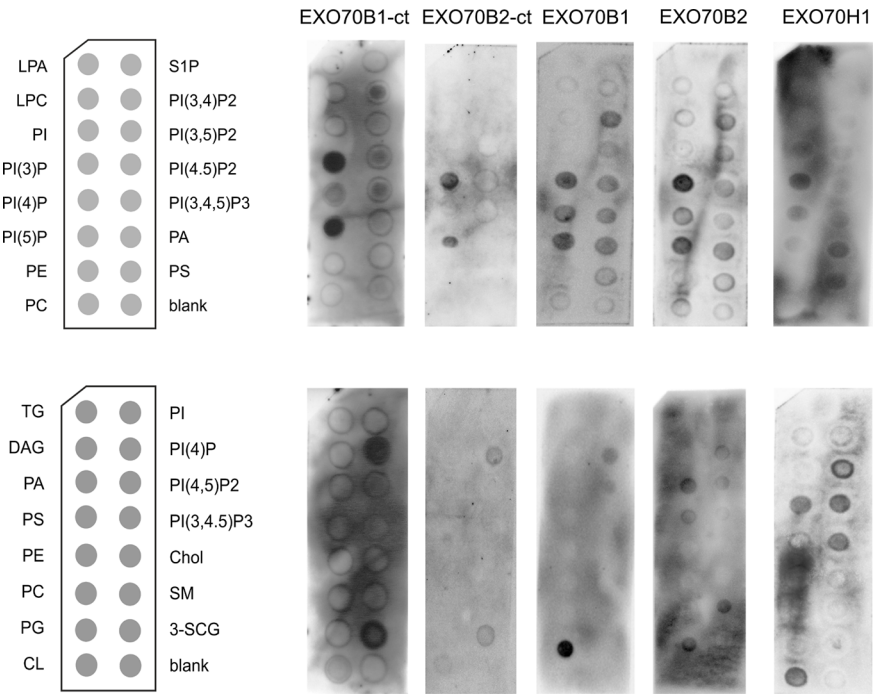

FIGURE 6 | Phosphoinositide-(upper row) and membrane lipid-binding capacity (lower row) of EXO70B1 and EXO70B2 C-terminal fragments (-ct; left) and full length variants (right) of EXO70B1, B2, and H1. For lipid terminology see *Abbreviations*.

mutations leads to more severe phenotypic manifestations compared to single mutations.

Similarly to other rapidly diversifying gene families, the expression pattern of *A. thaliana* EXO70 isoforms does not mirror their mutual relationships inferred by phylogenetic analyses (compare *e.g.* Dvořáková et al., 2007). Also isoforms with similar expression patterns may have unique roles; for instance, the two paralogs with the highest expression throughout the Arabidopsis development are EXO70A1 and EXO70B1, documented to function differently—while EXO70A1 plays a part in the exocytosis related to the polar growth, cytokinesis, cell expansion, and endosomal recycling, B1 engages in the autophagic route to the vacuole (Kulich et al., 2013). The *exo70A1* mutant has pleiotropic developmental defects, including very obvious stunted growth of both roots and rosettes (Synek et al., 2006), while *exo70B1* plants first develop normally; however, in adult rosettes, they develop spontaneous hypersensitive response (HR)-like leaf lesions, display partial loss of anthocyanin vacuolar accumulation, and are more resistant to biotrophic and hemi-biotrophic pathogens due to elevated salicylic acid (SA) levels in fully mature plants (Kulich et al., 2013; Zhao et al., 2015). HR- and SA-related *exo70B1* phenotypes can be suppressed by mutations in the R-related protein TIR-NBS2 [TN2 (Zhao et al., 2015)]. Considering that the two isoforms have high overall sequence similarity (including the C-terminal membrane-binding motif), it is possible to speculate that additional isoform-specific protein interactors are instrumental for the observed differences—*e.g.* the known defense-related protein RIN4 has been shown to specifically interact with EXO70B1 but not with EXO70A1 (Sabol et al., 2017).

Surprisingly, according to our bacterial flooding assays, EXO70A1 loss-of-function has significant impact on plant defense capability, a finding never reported before, mainly due to the expectation that the biotic-stress induced isoforms play more important role in plant defense. Nevertheless, it is obvious that EXO70A1 has an important general background role in defense as well, probably due to its influence on biogenesis and maintenance of plasma membrane and especially on cell wall biogenesis and properties (Fendrych et al., 2013; Vukašinović et al., 2017). Surprisingly, unlike some other dwarf and esp. *atg* mutants (Zhang et al., 2007; van Wersch et al., 2016) and also unlike other exocyst mutants such as *exo70B1* and *Ossec3A* (Kulich et al., 2013; Ma et al., 2018), *exo70A1* shows no elevation of either salicylic acid (SA) biosynthetic machinery or in overall SA content (Žárský et al., in preparation). Based on all of this, we could speculate that the increased susceptibility in the case of double mutant *exo70A1 exo70B1*, which otherwise has the same developmental phenotype as the single *exo70A1* mutant, is rather a cumulative effect of the two mutations converging in the situation of biotic stress than the aggravation of the single mutants' phenotypes.

The second Arabidopsis EXO70B isoform, EXO70B2, is important for efficient defense against pathogens (Pecenková

et al., 2011; Stegmann et al., 2012; Stegmann et al., 2014; Du et al., 2015; Du et al., 2018);. EXO70A1 and B2 have different expression patterns and highly diversified lipid binding domains. The B1 and B2 isoforms are closely related and interact with both common and specific protein partners, some of them important components of the pathogen-associated molecular patterns-triggered immunity (PTI) and effector-triggered susceptibility and immunity pathways [ETS and ETI; see (Jones and Dangl, 2006)]. Interestingly in most Angiosperm families such diversification of EXO70B functions did not happen, and only a single EXO70B isoform is present (Cvrčková et al., 2012). Recently co-operation of the Arabidopsis EXO70B1 and B2 isoforms in the regulation of FLS2 flagellin receptor kinase plasma membrane localization was described (Wang et al., 2020). Despite the overlaps in expression and lipid-binding capacity, there may be a compensatory effect between the two mutations (Drs et al., unpublished observation). It is possible that the clue for this unexpected outcome lies within the EXO70Bs different protein interacting repertoire (Zhao et al., 2015; Sabol et al., 2017).

Similarly to the double mutants *exo70A1exo70B1*, and in conflict with the *exo70B1exo70B2* phenotype case, *exo70A1exo70B2* appears to be more severely compromised in the defense responses analyzed in the present work compared to the single mutant counterparts, similarly to what has been found in the *exo70A1exo70B2* defense reaction to *Blumeria graminis* (Žárský et al., 2013). Unlike the case of the double mutant *exo70A1exo70B1* with secretory impairment caused by *exo70A1* and additional defect in autophagy/vacuolar transport imposed by *exo70B1* (Kulich et al., 2013), the double mutant *exo70A1exo70B2* severe phenotype may be the consequence of the lack of partial redundancy between the EXO70A1-related constitutive secretion and EXO70B2-related defense secretion.

The complexity of relationships among EXO70s is well-illustrated by the example of root hair growth enhancement in *exo70B1exo70B2* mutants, consistent with the possible competition of the EXO70B clade paralogs and the tip growth-promoting EXO70A1 paralog for exocyst core subunits. Neither the of two EXO70Bs isoforms has prominent affinity for phosphatidyl serine (PS), a tip-growth localized lipid in root hairs (Platre et al., 2018). We could thus speculate that in the absence of both EXO70Bs, the whole pool of exocyst core subunits in root hair cells is available for tip-growth-related and preferentially PS-binding EXO70 isoform(s), possibly the most abundant EXO70A1 (Fendrych et al., 2013). The ability of EXO70B1 and B2 to bind PI(3)P and PI(5)P suggests their possible involvement in processes not directly related to cell enlargement. Although PI(3)P is a minor lipid in the cell, it is a key player in membrane protein recruitment, especially late endosomal vesicle trafficking and autophagosome formation (Balla, 2013; van Wersch et al., 2016). This is in concordance with the autophagy-related function of EXO70B1 (Kulich et al., 2013), and it remains to be seen if and how the EXO70B2 could be as well involved in autophagy.

The EXO70E1, F1 and H1 are probably the least studied Arabidopsis EXO70 paralogs. Our observation of compensatory E1/F1 and B2/H1 (also A1/B2/H1) effects thus may be opening a new field that would deserve attention in the nearest future.

In our pathogen sensitivity assays, we could often see a complementarity of responses between the root hair growth and general defense. The single mutant lines that did not respond to root hair growth enhancement to the same level as the WT were also found to be more sensitive in the overall immunity to *P. syringae* in flooding assays. Also the double mutants that had diminished capacity to enhance root hair growth after bacteria inoculation were more sensitive to bacteria in flooding experiments (*e.g. exo70A1exo70B1* and *exo70A1exo70B2*) in comparison to corresponding single mutants. This strengthens a suitability of the root hair growth response assay as a readout of the general defense capacity. On the other hand, the case of the triple mutant *exo70A1exo70B2exo70H1* fully reflects the complexity of relationships among isoforms—even though it is the mutant with the most prominent reduction of root hair growth (possibly also due to a general cell expansion defect), it is not the one to be the most sensitive toward bacteria in flooding assay.

Our analysis of lipid-interacting motifs suggests that Arabidopsis EXO70 isoforms might have multiple lipid interaction specificities, some of them located outside the C-terminal motif predicted to be the a major specificity determinant based on animal and yeast PI(4,5)P_2-binding homologs, similarly to what has been suggested for yeast Exo70p (Pleskot et al., 2015). The EXO70 lipid binding specificity can also be modulated by additional protein interactions, including putative EXO70s homo- or hetero-dimerization, which could help a particular isoform to achieve a highly specific function, that may even be independent from the rest of the complex, as shown for membrane curvature in animal cells (Zhao et al., 2013) or EXO70C2 in pollen tubes (Synek et al., 2017). Although the EXO70B2 isoform can homodimerize in the yeast two hybrid assay (Pecenková et al., 2011), biological relevance of plant EXO70 dimerization capability *in vivo* remains elusive (Žárský et al., 2020) and only recently was implied in the FLS2 plasma membrane localization (Wang et al., 2020).

To conclude, our results demonstrate that despite evolutionary relatedness, overlapping mRNA expression patterns, and similar lipid binding affinities, each EXO70 isoform might have a unique function. When one isoform is missing, there is mostly no simple full replacement of one isoform function by another one. Our data indicate that the pool of exocyst core subunits is possibly available for several EXO70 isoforms present in the same cell so that the overall endomembrane dynamics within the cell is also regulated in different situations by the competition of different EXO70s for the same core subunits (Žárský et al., 2013). The main question of other isoforms' involvement in secretion *versus* autophagy will necessitate creation of additional multiple mutants involving other paralogs (especially H1 and H2) and further analysis of multiple mutants' phenotypes beyond defense-related phenomena.

DATA AVAILABILITY STATEMENT

Publicly available datasets were analyzed in this study. This data can be found here: GSE18986.

AUTHOR CONTRIBUTIONS

TP performed root hair assays, RNA expression analysis, mutant crossing, recombinant protein expression, lipid-binding experiments and wrote the manuscript. AP performed Pseudomonas flooding experiments. MP conceptualized and performed lipid-binding domain *in silico* analysis and statistical analysis of biotic assay results. JO performed mutant propagation, protein expression *in vitro*, crossings, and root hair analysis. MD performed mutant propagation, image analysis, and text editing. EJ and LS performed RNA microarray experiments and data analysis. PP performed cloning. HS performed mutant propagation and crossings. VŽ performed planning of experiments, interpretation and writing. FC performed data analysis, figure design, and participated in data interpretation and manuscript writing. All authors contributed to the article and approved the submitted version.

FUNDING

This research was funded by the Ministry of Education, Youth and Sports of the Czech Republic (MŠMT) project and European Regional Development Fund project CZ.02.1.01/0.0/0.0/16_019/0000738 "Centre for Experimental Plant Biology" at the Institute of Experimental Botany and by the Czech Science Foundation (GAČR) grants number CSF 19-02242J and GC18-18290J.

ACKNOWLEDGMENTS

We thank Juraj Sekereš and Roman Pleskot for methodological guidance and helpful suggestions and Jana Šťovíčková for technical assistance.

SUPPLEMENTARY MATERIAL

The Supplementary Material for this article can be found online at: https://www.frontiersin.org/articles/10.3389/fpls.2020.00960/full#supplementary-material

REFERENCES

Baker, N. A., Sept, D., Joseph, S., Holst, M. J., and McCammon, J. A. (2001). Electrostatics of nanosystems: Application to microtubules and the ribosome. *Proc. Natl. Acad. Sci. U. S. A.* 98, 1019–1137. doi: 10.1073/pnas.181342398

Balla, T. (2013). Phosphoinositides: Tiny lipids with giant impact on cell regulation. *Physiol. Rev.* 93, 1019–1137. doi: 10.1152/physrev.00028.2012

Boyd, C., Hughes, T., Pypaert, M., and Novick, P. (2004). Vesicles carry most exocyst subunits to exocytic sites marked by the remaining two subunits, Sec3p and Exo70p. *J. Cell Biol.* 167, 889–901. doi: 10.1083/jcb.200408124

Chong, Y. T., Gidda, S. K., Sanford, C., Parkinson, J., Mullen, R. T., and Goring, D. R. (2010). Characterization of the Arabidopsis thaliana exocyst complex gene families by phylogenetic, expression profiling, and subcellular localization studies. *New Phytol.* 185, 401–419. doi: 10.1111/j.1469-8137.2009.03070.x

Cole, R. A., Synek, L., Zarsky, V., and Fowler, J. E. (2005). SEC8, a subunit of the putative arabidopsis exocyst complex, facilitates pollen germination and competitive pollen tube growth. *Plant Physiol.* 138, 2005–2018. doi: 10.1104/pp.105.062273

Cvrčková, F., Grunt, M., Bezvoda, R., Hála, M., Kulich, I., Rawat, A., et al. (2012). Evolution of the land plant exocyst complexes. *Front. Plant Sci.* 3, 159. doi: 10.3389/fpls.2012.00159

Drdová, E. J., Synek, L., Pečenková, T., Hála, M., Kulich, I., Fowler, J. E., et al. (2013). The exocyst complex contributes to PIN auxin efflux carrier recycling and polar auxin transport in Arabidopsis. *Plant J.* 73, 709–719 doi: 10.1111/tpj.12074

Du, Y., Mpina, M. H., Birch, P. R. J., Bouwmeester, K., and Govers, F. (2015). Phytophthora infestans RXLR effector AVR1 interacts with exocyst component Sec5 to manipulate plant immunity. *Plant Physiol.* 169, 1975–1990. doi: 10.1104/pp.15.01169

Du, Y., Overdijk, E. J. R., Berg, J. A., Govers, F., and Bouwmeester, K. (2018). Solanaceous exocyst subunits are involved in immunity to diverse plant pathogens. *J. Exp. Bot.* 69, 655–666. doi: 10.1093/jxb/erx442

Dubuke, M. L., Maniatis, S., Shaffer, S. A., and Munson, M. (2015). The exocyst subunit Sec6 interacts with assembled exocytic SNARE complexes. *J. Biol. Chem.* 290, 28245–28256. doi: 10.1074/jbc.M115.673806

Dvořáková, L., Cvrčková, F., and Fischer, L. (2007). Analysis of the hybrid proline-rich protein families from seven plant species suggests rapid diversification of their sequences and expression patterns. *BMC Genomics.* 8, 412. doi: 10.1186/1471-2164-8-412

Elias, M., Drdova, E., Ziak, D., Bavlnka, B., Hala, M., Cvrckova, F., et al. (2003). The exocyst complex in plants. *Cell Biol. Int.* 27, 199–201. doi: 10.1016/S1065-6995(02)00349-9

Fendrych, M., Synek, L., Pecenková, T., Toupalová, H., Cole, R., Drdová, E., et al. (2010). The Arabidopsis exocyst complex is involved in cytokinesis and cell plate maturation. *Plant Cell* 22, 3053–3065. doi: 10.1105/tpc.110.074351

Fendrych, M., Synek, L., Pečenková, T., Drdová, E. J., Sekereš, J., de Rycke, R., et al. (2013). Visualization of the exocyst complex dynamics at the plasma membrane of *Arabidopsis thaliana*. *Mol. Biol. Cell.* 24, 510-520. doi: 10.1091/mbc.E12-06-0492

Guo, W., Roth, D., Walch-Solimena, C., and Novick, P. (1999). The exocyst is an effector for Sec4P, targeting secretory vesicles to sites of exocytosis. *EMBO J.f.* 18, 1071–1080. doi: 10.1093/emboj/18.4.1071

Hála, M., Cole, R., Synek, L., Drdová, E., Pečenková, T., Nordheim, A., et al. (2008). An exocyst complex functions in plant cell growth in Arabidopsis and tobacco. *Plant Cell.* 20, 1330–1345. doi: 10.1105/tpc.108.059105

Hála, M., Soukupová, H., Synek, L., and Žárský, V. (2010). Arabidopsis RAB geranylgeranyl transferase β-subunit mutant is constitutively photomorphogenic, and has shoot growth and gravitropic defects. *Plant J.* 62, 615–627. doi: 10.1111/j.1365-313X.2010.04172.x

Hall, T. A. (1999). BIOEDIT: a user-friendly biological sequence alignment editor and analysis program for Windows 95/98/ NT. *Nucleic Acids Symp. Ser.* 41, 95–98.

He, B., Xi, F., Zhang, X., Zhang, J., and Guo, W. (2007). Exo70 interacts with phospholipids and mediates the targeting of the exocyst to the plasma membrane. *EMBO J.* 26, 4053–4065. doi: 10.1038/sj.emboj.7601834

Hekkelman, M. L., te Beek, T. A. H., Pettifer, S. R., Thorne, D., Attwood, T. K., and Vriend, G. (2010). WIWS: A protein structure bioinformatics web service collection. *Nucleic Acids Res.* 38, W719–W723. doi: 10.1093/nar/gkq453

Hruz, T., Laule, O., Szabo, G., Wessendorp, F., Bleuler, S., Oertle, L., et al. (2008). Genevestigator V3: A reference expression database for the meta-analysis of transcriptomes. *Adv. Bioinf.* 2008, 420747. doi: 10.1155/2008/420747

Hsu, S. C., TerBush, D., Abraham, M., and Guo, W. (2004). The exocyst complex in polarized exocytosis. *Int. Rev. Cytol.* 21, 537–542. doi: 10.1016/S0074-7696(04)33006-8

Ishiga, Y., Ishiga, T., Uppalapati, S. R., and Mysore, K. S. (2011). Arabidopsis seedling flood-inoculation technique: A rapid and reliable assay for studying plant-bacterial interactions. *Plant Methods*. 7, 32. doi: 10.1186/1746-4811-7-32

Janková Drdová, E., Klejchová, M., Janko, K., Hála, M., Soukupová, H., Cvrćková, F., et al. (2019). Developmental plasticity of Arabidopsis hypocotyl is dependent on exocyst complex function. *J. Exp. Bot*. 70, 1255–1265. doi: 10.1093/jxb/erz005

Jones, J. D. G., and Dangl, J. L. (2006). The plant immune system. *Nature*. 444, 323–329. doi: 10.1038/nature05286

Kalachova, T., Janda, M., Šašek, V., Ortmannová, J., Nováková, P., Dobrev, I. P., et al. (2019). Identification of salicylic acid-independent responses in an Arabidopsis phosphatidylinositol 4-kinase beta double mutant. *Ann. Bot*. 125, 775–784. doi: 10.1093/aob/mcz112

Koumandou, V. L., Dacks, J. B., Coulson, R. M. R., and Field, M. C. (2007). Control systems for membrane fusion in the ancestral eukaryote; Evolution of tethering complexes and SM proteins. *BMC Evol. Biol*. 7, 29. doi: 10.1186/1471-2148-7-29

Kulich, I., Pečenková, T., Sekereš, J., Smetana, O., Fendrych, M., Foissner, I., et al. (2013). Arabidopsis exocyst subcomplexcontaining subunit EXO70B1 is involved in autophagy-related transport to the vacuole. *Traffic*. 14, 1155–1165. doi: 10.1111/tra.12101

Kulich, I., Vojtíková, Z., Glanc, M., Ortmannová, J., Rasmann, S., and Zárský, V. (2015). Cell wall maturation of arabidopsis trichomes is dependent on exocyst subunit EXO70H4 and involves callose deposition. *Plant Physiol*. 168, 120–131. doi: 10.1104/pp.15.00112

Kulich, I., Vojtíková, Z., Sabol, P., Ortmannová, J., Neděla, V., Tihlaříková, E., et al. (2018). Exocyst subunit EXO70H4 has a specific role in callose synthase secretion and silica accumulation. *Plant Physiol*. 176, 2040–2051. doi: 10.1104/pp.17.01693

Laxalt, A. M., and Munnik, T. (2002). Phospholipid signalling in plant defence. *Curr. Opin. Plant Biol*. 5, 332–338. doi: 10.1016/s1369-5266(02)00268-6

Liu, J., Zuo, X., Yue, P., and Guo, W. (2007). Phosphatidylinositol 4,5-bisphosphate mediates the targeting of the exocyst to the plasma membrane for exocytosis in mammalian cells. *Mol. Biol. Cell*. 18, 4483–4492. doi: 10.1091/mbc.E07-05-0461

Ma, J., Chen, J., Wang, M., Ren, Y., Wang, S., Lei, C., et al. (2018). Disruption of OsSEC3A increases the content of salicylic acid and induces plant defense responses in rice. *J. Exp. Bot*. 69, 1051–1064. doi: 10.1093/jxb/erx458

Markovic, V., Cvrckova, F., Potocky, M., Pejchar, P., Kolarova, E., Kulich, I., et al. (2020). EXO70A2 is critical for the exocyst complex function in Arabidopsis pollen. *bioRxiv*. doi: 10.1101/831875

Martin-Urdiroz, M., Deeks, M. J., Horton, C. G., Dawe, H. R., and Jourdain, I. (2016). The exocyst complex in health and disease. *Front. Cell Dev. Biol*. 4, 24. doi: 10.3389/fcell.2016.00024

Moskalenko, S., Henry, D. O., Rosse, C., Mirey, G., Camonis, J. H., and White, M. A. (2002). The exocyst is a Ral effector complex. *Nat. Cell Biol*. 4, 66–72. doi: 10.1038/ncb728

Pečenková, T., Janda, M., Ortmannová, J., Hajná, V., Stehlíková, Z., and Žárský, V. (2017a). Early Arabidopsis root hair growth stimulation by pathogenic strains of Pseudomonas syringae. *Ann. Bot*. 120, 437–446. doi: 10.1093/aob/mcx073

Pečenková, T., Marković, V., Sabol, P., Kulich, I., and Zárský, V. (2017b). Exocyst and autophagy-related membrane trafficking in plants. *J. Exp. Bot*. 69, 47–57. doi: 10.1093/jxb/erx363

Pecenková, T., Hála, M., Kulich, I., Kocourková, D., Drdová, E., Fendrych, M., et al. (2011). The role for the exocyst complex subunits Exo70B2 and Exo70H1 in the plant-pathogen interaction. *J. Exp. Bot*. 62, 2107–2116. doi: 10.1093/jxb/erq402

Picco, A., Irastorza-Azcarate, I., Specht, T., Böke, D., Pazos, I., Rivier-Cordey, A. S., et al. (2017). The in vivo architecture of the exocyst provides structural basis for exocytosis. *Cell*. 168, 400–412.e18. doi: 10.1016/j.cell.2017.01.004

Platre, M. P., Noack, L. C., Doumane, M., Bayle, V., Simon, M. L. A., Maneta-Peyret, L., et al. (2018). A combinatorial lipid code shapes the electrostatic landscape of plant endomembranes. *Dev. Cell*. 45, 465–480. doi: 10.1016/j.devcel.2018.04.011

Pleskot, R., Cwiklik, L., Jungwirth, P., Žárský, V., and Potocký, M. (2015). Membrane targeting of the yeast exocyst complex. *Biochim. Biophys. Acta Biomembr*. 1848, 1481–1489. doi: 10.1016/j.bbamem.2015.03.026

Rawat, A., Brejšková, L., Hála, M., Cvrčková, F., and Žárský, V. (2017). The Physcomitrella patens exocyst subunit EXO70.3d has distinct roles in growth and development, and is essential for completion of the moss life cycle. *New Phytol*. 216, 438–454. doi: 10.1111/nph.14548

Redditt, T. J., Chung, E. H., Zand Karimi, H., Rodibaugh, N., Zhang, Y., Trinidad, J. C., et al. (2019). AvrRpm1 functions as an ADP-ribosyl transferase to modify NOI-domain containing proteins, including Arabidopsis and soybean RPM1-interacting protein 4. *Plant Cell*. (Epub ahead of print). doi: 10.1105/tpc.19.00020

Rossi, G., Lepore, D., Kenner, L., Czuchra, A. B., Plooster, M., Frost, A., et al. (2020). Exocyst structural changes associated with activation of tethering downstream of Rho/Cdc42 GTPases. *J. Cell Biol*. 219, e201904161. doi: 10.1083/jcb.201904161

Roth, D., Guo, W., and Novick, P. (1998). Dominant negative alleles of SEC10 reveal distinct domains involved in secretion and morphogenesis in yeast. *Mol. Biol. Cell*. 9, 1725–1739. doi: 10.1091/mbc.9.7.1725

Sabol, P., Kulich, I., and Žárský, V. (2017). RIN4 recruits the exocyst subunit EXO70B1 to the plasma membrane. *J. Exp. Bot*. 68, 3253–3265. doi: 10.1093/jxb/erx007

Schindelin, J., Rueden, C. T., Hiner, M. C., and Eliceiri, K. W. (2015). The ImageJ ecosystem: An open platform for biomedical image analysis. *Mol. Reprod. Dev*. 82, 518–529. doi: 10.1002/mrd.22489

Sekereš, J., Pejchar, P., Šantrůček, J., Vukasinovic, N., Žárský, V., and Potocký, M. (2017). Analysis of exocyst subunit EXO70 family reveals distinct membrane polar domains in Tobacco pollen tubes. *Plant Physiol*. 173, 1659–1675. doi: 10.1104/pp.16.01709

Stegmann, M., Anderson, R. G., Ichimura, K., Pecenkova, T., Reuter, P., Žárský, V., et al. (2012). The ubiquitin ligase PUB22 targets a subunit of the exocyst complex required for PAMP-triggered responses in arabidopsis c w. *Plant Cell*. 24, 4703–4716. doi: 10.1105/tpc.112.104463

Stegmann, M., Anderson, R. G., Westphal, L., Rosahl, S., McDowell, J. M., and Trujillo, M. (2014). The exocyst subunit Exo70B1 is involved in the immune response of Arabidopsis thaliana to different pathogens and cell death. *Plant Signal. Behav*. 8, e27421. doi: 10.4161/psb.27421

Synek, L., Schlager, N., Eliáš, M., Quentin, M., Hauser, M. T., and Žárský, V. (2006). AtEXO70A1, a member of a family of putative exocyst subunits specifically expanded in land plants, is important for polar growth and plant development. *Plant J*. 48, 54–72. doi: 10.1111/j.1365-313X.2006.02854.x

Synek, L., Vukašinović, N., Kulich, I., Hála, M., Aldorfová, K., Fendrych, M., et al. (2017). EXO70C2 is a key regulatory factor for optimal tip growth of pollen. *Plant Physiol*. 174, 223–240. doi: 10.1104/pp.16.01282

TerBush, D. R., Maurice, T., Roth, D., and Novick, P. (1996). The Exocyst is a multiprotein complex required for exocytosis in Saccharomyces cerevisiae. *EMBO J*. 15, 6483–6494. doi: 10.1002/j.1460-2075.1996.tb01039.x

van Wersch, R., Li, X., and Zhang, Y. (2016). Mighty dwarfs: Arabidopsis autoimmune mutants and their usages in genetic dissection of plant immunity. *Front. Plant Sci*. 7, 1717. doi: 10.3389/fpls.2016.01717

Vukašinović, N., Oda, Y., Pejchar, P., Synek, L., Pečenková, T., Rawat, A., et al. (2017). Microtubule-dependent targeting of the exocyst complex is necessary for xylem development in Arabidopsis. *New Phytol*. 213, 1052–1067. doi: 10.1111/nph.14267

Wang, W., Liu, N., Gao, C., Cai, H., Romeis, T., and Tang, D. (2020). The Arabidopsis exocyst subunits EXO70B1 and EXO70B2 regulate FLS2 homeostasis at the plasma membrane. *New Phytol*. 227, 529–544. doi: 10.1111/nph.16515

Wang, X. (2004). Lipid signaling. *Curr. Opin. Plant Biol*. 7, 329–336. doi: 10.1016/j.pbi.2004.03.012

Webb, B., and Sali, A. (2016). Comparative protein structure modeling using MODELLER. *Curr. Protoc. Bioinforma*. 1654, 39–54. doi: 10.1002/cpbi.3

Wiederstein, M., and Sippl, M. J. (2007). ProSA-web: Interactive web service for the recognition of errors in three-dimensional structures of proteins. *Nucleic Acids Res*. 35, W407–W410. doi: 10.1093/nar/gkm290

Wu, H., Turner, C., Gardner, J., Temple, B., and Brennwald, P. (2010). The Exo70 subunit of the exocyst is an effector for both Cdc42 and Rho3 function in polarized exocytosis. *Mol. Biol. Cell*. 21, 430–442. doi: 10.1091/mbc.E09-06-0501

Yuan, J., and He, S. Y. (1996). The Pseudomonas syringae Hrp regulation and secretion system controls the production and secretion of multiple extracellular proteins. *J. Bacteriol.* 178, 6399–6402. doi: 10.1128/jb.178.21.6399-6402.1996

Yuan, S., Chan, H. C. S., Filipek, S., and Vogel, H. (2016). PyMOL and inkscape bridge the data and the data visualization. *Structure*. 24, 2041–2042. doi: 10.1016/j.str.2016.11.012

Žárský, V., Cvrčková, F., Potocký, M., and Hála, M. (2009). Exocytosis and cell polarity in plants - Exocyst and recycling domains: Tansley review. *New Phytol.* 183, 255–272. doi: 10.1111/j.1469-8137.2009.02880.x

Žárský, V., Kulich, I., Fendrych, M., and Pečenková, T. (2013). Exocyst complexes multiple functions in plant cells secretory pathways. *Curr. Opin. Plant Biol.* 16, 726–733. doi: 10.1016/j.pbi.2013.10.013

Žárský, V., Sekereš, J., Kubátová, Z., Pečenková, T., and Cvrčková, F. (2020). Three subfamilies of exocyst EXO70 family subunits in land plants: early divergence and ongoing functional specialization. *J. Exp. Bot.* 71, 49–62. doi: 10.1093/jxb/erz423

Zhang, Z., Feechan, A., Pedersen, C., Newman, M. A., Qiu, J. L., Olesen, K. L., et al. (2007). A SNARE-protein has opposing functions in penetration resistance and defense signalling pathways. *Plant J.* 49, 302–312. doi: 10.1111/j.1365-313X.2006.02961.x

Zhao, Y., Liu, J., Yang, C., Capraro, B. R., Baumgart, T., Bradley, R. P., et al. (2013). Exo70 generates membrane curvature for morphogenesis and cell migration. *Dev. Cell.* 26, 266–278. doi: 10.1016/j.devcel.2013.07.007

Zhao, T., Rui, L., Li, J., Nishimura, M. T., Vogel, J. P., Liu, N., et al. (2015). A Truncated NLR protein, TIR-NBS2, is required for activated defense responses in the exo70B1 mutant. *PloS Genet.* 11, e1004945. doi: 10.1371/journal.pgen.1004945

Conflict of Interest: The authors declare that the research was conducted in the absence of any commercial or financial relationships that could be construed as a potential conflict of interest.

frontiers in Plant Science

MINI REVIEW
published: 03 November 2020
doi: 10.3389/fpls.2020.579875

Knowing When to Self-Eat – Fine-Tuning Autophagy Through ATG8 Iso-forms in Plants

Svetlana Boycheva Woltering[1,2]* *and Erika Isono*[1]

[1] Department of Biology, University of Konstanz, Konstanz, Germany, [2] Zukunftskolleg, University of Konstanz, Konstanz, Germany

Autophagy is a catabolic process that takes place under both normal and adverse conditions and is important for the degradation of various organelles and proteins that are no longer needed. Thus, it can be viewed as both a constitutive recycling machinery and an adaptation mechanism. Increase in the activity of autophagy can be caused by multiple biotic and abiotic stress factors. Though intensive research in the past decade has elucidated many molecular details of plant autophagy, the mechanisms of induction and regulation of the process remain understudied. Here, we discuss the role of ATG8 proteins in autophagic signaling and regulation with an emphasis on the significance of ATG8 diversification for adapting autophagy to the changing needs of plants.

Keywords: plant autophagy, adaptation mechanism, recycling, abiotic stress, regulator, regulation target

OPEN ACCESS

Edited by:
Kendal Hirschi,
Baylor College of Medicine,
United States

Reviewed by:
Ping Wang,
Iowa State University, United States
Toshiro Shigaki,
The University of Tokyo, Japan

***Correspondence:**
Svetlana Boycheva Woltering
svetlana.boycheva-woltering@uni-konstanz.de

Specialty section:
This article was submitted to Plant Membrane Traffic and Transport, a section of the journal Frontiers in Plant Science

Received: *03 July 2020*
Accepted: *30 September 2020*
Published: *03 November 2020*

Citation:
Boycheva Woltering S and Isono E (2020) Knowing When to Self-Eat – Fine-Tuning Autophagy Through ATG8 Iso-forms in Plants. Front. Plant Sci. 11:579875. doi: 10.3389/fpls.2020.579875

INTRODUCTION

Plants are unable to escape from unfavorable environmental conditions or damaging interactions with other organisms. Hence, in order to survive, they need to adapt to the changes in their surroundings as fast as possible. Due to these characteristics, it is important for plants to efficiently acquire essential elements, produce and reuse metabolites, and optimize energy consumption by recycling of cellular components.

One mechanism to degrade and recycle cytoplasmic material and provide building blocks in eukaryotic cells is autophagy (Li and Vierstra, 2012; Liu and Bassham, 2012; Avin-Wittenberg et al., 2018). Microautophagy occurs through invagination of the tonoplast engulfing cytoplasmic material in autophagic bodies while macroautophagy, hereafter referred to as autophagy, involves the formation of a cup-shaped phagophore which closes to form the autophagosome. Research conducted in the yeast *Saccharomyces cerevisiae* identified the main players in autophagy and revealed the detailed molecular mechanisms of autophagic degradation (Tsukada and Ohsumi, 1993; Noda et al., 1995; Ohsumi, 2001). Further studies with model organisms, including *Arabidopsis thaliana*, demonstrated high degree of conservation for the autophagic proteins in plants (Liu and Bassham, 2012).

The induction of autophagy in plants involves several protein kinases (**Figures 1A,B**). The best studied example is the target of rapamycin (TOR) kinase which is a negative regulator of autophagy and its downregulation or inhibition leads to constitutive activation of autophagy (Liu and Bassham, 2010). TOR belongs to the TORC1 complex together with its target recognition cofactor REGULATORY-ASSOCIATED PROTEIN OF mTOR (RAPTOR), and the stabilizer LETHAL WITH SEC13 8 (LST8) (Shi et al., 2018). Once activated, the TOR kinase transfers the

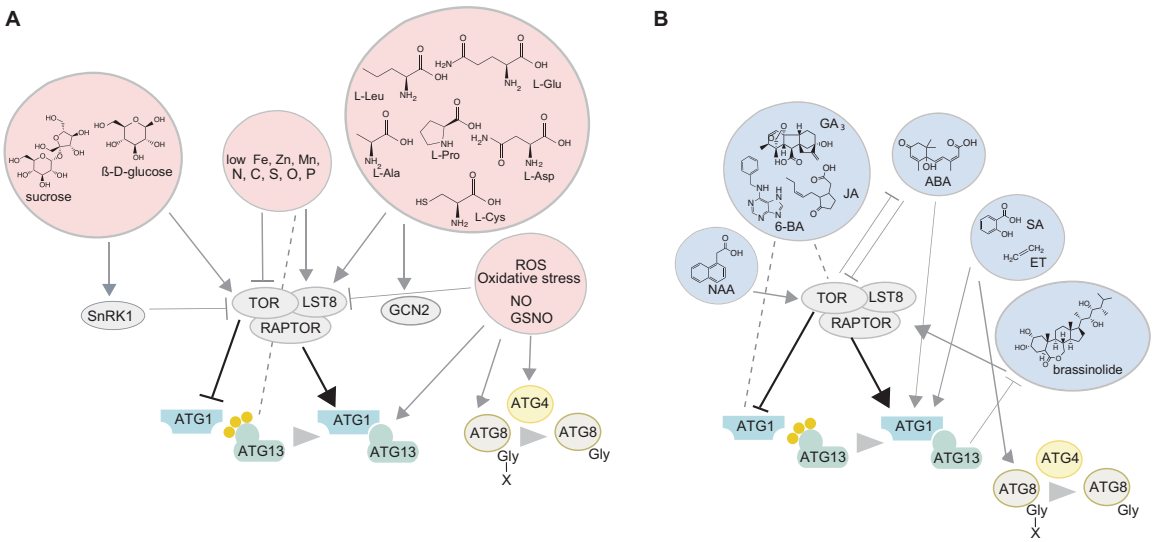

FIGURE 1 | Autophagy sensors and regulators with or without the involvement of the TOR kinase. **(A)** Sugars, mineral nutrients, amino acids, and ROS affect autophagy. Glucose activates TOR while the lack of it inhibits the TOR kinase thus activating autophagy. Furthermore, SnRK1 kinase can be involved in sugar sensing upstream of TOR. Low availability of nutrients activates autophagy with C and N starvation acting through TOR inhibition. P-deficiency stimulates autophagy independently of TOR, although LST8 was shown to act as an intermediate. Lack of Fe, Zn, and Mn also activates autophagy but the participation of TOR is not clear. Changes in the levels of branched chain amino acids, with or without the involvement of TOR have been reported to modulate TOR and autophagic activity in mammals. However, the only well-studied amino acid in plants in this aspect is cysteine where the levels of the sulfur precursor affect the activity of the TOR kinase itself, while the C/N precursor levels are perceived by GCN2 kinase. ROS can activate autophagy via TOR inhibition or directly influencing multiple ATG genes/proteins downstream of the TOR kinase. **(B)** Phytohormones modulate the activity of TOR and/or autophagy. Auxin (NAA) stimulates TOR thereby inhibiting the autophagy process. Brassinosteroids are also able to inhibit autophagy through TOR activation while autophagy itself can affect BR signaling by degrading components of it. ABA is involved in an interplay with the TOR kinase by inhibiting its activity under stress, thereby promoting autophagy, while under favorable conditions TOR suppresses ABA signaling. A direct connection between ABA and autophagy is indicated by the involvement of two ATG8-interacting proteins ATI1 and ATI2 in ABA-mediated germination and salt tolerance. The presence of less GA in autophagy mutants indicates its possible involvement in autophagy regulation although the exact mechanisms have not been established. Ethylene stimulates autophagy by directly activating ATG8 homologs or via ROS. The exact relationships of JA and CK with TOR and autophagy have not been established. SA stimulates autophagy involved in senescence and plant immunity possibly with the involvement of ROS. NO can regulate hypoxia responses by S-nitrosylating various proteins including the master regulator of NO signaling *S*-nitrosoglutathione reductase thus exposing its ATG8-interacting motif and targeting it for degradation. TOR, target of rapamycin; RAPTOR, regulatory-associated protein of mTOR; LST8, lethal with sec 13 8; SnRK1, sucrose non-fermenting related kinase 1; GCN2, general control non-depressible 2; ROS, reactive oxygen species; ATG, autophagy-related; NAA, naphthaleneacetic acid; 6-BA, 6-benzyladenine; GA3, gibberellic acid; JA, jasmonic acid; ABA, abscisic acid; SA, salicylic acid; ET, ethylene; BR, brassinolide; NO, nitric oxide.

signals downstream by phosphorylating the ATG1/ATG13 complex thus stimulating autophagic vesiculation that involves the decoration of the phagophore with phosphatidylinositol-3 phosphate (PI3P) and the delivery of lipids to the expanding phagophore (Suttangkakul et al., 2011). The ubiquitin-like ATG8 is then processed by the cysteine protease ATG4, which leads to the exposure of the c-terminal glycine of ATG8, allowing its recruitment to the phagophore through the attachment of the phospholipid phosphatidylethanolamine (PE) (Kirisako et al., 2000). Following closure, the newly formed double membrane delimited autophagosome is transported to the vacuole and fuses with the tonoplast, subsequently releasing its single-membrane content as an autophagic body into the vacuole.

Autophagy in plants was initially described as a system for bulk recycling of cytoplasmic material (Bassham, 2009). However, it is becoming increasingly evident that the process can be highly selective and requires strict regulation on multiple levels. An enormous body of studies of autophagy in plants elucidated the functions of core components and has been discussed in multiple excellent review articles (Ohsumi, 2001; Marshall and Vierstra, 2018; Shi et al., 2018; Yoshimoto and Ohsumi, 2018). Although some aspects of autophagy modulation have been well-studied, the detailed mechanisms remain elusive. In this review, we focus on regulation of autophagy mainly through ATG8 diversification and specialization.

TOR KINASE AS A CENTRAL MODULATOR OF ATG PROTEINS

Small molecules, mineral nutrients, reactive oxygen species (ROS) and phytohormones can influence the activity of autophagy and ATG proteins in plants in a TOR-dependent manner. Amino acid availability and abundance of their degradation products affect metabolic and developmental processes (Hildebrandt et al., 2015) including autophagy (Meijer et al., 2015). However, only cysteine has been described in detail in plants, with sulfur availability being sensed by the TOR kinase and the carbon/nitrogen (C/N) precursors by GENERAL CONTROL NON-DEPRESSIBLE2 (GCN2) kinase

(Dong et al., 2017) (**Figure 1A**). High levels of sulfur lead to increased glucose levels, and subsequently activate TOR, whereas reduced glucose levels during sulfur deficiency or impaired photosynthesis inhibit TOR and activate autophagy (reviewed in Fu et al., 2020). Glucose is the likely transmitter of the signal between sulfur and TOR (Dong et al., 2017) but whether it could convey the availability of other nutrients in the context of autophagy is unclear. The mechanisms of GCN2 perception in plants are unknown, although GCN2 activation by uncharged tRNAs appears to be universal in eukaryotes (Li et al., 2013) (**Figure 1A**). Prolonged carbon starvation (Huang et al., 2019) and phosphate deficit which causes ER stress (Naumann et al., 2019) induce autophagy independently of TOR, although recent research in Chlamydomonas suggests LST8, the stabilizer of TOR, is involved in phosphate starvation response (Couso et al., 2020).

The connection between autophagy and nitrogen metabolism, transport, and remobilization has been explored by the Masclaux-Daubresse lab and is covered in recent reviews (Masclaux-Daubresse et al., 2017; Chen et al., 2018). We will only mention that N depletion strongly inhibits TOR and activates autophagy, although its deficit also leads to accumulation of sugars, including glucose, which activates TOR and inhibits autophagy (Cao et al., 2019). Zinc deficit has also been shown to induce autophagy in *Arabidopsis thaliana* although the mechanisms are unclear (Shinozaki et al., 2020). In mammalian cells, iron is released from storage by Nuclear Receptor Coactivator4 (NCOA4) autophagy receptor mediated ferritin degradation in the lysosome (ferritinophagy) (Mancias et al., 2014; Mancias et al., 2015). In plants, multiple autophagy mutants of Arabidopsis have impaired translocation of iron, zinc and manganese, to the seeds, suggesting that deficit of these elements could induce autophagy (Pottier et al., 2018) (**Figure 1A**).

Phytohormones have been shown to regulate the TOR kinase and thus have the potential to affect TOR-dependent autophagy (reviewed in Fu et al., 2020). For example, auxin inhibits stress-induced autophagy by stimulating TOR activity (Schepetilnikov et al., 2017) (**Figure 1B**) or blocking autophagosome formation under certain stresses (Pu et al., 2017). Brassinosteroids (BRs) use the TOR kinase to inhibit autophagy and enhance their signaling through brassinazole-resistant (BZR)1 transcription factor at the same time (Zhang et al., 2016) (**Figure 1B**). BZR1 itself was shown to activate the transcription of the autophagy adaptor *Neighbour of BRCA (NBR)1,* promoting its own selective degradation (Chi et al., 2020). Direct involvement of gibberellins (GA) in the regulation of autophagy is unclear although lower levels of GA were detected in the rice autophagy mutant *osatg7-1* (Kurusu et al., 2017). The stress hormone abscisic acid (ABA) represses TOR activity (Wang et al., 2018), leading to autophagy activation while TOR itself inhibits ABA signaling under favorable environmental conditions. High levels of salicylic acid (SA) have been associated with autophagy-mediated senescence and programmed cell death (PCD) (Yoshimoto et al., 2009). In Arabidopsis, SA also accumulates during flooding increasing ROS levels, and stimulating autophagy (Chen et al., 2015). Both SA and PCD are strongly associated with pathogen response and plant immunity (Liu et al., 2016; Leary et al., 2019). Autophagy regulation in the context of plant immunity is extensively covered in other recent reviews (Üstün et al., 2017; Leary et al., 2019).

FINE-TUNING AUTOPHAGY THROUGH ATG8

One of the proteins central to the autophagic process, the ubiquitin-like ATG8, usually requires activation through post-translational cleavage by the ATG4 protease at the c-terminus. This process seems to be controlled for instance by ROS, that were shown to activate ATG4 in Chlamydomonas (Pérez-Pérez et al., 2012, 2016). Both ATG8 and ATG4 have more than one homolog in most plant species and several ATG4 homologs have been shown to interact preferentially with distinct ATG8 iso-forms (Woo et al., 2014; Seo et al., 2016). These observations imply that ATG8s and ATG4s could contribute to fine-tune specific and efficient induction of autophagy.

ATG8 can interact with receptor and adaptor proteins containing either ATG8-interacting motif [AIM/LIR; LIR-docking site (LDS)] or Ubiquitin-interacting motif [UIM; UIM-docking site (UDS)] (Marshall et al., 2019). UDS-interacting adaptors are the proteasome degradation subunit Regulatory particle non-ATPase (RPN)10 and the proteins from the Plant Ubiquitin Regulatory X Domain (PUX) family, which have diverse cellular functions (Marshall et al., 2015; Wen and Klionsky, 2016). LDS-interacting are NBR1 and the ATI (ATG8-interacting protein)1 and ATI2 proteins targeting plastid proteins for degradation upon carbon starvation (Honig et al., 2012; Michaeli et al., 2014). Known autophagy receptors are: the Arabidopsis Orosomucoid (ORM) proteins 1 and 2, involved in Flagellin-Sensing 2 (FLS2) receptor kinase degradation (Yang et al., 2019); DSK2, targeting the brassenosteroid pathway regulator BES1 for degradation (Nolan et al., 2017); the Arabidopsis TSPO protein regulating the levels of PIP2;7 aquaporin on the cell surface (Hachez et al., 2014). Most recently, a dehydrin in *Medicago truncatula* MtCAS31 was found to promote autophagy under drought stress through interaction with ATG8 (Li et al., 2019). Autophagy in the context of hypoxia responses can be regulated by nitric oxide (NO) which can *S*-nitrosylate various proteins including the master regulator of NO signaling *S*-nitrosoglutathione reductase, thus exposing its ATG8-interacting motif and targeting it for degradation (Zhan et al., 2018). It is unclear whether the highly variable AIM/LIR provides another layer of specificity in terms of different ATG8 iso-forms interacting with different variants of the motif.

Given the diversity of ATG8s in higher plants, it is difficult to conclude on the importance of each iso-form based on single knockout mutants due to functional redundancy. Different ATG8s appear to be induced by varying stress factors or to alleviate them although some overlap has been discovered (Vanhee et al., 2011; Xia et al., 2012; Luo et al., 2017; Chen et al., 2018; Li et al., 2019). The ability of different ATG8 iso-forms to interact with different effectors implies the existence of unique functions of the ATG8 homologs. Unfortunately, all the functional data so far have been obtained from a handful of model organisms and is not equally covering all the homologs. While it

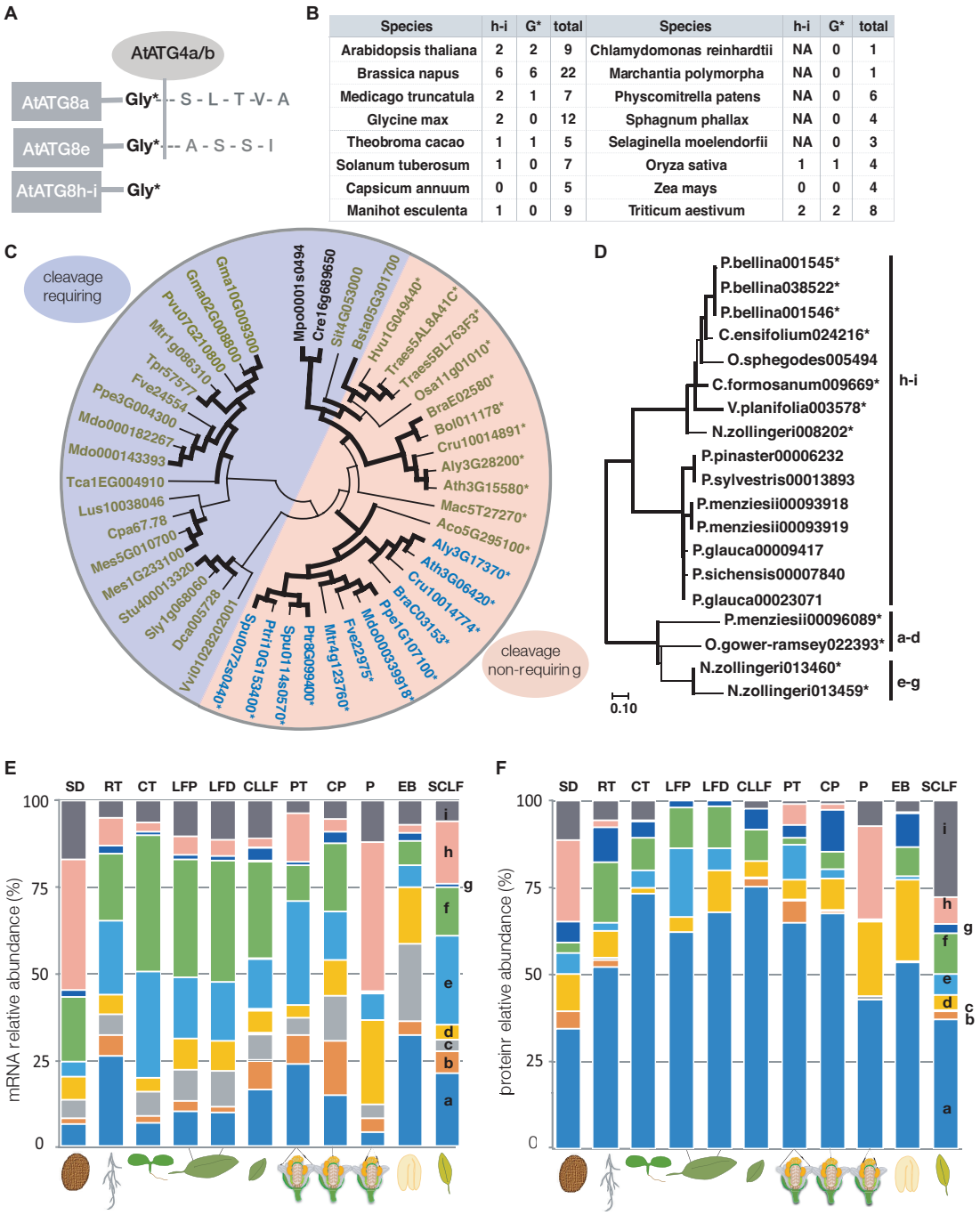

Species	h-i	G*	total	Species	h-i	G*	total
Arabidopsis thaliana	2	2	9	Chlamydomonas reinhardtii	NA	0	1
Brassica napus	6	6	22	Marchantia polymorpha	NA	0	1
Medicago truncatula	2	1	7	Physcomitrella patens	NA	0	6
Glycine max	2	0	12	Sphagnum phallax	NA	0	4
Theobroma cacao	1	1	5	Selaginella moelendorfii	NA	0	3
Solanum tuberosum	1	0	7	Oryza sativa	1	1	4
Capsicum annuum	0	0	5	Zea mays	0	0	4
Manihot esculenta	1	0	9	Triticum aestivum	2	2	8

FIGURE 2 | ATG8 analysis. **(A)** Schematic representation of cleavable and non-cleavable ATG8 iso-forms in Arabidopsis. **(B)** The table lists the homologs in the ATG8h-i group for a given species, the total number and the number of homologs with an exposed glycine. In some cases, the ATG8h-i group members have been secondarily lost such as in *C. annuum* and *Z. mays*. **(C,D)** Phylogenetic tree of ATG8h-i homologs of selected mono- and eudicot species and gymnosperms and orchids, respectively. Protein coding sequences were taken from Phytozome 12 (Goodstein et al., 2012) in **(C)** and from Gymno Plaza 1.0 (Proost et al., 2009) and Orchidstra 2.0 (Chao et al., 2017) for **(D)**. **(C)** Unicellular algae have a single ATG8, while mosses can have one or multiple homologs both groups clustering together and completely separately from the ATG8h-i group of homologs of the higher plants. Some homologs of the ATG8h-i group have an exposed catalytic glycine (marked with an asterisk) such as all the sequenced *Brassicaceae* species. ATG8h-i members with and without an exposed glycine could be in the same species. The ATG8h-homologs are shown in blue and the ATG8i-homologs are depicted in green. The algae/mosses group is shown in black. In **(C)**, all homologs with an exposed catalytic glycine are marked with an asterisk and the entire segment of the tree is colored in orange and the cleavable iso-forms are colored in blue. **(D)** The clades are indicated next to the tree, while the homologs with an exposed G are marked with an asterisk. The Evolutionary analysis was conducted using the Maximum Likelihood method and General Time Reversible model (Nei and Kumar, 2000) for both **(C,D)**. The bootstrap consensus tree inferred from 1000 replicates

(Continued)

FIGURE 2 | Continued
is taken to represent the evolutionary history of the taxa analyzed (Felsenstein, 1985). Branches corresponding to partitions reproduced in less than 50% bootstrap replicates are collapsed. The percentage of replicate trees in which the associated taxa clustered together in the bootstrap test (1000 replicates) are shown next to the branches and the ones equal to or above 60% are indicated by a bold black line (Felsenstein, 1985). Initial trees for the heuristic search were obtained automatically by applying Neighbor-Join and BioNJ algorithms to a matrix of pairwise distances estimated using the maximum composite likelihood (MCL) approach, and then selecting the topology with superior log likelihood value. A discrete Gamma distribution was used to model evolutionary rate differences among sites [5 categories (+ G, parameter = 0.9115)]. The rate variation model allowed for some sites to be evolutionarily invariable ([+ I], 15.22% sites). This analysis involved 45 and 19 protein coding nucleotide sequences with 335 and 309 positions in the final dataset for **(C)** and **(D)** respectively. Evolutionary analyses were conducted in MEGA X (Kumar et al., 2018; Stecher et al., 2020). **(E,F)** Relative abundance of ATG8 transcript and protein, respectively, based on a dataset from Mergner et al. (2020) (data file 41568_2020_2094_MOESM4) containing experimental data for 30 different tissues and in both **(E)** and **(F)** non-transformed values were used for generating the graphical representation. Transcript abundance was estimated using TPM (transcript per million) and protein abundance estimation was based on iBAQ (intensity-based absolute quantification). ATG8 protein iso-forms a, d, and f can be found in every tissue examined. Values are for selected organs, tissues, and developmental stages: SD – dry seed; RT – root; CT – cotyledon; LFP – rosette leaf 7 proximal part; LFD – rosette leaf 7 distal part of the leaf; CLLF – cauline leaf 1; PT – petal; CP – carpel; P – pollen; EB – embryo; SCLF – senescent leaf.

is essential that more *in vivo* and *in planta* data are acquired, in the next section we use existing resources such as available plant genomes together with transcriptomics and proteomics data to explore ATG8 specificities in the plant kingdom.

SIGNIFICANCE OF THE ATG8 DIVERSITY

ATG8 proteins have shown a tendency toward increase in number of iso-forms and diversification in multicellular organisms. Yeast and algae have a single homolog while in the genomes of higher plants, multiple homologs can be found (Kellner et al., 2017). The nine iso-forms (ATG8a-i) of Arabidopsis have been investigated more in depth revealing that they belong to three separate groups – a-d, e-g, and h-i (Seo et al., 2016; Kellner et al., 2017). A characteristic of many members of the ATG8h-i group is that they have an exposed catalytic glycine residue, and do not require cleavage by the ATG4 protease for activation (**Figure 2A**) (Seo et al., 2016; Kellner et al., 2017).

Analyzing several model and crop species showed that the presence of ATG8h-i group members is not strictly associated with the total number of ATG8 homologs in each species (**Figure 2B**). For example, in maize (*Zea mays*), none of the four ATG8s belong to the ATG8h-i group, while one of the four rice (*Oryza sativa*) homologs is cleavage-free. Additionally, while Medicago (*Medicago truncatula*) and soybean (*Glycine max*) have two ATG8h-i iso-forms each, only one in Medicago is cleavage-free. The rapeseed (*Brassica napus*) has six h-i homologs, all ending with a glycine (G) and as the plant is a recent alopolyploid (Lu et al., 2019), it could serve as a model to study ATG8 diversification and mechanisms of retention. While *Brassicaceae* species have only ATG8h-i iso-forms with an exposed glycine, some ATG8i-homologs from other taxonomic groups have additional amino acids at the C-terminus. The cleavage-free and cleavage-requiring forms separate from each other as shown by Maximum likelihood analysis (**Figure 2C**). It is yet to be established whether this exposed glycine residue provides any advantage to the ATG8 protein that possesses it. If cleavage free iso-forms are constitutively active, they might be important for fast induction of autophagy under stress conditions. However, involvement in a developmental process cannot be excluded based on the current understanding of the iso-forms which prompted further analyses of the ATG8 family. Exploring several gymnosperm genomes indicated, that while acquisition of multiple ATG8 homologs can be associated with multicellularity, the non-cleavable forms appeared together with seeds. Interestingly, the gymnosperms homologs with an exposed G belong to the a-d group (**Figure 2D**) and the limited number makes it difficult to conclude on their significance. Analyzing additional mono- and dicots such as the primitive *Amborella trichopoda* (*Amborellaceae* family) (Endress and Igersheim, 2000) and members of the *Orchidaceae* family, showed that cleavage free ATG8s exist in each case and with only two exceptions belong to the h-i group (**Figure 2D**). Whether the mass appearance of cleavage free ATG8s can be associated with any of the characteristics new to seed plants remains to be investigated. It is however established, that autophagy plays an important role in male reproduction in plants (reviewed in Norizuki et al., 2020) and in rice, endosperm development (Sera et al., 2019). However, the current advances in ATG8s do not allow conclusions on specific functions of the homologs to be made. A step in the right direction would be investigating the possible unique roles of ATG8 iso-forms.

EXPRESSION AND ABUNDANCE OF ATG8s

In order to estimate the potential for diversity of function of the ATG8s, we next analyzed data from two recent large-scale studies dealing with transcriptional regulation and with proteomics, respectively, conducted in Arabidopsis. The first study identified 225 transcription factors (TFs) by yeast one-hybrid screen able to bind the promoters of four *ATG8* genes, namely *ATG8a*, *b*, *e,* and *h* (Wang et al., 2019) and thus having the potential to activate their transcription. Surprisingly, only 19 of those TFs were shared by all four genes. The *ATG8e* promoter interacted with 71 unique TFs. Transcriptional activation by phytohormones such as ET can affect the expression of various *ATG* genes which makes it essential for survival during submergence in Arabidopsis (Chen et al., 2015; Hartman et al., 2019), most likely mediating the switch from hypoxia-associated fermentation to degradation of amino acids and fatty acids (Okuda et al., 2011; Zhu et al., 2018) (**Figure 1B**). ET is also able to stimulate the expression of *ATG8* homologs specifically in autophagy-dependent pollen development in petunia (*Petunia hybrida*) likely through ROS

signaling or direct binding to their promoters (Okuda et al., 2011; Zhu et al., 2018). It is however currently unknown whether ET has identical affinity toward all *ATG8* promoters.

Apart from the evidence for differential transcriptional regulation of the ATG8 homologs, differences in protein levels have recently been documented by large scale quantitative transcriptome and proteome analysis of 30 different tissues (Mergner et al., 2020). While all *ATG8* genes seem to be expressed in every analyzed tissue (**Figure 2E**), only AtATG8a, d, and f protein iso-forms are ubiquitously present (**Figure 2F**). Notably, in root, petal, carpel and senescing leaves all ATG8 proteins can be found and ATG8a appears to be the predominant iso-form in all tissues (**Figure 2F**) (Mergner et al., 2020). The AtATG8h protein is very strongly expressed in pollen and dry seed, reflecting high mRNA levels in the same tissues, but completely missing in rosette and cauline leaves. The other member of the clade, AtATG8i, also has the highest relative protein abundance in senescent leaves but is also strongly present in pollen and dry seed, and cotyledons also contain relatively high levels. One possible explanation for the discrepancies in transcript and protein abundance of the ATG8 could be different turnover rates of the proteins. It also remains to be established to what extent the exposed c-terminal glycine could offer an advantage in different autophagy inducing conditions and whether the h and i iso-forms would require some other type of activation.

DISCUSSION

The presence of multiple regulation targets providing grounds for activity modulation of autophagy could be considered as an indicator that such intricate regulatory system is in fact necessary. It is without a doubt, that understanding the molecules and signals affecting the autophagy machinery would contribute to the elucidation of autophagy induction and regulation.

One of the most upstream targets of autophagy modulation, the TOR kinase, has recently featured in a phosphoproteomic screen combined with targeted proteomics analysis of interacting proteins, in *Arabidopsis thaliana*, identifying potential upstream and downstream components of the TOR network (Van Leene et al., 2019) that could be investigated together with many non-protein molecules in relation to autophagy regulation.

Increase in number of iso-forms and diversification of ATG8 in plants along the course of evolution might reflect the need to accommodate the requirements of the increased complexity of flowering species. It is possible that iso-form specific or clade-specific ATG8 functions exist or that certain homologs are more abundant in autophagosomes under given conditions, in specific tissues and organs or during certain developmental stages. Additionally, exploring the specificity of the ATG8 interactions and the significance of the cleavage free iso-forms, also by obtaining more functional data could further clarify the diversity of the ATG8 homologs in plants and contribute to the understanding of autophagy induction and regulation. In this line of thought, clarifying the molecular mechanisms regulating ATG4 and ATG8 would provide more insight into the process of fine-tuning autophagy.

AUTHOR CONTRIBUTIONS

SBW provided the initial draft while both SBW and EI were involved in the further editing of the manuscript and the preparation of the figures. Both authors conceptualized the idea.

FUNDING

SBW was a recipient of a Humboldt-Bayer research fellowship of the Alexander von Humboldt Foundation. Work in the authors' lab was supported by grants from the German Science Foundation (DFG: SFB969 and IS 221/6-1) to EI. The publication cost was supported by the Open Access Publication Fund of the University of Konstanz.

REFERENCES

Avin-Wittenberg, T., Baluška, F., Bozhkov, P. V., Elander, P. H., Fernie, A. R., Galili, G., et al. (2018). Autophagy-related approaches for improving nutrient use efficiency and crop yield protection. *J. Exp. Bot.* 69, 1335–1353. doi: 10.1093/jxb/ery069

Bassham, D. C. (2009). Function and regulation of macroautophagy in plants. *Biochim. Biophys. Acta* 1793, 1397–1403. doi: 10.1016/j.bbamcr.2009.01.001

Cao, P., Kim, S. J., Xing, A., Schenck, C. A., Liu, L., Jiang, N., et al. (2019). Homeostasis of branched-chain amino acids is critical for the activity of TOR signaling in *Arabidopsis*. *Elife* 8:e50747. doi: 10.7554/eLife.50747.sa2

Chao, Y. T., Yen, S. H., Yeh, J. H., Chen, W. C., and Shih, M. C. (2017). Orchidstra 2.0-A transcriptomics resource for the orchid family. *Plant Cell Physiol.* 58:e9. doi: 10.1093/pcp/pcw220

Chen, L., Liao, B., Qi, H., Xie, L. J., Huang, L., Tan, W. J., et al. (2015). Autophagy contributes to regulation of the hypoxia response during submergence in *Arabidopsis thaliana*. *Autophagy* 11, 2233–2246. doi: 10.1080/15548627.2015.1112483

Chen, Q., Soulay, F., Saudemont, B., Elmayan, T., Marmagne, A., and Masclaux-Daubresse, C. (2018). Overexpression of *ATG8* in *Arabidopsis* Stimulates autophagic activity and increases nitrogen remobilization efficiency and grain filling. *Plant Cell Physiol.* 60, 343–352. doi: 10.1093/pcp/pcy214

Chi, C., Li, X., Fang, P., Xia, X., Shi, K., Zhou, Y., et al. (2020). Brassinosteroids act as a positive regulator of NBR1-dependent selective autophagy in response to chilling stress in tomato. *J. Exp. Bot.* 71, 1092–1106. doi: 10.1093/jxb/erz466

Couso, I., Pérez-Pérez, M. E., Ford, M. M., Martínez-Force, E., Hicks, L. M., Umen, J. G., et al. (2020). Phosphorus availability regulates TORC1 signaling via LST8 in Chlamydomonas. *Plant Cell* 32, 69–80. doi: 10.1105/tpc.19.00179

Dong, Y., Silbermann, M., Speiser, A., Forieri, I., Linster, E., Poschet, G., et al. (2017). Sulfur availability regulates plant growth via glucose-TOR signaling. *Nat. Commun.* 8:1174. doi: 10.1038/s41467-017-01224-w

Endress, P. K., and Igersheim, A. (2000). The reproductive structures of the basal angiosperm *Amborella Trichopoda* (Amborellaceae). *Int. J. Plant Sci.* 161, S237–S248. doi: 10.1086/317571

Felsenstein, J. (1985). CONFIDENCE limits on phylogenies: an approach using the bootstrap. *Evolution* 39, 783–791. doi: 10.1111/j.1558-5646.1985.tb00420.x

Fu, L., Wang, P., and Xiong, Y. (2020). Target of Rapamycin signaling in plant stress responses. *Plant Physiol.* 182, 1613–1623. doi: 10.1104/pp.19.01214

Goodstein, D. M., Shu, S., Howson, R., Neupane, R., Hayes, R. D., Fazo, J., et al. (2012). Phytozome: a comparative platform for green plant genomics. *Nucleic Acids Res.* 40, D1178–1186. doi: 10.1093/nar/gkr944

Hachez, C., Veljanovski, V., Reinhardt, H., Guillaumot, D., Vanhee, C., Chaumont, F., et al. (2014). The *Arabidopsis* abiotic stress-induced TSPO-related protein reduces cell-surface expression of the aquaporin PIP2;7 through protein-protein interactions and autophagic degradation. *Plant Cell* 26, 4974–4990. doi: 10.1105/tpc.114.134080

Hartman, S., Sasidharan, R., and Voesenek, L. (2019). The role of ethylene in metabolic acclimations to low oxygen. *New Phytol.* doi: 10.1111/nph.16378 [Epub ahead of print].

Hildebrandt, T. M., Nunes Nesi, A., Araujo, W. L., and Braun, H. P. (2015). Amino acid catabolism in plants. *Mol. Plant* 8, 1563–1579. doi: 10.1016/j.molp.2015.09.005

Honig, A., Avin-Wittenberg, T., Ufaz, S., and Galili, G. (2012). A new type of compartment, defined by plant-specific atg8-interacting proteins, is induced upon exposure of *Arabidopsis* Plants to carbon starvation. *Plant Cell* 24, 288–303. doi: 10.1105/tpc.111.093112

Huang, X., Zheng, C., Liu, F., Yang, C., Zheng, P., Lu, X., et al. (2019). Genetic analyses of the *Arabidopsis* ATG1 kinase complex reveal both kinase-dependent and independent autophagic routes during fixed-carbon starvation. *Plant Cell* 31:2973. doi: 10.1105/tpc.19.00066

Kellner, R., De La Concepcion, J. C., Maqbool, A., Kamoun, S., and Dagdas, Y. F. (2017). ATG8 Expansion: a driver of selective autophagy diversification? *Trends Plant Sci.* 22, 204–214. doi: 10.1016/j.tplants.2016.11.015

Kirisako, T., Ichimura, Y., Okada, H., Kabeya, Y., Mizushima, N., Yoshimori, T., et al. (2000). The reversible modification regulates the membrane-binding state of Apg8/Aut7 essential for autophagy and the cytoplasm to vacuole targeting pathway. *J. Cell Biol.* 151, 263–276. doi: 10.1083/jcb.151.2.263

Kumar, S., Stecher, G., Li, M., Knyaz, C., and Tamura, K. (2018). MEGA X: molecular evolutionary genetics analysis across computing platforms. *Mol. Biol. Evol.* 35, 1547–1549. doi: 10.1093/molbev/msy096

Kurusu, T., Koyano, T., Kitahata, N., Kojima, M., Hanamata, S., Sakakibara, H., et al. (2017). Autophagy-mediated regulation of phytohormone metabolism during rice anther development. *Plant Signal. Behav.* 12:e1365211. doi: 10.1080/15592324.2017.1365211

Leary, A. Y., Savage, Z., Tumtas, Y., and Bozkurt, T. O. (2019). Contrasting and emerging roles of autophagy in plant immunity. *Curr. Opin. Plant Biol.* 52, 46–53. doi: 10.1016/j.pbi.2019.07.002

Li, B., Liu, G., Wang, Y., Wei, Y., and Shi, H. (2019). Overexpression of banana *ATG8f* modulates drought stress resistance in *Arabidopsis*. *Biomolecules* 9:814. doi: 10.3390/biom9120814

Li, F., and Vierstra, R. D. (2012). Autophagy: a multifaceted intracellular system for bulk and selective recycling. *Trends Plant Sci.* 17, 526–537. doi: 10.1016/j.tplants.2012.05.006

Li, M. W., Auyeung, W. K., and Lam, H. M. (2013). The GCN2 homologue in *Arabidopsis thaliana* interacts with uncharged tRNA and uses *Arabidopsis* eIF2α molecules as direct substrates. *Plant Biol.* 15, 13–18. doi: 10.1111/j.1438-8677.2012.00606.x

Liu, L., Sonbol, F. M., Huot, B., Gu, Y., Withers, J., Mwimba, M., et al. (2016). Salicylic acid receptors activate jasmonic acid signalling through a non-canonical pathway to promote effector-triggered immunity. *Nat. Commun.* 7:13099. doi: 10.1038/ncomms13099

Liu, Y., and Bassham, D. C. (2010). TOR is a negative regulator of autophagy in *Arabidopsis thaliana*. *PLoS One* 5:e11883. doi: 10.1371/journal.pone.0011883

Liu, Y., and Bassham, D. C. (2012). Autophagy: pathways for self-eating in plant cells. *Annu. Rev. Plant Biol.* 63, 215–237. doi: 10.1146/annurev-arplant-042811-105441

Lu, K., Wei, L., Li, X., Wang, Y., Wu, J., Liu, M., et al. (2019). Whole-genome resequencing reveals Brassica napus origin and genetic loci involved in its improvement. *Nat. Commun.* 10:1154. doi: 10.1038/s41467-019-09134-9

Luo, L., Zhang, P., Zhu, R., Fu, J., Su, J., Zheng, J., et al. (2017). Autophagy is rapidly induced by salt stress and is required for salt tolerance in *Arabidopsis*. *Front. Plant Sci* 8:1459. doi: 10.3389/fpls.2017.01459

Mancias, J. D., Pontano Vaites, L., Nissim, S., Biancur, D. E., Kim, A. J., Wang, X., et al. (2015). Ferritinophagy via NCOA4 is required for erythropoiesis and is regulated by iron dependent HERC2-mediated proteolysis. *Elife* 4:e10308. doi: 10.7554/eLife.10308.014

Mancias, J. D., Wang, X., Gygi, S. P., Harper, J. W., and Kimmelman, A. C. (2014). Quantitative proteomics identifies NCOA4 as the cargo receptor mediating ferritinophagy. *Nature* 509, 105–109. doi: 10.1038/nature13148

Marshall, R. S., Hua, Z., Mali, S., Mcloughlin, F., and Vierstra, R. D. (2019). ATG8-Binding UIM proteins define a new class of autophagy adaptors and receptors. *Cell* 177, 766–781.e24. doi: 10.1016/j.cell.2019.02.009

Marshall, R. S., Li, F., Gemperline, D. C., Book, A. J., and Vierstra, R. D. (2015). Autophagic degradation of the 26S proteasome is mediated by the dual ATG8/Ubiquitin receptor RPN10 in *Arabidopsis*. *Mol. Cell* 58, 1053–1066. doi: 10.1016/j.molcel.2015.04.023

Marshall, R. S., and Vierstra, R. D. (2018). Autophagy: the master of bulk and selective recycling. *Annu. Rev. Plant Biol.* 69, 173–208. doi: 10.1146/annurev-arplant-042817-040606

Masclaux-Daubresse, C., Chen, Q., and Havé, M. (2017). Regulation of nutrient recycling via autophagy. *Curr. Opin. Plant Biol.* 39, 8–17. doi: 10.1016/j.pbi.2017.05.001

Meijer, A. J., Lorin, S., Blommaart, E. F., and Codogno, P. (2015). Regulation of autophagy by amino acids and MTOR-dependent signal transduction. *Amino Acids* 47, 2037–2063. doi: 10.1007/s00726-014-1765-4

Mergner, J., Frejno, M., List, M., Papacek, M., Chen, X., Chaudhary, A., et al. (2020). Mass-spectrometry-based draft of the *Arabidopsis* proteome. *Nature* 579, 409–414. doi: 10.1038/s41586-020-2094-2

Michaeli, S., Honig, A., Levanony, H., Peled-Zehavi, H., and Galili, G. (2014). *Arabidopsis* ATG8-INTERACTING PROTEIN1 is involved in autophagy-dependent vesicular trafficking of plastid proteins to the vacuole. *Plant Cell* 26, 4084–4101. doi: 10.1105/tpc.114.129999

Naumann, C., Müller, J., Sakhonwasee, S., Wieghaus, A., Hause, G., Heisters, M., et al. (2019). The local phosphate deficiency response activates endoplasmic reticulum stress-dependent autophagy. *Plant Physiol.* 179:460. doi: 10.1104/pp.18.01379

Nei, M., and Kumar, S. (2000). *Molecular Evolution and Phylogenetics*. Oxford: Oxford University Press.

Noda, T., Matsuura, A., Wada, Y., and Ohsumi, Y. (1995). Novel system for monitoring autophagy in the yeast *Saccharomyces cerevisiae*. *Biochem. Biophys. Res. Commun.* 210, 126–132. doi: 10.1006/bbrc.1995.1636

Nolan, T. M., Brennan, B., Yang, M., Chen, J., Zhang, M., Li, Z., et al. (2017). Selective autophagy of BES1 mediated by DSK2 balances plant growth and survival. *Dev. Cell* 41, 33–46.e7. doi: 10.1016/j.devcel.2017.03.013

Norizuki, T., Minamino, N., and Ueda, T. (2020). Role of autophagy in male reproductive processes in land plants. *Front. Plant Sci.* 11:756. doi: 10.3389/fpls.2020.00756

Ohsumi, Y. (2001). Molecular dissection of autophagy: two ubiquitin-like systems. *Nat. Rev. Mol. Cell Biol.* 2, 211–216. doi: 10.1038/35056522

Okuda, M., Nang, M. P., Oshima, K., Ishibashi, Y., Zheng, S. H., Yuasa, T., et al. (2011). The ethylene signal mediates induction of GmATG8i in soybean plants under starvation stress. *Biosci. Biotechnol. Biochem.* 75, 1408–1412. doi: 10.1271/bbb.110086

Pérez-Pérez, M. E., Couso, I., and Crespo, J. L. (2012). Carotenoid deficiency triggers autophagy in the model green alga Chlamydomonas reinhardtii. *Autophagy* 8, 376–388. doi: 10.4161/auto.18864

Pérez-Pérez, M. E., Lemaire, S. D., and Crespo, J. L. (2016). Control of autophagy in chlamydomonas is mediated through redox-dependent inactivation of the ATG4 protease. *Plant Physiol.* 172, 2219–2234. doi: 10.1104/pp.16.01582

Pottier, M., Dumont, J., Masclaux-Daubresse, C., and Thomine, S. (2018). Autophagy is essential for optimal translocation of iron to seeds in *Arabidopsis*. *J. Exp. Botany* 70, 859–869. doi: 10.1093/jxb/ery388

Proost, S., Van Bel, M., Sterck, L., Billiau, K., Van Parys, T., Van De Peer, Y., et al. (2009). PLAZA: a comparative genomics resource to study gene and genome evolution in plants. *Plant Cell* 21, 3718–3731. doi: 10.1105/tpc.109.071506

Pu, Y., Luo, X., and Bassham, D. C. (2017). TOR-dependent and -independent pathways regulate autophagy in *Arabidopsis thaliana*. *Front. Plant Sci.* 8:1204. doi: 10.3389/fpls.2017.01204

Schepetilnikov, M., Makarian, J., Srour, O., Geldreich, A., Yang, Z., Chicher, J., et al. (2017). GTPase ROP2 binds and promotes activation of target of rapamycin, TOR, in response to auxin. *EMBO J.* 36, 886–903. doi: 10.15252/embj.201694816

Seo, E., Woo, J., Park, E., Bertolani, S. J., Siegel, J. B., Choi, D., et al. (2016). Comparative analyses of ubiquitin-like ATG8 and cysteine protease ATG4 autophagy genes in the plant lineage and cross-kingdom processing of

ATG8 by ATG4. *Autophagy* 12, 2054–2068. doi: 10.1080/15548627.2016.1217373

Sera, Y., Hanamata, S., Sakamoto, S., Ono, S., Kaneko, K., Mitsui, Y., et al. (2019). Essential roles of autophagy in metabolic regulation in endosperm development during rice seed maturation. *Sci. Rep.* 9:18544. doi: 10.1038/s41598-019-54361-1

Shi, L., Wu, Y., and Sheen, J. (2018). TOR signaling in plants: conservation and innovation. *Development* 145:dev160887. doi: 10.1242/dev.160887

Shinozaki, D., Merkulova, E. A., Naya, L., Horie, T., Kanno, Y., Seo, M., et al. (2020). Autophagy increases Zinc bioavailability to avoid light-mediated reactive oxygen species production under Zinc deficiency. *Plant Physiol.* 182, 1284–1296. doi: 10.1104/pp.19.01522

Stecher, G., Tamura, K., and Kumar, S. (2020). Molecular evolutionary genetics analysis (MEGA) for macOS. *Mol. Biol. Evol.* 37, 1237–1239. doi: 10.1093/molbev/msz312

Suttangkakul, A., Li, F., Chung, T., and Vierstra, R. D. (2011). The ATG1/ATG13 protein kinase complex is both a regulator and a target of autophagic recycling in *Arabidopsis*. *Plant Cell* 23, 3761–3779. doi: 10.1105/tpc.111.090993

Tsukada, M., and Ohsumi, Y. (1993). Isolation and characterization of autophagy-defective mutants of *Saccharomyces cerevisiae*. *FEBS Lett.* 333, 169–174. doi: 10.1016/0014-5793(93)80398-E

Üstün, S., Hafrén, A., and Hofius, D. (2017). Autophagy as a mediator of life and death in plants. *Curr. Opin. Plant Biol.* 40, 122–130. doi: 10.1016/j.pbi.2017.08.011

Van Leene, J., Han, C., Gadeyne, A., Eeckhout, D., Matthijs, C., Cannoot, B., et al. (2019). Capturing the phosphorylation and protein interaction landscape of the plant TOR kinase. *Nat. Plants* 5, 316–327. doi: 10.1038/s41477-019-0378-z

Vanhee, C., Zapotoczny, G., Masquelier, D., Ghislain, M., and Batoko, H. (2011). The *Arabidopsis* multistress regulator TSPO is a heme binding membrane protein and a potential scavenger of porphyrins via an autophagy-dependent degradation mechanism. *Plant Cell* 23, 785–805. doi: 10.1105/tpc.110.081570

Wang, P., Nolan, T. M., Yin, Y., and Bassham, D. C. (2019). Identification of transcription factors that regulate ATG8 expression and autophagy in *Arabidopsis*. *Autophagy* 16, 123–139. doi: 10.1080/15548627.2019.1598753

Wang, P., Zhao, Y., Li, Z., Hsu, C.-C., Liu, X., Fu, L., et al. (2018). Reciprocal regulation of the TOR kinase and ABA receptor balances plant growth and stress response. *Mol. Cell* 69, 100–112.e6. doi: 10.1016/j.molcel.2017.12.002

Wen, X., and Klionsky, D. J. (2016). The proteasome subunit RPN10 functions as a specific receptor for degradation of the 26S proteasome by macroautophagy in *Arabidopsis*. *Autophagy* 12, 905–906. doi: 10.1080/15548627.2016.1171949

Woo, J., Park, E., and Dinesh-Kumar, S. P. (2014). Differential processing of *Arabidopsis* ubiquitin-like Atg8 autophagy proteins by Atg4 cysteine proteases. *Proc. Natl. Acad. Sci. U.S.A.* 111, 863–868. doi: 10.1073/pnas.1318207111

Xia, T., Xiao, D., Liu, D., Chai, W., Gong, Q., and Wang, N. N. (2012). Heterologous expression of ATG8c from soybean confers tolerance to nitrogen deficiency and increases yield in *Arabidopsis*. *PLoS One* 7:e37217. doi: 10.1371/journal.pone.0037217

Yang, F., Kimberlin, A. N., Elowsky, C. G., Liu, Y., Gonzalez-Solis, A., Cahoon, E. B., et al. (2019). A plant immune receptor degraded by selective autophagy. *Mol. Plant* 12, 113–123. doi: 10.1016/j.molp.2018.11.011

Yoshimoto, K., Jikumaru, Y., Kamiya, Y., Kusano, M., Consonni, C., Panstruga, R., et al. (2009). Autophagy negatively regulates cell death by controlling NPR1-dependent salicylic acid signaling during senescence and the innate immune response in *Arabidopsis*. *Plant Cell* 21, 2914–2927. doi: 10.1105/tpc.109.068635

Yoshimoto, K., and Ohsumi, Y. (2018). Unveiling the molecular mechanisms of plant autophagy-from autophagosomes to vacuoles in plants. *Plant Cell Physiol.* 59, 1337–1344. doi: 10.1093/pcp/pcy112

Zhan, N., Wang, C., Chen, L., Yang, H., Feng, J., Gong, X., et al. (2018). S-nitrosylation targets GSNO reductase for selective autophagy during hypoxia responses in plants. *Mol. Cell* 71, 142–154.e6. doi: 10.1016/j.molcel.2018.05.024

Zhang, Z., Zhu, J. Y., Roh, J., Marchive, C., Kim, S. K., Meyer, C., et al. (2016). TOR signaling promotes accumulation of BZR1 to balance growth with carbon availability in *Arabidopsis*. *Curr. Biol.* 26, 1854–1860. doi: 10.1016/j.cub.2016.05.005

Zhou, J., Wang, J., Cheng, Y., Chi, Y. J., Fan, B., Yu, J. Q., et al. (2013). NBR1-mediated selective autophagy targets insoluble ubiquitinated protein aggregates in plant stress responses. *PLoS Genet.* 9:e1003196. doi: 10.1371/journal.pgen.1003196

Zhu, T., Zou, L., Li, Y., Yao, X., Xu, F., Deng, X., et al. (2018). Mitochondrial alternative oxidase-dependent autophagy involved in ethylene-mediated drought tolerance in *Solanum lycopersicum*. *Plant Biotechnol. J.* 16, 2063–2076. doi: 10.1111/pbi.12939

Conflict of Interest: The authors declare that the research was conducted in the absence of any commercial or financial relationships that could be construed as a potential conflict of interest.

frontiers in Plant Science

MINI REVIEW
published: 08 December 2020
doi: 10.3389/fpls.2020.609516

Differentiation of Trafficking Pathways at Golgi Entry Core Compartments and Post-Golgi Subdomains

Yoko Ito and Yohann Boutté**

Laboratoire de Biogenèse Membranaire, Université de Bordeaux, Villenave d'Ornon, France

Eukaryotic cells have developed specialized membrane structures called organelles, which compartmentalize cellular functions and chemical reactions. Recent improvements in microscopy and membrane compartment isolation techniques are now sophisticating our view. Emerging evidences support that there are distinct sub-populations or subdomains, which are spatially and/or temporally segregated within one type of organelle, contributing to specify differential sorting of various cargos to distinct destinations of the cell. In plant cells, the Golgi apparatus represents a main trafficking hub in which entry occurs through a Golgi Entry Core Compartment (GECCO), that remains to be further characterized, and sorting of cargos is mediated through multiple transport pathways with different sets of regulator proteins at the post-Golgi compartment *trans*-Golgi network (TGN). Both GECCO and TGN are differentiated sub-populations as compared to the rest of Golgi, and moreover, further subdomain formation within TGN is suggested to play a key role for cargo sorting. In this review, we will summarize recent findings obtained on organelle subdomains, and their relationship with cargo entry at and exit from the Golgi apparatus.

Keywords: membrane traffic, subdomains, secretion, endocytosis, lipids, trans-Golgi network, Golgi apparatus, protein sorting

OPEN ACCESS

Edited by:
Eugenia Russinova, Ghent University, Belgium

Reviewed by:
Charlotte Kirchhelle, University of Oxford, United Kingdom
Georgia Drakakaki, University of California, Davis, United States

****Correspondence:***
Yoko Ito
yoko.ito@u-bordeaux.fr
Yohann Boutté
yohann.boutte@u-bordeaux.fr

Specialty section:
This article was submitted to Plant Membrane Traffic and Transport, a section of the journal Frontiers in Plant Science

Received: *23 September 2020*
Accepted: *23 November 2020*
Published: *08 December 2020*

Citation:
Ito Y and Boutté Y (2020) Differentiation of Trafficking Pathways at Golgi Entry Core Compartments and Post-Golgi Subdomains. Front. Plant Sci. 11:609516. doi: 10.3389/fpls.2020.609516

INTRODUCTION

Membrane trafficking in eukaryotic cells substantially contributes to tissue and whole organism patterning by secretion to the extracellular space or controlling protein localization at the plasma membrane (PM) sometimes in a polar way at proper timings. The secretory trafficking partly relies on the Golgi apparatus, which consists of multiple flat cisternae piled up to form stacks in most eukaryotic cells including plants. Those cisternae are polarized across the stack between the *cis* side, which receives materials from the endoplasmic reticulum (ER), and the *trans* side, which sends them forward to their destinations. In addition to these flat cisternae, morphological studies in mammalian cells demonstrated that there are vesicular-tubular structures both on the *cis* and *trans* ends of the stack, which are suggested to be the specialized compartments for cargo sorting at the entry and exit sides of the Golgi (Griffiths and Simons, 1986; Mellman and Simons, 1992). The one at the *trans* side was named *trans*-Golgi network (TGN), and now its dynamics in plant cells is attracting interests from wide range of scientists in the trial to understand the complex sorting mechanisms taking place in this compartment. In addition, it clearly appears now that TGN is further divided into subdomains or sub-populations whose composition, dynamics

and function remains to be fully deciphered. The one at the *cis* side, which was named ER-Golgi intermediate compartment (ERGIC) in mammalian cells, was not recognized in plants before, but recent studies are revealing the existence of specialized compartment at the ER-Golgi interface in plant cells as well.

THE Golgi ENTRY FACE: *cis*-COMPARTMENTS AS THE ER-Golgi FERRYMAN

The ER produces COPII vesicles at specialized domains called ER exit/export sites (ERES) for anterograde trafficking to the Golgi and the Golgi sends ER components back by COPI vesicles to the ER (**Figure 1**). In spite of this continuous communication between the ERES and Golgi, about a half of total ERES are located far from the Golgi in vertebrate cells (Stephens, 2003). Instead of direct ER-Golgi interaction, some vesicular-tubular structures are obviously separated from the other Golgi cisternae in vertebrate cells, and now recognized as the pre-Golgi compartment that receives cargoes from the ER before the *cis*-Golgi. It is commonly termed as Vesicular Tubular Cluster (VTC), ER-Golgi Intermediate Compartments (ERGIC), or just intermediate compartment (IC). Since it contains both anterograde and retrograde cargos (Palokangas et al., 1998; Simpson et al., 2006), depends on both COPI and COPII machineries (Scales et al., 1997), and furthermore, provided that some protein sorting receptors cycle between the ER and ERGIC (Dancourt and Barlowe, 2010), ERGIC is thought as the place for sorting between the ER and Golgi. Recently, a new model suggests that ERGIC can be divided into stationary globular domain, which is associated with ERES, and dynamic tubular domain which protrudes from the globular domain. This is based on the observations that a GTPase RAB1 preferentially localizes to the tubular domain than the globular domain, while some other proteins including the ERGIC marker p58/ERGIC-53 show the opposite distribution, which indicates the differentiation of these domains (Sannerud et al., 2006; Saraste and Marie, 2018).

In plant cells, the Golgi stacks are dispersed throughout the cytoplasm with continuous association with ERES, although it has been observed that there are some free and small ERES without being associated with Golgi (Ito et al., 2014; Brandizzi, 2018; Takagi et al., 2020). In the associated pairs, ERES and Golgi are physically tethered by a long coiled-coil protein and keep the close distance during rapid movement along actin filaments (Osterrieder et al., 2017). Most of the COPII budding from the ER occurs within only 300 nm from the *cis*-Golgi, while the size of a single COPII bud in *Arabidopsis* is approximately 60 nm in diameter (Kang and Staehelin, 2008; Staehelin and Kang, 2008). Due to these constraints, an "ERGIC-like structure" has never been morphologically determined within this limited space. However, electron tomography has demonstrated that the size and shape of the very first *cis* cisternae are tremendously variable from a small "blob," with the size corresponding to only several vesicles, to branched tubules or disc-shaped cisternae, suggesting that they are in the course of cisternal assembly (Staehelin and Kang, 2008). α-1,2-Mannosidase I (ManI), the first enzyme that works in the *N*-glycosylation reaction of proteins at Golgi, was revealed to mainly localize at the third and fourth

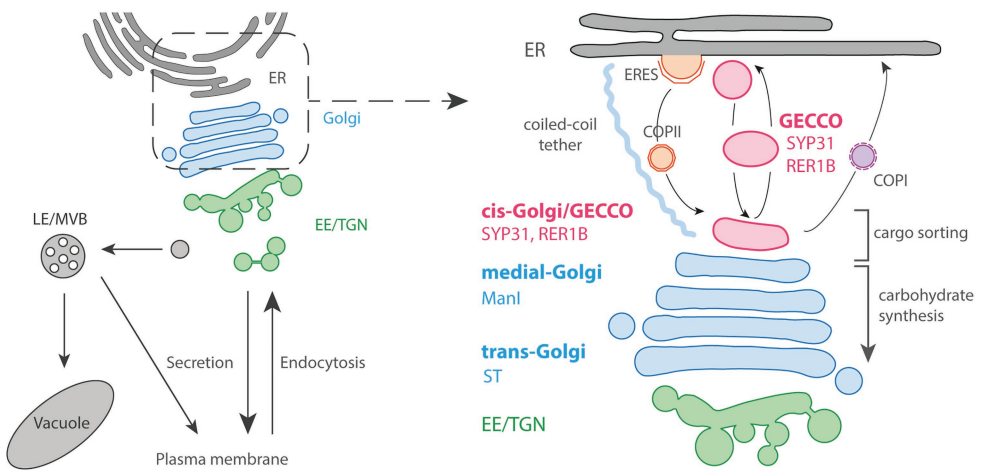

FIGURE 1 | The Golgi entry face. **Left panel**: general schematic representation of the endomembrane trafficking starting with ER: Endoplasmic Reticulum followed by Golgi and post-Golgi trafficking with the Early Endosome (EE)/*trans*-Golgi Network (TGN), the Late Endosome (LE)/Multi-Vesicular Bodies (MVBs), vacuole and plasma membrane (PM). **Right panel**: the pre-Golgi trafficking involves COPII-anterograde transport through Endoplasmic Reticulum Export Sites (ERES) as well as COPI-retrograde transport. The Golgi Entry Core Compartment (GECCO) is a compartment independent from the COPII machinery, and could function as an intermediate compartment between ER and Golgi. GECCO shares its localizing proteins (SYP31 and RER1B) with the *cis*-most Golgi cisternae. GECCO and the first *cis*-Golgi cisternae might be specialized in cargo sorting, while carbohydrate synthesis occurs only from *medial* and *trans* cisternae due to the specific localization of glycosylation enzymes (e.g., ManI or sialyltransferase; ST) at these later cisternae. The Golgi stacks are physically tethered to the ER by long coiled-coil tethering elements.

cisternae, not to the first and second ones by immuno-electron tomography (Donohoe et al., 2013). Since the glycosylation enzymes are distributed within the Golgi largely in the order that they act, this data indicates that the cisternae at the most *cis* side in plant cells are biochemically inactive, similarly to mammalian ERGIC.

Live-cell observations have also demonstrated that the *cis*-most cisternae have a distinct nature from the others cisternae in plant cells. Brefeldin A, a drug that inhibits the activation of ARF1 GTPase, causes Golgi disassembly and relocalization of Golgi enzymes to the ER in many organisms and cell types including tobacco cultured cells (Lippincott-Schwartz et al., 1989; Ritzenthaler et al., 2002). In tobacco BY-2 cultured cells, *cis*-Golgi proteins SYP31 and RER1B were found to localize at unknown punctate structures close to ERES upon brefeldin A (BFA) treatment, while other Golgi markers including ManI were distributed in the ER (Ito et al., 2012, 2018). In addition, because the punctate structures labeled by SYP31 received other Golgi components from the ER and the Golgi stacks were regenerated from them after removal of BFA, these structures can be thought as the entry site of the Golgi and the scaffold for stack assembly. Thus, the structure was given the name "Golgi entry core compartment" (GECCO; **Figure 1**; Ito et al., 2012, 2018). In mammalian cells, an ERGIC marker protein ERGIC-53 shows a similar behavior upon BFA treatment by localizing to punctate structures called Golgi remnants (Lippincott-Schwartz et al., 1990). Therefore, GECCO that appears by BFA treatment would be corresponding to the Golgi remnants, and the *cis*-most cisternae in plant cells would be the counterpart of ERGIC. However, contrastingly to the mammalian ERGIC-53, which is trapped in the ER by the expression of a dominant mutant of SAR1 GTPase, the localization of SYP31 to GECCO in tobacco BY-2 cells is not affected by SAR1 dominant mutant, indicating that ER-to-GECCO transport independent from COPII machinery exists in plant cells (Shima et al., 1998; Hauri et al., 2000; Ito et al., 2018). In *Saccharomyces cerevisiae*, although it is impossible to define pre-Golgi compartment by spatial relationship among cisternae, 3D live-cell imaging has revealed that only the *cis* cisternae approach to ERES and contact transiently to receive COPII-mediated cargos ("hug-and-kiss" action; Kurokawa et al., 2014). Considering their function as the Golgi entry compartment, the cisternae that show this hug-and-kiss action would correspond to mammalian ERGIC and plant *cis*-Golgi/GECCO. If the COPII-mediated transport occurs by hug-and-kiss also during the formation of new *cis* cisternae, some preexisting compartment should be in front of the ER to capture the first COPII carriers. The finding of GECCO as a COPII-independent structure in plants might contribute to understand the process of cisterna initiation.

THE Golgi EXIT FACE: THE MULTIFACETED TGN IS DIFFERENTIATED IN FUNCTIONAL SUBDOMAINS

The TGN is generally defined as a vesicular-tubular structure at the *trans* side of Golgi. In plants, 3D tomographic studies showed that the *trans*-most cisternae seem to peel off from the stack and mature by changing their morphology from early TGN with central flat domain into late TGN with many vesicles connected by tubules (Staehelin and Kang, 2008; Kang et al., 2011). It is also reported in *Arabidopsis* that impaired TGN biogenesis in the *lot* (loss of TGN, a Golgi-localized putative activator for the small GTPase Rab6) mutant is accompanied by the overstacking of the Golgi, supporting that the TGN is generated by the maturation of the Golgi cisternae (Jia et al., 2018). However, in tobacco cells, pharmacological induction of the disassembly and reassembly of the TGN suggested that TGN biogenesis would not fully depend on the cisternal maturation from the *trans*-Golgi (Ito et al., 2017).

Once formed, TGN are able to further differentiate into other compartments of different composition. A striking example is the differentiation of TGN into pre-vacuolar compartments (PVCs)/multi vesicular bodies (MVBs; Scheuring et al., 2011). Other examples are the compartments labeled by either RAB-A5c or RAB-A4b. In both cases, these compartments are thought to be derived from TGN but at some point they become so differentiated that they do not co-localize any longer with any TGN or other known endomembrane compartments markers (Preuss et al., 2004; Kirchhelle et al., 2016).

The multiple identity of TGN is also seen at the level of trafficking routes crossing the TGN. The TGN is known to not only receive secretory cargos from the Golgi but also cargos from the endocytic pathway. In mammalian cells, the early endosomes (EE) first receive the proteins endocytosed from the PM, and some of those proteins are recycled back to the PM directly from the EE or *via* tubular compartments called the recycling endosomes (RE), or transported to the late endosomes/multi vesicular bodies (LE/MVB) generated by the maturation of the EE (Naslavsky and Caplan, 2018). The TGN exchanges materials with them, and some endocytic cargos are known to reach the TGN *via* those endosomes (Bonifacino and Rojas, 2006; Makaraci and Kim, 2018). The TGN in plant cells also receives endocytic cargos. However, by contrast to mammalian cells, since the endocytic tracer FM4-64 reaches the TGN within a few minutes before accumulating at the LE/MVB, it is thought that the TGN itself is equivalent to the EE in plant cells (Dettmer et al., 2006; Viotti et al., 2010). A recent study revealed that the TGN receives some proteins and FM4-64 endocytosed from the PM before the LE/prevacuolar compartment in budding yeast as well, suggesting the function of the TGN as the EE in the ancestral membrane trafficking system (Day et al., 2018). The mechanisms that achieve this complex cargo receiving and sorting at the TGN are largely unknown. However, recent studies are revealing that the division of roles between sub-populations of TGN contributes to those sorting processes.

At the dynamic level, live-cell observations have demonstrated that TGN can either be associated with the *trans* side of the Golgi apparatus (Golgi-associated TGN/GA-TGN), or can be disassociated and moves independently from the Golgi (Golgi-independent TGN/GI-TGN or free TGN; **Figure 2**; Viotti et al., 2010; Kang et al., 2011; Uemura et al., 2014).

GA-TGN and GI-TGN can undergo homotypic or heterotypic fusion and fission, and GI-TGN sometimes associates with the Golgi apparatus transiently, indicating that they might exchange materials with each other (Viotti et al., 2010).

These two types of TGN sub-populations are labeled by the syntaxin SYP43 (SYntaxin of Plants43), a component of a SNARE (Soluble *N*-ethylmaleimide sensitive factor Attachment protein REceptor) complex localized at TGN. Most of the SYP43 labels GA-TGN co-localize with the SNAREs VAMP721, VAMP722, and VAMP727. Although these three VAMP7 proteins are close homologs, it is known that VAMP721 and VAMP722 are involved in the trafficking to the PM and cell plate while VAMP727 mainly functions in the trafficking to vacuoles (Ebine et al., 2008; Kwon et al., 2008; Zhang et al., 2011; El Kasmi et al., 2013). In contrast to the GA-TGN, GI-TGN shows less co-localization with VAMP727, whereas VAMP721 and VAMP722 still co-localize well with GI-TGN. In addition, the GI-TGN co-localize with FM4-64 much less compared to the GA-TGN, indicating that the GI-TGN is more specialized to the trafficking to the PM as compared to the vacuolar trafficking or endocytic recycling (Uemura et al., 2019). This is consistent with a previous report that CONTINUOUS VASCULAR RING (COV1), a TGN-localized protein which is required for vacuolar protein sorting, is involved in the association of the GA-TGN to the *trans*-most cisternae of the Golgi (Shirakawa et al., 2014). In contrast, ECHIDNA (ECH) and its interactors YPT/RAB GTPase Interacting Protein 4a (YIP4a) and YIP4b are also known to localize to the TGN and contribute to the proper association between the Golgi and GA-TGN, but they function in the secretory transport of specific proteins and polysaccharides to the PM, not in the vacuolar or endocytic trafficking (Gendre et al., 2011, 2013). This might indicate that the trafficking routes of SYP4-VAMP721 and ECH-YIP4 are differentiated within the TGN. Although it is not yet clear, the GA- and GI-TGN are also presumed to be involved in plant growth and development differently from the fact that the GI-TGN is found more frequently in root differentiation zone compared to meristematic zone (Uemura et al., 2014).

Besides, it also becomes increasingly clear that TGN vesicles are morphologically and functionally diverse. Originally, subdomains at the TGN were first suggested by immunogold electron microscopy which found that the TGN SNAREs SYP41 and SYP42 localized to distinct parts of the same TGN (Bassham et al., 2000; Sanderfoot et al., 2001). Later on, it was observed that two TGN-localized proteins, the vacuolar V-ATPase VHA-a1 and the Rab GTPase RAB-A2a only weakly overlap by confocal microscopy (Chow et al., 2008). From electron tomography analyses, it is clear that at least two populations co-exist at TGN according to that they are either coated with clathrin for CCVs (clathrin coated vesicles) or uncoated for secretory vesicles (SVs; **Figure 2**; Kang et al., 2011; Boutté et al., 2013; Wattelet-Boyer et al., 2016). Electron microscopy analyzes revealed that VHA-a1 and the syntaxin SYP61 localize at SVs (Kang et al., 2011). Confocal microscopy additionally revealed strong co-localization of the protein ECHIDNA with the SVs markers VHA-a1 or SYP61 while ECHIDNA or VHA-a1 displayed only weak co-localization with clathrin (Gendre et al., 2011; Boutté et al., 2013). Oppositely, RAB-A2a displays strong co-localization with clathrin compared to SYP61 (Doyle et al., 2015; Wattelet-Boyer et al., 2016). These results suggest that VHA-a1/SYP61/ECHIDNA are present in one subdomain of TGN while RAB-A2a/clathrin would constitute another subdomain of TGN. The presence of CCVs at TGN was first attributed to involvement of clathrin-mediated trafficking from TGN to vacuoles (Sanderfoot et al., 1998; Sauer et al., 2013; Reynolds et al., 2018). However, recently, an elegant study revealed that CCVs at TGN also originate from the endocytic trafficking (**Figure 2**; Narasimhan et al., 2020). Interestingly, while in mammalian cells the CCVs formed at PM shortly release their clathrin coat, CCVs of plant cells get only partially uncoated while being collected by EE/TGN at close proximity of PM (Narasimhan et al., 2020). Consistent with the endocytic nature of CCVs at TGN, RAB-A2a- colocalizes with the endocytic tracer FM4-64 within a couple of minutes after external application (Chow et al., 2008). Partially uncoated CCVs could be a central place of recycling at TGN and a way for TGN to segregate the endocytic recycling material from the *de novo* secretory material. However, further investigations are required to decipher the complete role and dynamics of CCVs at TGN (Reynolds et al., 2018). Similarly, the function of SVs at TGN attracts increasing attention. As CCVs, SVs are thought to play a role during early stages of endocytosis based on the accumulation of FM4-64 a few minutes after application (Dettmer et al., 2006; Viotti et al., 2010). This is conceivable due to the partial fusion of CCVs with EE/SVs and the non-specific lipophilic nature of FM4-64. At the functional level, ECHIDNA and VHA-a1 are involved in cell elongation while RAB-A2a or DYNAMIN-RELATED PROTEINS (DRPs) are involved in cell division. Consistently, RAB-A2a or DRPs localize to the cell plate while ECHIDNA or VHA-a1 do not (Dettmer et al., 2006; Chow et al., 2008; Konopka et al., 2008; Boutté et al., 2010; Gendre et al., 2011). However, it would be hasty and oversimple to state that the division of labor between cell elongation and cell division is supported by either SVs or CCVs. The localization of CCV-proteins at the cell plate probably reflects the contribution of the endocytosis to the building of new membranes, which is possible considering the partial uncoating of CCVs, and/or it reflects the vesicular recycling from the middle to the edges of the cell plate as the division plane is extending (Chow et al., 2008; Richter et al., 2014). Moreover, RAB-A2a is not only involved in cell division but also in cell elongation (Chow et al., 2008; Li et al., 2017). Similarly, SVs do not contribute only to cell elongation but are also involved in the building of the cell plate by delivering *de novo* synthesized materials (Reichardt et al., 2007; Richter et al., 2014). For example, the syntaxin SYP61 and the TRS120 subunit of the Transport Protein Particle II (TRAPP II) tethering complex both localize to SVs and at the cell plate (Kang et al., 2011; Ravikumar et al., 2018). Interestingly, TRAPPII and ECHIDNA co-localize very well at SVs but are involved in two distinct cellular processes as loss-of function of *ECHIDNA* does not lead to obvious cell division defect contrarily to loss-of

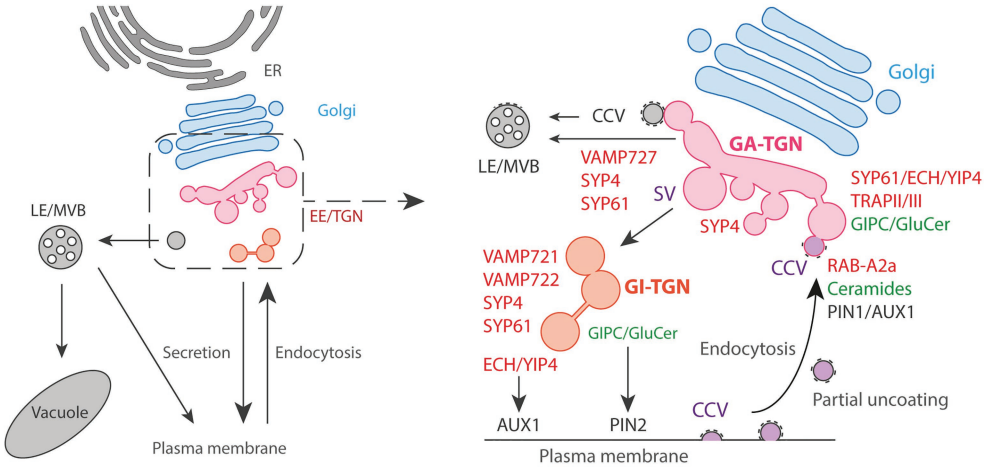

FIGURE 2 | The Golgi exit face. **Left panel**: general schematic representation of the endomembrane trafficking starting with ER: Endoplasmic Reticulum followed by Golgi and post-Golgi trafficking with the EE/TGN, the LE/MVBs, vacuole and PM. **Right panel**: the post-Golgi trafficking is complex and involves multiple pathways interconnected at TGN. Golgi-Associated (GA) TGN can mature and detach from Golgi to become a Golgi-independent (GI) TGN. Trafficking from TGN to LE/MVBs is thought to partly rely on Clathrin-Coated Vesicles (CCVs) and the SNARE VAMP727. Presence of CCVs at TGN is also attributed to the endocytic pathway from the PM due to the partial uncoating of endocytic clathrin-coated vesicles that are collected by the EE/TGN. At clathrin/TGN subdomain, the small GTPase RAB-A2a is involved in PIN1 and AUX1 endocytic sorting through the action of the sphingolipid ceramides. At Secretory Vesicles (SVs)/TGN, the ECH/YIP4 complex is involved in AUX1 secretory sorting to PM while the sphingolipids GIPC/GluCer are involved in PIN2 secretory sorting to PM.

function of *TRS120*/*TRAPPII* (Ravikumar et al., 2018). Moreover, an element of a TRAPPIII complex has been shown to play a role at TGN in a yet different trafficking route involved in endocytic trafficking (Rosquete et al., 2019). Thus, trafficking pathways at SVs are diverse and rely on distinct molecular machineries.

Another striking evidence for such a sub-compartmentalization is coming from the lipid composition of these compartments. Immuno-isolation of SYP61-positive TGN and RAB-A2a-positive TGN using the corresponding proteins as baits revealed a specific enrichment of α-hydroxylated VLCFAs (hVLCFAs) at SYP61-TGN but not RAB-A2a-TGN, as compared to Golgi (Wattelet-Boyer et al., 2016). hVLCFAs are a specific signature of sphingolipids (SLs) and enrichment of sterols was also detected at SVs, which suggest that SLs and sterols could form small lipid platforms within SVs to sort specific cargos (Boutté et al., 2010; Wattelet-Boyer et al., 2016). Interestingly, while hVLCFAs of the final form of SLs, namely glucosylceramide (GluCer) and glycosylinositolphosphorylceramides (GIPCs), have been shown to play a role in secretory sorting of the efflux auxin carrier PIN2 at SVs, they do not act in secretory sorting of the auxin efflux carrier PIN1 or the auxin influx carrier AUX1 (**Figure 2**; Wattelet-Boyer et al., 2016). Contrastingly, ECHIDNA which is localized at SVs is involved in secretory sorting of AUX1 but not PIN1 or PIN2 (**Figure 2**; Gendre et al., 2011; Boutté et al., 2013; Jonsson et al., 2017). Intriguingly, intermediate forms of SLs, namely the ceramides, play a role in endocytic trafficking of PIN1 and AUX1 at RAB-A2/clathrin compartments, but not PIN2 (**Figure 2**; Markham et al., 2011). Hence, we should not think of TGN as a single homogeneous population. Even within SVs, protein cargos are segregated according to specific protein- and lipid-mediated sorting mechanisms.

CONCLUSION AND OUTLOOK

It is clear that Golgi trafficking can no longer be seen as a general bulk flow. Both pre- and post-Golgi are divided into subdomains defining distinct protein sorting mechanisms and trafficking pathways. This subdivision represents most likely a phenomenon commonly found in endomembrane trafficking. Indeed, the rims or even a part within the rim region of the Golgi cisternae were also suggested to function as specialized subdomains based on the concentrated localization of specific proteins, which might indicate the existence of a subdomain sorting system at the Golgi cisternae as well (Pimpl et al., 2000; Naramoto et al., 2014; Meents et al., 2019). In the future, the use of super-resolution techniques such as stimulated emission depletion (STED), structured illumination microcopy (SIM), or super-resolution confocal live imaging microscopy (SCLIM) will be essential to distinguish subdomains with enough resolution. Moreover, the complete biochemical characterization of pre- and post-Golgi subdomains, both at the proteins and lipids level, would be a great advance to decipher the mechanisms through which lipids and proteins synergistically act during maturation of subdomains and differentiation of trafficking pathways. Protein and lipid characterization of TGN subdomains has already been supported by several studies but requires further investigations. In contrast, GECCO vesicles have not been isolated yet, while this would help us to define the nature and dynamics of GECCO and would be an important key in understanding ER to Golgi sorting mechanisms. Moreover, in spite of the accumulating evidences as described in this mini-review, the cargo transport *via* the membrane subdomains has never been directly observed in plant cells due to the lack of microscopic resolution and

techniques to visualize cargo proteins. The improvement in those techniques would bring us a breakthrough in the near future. Finally, the complexity of membrane compartmentalization has to be accounted for its function in cellular organization sustaining developmental processes. Although, we did not address it in this mini-review due to lack of space, this question is indeed central to understand how protein sorting and membrane sub-compartmentalization is acting across cellular and developmental scales.

AUTHOR CONTRIBUTIONS

YI and YB wrote and edited the manuscript and prepared figures. All authors contributed to the article and approved the submitted version.

FUNDING

This work was supported by a research grant from the French National Research Agency (ANR-18-CE13-0025) to YB and an Overseas Research Fellowship granted from Japan Society for Promotion of Science (JSPS) to YI.

ACKNOWLEDGMENTS

We would like to thank the topic editors of this special issue and the reviewers that took time to read and help improving our manuscript. We warmly acknowledge Patrick Moreau for his help to improve this manuscript prior submission. We apologize to colleagues whose work could not be included in this manuscript due to space constraints.

REFERENCES

Bassham, D. C., Sanderfoot, A. A., Kovaleva, V., Zheng, H., and Raikhel, N. V. (2000). AtVPS45 complex formation at the trans-Golgi network. *Mol. Biol. Cell* 11, 2251–2265. doi: 10.1091/mbc.11.7.2251

Bonifacino, J. S., and Rojas, R. (2006). Retrograde transport from endosomes to the *trans*-golgi network. *Nat. Rev. Mol. Cell Biol.* 7, 568–579. doi: 10.1038/nrm1985

Boutté, Y., Frescatada-Rosa, M., Men, S., Chow, C., Ebine, K., Gustavsson, A., et al. (2010). Endocytosis restricts *Arabidopsis* KNOLLE syntaxin to the cell division plane during late cytokinesis. *EMBO J.* 29, 546–558. doi: 10.1038/emboj.2009.363

Boutté, Y., Jonsson, K., McFarlane, H. E., Johnson, E., Gendre, D., Swarup, R., et al. (2013). ECHIDNA-mediated post-golgi trafficking of auxin carriers for differential cell elongation. *Proc. Natl. Acad. Sci. U. S. A.* 110, 16259–16264. doi: 10.1073/pnas.1309057110

Brandizzi, F. (2018). Transport from the endoplasmic reticulum to the golgi in plants: where are we now? *Semin. Cell Dev. Biol.* 80, 94–105. doi: 10.1016/j.semcdb.2017.06.024

Chow, C. -M., Neto, H., Foucart, C., and Moore, I. (2008). Rab-A2 and Rab-A3 GTPases define a *trans*-golgi endosomal membrane domain in *Arabidopsis* that contributes substantially to the cell plate. *Plant Cell* 20, 101–123. doi: 10.1105/tpc.107.052001

Dancourt, J., and Barlowe, C. (2010). Protein sorting receptors in the early secretory pathway. *Annu. Rev. Biochem.* 79, 777–802. doi: 10.1146/annurev-biochem-061608-091319

Day, K. J., Casler, J. C., and Glick, B. S. (2018). Budding yeast has a minimal endomembrane system. *Dev. Cell* 44, 56.e4–72.e4. doi: 10.1016/j.devcel.2017.12.014

Dettmer, J., Hong-Hermesdorf, A., Stierhof, Y. -D., and Schumacher, K. (2006). Vacuolar H^+ -ATPase activity is required for endocytic and secretory trafficking in *Arabidopsis*. *Plant Cell* 18, 715–730. doi: 10.1105/tpc.105.037978

Donohoe, B. S., Kang, B. -H., Gerl, M. J., Gergely, Z. R., McMichael, C. M., Bednarek, S. Y., et al. (2013). *Cis*-golgi cisternal assembly and biosynthetic activation occur sequentially in plants and algae. *Traffic* 14, 551–567. doi: 10.1111/tra.12052

Doyle, S. M., Haeger, A., Vain, T., Rigal, A., Viotti, C., Łangowska, M., et al. (2015). An early secretory pathway mediated by GNOM-LIKE 1 and GNOM is essential for basal polarity establishment in *Arabidopsis thaliana*. *Proc. Natl. Acad. Sci. U. S. A.* 112, E806–E815. doi: 10.1073/pnas.1424856112

Ebine, K., Okatani, Y., Uemura, T., Goh, T., Shoda, K., Niihama, M., et al. (2008). A SNARE complex unique to seed plants is required for protein storage vacuole biogenesis and seed development of *Arabidopsis thaliana*. *Plant Cell* 20, 3006–3021. doi: 10.1105/tpc.107.057711

El Kasmi, F., Krause, C., Hiller, U., Stierhof, Y. -D., Mayer, U., Conner, L., et al. (2013). SNARE complexes of different composition jointly mediate membrane fusion in *Arabidopsis* cytokinesis. *Mol. Biol. Cell* 24, 1593–1601. doi: 10.1091/mbc.e13-02-0074

Gendre, D., McFarlane, H. E., Johnson, E., Mouille, G., Sjödin, A., Oh, J., et al. (2013). *Trans*-golgi network localized ECHIDNA/Ypt interacting protein complex is required for the secretion of cell wall polysaccharides in *Arabidopsis*. *Plant Cell* 25, 2633–2646. doi: 10.1105/tpc.113.112482

Gendre, D., Oh, J., Boutté, Y., Best, J. G., Samuels, L., Nilsson, R., et al. (2011). Conserved *Arabidopsis* ECHIDNA protein mediates trans–golgi-network trafficking and cell elongation. *Proc. Natl. Acad. Sci. U. S. A.* 108, 8048–8053. doi: 10.1073/pnas.1018371108

Griffiths, G., and Simons, K. (1986). The *trans* golgi network: sorting at the exit site of the golgi complex. *Science* 234, 438–443. doi: 10.1126/science.2945253

Hauri, H. P., Kappeler, F., Andersson, H., and Appenzeller, C. (2000). ERGIC-53 and traffic in the secretory pathway. *J. Cell Sci.* 113, 587–596.

Ito, Y., Toyooka, K., Fujimoto, M., Ueda, T., Uemura, T., and Nakano, A. (2017). The *trans*-golgi network and the golgi stacks behave independently during regeneration after brefeldin A treatment in tobacco BY-2 cells. *Plant Cell Physiol.* 58, 811–821. doi: 10.1093/pcp/pcx028

Ito, Y., Uemura, T., and Nakano, A. (2014). Formation and maintenance of the Golgi apparatus in plant cells. *Int. Rev. Cell Mol. Biol.* 310, 221–287. doi: 10.1016/B978-0-12-800180-6.00006-2

Ito, Y., Uemura, T., and Nakano, A. (2018). The golgi entry core compartment functions as a COPII-independent scaffold for ER-to-golgi transport in plant cells. *J. Cell Sci.* 131:jcs203893. doi: 10.1242/jcs.203893

Ito, Y., Uemura, T., Shoda, K., Fujimoto, M., Ueda, T., and Nakano, A. (2012). *cis*-golgi proteins accumulate near the ER exit sites and act as the scaffold for golgi regeneration after brefeldin A treatment in tobacco BY-2 cells. *Mol. Biol. Cell* 23, 3203–3214. doi: 10.1091/mbc.E12-01-0034

Jia, P. -F., Xue, Y., Li, H. -J., and Yang, W. -C. (2018). Golgi-localized LOT regulates *trans*-golgi network biogenesis and pollen tube growth. *Proc. Natl. Acad. Sci. U. S. A.* 115, 12307–12312. doi: 10.1073/pnas.1809206115

Jonsson, K., Boutté, Y., Singh, R. K., Gendre, D., and Bhalerao, R. P. (2017). Ethylene regulates differential growth via BIG ARF-GEF-dependent post-golgi secretory trafficking in *Arabidopsis*. *Plant Cell* 29, 1039–1052. doi: 10.1105/tpc.16.00743

Kang, B. -H., Nielsen, E., Preuss, M. L., Mastronarde, D., and Staehelin, L. A. (2011). Electron tomography of RabA4b- and PI-4Kβ1-labeled *trans* golgi network compartments in *Arabidopsis*. *Traffic* 12, 313–329. doi: 10.1111/j.1600-0854.2010.01146.x

Kang, B. -H., and Staehelin, L. A. (2008). ER-to-golgi transport by COPII vesicles in *Arabidopsis* involves a ribosome-excluding scaffold that is transferred with the vesicles to the golgi matrix. *Protoplasma* 234, 51–64. doi: 10.1007/s00709-008-0015-6

Kirchhelle, C., Chow, C. -M., Foucart, C., Neto, H., Stierhof, Y. -D., Kalde, M., et al. (2016). The specification of geometric edges by a plant Rab GTPase

is an essential cell-patterning principle during organogenesis in *Arabidopsis*. *Dev. Cell* 36, 386–400. doi: 10.1016/j.devcel.2016.01.020

Konopka, C. A., Backues, S. K., and Bednarek, S. Y. (2008). Dynamics of *Arabidopsis* dynamin-related protein 1C and a clathrin light chain at the plasma membrane. *Plant Cell* 20, 1363–1380. doi: 10.1105/tpc.108.059428

Kurokawa, K., Okamoto, M., and Nakano, A. (2014). Contact of *cis*-golgi with ER exit sites executes cargo capture and delivery from the ER. *Nat. Commun.* 5:3653. doi: 10.1038/ncomms4653

Kwon, C., Neu, C., Pajonk, S., Yun, H. S., Lipka, U., Humphry, M., et al. (2008). Co-option of a default secretory pathway for plant immune responses. *Nature* 451, 835–840. doi: 10.1038/nature06545

Li, R., Rodriguez-Furlan, C., Wang, J., van de Ven, W., Gao, T., Raikhel, N. V., et al. (2017). Different endomembrane trafficking pathways establish apical and basal polarities. *Plant Cell* 29, 90–108. doi: 10.1105/tpc.16.00524

Lippincott-Schwartz, J., Donaldson, J. G., Schweizer, A., Berger, E. G., Hauri, H. -P., Yuan, L. C., et al. (1990). Microtubule-dependent retrograde transport of proteins into the ER in the presence of brefeldin a suggests an ER recycling pathway. *Cell* 60, 821–836. doi: 10.1016/0092-8674(90)90096-W

Lippincott-Schwartz, J., Yuan, L. C., Bonifacino, J. S., and Klausner, R. D. (1989). Rapid redistribution of golgi proteins into the ER in cells treated with brefeldin A: evidence for membrane cycling from golgi to ER. *Cell* 56, 801–813. doi: 10.1016/0092-8674(89)90685-5

Makaraci, P., and Kim, K. (2018). *Trans*-golgi network-bound cargo traffic. *Eur. J. Cell Biol.* 97, 137–149. doi: 10.1016/j.ejcb.2018.01.003

Markham, J. E., Molino, D., Gissot, L., Bellec, Y., Hématy, K., Marion, J., et al. (2011). Sphingolipids containing very-long-chain fatty acids define a secretory pathway for specific polar plasma membrane protein targeting in *Arabidopsis*. *Plant Cell* 23, 2362–2378. doi: 10.1105/tpc.110.080473

Meents, M. J., Motani, S., Mansfield, S. D., and Samuels, A. L. (2019). Organization of Xylan production in the golgi during secondary cell wall biosynthesis. *Plant Physiol.* 181, 527–546. doi: 10.1104/pp.19.00715

Mellman, I., and Simons, K. (1992). The golgi complex: in vitro veritas? *Cell* 68, 829–840. doi: 10.1016/0092-8674(92)90027-A

Naramoto, S., Otegui, M. S., Kutsuna, N., de Rycke, R., Dainobu, T., Karampelias, M., et al. (2014). Insights into the localization and function of the membrane trafficking regulator GNOM ARF-GEF at the golgi apparatus in *Arabidopsis*. *Plant Cell* 26, 3062–3076. doi: 10.1105/tpc.114.125880

Narasimhan, M., Johnson, A., Prizak, R., Kaufmann, W. A., Tan, S., Casillas-Pérez, B., et al. (2020). Evolutionarily unique mechanistic framework of clathrin-mediated endocytosis in plants. *Elife* 9:e52067. doi: 10.7554/eLife.52067

Naslavsky, N., and Caplan, S. (2018). The enigmatic endosome–sorting the ins and outs of endocytic trafficking. *J. Cell Sci.* 131:jcs216499. doi: 10.1242/jcs.216499

Osterrieder, A., Sparkes, I. A., Botchway, S. W., Ward, A., Ketelaar, T., de Ruijter, N., et al. (2017). Stacks off tracks: a role for the golgin AtCASP in plant endoplasmic reticulum-golgi apparatus tethering. *J. Exp. Bot.* 68, 3339–3350. doi: 10.1093/jxb/erx167

Palokangas, H., Ying, M., Väänänen, K., and Saraste, J. (1998). Retrograde transport from the pre-golgi intermediate compartment and the golgi complex is affected by the vacuolar H^+-ATPase inhibitor bafilomycin A1. *Mol. Biol. Cell* 9, 3561–3578. doi: 10.1091/mbc.9.12.3561

Pimpl, P., Movafeghi, A., Coughlan, S., Denecke, J., Hillmer, S., and Robinson, D. G. (2000). In situ localization and in vitro induction of plant COPI-coated vesicles. *Plant Cell* 12, 2219–2235. doi: 10.1105/tpc.12.11.2219

Preuss, M. L., Serna, J., Falbel, T. G., Bednarek, S. Y., and Nielsen, E. (2004). The *Arabidopsis* Rab GTPase RabA4b localizes to the tips of growing root hair cells. *Plant Cell* 16, 1589–1603. doi: 10.1105/tpc.021634

Ravikumar, R., Kalbfuß, N., Gendre, D., Steiner, A., Altmann, M., Altmann, S., et al. (2018). Independent yet overlapping pathways ensure the robustness and responsiveness of *trans*-golgi network functions in *Arabidopsis*. *Development* 145:dev169201. doi: 10.1242/dev.169201

Reichardt, I., Stierhof, Y. -D., Mayer, U., Richter, S., Schwarz, H., Schumacher, K., et al. (2007). Plant cytokinesis requires de novo secretory trafficking but not endocytosis. *Curr. Biol.* 17, 2047–2053. doi: 10.1016/j.cub.2007.10.040

Reynolds, G. D., Wang, C., Pan, J., and Bednarek, S. Y. (2018). Inroads into internalization: five years of endocytic exploration. *Plant Physiol.* 176, 208–218. doi: 10.1104/pp.17.01117

Richter, S., Kientz, M., Brumm, S., Nielsen, M. E., Park, M., Gavidia, R., et al. (2014). Delivery of endocytosed proteins to the cell–division plane requires change of pathway from recycling to secretion. *Elife* 3:e02131. doi: 10.7554/eLife.02131

Ritzenthaler, C., Nebenführ, A., Movafeghi, A., Stussi-Garaud, C., Behnia, L., Pimpl, P., et al. (2002). Reevaluation of the effects of brefeldin A on plant cells using tobacco bright yellow 2 cells expressing golgi-targeted green fluorescent protein and COPI antisera. *Plant Cell* 14, 237–261. doi: 10.1105/tpc.010237

Rosquete, M. R., Worden, N., Ren, G., Sinclair, R. M., Pfleger, S., Salemi, M., et al. (2019). AtTRAPPC11/ROG2: a role for TRAPPs in maintenance of the plant *trans*-golgi network/early endosome organization and function. *Plant Cell* 31, 1879–1898. doi: 10.1105/tpc.19.00110

Sanderfoot, A. A., Ahmed, S. U., Marty-Mazars, D., Rapoport, I., Kirchhausen, T., Marty, F., et al. (1998). A putative vacuolar cargo receptor partially colocalizes with AtPEP12p on a prevacuolar compartment in *Arabidopsis* roots. *Proc. Natl. Acad. Sci. U. S. A.* 95, 9920–9925. doi: 10.1073/pnas.95.17.9920

Sanderfoot, A. A., Pilgrim, M., Adam, L., and Raikhel, N. V. (2001). Disruption of individual members of *Arabidopsis* syntaxin gene families indicates each has essential functions. *Plant Cell* 13, 659–666. doi: 10.1105/tpc.13.3.659

Sannerud, R., Marie, M., Nizak, C., Dale, H. A., Pernet-Gallay, K., Perez, F., et al. (2006). Rab1 defines a novel pathway connecting the pre-golgi intermediate compartment with the cell periphery. *Mol. Biol. Cell* 17, 1514–1526. doi: 10.1091/mbc.e05-08-0792

Saraste, J., and Marie, M. (2018). Intermediate compartment (IC): from pre-golgi vacuoles to a semi-autonomous membrane system. *Histochem. Cell Biol.* 150, 407–430. doi: 10.1007/s00418-018-1717-2

Sauer, M., Delgadillo, M. O., Zouhar, J., Reynolds, G. D., Pennington, J. G., Jiang, L., et al. (2013). MTV1 and MTV4 encode plant-specific ENTH and ARF GAP proteins that mediate clathrin-dependent trafficking of vacuolar cargo from the *trans-Golgi* network. *Plant Cell* 25, 2217–2235. doi: 10.1105/tpc.113.111724

Scales, S. J., Pepperkok, R., and Kreis, T. E. (1997). Visualization of ER-to-golgi transport in living cells reveals a sequential mode of action for COPII and COPI. *Cell* 90, 1137–1148. doi: 10.1016/S0092-8674(00)80379-7

Scheuring, D., Viotti, C., Krüger, F., Künzl, F., Sturm, S., Bubeck, J., et al. (2011). Multivesicular bodies mature from the *trans*-golgi network/early endosome in *Arabidopsis*. *Plant Cell* 23, 3463–3481. doi: 10.1105/tpc.111.086918

Shima, D. T., Cabrera-Poch, N., Pepperkok, R., and Warren, G. (1998). An ordered inheritance strategy for the golgi apparatus: visualization of mitotic disassembly reveals a role for the mitotic spindle. *J. Cell Biol.* 141, 955–966. doi: 10.1083/jcb.141.4.955

Shirakawa, M., Ueda, H., Koumoto, Y., Fuji, K., Nishiyama, C., Kohchi, T., et al. (2014). Continuous vascular ring (COV1) is a *trans*-golgi network-localized membrane protein required for golgi morphology and vacuolar protein sorting. *Plant Cell Physiol.* 55, 764–772. doi: 10.1093/pcp/pct195

Simpson, J. C., Nilsson, T., and Pepperkok, R. (2006). Biogenesis of tubular ER-to-golgi transport intermediates. *Mol. Biol. Cell* 17, 723–737. doi: 10.1091/mbc.e05-06-0580

Staehelin, L. A., and Kang, B. -H. (2008). Nanoscale architecture of endoplasmic reticulum export sites and of golgi membranes as determined by electron tomography. *Plant Physiol.* 147, 1454–1468. doi: 10.1104/pp.108.120618

Stephens, D. J. (2003). De novo formation, fusion and fission of mammalian COPII-coated endoplasmic reticulum exit sites. *EMBO Rep.* 4, 210–217. doi: 10.1038/sj.embor.embor736

Takagi, J., Kimori, Y., Shimada, T., and Hara-Nishimura, I. (2020). Dynamic capture-and-release of endoplasmic reticulum exit sites by golgi stacks in *Arabidopsis*. *iScience* 23:101265. doi: 10.1016/j.isci.2020.101265

Uemura, T., Nakano, R. T., Takagi, J., Wang, Y., Kramer, K., Finkemeier, I., et al. (2019). A golgi-released subpopulation of the *trans*-golgi network mediates protein secretion in *Arabidopsis*. *Plant Physiol.* 179, 519–532. doi: 10.1104/pp.18.01228

Uemura, T., Suda, Y., Ueda, T., and Nakano, A. (2014). Dynamic behavior of the *trans*-golgi network in root tissues of *Arabidopsis* revealed by super-resolution live imaging. *Plant Cell Physiol.* 55, 694–703. doi: 10.1093/pcp/pcu010

Viotti, C., Bubeck, J., Stierhof, Y. -D., Krebs, M., Langhans, M., van den Berg, W., et al. (2010). Endocytic and secretory traffic in *Arabidopsis*

merge in the *trans*-golgi network/early endosome, an independent and highly dynamic organelle. *Plant Cell* 22, 1344–1357. doi: 10.1105/tpc.109.072637

Wattelet-Boyer, V., Brocard, L., Jonsson, K., Esnay, N., Joubès, J., Domergue, F., et al. (2016). Enrichment of hydroxylated C24- and C26-acyl-chain sphingolipids mediates PIN2 apical sorting at *trans*-golgi network subdomains. *Nat. Commun.* 7:12788. doi: 10.1038/ncomms12788

Zhang, L., Zhang, H., Liu, P., Hao, H., Jin, J. B., and Lin, J. (2011). *Arabidopsis* R-SNARE proteins VAMP721 and VAMP722 are required for cell plate formation. *PLoS One* 6:e26129. doi: 10.1371/journal.pone.0026129

Conflict of Interest: The authors declare that the research was conducted in the absence of any commercial or financial relationships that could be construed as a potential conflict of interest.

frontiers in Plant Science

ORIGINAL RESEARCH
published: 19 March 2021
doi: 10.3389/fpls.2021.538580

Nanobody-Dependent Delocalization of Endocytic Machinery in *Arabidopsis* Root Cells Dampens Their Internalization Capacity

Joanna Winkler[1,2†], Andreas De Meyer[1,2†], Evelien Mylle[1,2], Veronique Storme[1,2], Peter Grones[1,2] and Daniël Van Damme[1,2]*

[1]Department of Plant Biotechnology and Bioinformatics, Ghent University, Ghent, Belgium, [2]VIB Center for Plant Systems Biology, Ghent, Belgium

OPEN ACCESS

Edited by:
Erika Isono,
University of Konstanz, Germany

Reviewed by:
Takashi Ueda,
Graduate University for Advanced Studies (Sokendai), Japan
Matthieu Platre
Salk Institute for Biological Studies, United States

***Correspondence:**
Daniël Van Damme
daniel.vandamme@psb.vib-ugent.be;
dadam@psb.vib-ugent.be

[†]These authors have contributed equally to this work

Specialty section:
This article was submitted to Plant Membrane Traffic and Transport, a section of the journal Frontiers in Plant Science

Received: 24 July 2020
Accepted: 23 February 2021
Published: 19 March 2021

Citation:
Winkler J, De Meyer A, Mylle E, Storme V, Grones P and Van Damme D (2021) Nanobody-Dependent Delocalization of Endocytic Machinery in Arabidopsis Root Cells Dampens Their Internalization Capacity. Front. Plant Sci. 12:538580. doi: 10.3389/fpls.2021.538580

Plant cells perceive and adapt to an ever-changing environment by modifying their plasma membrane (PM) proteome. Whereas secretion deposits new integral membrane proteins, internalization by endocytosis removes membrane proteins and associated ligands, largely with the aid of adaptor protein (AP) complexes and the scaffolding molecule clathrin. Two AP complexes function in clathrin-mediated endocytosis at the PM in plant cells, the heterotetrameric AP-2 complex and the hetero-octameric TPLATE complex (TPC). Whereas single subunit mutants in AP-2 develop into viable plants, genetic mutation of a single TPC subunit causes fully penetrant male sterility and silencing single subunits leads to seedling lethality. To address TPC function in somatic root cells, while minimizing indirect effects on plant growth, we employed nanobody-dependent delocalization of a functional, GFP-tagged TPC subunit, TML, in its respective homozygous genetic mutant background. In order to decrease the amount of functional TPC at the PM, we targeted our nanobody construct to the mitochondria and fused it to TagBFP2 to visualize it independently of its bait. We furthermore limited the effect of our delocalization to those tissues that are easily accessible for live-cell imaging by expressing it from the PIN2 promoter, which is active in root epidermal and cortex cells. With this approach, we successfully delocalized TML from the PM. Moreover, we also show co-recruitment of TML-GFP and AP2A1-TagRFP to the mitochondria, suggesting that our approach delocalized complexes, rather than individual adaptor complex subunits. In line with the specific expression domain, we only observed minor effects on root growth, yet realized a clear reduction of endocytic flux in epidermal root cells. Nanobody-dependent delocalization in plants, here exemplified using a TPC subunit, has the potential to be widely applicable to achieve specific loss-of-function analysis of otherwise lethal mutants.

Keywords: nanobody, endocytosis, *Arabidopsis*, protein delocalization, fluorescence microscopy, TPLATE complex (TPC)

INTRODUCTION

Cells are delineated by their plasma membrane (PM). The PM houses a plethora of proteins ranging from receptors and ion channels to structural membrane proteins. Many of these PM proteins, commonly termed cargo, are responsible for cellular communication with the outside world. In eukaryotes, endocytosis is the cellular process where cargoes, associated ligands as well as lipids are internalized from the PM. Endocytosis thereby provides a way to regulate the content and consequently modulate protein activity at the PM. A predominant and well-studied form of endocytosis is clathrin-mediated endocytosis (CME; Bitsikas et al., 2014). CME refers to the dependency of the scaffolding protein clathrin, which coats the developing and mature vesicles (Robinson, 2015). In plants, CME plays a role in hormone signaling (Irani et al., 2012; Martins et al., 2015; Zhang et al., 2017), nutrient availability (Wang et al., 2017; Dubeaux et al., 2018; Yoshinari et al., 2019), pathogen defense and susceptibility (Mbengue et al., 2016; Li and Pan, 2017), and other biotic and abiotic stresses (Li et al., 2011). Consequently, CME is essential for plant development.

Two early-arriving adaptor complexes, the heterotetrameric Adaptor Protein-2 complex (AP-2) and the hetero-octameric TPLATE complex (TPC) facilitate CME in plants (Gadeyne et al., 2014). In contrast to AP-2, TPC represents an evolutionary ancient protein complex, which is lost in yeast and mammalian cells (Hirst et al., 2014). The slime mold *Dictyostelium discoideum* contains a similar complex, named TSET. TSET, however, is a hexameric complex in contrast to TPC in *Arabidopsis thaliana*, which has two additional subunits. Also contrary to TPC, TSET is dispensable in *D. discoideum* (Hirst et al., 2014). The presence of a full or partial TSET complex in other eukaryotes was confirmed by additional homology searches, indicative of its ancient evolutionary origin (Hirst et al., 2014).

Adaptor Protein-2 complex and TPC have both common and distinct functions, possibly relating to cargo specificity and/or fate of the internalized cargo (Bashline et al., 2015; Sánchez-Rodríguez et al., 2018; Wang et al., 2019; Yoshinari et al., 2019). In addition, functional diversification of both complexes is reflected in their mutant phenotypes. Knockout plants in individual AP-2 subunits are affected at various stages of development but viable (Bashline et al., 2013; Di Rubbo et al., 2013; Fan et al., 2013; Kim et al., 2013; Yamaoka et al., 2013). However, *ap2* mutants show reduced internalization of the styryl dye N-(3-Triethylammoniumpropyl)-4-(6-(4-(Diethylamino) Phenyl) Hexatrienyl) Pyridinium Dibromide (FM4-64), which can be seen as proxy to a difference in cargo uptake (Jelínková et al., 2010), as well as known endocytic cargoes like the brassinosteroid receptor BRASSINOSTEROID INSENSITIVE 1 (BRI1), the boron exporter BOR1, and auxin efflux carriers of the PIN-FORMED protein family (Di Rubbo et al., 2013; Fan et al., 2013; Kim et al., 2013; Yoshinari et al., 2016, 2019).

The relatively mild phenotype of *ap2* single subunit mutants in plants contrasts with the lethal phenotype of a single *ap2* subunit knockout in mice (Mitsunari et al., 2005). Alternatively, the complex does not seem to be essential for yeast (Yeung et al., 2013). In *Caenorhabditis elegans*, AP-2 subunits are capable of assembling into hemicomplexes which partially retain their functionality (Gu et al., 2013). In plants, AP2M and AP2S are still recruited to the PM in *ap2s* and *ap2m* mutants, respectively (Wang et al., 2016), suggesting that AP-2 hemicomplexes might also confer partial functionality in plants.

In contrast to AP-2, single knockouts of TPC subunits result in fully penetrant male sterility with shriveled pollen and ectopic callose accumulation (Gadeyne et al., 2014). Similar pollen-lethal phenotypes are also reported for a mutant in DYNAMIN-RELATED PROTEIN 1C protein (*drp1c*; Backues et al., 2010), as well as a CLATHRIN LIGHT CHAIN mutant, *clc1* (Wang et al., 2013), involved in vesicle fission and clathrin triskelion assembly, respectively.

So far, there is only one viable weak allele of one TPC subunit identified. This *twd40-2-3* mutant (Bashline et al., 2015) is however likely merely a knockdown as *twd40-2-1* and *twd40-2-2* mutants are pollen lethal (Gadeyne et al., 2014). Knockdowns of *TML* and *TPLATE* resulted in seedling lethality with a reduced internalization of FM4-64, BRI1, RECEPTOR-LIKE PROTEIN 44 (RLP44), and the cellulose synthase subunit CESA6 (Irani et al., 2012; Gadeyne et al., 2014; Sánchez-Rodríguez et al., 2018; Gómez et al., 2019). Silencing works on the messenger level and phenotypes only become apparent following degradation of pre-made proteins. As AP complexes can be recycled following each round of internalization, approaches affecting these complexes at the protein level have a more direct effect. In animal cells, conditional delocalization using rapamycin to target AP-2 to mitochondria has been successfully applied to interfere with endocytosis (Robinson et al., 2010). Also, epidermal growth factor receptor substrate 15 (EPS15), a pioneer endocytic accessory protein, was successfully inactivated in HeLa cells by expressing an anti-EPS15 nanobody on endosomes or mitochondria (Traub, 2019).

Since their discovery, nanobodies, derived from camelid heavy chain-only antibodies (HCAb), have found their way into a wide variety of applications in biological fields. Nanobodies are similar to antibodies (Ab) in the sense that they can bind epitopes with high affinity in a highly selective manner (Ingram et al., 2018). Their applications range from drug discovery, crystallography, and imaging techniques to probing protein functions by degradation or delocalization (Caussinus et al., 2012; Früholz et al., 2018; Ingram et al., 2018). Nanobodies can be expressed as a single chain, compact and stable protein while still retaining high selectivity and affinity for its epitope (Muyldermans, 2013). This makes them more convenient to clone and to express compared to conventional Ab.

In plants, nanobodies have been used to selectively degrade proteins using the deGradFP method, originally developed in *Drosophila melanogaster*. DeGradFP links an anti-GFP nanobody to an F-box protein, thereby targeting it for ubiquitin-dependent degradation (Caussinus et al., 2012). This approach was shown to be functional in plants (Baudisch et al., 2018) and successfully used to deplete WUSCHEL-GFP in the *Arabidopsis* flowering meristem (Ma et al., 2019) and the centromeric Histon H3 of *Arabidopsis* in transgenic tobacco plants (Sorge et al., 2021). Nanobodies have also been used in *Arabidopsis* seedlings to

lock down vacuolar sorting receptors (VSRs) in cellular compartments upstream of trans-Golgi network/early endosomes, allowing to determine their retrograde trafficking pathway (Früholz et al., 2018).

Here, we explore, similar to what has been done in animal cells (Robinson et al., 2010; Traub, 2019), the effects on CME caused by lockdown of the endocytic machinery. We use a GFP-tagged functional TML-GFP fusion protein in the homozygous *tml-1(−/−)* mutant background and delocalized it to the mitochondria using a nanobody directed against eGFP.

MATERIALS AND METHODS

Cloning

Gateway entry clones pDONR221-TagBFP2, pDONR221-MITOTagBFP2 and pDONRP2RP3-GFPNb were generated according to the manufacturer's instructions (ThermoFisher Scientific BP clonase). pDONR221-TagBFP2 was amplified from pSN.5 mTagBFP2 (Pasin et al., 2014) with primers:

AttB1-GGGGACAAGTTTGTACAAAAAAGCAGGCTATGT CATCTAAGGGTGAAGAGC TTATC AAAGAGAAT and AttB2-GGGGACCACTTTGTACAAGAAAGCTGGGTCACCTCCGCC ACCTCCACCTCCCAGTCCTGCGTA.

pDONR221-MITOTagBFP2 was generated from pDONR221-TagBFP2 by including the import signal of the yeast mitochondrial outer membrane protein Tom70p as described before (Robinson et al., 2010). The following primers sequences were used:

AttB1-GGGGACAAGTTTGTACAAAAAAGCAGGCTCAAT GAAGAGCTTCATTACAAGGAACAAGACAGCCATTTTGGC AACCGTTGCTGCTACAGGTACTGCCATCGGTGCCTACTA TTATTACAACCAATTGCAACAGGATCCACCGGTCGCCA CCATGTCATCTAAGGGTGAAGAGCTT and AttB2-GGGGA CCACTTTGTACAAGAAAGCTGGGTACGCTAAGTCTTC CTCTGAAATCAA.

pDONRP2RP3-GFPNb was generated from an anti-GFP Nanobody construct (Künzl et al., 2016) with primers attB2-GGGGACAGCT TTCTTGTACAAAG TGGGGATGTATCCTTA TGATGTTC and attB3r-GGGGACAACTT TGTATAATAAAGT TGTTTAAT GATGATGATGA TGATGAGAAGA including a HA-tag, a 3xHis-tag, and a stop codon.

The entry clones of the PIN2 promoter pDONRP4P1R_PIN2prom (Marquès-Bueno et al., 2016) or 35 s promoter, pDONR221-MITOTagBFP2 and pDONRP2RP3-GFPNb were used in a triple Gateway LR reaction, combining pB7m34GW (Karimi et al., 2005) to yield pB7m34GW_PIN2prom::MITOTagBFP2-GFPNb or pB7m34GW_p35sprom::MITOTagBFP2-GFPNb.

Nicotiana benthamiana Plant Growth and Transient Expression Assay

Nicotiana benthamiana plants were grown in a greenhouse under long-day conditions (6–22 h light, 100 PAR, 21°C) in soil (Saniflo Osmocote pro NPK: 16 − 11 − 10+ magnesium and trace elements). Transient expression was performed by leaf infiltration according to (Sparkes et al., 2006). The abaxial epidermis was imaged 48 h after infiltration.

Arabidopsis Plant Material and Transformation

Plants expressing pB7m34GW_PIN2prom::MITOTagBFP2-GFPNb were generated by floral dip (Clough and Bent, 1998). Constructs were dipped into Col-0 and *tml-1(−/−)* (At5g57460) mutant lines described previously (Gadeyne et al., 2014). Primary transformants (T1) were selected on BASTA containing ½ strength MS medium without sucrose and 0.6% Gelrite (Duchefa, Netherlands). PIN2prom::MITOTagBFP2-GFPNb expression was analyzed in the progeny of BASTA-resistant primary transformants (T2 seeds) by microscopy and T2 lines demonstrating strong expression were selected regardless of insert copy number. Next, T2 lines were crossed with the previously described TML-GFP complemented *tml-1(−/−)* mutant line expressing also RPS5Aprom::AP2A1-TagRFP (Gadeyne et al., 2014). Primary hybrids were analyzed *via* microscopy and best lines were selected on the basis of both PIN2prom::MITOTagBFP2-GFPNb and RPS5Aprom::AP2A1-TagRFP expression. For both Col-0 and *tml-1(−/−)* backgrounds, two independent lines (-Nb1 and -Nb2) were generated. Namely, Col-Nb1, Col-Nb2, TML-Nb1, and TML-Nb2. In order to synchronize the age and overall fitness of the seeds, all lines used in the root growth and carbon starvation study, including the Col-0 and *tml-1(−/−)* lines, were propagated together and collected at the same time.

Quantification of TML-GFP Endocytic Foci

Four to five days old seedlings of TML, TML-Nb1, and TML-Nb2 were grown on ½ strength MS medium without sucrose and 0.6% Gelrite (Duchefa, Netherlands). Acquired pictures were analyzed in Fiji/ImageJ (Schindelin et al., 2012; Schneider et al., 2012). In each analyzed root an ROI of constant dimensions was selected. In addition in TML-Nb1 and TML-Nb2, the ROI did not overlap with mitochondrial clusters. The median intensity in each root was recorded, followed by the counts of the endocytic foci using the Find Maxima function. Statistical differences in median intensity and foci count between the lines were analyzed with pairwise Wilcoxon tests. *p*-values were adjusted using the Bonferroni method.

Phenotypical Quantification of Root Growth

Arabidopsis seedlings were grown on ½ strength MS medium without sucrose and 0.6% Gelrite (Duchefa, Netherlands). Seeds of all lines were equally placed on the plates (3 seeds per line per plate, distributed over 14 plates). Plates were left for the stratification for 48 h at 4°C, and then placed at 21°C in continuous light. Two days after transfer to the light, seeds which did not germinate were marked and excluded in the further analysis. For root growth analysis, seedlings were grown in continuous light and 2 days after germination the root growth of every seedling was marked for 7 days, daily. For carbon starvation, seedlings were grown for 5 days, including the germination period, in continuous light after which the root growth of every seedling was marked. Subsequently, the plates were covered with aluminum foil and left for 7 days

in dark after which root growth was marked again. Root growth and carbon starvation assays measurements were carried out with Fiji/ImageJ (Schindelin et al., 2012; Schneider et al., 2012). Seedlings, which stopped growing at early time points of the study, have grown into the medium or have grown in direct contact with the plate edge, were excluded from further analysis. Statistical differences for root growth assays were determined *via* a mixed model analysis. Mixed linear model analysis was applied to the root length of the lines Col-0, Col-Nb1, Col-Nb2, TML, TML-Nb1, and TML-Nb2 using the mixed procedure from SAS (SAS Studio 3.8 and SAS 9.4, SAS Institute Inc., Cary, NC). Fixed effects in the model were Line, Day, and the interaction term. An unstructured covariance structure was estimated to model the correlations between measurements done on the same plant. The degrees of freedom of the fixed effects were approximated with the Kenward-Rogers method. The hypotheses of interests were the differences between Col-0 and its respective nanobody lines, between TML and its respective nanobody lines and between the nanobody lines with the same background. These hypotheses were tested using the plm procedure. *p*-values were adjusted for multiple testing using the maxT procedure as implemented in the plm procedure. For the carbon starvation assay, statistical differences in root growth between the lines were analyzed with pairwise Wilcoxon tests. *p*-values were adjusted using the Bonferroni method.

FM-Uptake Quantification

Endocytic tracer FM4-64 stock solution was prepared prior to treatment (2 mM in DMSO, Thermo Fisher). Roots were stained with 2 μM FM4-64 by incubating the seedlings in FM-containing ½ strength MS medium without sucrose for 30 min. Treatment was followed by microscopy. Acquired pictures were analyzed in Fiji/ImageJ (Schindelin et al., 2012; Schneider et al., 2012). PM and cytosol of individual epidermal cells were outlined (using the Select Brush Tool and Freehand selections, respectively) and histograms of pixel intensities were generated. Pictures which contained more than 1% saturated pixels were excluded from the quantification. Cytoplasm/PM ratios were calculated from average intensities of the top 1% highest intensity pixels based on the histograms. Outliers were removed *via* interquartile range (IQR, data point ruled out if its value was either lower than first quartile Q1-1.5 × IQR, or higher than third quartile Q3-1.5 × IQR) in a single step. The normality assumption of the measurements was verified with the Shapiro-Wilk normality test. Due to violation of the normality assumption, statistical differences in intensity values between the lines were analyzed with pairwise Wilcoxon tests. *p*-values were adjusted using the Bonferroni method. All Shapiro-Wilk normality tests and Wilcoxon tests were performed using the R statistical software. (Rstudio Team, 2019, Version 1.2.5033, R Version 3.6.2).

Image Acquisition

Nicotiana benthamiana infiltration assay imaging (**Figure 1A**) was performed on a PerkinElmer UltraView spinning-disk system, attached to a Nikon Ti inverted microscope and operated using the Volocity software package. Images were acquired on an ImagEMccd camera (Hamamatsu C9100-13) using frame-sequential imaging with a 60x water immersion objective (NA = 1.20). Specific excitation and emission was performed using a 405 nm laser excitation combined with a single band pass filter (454–496 nm) for TagBFP2 and 561 nm laser excitation combined with a dual band pass filter (500–530 and 570–625 nm) for RFP. Images shown are Z-stack projections. Z-stacks were acquired in sequential frame mode with a 1 μm interval using the UltraView (Piezo) focus drive module.

Confocal *Arabidopsis* images were taken using Leica SP8X confocal microscope equipped with a White Light Laser and using the LASX software (**Figures 1B-D, 2, 4**). Images were acquired on Hybrid (HyD, gating 0.3–10.08 ns) and Photomultiplier (PMT) Detectors using bidirectional line-sequential imaging with a 40x water objective (NA = 1.10) and frame or line signal averaging. Specific excitation and emission were used: 405 nm laser and filter range 410–470 nm for TagBFP2, 488 nm laser and filter range 500–550 nm for GFP, 488 nm laser, and filter range 600–740 nm for FM4-64, 555nm laser and filter range 560–670 for TagRFP. Focal planes of PMs (**Figure 1E**) were acquired with the PerkinElmer UltraView spinning-disk system using a 100x oil immersion objective (NA = 1.45). Specific excitation and emission was performed using a 488 nm laser combined with a single band pass filter (500–550 nm) for GFP. Images shown are single-slice.

RESULTS

The Targeting Sequence of Yeast Tom70p Targets the Nanobody to the Mitochondria

We expressed a nanobody directed against eGFP (GFPNb; Künzl et al., 2016), which we visualized by fusing it to TagBFP2. We targeted the fusion protein to the mitochondria using the import signal of the yeast mitochondrial outer membrane protein Tom70p as described before (Robinson et al., 2010). This targeting signal is functional in plants as constructs containing this signal colocalized with MitoTracker in *N. benthamiana* leaf epidermal cells (Winkler et al., 2021). To verify that the GFP nanobody did not interfere with the mitochondrial targeting, we expressed it under the control of the 35Sprom together with the red mitochondrial mt-rk marker (Nelson et al., 2007) in *N. benthamiana* abaxial leaf epidermal cells and visualized both fusion proteins using spinning disk confocal microscopy. Both constructs colocalized at discrete punctae, but not exclusively. We observed that the mt-rk marker did not localize to big aggregates labeled with the GFPNb (**Figure 1A**). The mt-rk marker line consists of yeast cytochrome c oxidase IV (Nelson et al., 2007). It has been shown that release of cytochrome c oxidase into the cytosol is associated with changes of mitochondrial integrity (Kadenbach et al., 2004). It is, therefore, possible that the observed signal from aggregates originates from mitochondrial clustering similarly to what we observed with our knocksideways in plants system (Winkler et al., 2021). The absence of the mt-rk fusion protein

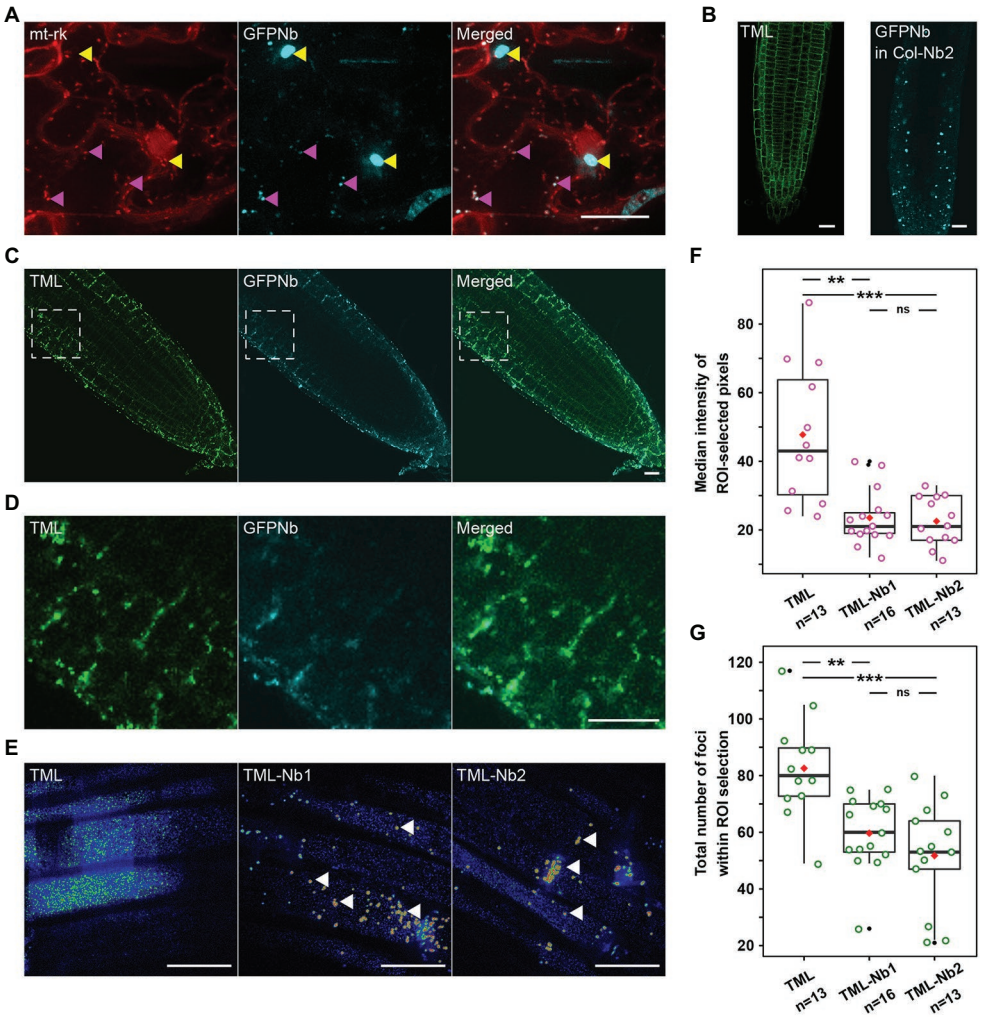

FIGURE 1 | Expression of a mitochondrial-targeted nanobody against GFP allows delocalization of TML-GFP. **(A)** Representative Z-stack projection of epidermal *Nicotiana benthamiana* cells transiently expressing the mitochondrial marker mt-rk (red) and the 35S::MITO-TagBFP2-GFP-Nanobody (GFPNb, cyan). Both fusion proteins colocalize at small cytosolic punctae (magenta arrowheads), but not at big aggregates, likely representing dysfunctional clustered mitochondria (yellow arrowheads). **(B)** Representative *Arabidopsis* root image of *tml-1(–/–)* complemented with TML-GFP showing that the functional TML fusion is predominantly targeted to the PM (left) as well as localization of GFPNb in cytosolic punctae in the WT (Col-0) background (right). **(C,D)** Representative overview images and respective zooms of the outlined region of *Arabidopsis* roots where TML-GFP in *tml-1(–/–)* was combined with MITOTagBFP2-GFPNb expression, leading to its delocalization from the PM. **(E)** Representative, rainbow intensity colored, grazing sections through the PM, showing the recruitment of TML to endocytic foci without (left) and with partial delocalization of TML-Nb1 and TML-Nb2 (middle, right, white arrowheads). Scale bars equal 20 μm. **(F,G)** Box plots showing the median intensity **(F)** or total number **(G)** of endosomal TML-GFP positive foci in the *Arabidopsis* roots. In the roots expressing GFPNb, both the intensity of the foci as well as their number are significantly reduced compared to TML-GFP (Wilcoxon pairwise comparison tests with Bonferroni adjusted *p*-values. $p < 0.001$ are represented as ***, <0.01 as **, and non-significant values as "ns"). The black lines represent the median and the red diamonds represent the mean of the analyzed values. Each magenta or green dot represents an individual cell. Black dot refers to outliers. *n* refers to the total number of analyzed cells.

from those clusters might therefore be a consequence of altered fitness of the clustered mitochondria.

A Mitochondrially Targeted Nanobody Can Delocalize TML

TPLATE complex is a robust multi-subunit complex functioning at the PM and can be affinity purified using any of its subunits as bait (Gadeyne et al., 2014). In order to delocalize, and thereby inactivate TPC, we took advantage of the functionally complemented homozygous *tml-1(–/–)* mutant expressing TMLprom::TML-GFP (Gadeyne et al., 2014). In complemented *tml-1(–/–) Arabidopsis* roots, TML-GFP is recruited predominantly at the PM (**Figure 1B**, left). We introduced our MITO-TagBFP2-GFPNb nanobody into this background and used PIN2prom to drive expression of the construct. PIN2prom expresses in epidermis and cortex root cell files, which, with respect to future experiments, would allow us easily to perform confocal microscopy. Two independent lines, TML-Nb1 and TML-Nb2, were selected. MITO-TagBFP2-GFPNb

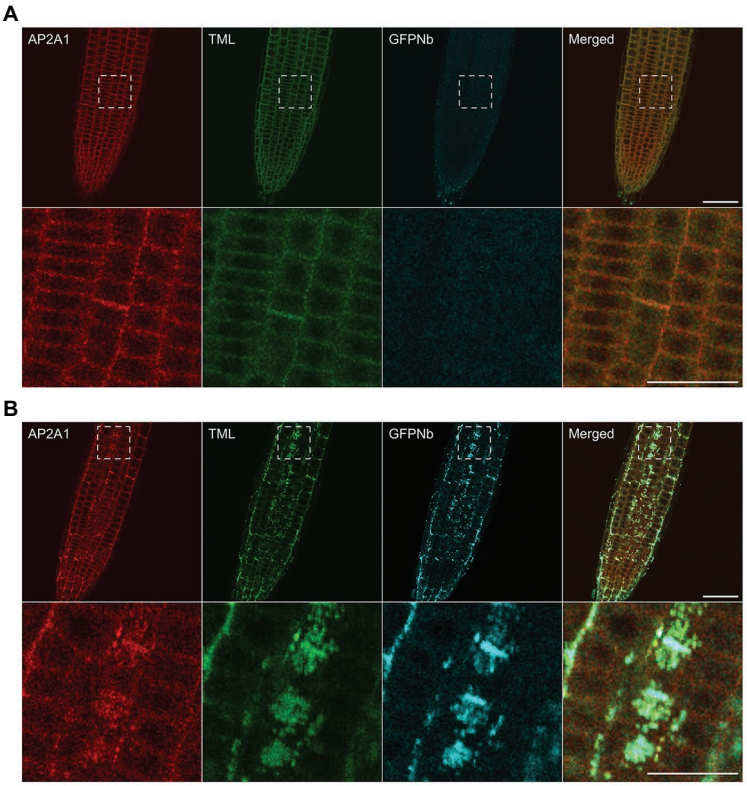

FIGURE 2 | Delocalization of TML also affects the targeting of other endocytic players. **(A,B)** Representative images and blow-ups of the outlined regions of *Arabidopsis* roots expressing TML-GFP and AP2A1-TagRFP without **(A)** and with **(B)** MITOTagBFP2-GFPNb expression. GFPNb expression causes delocalization of both TML and AP2A1. Scale bars equal 20 μm (overview pictures) or 10 μm (blow-up pictures).

(GFPNb) analogous to *N. benthamiana* leaves, localized to discrete punctae also in *Arabidopsis* wild type roots (**Figure 1B**, right).

Co-expression with GFPNb changed the uniform PM labeling of TML to a denser staining of discrete punctae in epidermis and cortex. Most of those were still near the PM and colocalized with the fluorescent signal from the nanobody, indicating effective delocalization of TML-GFP (**Figure 1C** and enhanced in **Figure 1D**). This delocalization was not apparent in the deeper layers of the root, where TML remained uniformly recruited to the PM (**Figure 1C**). Detailed analysis using spinning disk confocal microscopy confirmed the strong recruitment of TML to mitochondria that were present in the focal plane of the PM (**Figure 1E**, arrowheads). Next to the mitochondria, however, TML remained recruited to endocytic foci at the PM in root epidermal cells. The density of endocytic foci in epidermal root cells is very high (Dejonghe et al., 2016, 2019; Sánchez-Rodríguez et al., 2018). The density and intensity of the endocytic foci, marked by TML-GFP, appeared higher in epidermal cells in the complemented mutant (control) compared to the two independent lines expressing the GFPNb. Quantification showed a marked decrease in median signal intensity at the PM in the GFPNb expressing lines in regions devoid of mitochondria. The lower intensity of the signal also led to a statistically reduced number of foci (maxima) that could be detected. The reduced median intensity and lower amount of foci detected are in agreement with a substantial amount of TML-GFP accumulating at the mitochondria (**Figures 1F,G**).

Nanobody-Dependent Delocalization of TML Also Affects Other Endocytic Players

In plants, the heterotetrameric AP-2 complex and the octameric TPC are presumed to function largely, but not exclusively, together to execute CME (Gadeyne et al., 2014; Bashline et al., 2015; Wang et al., 2016; Adamowski et al., 2018). Both TPC and AP-2 have been shown to be involved in the internalization of cellulose synthase (CESA) complexes or the brassinosteroid receptor BRI1 for example (Bashline et al., 2013, 2015; Di Rubbo et al., 2013; Gadeyne et al., 2014; Sánchez-Rodríguez et al., 2018).

Moreover, a joint function is also suggested from proteomics analyses, which could identify subunits of both complexes when the AtEH1/Pan1 TPC subunit was used as bait in tandem-affinity purification assays (Gadeyne et al., 2014). To investigate whether our tool, aimed at delocalizing TPC, would also interfere with AP-2 recruitment at the PM, we tested the localization of AP-2 when TML was targeted to the mitochondria. To do so, we crossed our TML-GFP line, in *tml-1(−/−)* and expressing PIN2prom::MITOTagBFP2-GFPNb with the homozygous complemented *tml-1(−/−)* line, expressing

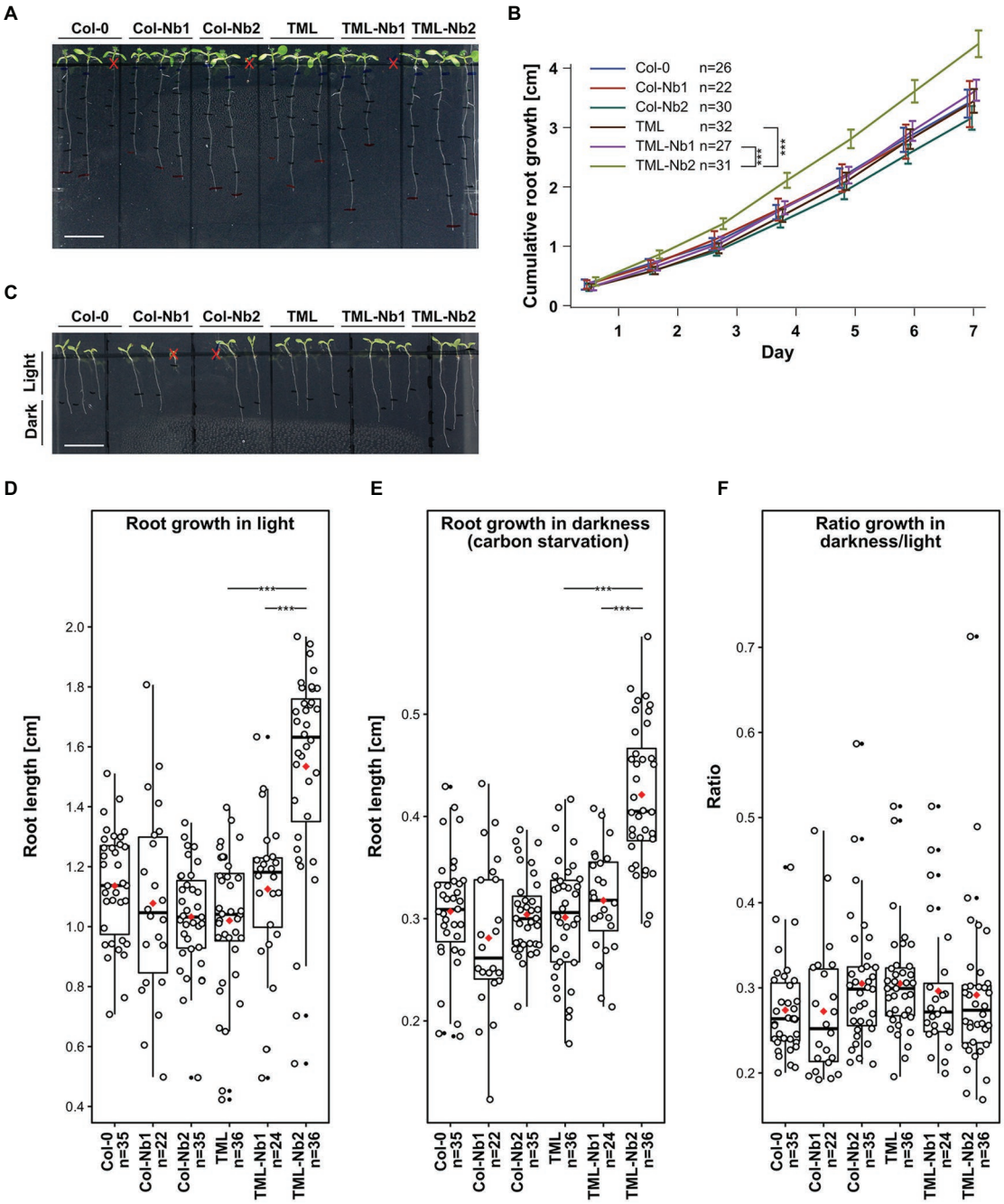

FIGURE 3 | Delocalizing TML-GFP in root epidermal and cortical cells does not adversely affect root growth. Comparison of wild type seedlings (Col-0), wild type seedlings expressing MITOTagBFP2-GFPNb (Col-Nb1 and Col-Nb2) complemented *tml-1(–/–)* mutants expressing TML-GFP (TML) and complemented *tml-1(–/–)* mutants expressing TML-GFP and MITOTagBFP2-GFPNb (TML-Nb1 and TML-Nb2) in different light conditions. **(A,B)** Representative images of seedlings and quantification of root growth in continuous light. There are no statistical differences between the lines except TML-Nb2 which showed enhanced cumulative root growth. **(C-F)** Representative images of seedlings grown for 5 days in continuous light and subsequently for 7 days in continuous dark. Consistent with the cumulative root growth assay, the TML-Nb2 grew bigger compared to the TML-GFP and TML-Nb1 under both growth conditions **(D,E)**. However, there were no significant differences in the analysis of the ratio of darkness/light growth **(F)**. Scale bars in A and C equal 1 cm. Red crosses in A and C are marking seedlings that were excluded from the analysis due to delayed germination or due to roots growing in the agar. The measurements of growth in light, dark, as well as the respective dark/light ratio, are represented as jitter box plots. The black lines represent the median and the red diamonds represent the mean of the analyzed values. Each dot represents an individual cell and black dost refer to outliers. *n* refers to the total number of analyzed cells. Significant statistical differences in growth between the lines, based on Wilcoxon pairwise comparisons tests are indicated. $p < 0.001$ are represented as *** (Bonferroni adjusted *p*-values).

TML-GFP as well as one of the large AP-2 subunits, AP2A1, fused to TagRFP (Gadeyne et al., 2014). Offspring plants that did not inherit the nanobody construct showed PM and cell plate recruitment of TML and AP2A1, and only background fluorescence in the TagBFP2 channel (**Figure 2A**). In the offspring plants that inherited the nanobody construct, however, the localization of the adaptor complex subunits changed. Both TML and AP2A1 accumulated at punctae, which clearly colocalized with the TagBFP2-fused nanobody construct (**Figure 2B**). The observed delocalization of AP2A1 to the mitochondria, together with TML strongly suggests that our approach has the capacity to delocalize TPC and AP-2 rather than TML alone, given that TPC and AP-2 are presumed to be linked *via* the AtEH1/Pan1 subunit (Gadeyne et al., 2014).

Mistargeting Adaptor Complexes in Epidermis and Cortex Affects Root Endocytic Uptake With Only Minor Effects on Root Growth

In contrast to AP-2, genetic interference with TPC subunits causes fully penetrant male sterility (Van Damme et al., 2006; Di Rubbo et al., 2013; Fan et al., 2013; Kim et al., 2013; Yamaoka et al., 2013; Gadeyne et al., 2014). TPC functionality, therefore, requires all subunits, and constitutive homozygous loss-of-function backgrounds are therefore non-existing. Abolishing endocytosis in plants, by silencing TPC subunits (Gadeyne et al., 2014) or overexpression of the uncaging proteins AUXILLIN-LIKE 1 or 2 (Adamowski et al., 2018) severely affects seedling development. The effect of silencing TPC subunits only indirectly affects protein levels and targeting clathrin might interfere with trafficking at endosomes besides the PM. As TPC and AP-2 only function at the PM, inactivating their function should not directly interfere with more downstream aspects of endosomal trafficking. Furthermore, by restricting the expression domain where the adaptor complex function is tuned down to the two outermost layers in the root should allow to study internalization from the PM, independently of possible indirect effects caused by the severe developmental alterations.

We evaluated the growth of several different lines expressing either GFPNb alone: Col-Nb1 and Col-Nb2, or GFPNb combined with TML-GFP in the complemented *tml-1(−/−)* mutant background: TML-Nb1 (−/−) and TML-Nb2 (−/−). At the seedling level, we did not observe any major adverse developmental effects (**Figure 3A**). Root length measurements of light grown seedlings revealed enhanced growth in the TML-Nb2 line compared to TML and TML-Nb1 (**Figure 3B**). The observed variability of this line, compared to all other lines that behaved similarly, probably results from a positional effect of the insertion. Nevertheless, our results show that nanobody expression in the PIN2prom domain and partial delocalization of TML has no negative effect on seedling development under normal growth conditions.

The AtEH/Pan1 TPC subunits were recently implicated in growth under nutrient-depleted conditions as downregulation of *AtEH1/Pan1* expression rendered plants hyper-susceptible to carbon starvation (Wang et al., 2019). We, therefore, assessed if delocalizing TML-GFP, as well as other endocytic players, would also render these plants susceptibility to nutrient stress. To do so, we measured root lengths of seedlings grown for 5 days in continuous light and afterwards we placed them in the dark for an additional 7 days. Measurements of root growth in the dark under carbon stress conditions did not show any differences between WT and Col-Nb lines. However, also here, the TML-Nb2 line exhibited increased root growth compared to TML and TML-Nb1 in both light and dark conditions (**Figures 3C-E**). We calculated the ratio of root growth in dark over root growth in light to avoid overestimation of the results due to the extraordinary growth of TML-Nb2 line. The ratios revealed that sequestering TML in TML-Nb lines did not cause any negative effect as the ratios were similar between all lines tested (**Figure 3F**). Overall, the effects of TML relocalization did not reveal any defects on seedling development, even under nutrient-stress conditions.

The subtle differences observed by comparing the effect of delocalization of TML on plant growth are likely a consequence of the restricted expression domain of GFPNb. We, therefore, monitored the effects of delocalizing TML more directly by visualizing the internalization of the styryl dye FM4-64, which in plants is commonly used as proxy for endocytic flux (Rigal et al., 2015; Jelínková et al., 2019). To rule out indirect effects of targeting GFPNb to the mitochondria, we compared endocytic flux between Col-Nb1, TML-GFP in *tml-1(−/−)*, TML-Nb1 (−/−), and TML-Nb2 (−/−). We observed a slight decrease in endocytic flux when comparing wild type seedlings with the complemented *tml-1(−/−)* line and a strong reduction in endocytic flux between the complemented mutant and both complemented mutant lines where TML was partially delocalized (**Figures 4A,B**). Direct visualization of endocytic flux, therefore, allowed us to conclude that expression of the PIN2prom:: MITOTagBFP2-GFPNb has the capacity to interfere with endocytosis in *Arabidopsis* root epidermal cells and that this tool certainly has the capacity to generate knockdown, and maybe even knockout lines at the protein level.

DISCUSSION

Analyzing how impaired TPC function directly affects endocytosis is hampered by the male sterility and/or seedling lethal mutant phenotypes following genetic interference of individual subunits (Gadeyne et al., 2014). Here, we explored to impair TPC function at the protein level by delocalizing a functional and essential subunit in its respective complemented mutant background. We were inspired by previous work in animal cells. However, instead of using rapamycin-dependent rerouting of one of the large AP-2 subunits, combined with silencing the endogenous subunit (Robinson et al., 2010), we took advantage of the complemented *tml-1(−/−)* mutant line expressing TML-GFP (Gadeyne et al., 2014) in combination with targeting a nanobody directed against GFP (GFPNb; Künzl et al., 2016) to the mitochondria. We expressed the GFPNb in epidermis, cortex and lateral root cap as we expected ubiquitous constitutive

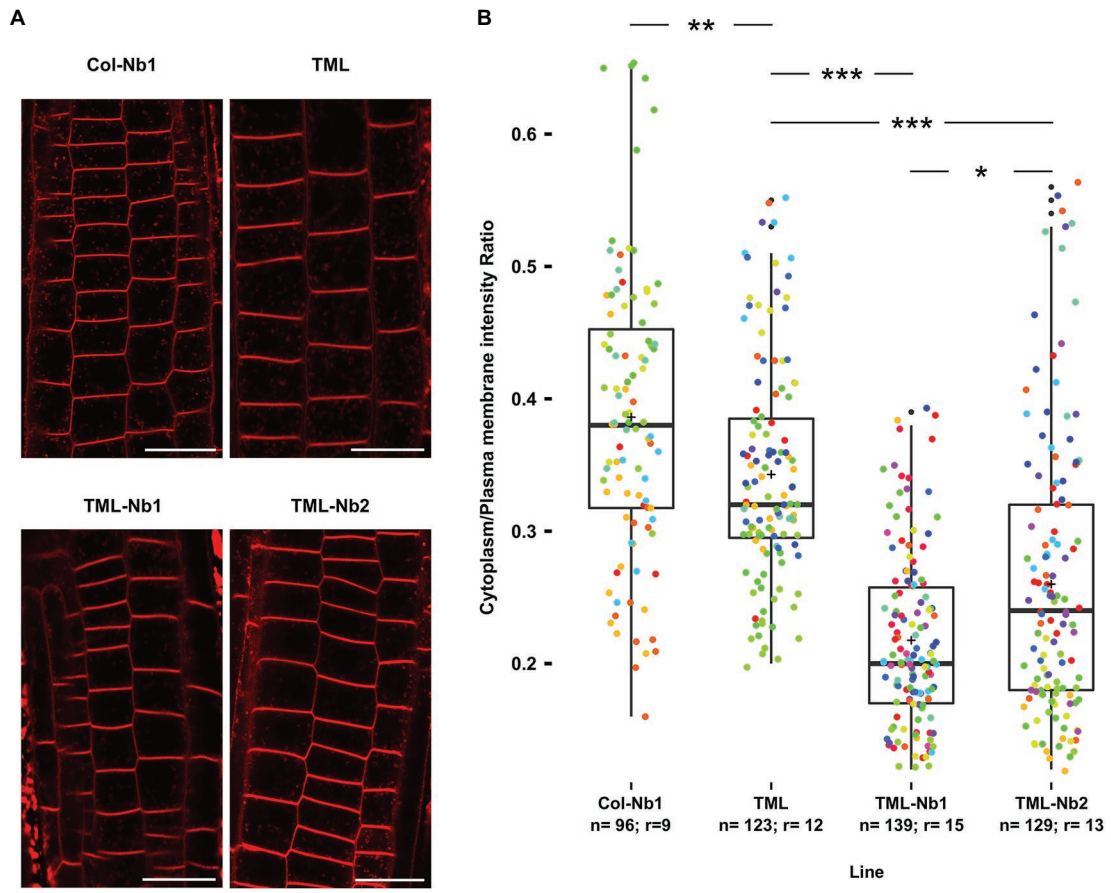

FIGURE 4 | Nanobody-dependent delocalization reduces endocytic flux. **(A)** Representative single confocal slices of FM4-64 stained root cells of the different lines for which endocytic flux was quantified. FM4-64 uptake was compared between wild type *Arabidopsis* expressing MITOTagBFP2-GFPNb (Col-Nb1), the TML-GFP expressing complemented *tml-1(–/–)* mutant (TML), and two independent lines of the TML-GFP expressing complemented *tml-1(–/–)* mutant expressing MITOTagBFP2-GFPNb (TML-Nb1 and TML-Nb2). Scale bars equal 20 μm. **(B)** Jittered box plot representation of the quantification of the cytoplasm/plasma membrane intensity of FM4-64 as proxy for endocytic flux. The black lines represent the median and the crosses represent the mean values. The dots represent individual measurements of cells. The rainbow-colored indication of the dots groups the cells from the different roots that were analyzed. The number of cells (*n*) and the number of individual roots (*r*) are indicated in the graph. The indicated *p*-values were calculated using pairwise Wilcoxon tests and corrected using the Bonferroni method. Significant statistical differences between the lines based on Wilcoxon pairwise comparisons tests are indicated. $p < 0.001$ are represented as ***, < 0.01 are represented as ** and < 0.1 are represented as * (Bonferroni adjusted *p*-values).

expression to be lethal for the plant. Moreover, the epidermis and cortex cell files are easily accessible for imaging purposes. Proteins fused to this mitochondrial targeting signal colocalized with MitoTracker in transient *N. benthamiana* experiments (Winkler et al., 2021) and also here, we found our GFPNb to colocalize with the mt-rk mitochondrial marker in small punctae (Nelson et al., 2007). We also observed larger aggregates of signal, which we assume to be clustered dysfunctional mitochondria, similar to what we observed with our knocksideways strategy (Winkler et al., 2021). Constitutively decorating mitochondria with a GFPNb construct in the root epidermis and cortex cell files, therefore, might affect mitochondrial functionality without however causing a severe penalty on overall plant growth. The GFPNb system was capable of delocalizing TML-GFP and this caused the appearance of strongly fluorescent GFP-positive aggregations. Detailed inspection revealed however that our approach was insufficient to remove all TML from the PM. Compared to the control cells, sequestration of TML-GFP led to an overall reduction in signal intensity at the endocytic foci, as well as a reduction in overall density of endocytic foci when this was calculated as the amount of maxima that could be identified within a region of interest. The observed reduction of TML at the PM correlated with a significant reduction in endocytic tracer uptake, a proxy for reduced endocytosis.

The absence of major developmental defects, observed when TML-GFP was delocalized in the GFPNb lines can be explained by the fact that not all complex was delocalized as well as by the limited-expression domain of the PIN2prom. The increased root growth observed for the TML-Nb2 line is likely not linked

to the delocalization of TML-GFP as we did not observe this in the TML-Nb1 line. An alternative explanation could be that the growth-promoting effect might possibly be a consequence of a positional effect of the insert. Inducible overexpression of AUXILIN-LIKE1/2 results in complete seedling growth arrest with drastic effects on cell morphology (Adamowski et al., 2018). The same holds true for inducible expression of dominant-negative clathrin HUB and DRP1A (Kitakura et al., 2011; Yoshinari et al., 2016). Furthermore, estradiol-inducible TPLATE and TML knockdown lines are noticeably shorter and show bulging cells (Gadeyne et al., 2014). As we did not observe cellular effects in epidermal or cortical cell files, we conclude that our approach lacked the required strength to block endocytosis, but only reduced it.

Recent results suggest that plant cells very likely contain a feedback loop controlling TPC expression, as carbon starved plants contained roughly the same amount of full-length TPLATE-GFP, next to an extensive amount of TPLATE-GFP degradation products (Wang et al., 2019). In case plant cells make more TPC upon depleting the complex at the PM, DeGradFP could provide a viable solution to this problem (Baudisch et al., 2018; Ma et al., 2019; Sorge et al., 2021). By applying this method in GFP-complemented *tml-1(−/−)* mutants, newly synthesized TML-GFP would be broken down immediately, preventing to achieve functional levels of TPC at the PM. Stronger or inducible promotors and/or the use of a different targeting location might also increase the delocalization capacity. To avoid lethality due to ubiquitous sequestration, engineered anti-GFP nanobodies, whose affinity can be controlled by small molecules, could also be used (Farrants et al., 2020).

Untangling the function of TPC and AP-2 in CME at the PM requires tools that allow interfering specifically with the functionality of both complexes. Our nanobody-dependent approach targeting TPC *via* TML resulted in the co-delocalization of one of the large subunits of AP-2, indicating that we likely are not only targeting TPC, but also AP-2 function. Whether a complementary approach, by delocalizing AP-2, using AP2S or AP2M in their respective complemented mutant backgrounds, would also delocalize TPC is something that would be worth trying. Furthermore, as AP2S and AP2M subunits are still recruited in *ap2m* and *ap2s* single mutant backgrounds (Wang et al., 2016), AP-2 in plants might also function as hemicomplexes similar to what is reported in *C. elegans* (Gu et al., 2013). Single mutants therefore might not reflect functional null *ap2* mutants and a similar approach as performed here might also provide tools to inactivate AP-2 as a whole, which can be highly complementary to working with the single subunit mutants.

In conclusion, the data presented here is a first step toward the development of specific tools, which are required to help us understand the functions of AP-2 and TPC. In the long-term, this will generate insight into endocytosis at the mechanistic level and this will bring us closer to being able to modulate CME-dependent processes, and thereby modulating plant development, nutrient uptake as well as defense responses to our benefit.

DATA AVAILABILITY STATEMENT

The raw data supporting the conclusions of this article will be made available by the authors, without undue reservation.

AUTHOR CONTRIBUTIONS

JW, ADM, EM, and PG designed and performed experiments. DVD designed experiments and wrote the initial draft together with ADM and JW. VS performed root growth assay statistical analysis. All authors contributed to the article and approved the submitted version.

FUNDING

Research in the Van Damme lab is supported by the European Research Council (T-Rex project number 682436 to DVD, JW, and ADM) and by the Research Foundation Flanders (FWO postdoctoral fellowship grant 1226420N to PG).

ACKNOWLEDGMENTS

We would like to thank the ENPER members for forming a vibrant and open research community for more than 20 years already. We would also like to thank Steffen Vanneste (PSB, VIB/UGent, Belgium) for providing research tools. This manuscript has been released as a pre-print at BioRxiv (Winkler et al., 2021).

REFERENCES

Adamowski, M., Narasimhan, M., Kania, U., Glanc, M., De Jaeger, G., and Friml, J. (2018). A functional study of AUXILIN-LIKE1 and 2, two putative clathrin uncoating factors in *Arabidopsis*. *Plant Cell* 30, 700–716. doi: 10.1105/tpc.17.00785

Backues, S. K., Korasick, D. A., Heese, A., and Bednarek, S. Y. (2010). The *Arabidopsis* dynamin-related protein2 family is essential for gametophyte development. *Plant Cell* 22, 3218–3231. doi: 10.1105/tpc.110.077727

Bashline, L., Li, S., Anderson, C. T., Lei, L., and Gu, Y. (2013). The endocytosis of cellulose synthase in *Arabidopsis* is dependent on μ2, a Clathrin-mediated endocytosis Adaptin. *Plant Physiol.* 163, 150–160. doi: 10.1104/pp.113.221234

Bashline, L., Li, S., Zhu, X., and Gu, Y. (2015). The TWD40-2 protein and the AP2 complex cooperate in the clathrin-mediated endocytosis of cellulose synthase to regulate cellulose biosynthesis. *Proc. Natl. Acad. Sci.* 112, 12870–12875. doi: 10.1073/pnas.1509292112

Baudisch, B., Pfort, I., Sorge, E., and Conrad, U. (2018). Nanobody-directed specific degradation of proteins by the 26S-proteasome in plants. *Front. Plant Sci.* 9:130. doi: 10.3389/fpls.2018.00130

Bitsikas, V., Corrêa, I. R., and Nichols, B. J. (2014). Clathrin-independent pathways do not contribute significantly to endocytic flux. *elife* 3:e03970. doi: 10.7554/eLife.03970

Caussinus, E., Kanca, O., and Affolter, M. (2012). Fluorescent fusion protein knockout mediated by anti-GFP nanobody. *Nat. Struct. Mol. Biol.* 19, 117–122. doi: 10.1038/nsmb.2180

Clough, S. J., and Bent, A. F. (1998). Floral dip: a simplified method for agrobacterium-mediated transformation of *Arabidopsis thaliana*. *Plant J.* 16, 735–743. doi: 10.1046/j.1365-313x.1998.00343.x

Dejonghe, W., Kuenen, S., Mylle, E., Vasileva, M., Keech, O., Viotti, C., et al. (2016). Mitochondrial uncouplers inhibit clathrin-mediated endocytosis largely through cytoplasmic acidification. *Nat. Commun.* 7:11710. doi: 10.1038/ncomms11710

Dejonghe, W., Sharma, I., Denoo, B., De Munck, S., Lu, Q., Mishev, K., et al. (2019). Disruption of endocytosis through chemical inhibition of clathrin heavy chain function. *Nat. Chem. Biol.* 15, 641–649. doi: 10.1038/s41589-019-0262-1

Di Rubbo, S., Irani, N. G., Kim, S. Y., Xu, Z. -Y., Gadeyne, A., Dejonghe, W., et al. (2013). The Clathrin adaptor complex AP-2 mediates endocytosis of BRASSINOSTEROID INSENSITIVE1 in *Arabidopsis*. *Plant Cell* 25, 2986–2997. doi: 10.1105/tpc.113.114058

Dubeaux, G., Neveu, J., Zelazny, E., and Vert, G. (2018). Metal sensing by the IRT1 transporter-receptor orchestrates its own degradation and plant metal nutrition. *Mol. Cell* 69, 953.e5–964.e5. doi: 10.1016/j.molcel.2018.02.009

Fan, L., Hao, H., Xue, Y., Zhang, L., Song, K., Ding, Z., et al. (2013). Dynamic analysis of *Arabidopsis* AP2 σ subunit reveals a key role in clathrin-mediated endocytosis and plant development. *Development* 140, 3826–3837. doi: 10.1242/dev.095711

Farrants, H., Tarnawski, M., Müller, T. G., Otsuka, S., Hiblot, J., Koch, B., et al. (2020). Chemogenetic control of nanobodies. *Nat. Methods* 17, 279–282. doi: 10.1038/s41592-020-0746-7

Früholz, S., Fäßler, F., Kolukisaoglu, Ü., and Pimpl, P. (2018). Nanobody-triggered lockdown of VSRs reveals ligand reloading in the Golgi. *Nat. Commun.* 9:643. doi: 10.1038/s41467-018-02909-6

Gadeyne, A., Sánchez-Rodríguez, C., Vanneste, S., Di Rubbo, S., Zauber, H., Vanneste, K., et al. (2014). The TPLATE adaptor complex drives clathrin-mediated endocytosis in plants. *Cell* 156, 691–704. doi: 10.1016/j.cell.2014.01.039

Gómez, B. G., Lozano-Durán, R., and Wolf, S. (2019). Phosphorylation-dependent routing of RLP44 towards brassinosteroid or phytosulfokine signalling. BioRxiv [Preprint]. doi: 10.1101/527754

Gu, M., Liu, Q., Watanabe, S., Sun, L., Hollopeter, G., Grant, B. D., et al. (2013). AP2 hemicomplexes contribute independently to synaptic vesicle endocytosis. *elife* 2:e00190. doi: 10.7554/eLife.00190

Hirst, J., Schlacht, A., Norcott, J. P., Traynor, D., Bloomfield, G., Antrobus, R., et al. (2014). Characterization of TSET, an ancient and widespread membrane trafficking complex. *elife* 3:e02866. doi: 10.7554/eLife.02866

Ingram, J. R., Schmidt, F. I., and Ploegh, H. L. (2018). Exploiting nanobodies' singular traits. *Annu. Rev. Immunol.* 36, 695–715. doi: 10.1146/annurev-immunol-042617-053327

Irani, N. G., Di Rubbo, S., Mylle, E., Van Den Begin, J., Schneider-Pizoń, J., Hniliková, J., et al. (2012). Fluorescent castasterone reveals BRI1 signaling from the plasma membrane. *Nat. Chem. Biol.* 8, 583–589. doi: 10.1038/nchembio.958

Jelínková, A., Malínská, K., and Petrášek, J. (2019). Using FM dyes to study endomembranes and their dynamics in plants and cell suspensions. *Methods Mol. Biol.* 1992, 173–187. doi: 10.1007/978-1-4939-9469-4_11

Jelínková, A., Malínská, K., Simon, S., Kleine-Vehn, J., Pařezová, M., Pejchar, P., et al. (2010). Probing plant membranes with FM dyes: tracking, dragging or blocking? *Plant J.* 61, 883–892. doi: 10.1111/j.1365-313X.2009.04102.x

Kadenbach, B., Arnold, S., Lee, I., and Hüttemann, M. (2004). The possible role of cytochrome c oxidase in stress-induced apoptosis and degenerative diseases. *Biochim. Biophys. Acta* 1655, 400–408. doi: 10.1016/j.bbabio.2003.06.005

Karimi, M., De Meyer, B., and Hilson, P. (2005). Modular cloning in plant cells. *Trends Plant Sci.* 10, 103–105. doi: 10.1016/j.tplants.2005.01.008

Kim, S. Y., Xu, Z. -Y., Song, K., Kim, D. H., Kang, H., Reichardt, I., et al. (2013). Adaptor protein complex 2-mediated endocytosis is crucial for male reproductive organ development in *Arabidopsis*. *Plant Cell* 25, 2970–2985. doi: 10.1105/tpc.113.114264

Kitakura, S., Vanneste, S., Robert, S., Löfke, C., Teichmann, T., Tanaka, H., et al. (2011). Clathrin mediates endocytosis and polar distribution of PIN auxin transporters in *Arabidopsis*. *Plant Cell* 23, 1920–1931. doi: 10.1105/tpc.111.083030

Künzl, F., Früholz, S., Fäßler, F., Li, B., and Pimpl, P. (2016). Receptor-mediated sorting of soluble vacuolar proteins ends at the trans-Golgi network/early endosome. *Nat. Plants* 2:16017. doi: 10.1038/nplants.2016.17

Li, X., and Pan, S. Q. (2017). Agrobacterium delivers VirE2 protein into host cells *via* clathrin-mediated endocytosis. *Sci. Adv.* 3:e1601528. doi: 10.1126/sciadv.1601528

Li, X., Wang, X., Yang, Y., Li, R., He, Q., Fang, X., et al. (2011). Single-molecule analysis of PIP2;1 dynamics and partitioning reveals multiple modes of *Arabidopsis* plasma membrane aquaporin regulation. *Plant Cell* 23, 3780–3797. doi: 10.1105/tpc.111.091454

Ma, Y., Miotk, A., Šutiković, Z., Ermakova, O., Wenzl, C., Medzihradszky, A., et al. (2019). WUSCHEL acts as an auxin response rheostat to maintain apical stem cells in *Arabidopsis*. *Nat. Commun.* 10:5093. doi: 10.1038/s41467-019-13074-9

Marquès-Bueno, M. M., Morao, A. K., Cayrel, A., Platre, M. P., Barberon, M., Caillieux, E., et al. (2016). A versatile multisite gateway-compatible promoter and transgenic line collection for cell type-specific functional genomics in *Arabidopsis*. *Plant J.* 85, 320–333. doi: 10.1111/tpj.13099

Martins, S., Dohmann, E. M. N., Cayrel, A., Johnson, A., Fischer, W., Pojer, F., et al. (2015). Internalization and vacuolar targeting of the brassinosteroid hormone receptor BRI1 are regulated by ubiquitination. *Nat. Commun.* 6:6151. doi: 10.1038/ncomms7151

Mbengue, M., Bourdais, G., Gervasi, F., Beck, M., Zhou, J., Spallek, T., et al. (2016). Clathrin-dependent endocytosis is required for immunity mediated by pattern recognition receptor kinases. *Proc. Natl. Acad. Sci.* 113, 11034–11039. doi: 10.1073/pnas.1606004113

Mitsunari, T., Nakatsu, F., Shioda, N., Love, P. E., Grinberg, A., Bonifacino, J. S., et al. (2005). Clathrin adaptor AP-2 is essential for early embryonal development. *Mol. Cell. Biol.* 25, 9318–9323. doi: 10.1128/MCB.25.21.9318-9323.2005

Muyldermans, S. (2013). Nanobodies: natural single-domain antibodies. *Annu. Rev. Biochem.* 82, 775–797. doi: 10.1146/annurev-biochem-063011-092449

Nelson, B. K., Cai, X., and Nebenführ, A. (2007). A multicolored set of *in vivo* organelle markers for co-localization studies in *Arabidopsis* and other plants. *Plant J.* 51, 1126–1136. doi: 10.1111/j.1365-313X.2007.03212.x

Pasin, F., Kulasekaran, S., Natale, P., Simón-Mateo, C., and García, J. A. (2014). Rapid fluorescent reporter quantification by leaf disc analysis and its application in plant-virus studies. *Plant Methods* 10:22. doi: 10.1186/1746-4811-10-22

Rigal, A., Doyle, S. M., and Robert, S. (2015). Live cell imaging of FM4-64, a tool for tracing the endocytic pathways in *Arabidopsis* root cells. *Methods Mol. Biol.* 1242, 93–103. doi: 10.1007/978-1-4939-1902-4_9

Robinson, M. S. (2015). Forty years of Clathrin-coated vesicles. *Traffic* 16, 1210–1238. doi: 10.1111/tra.12335

Robinson, M. S., Sahlender, D. A., and Foster, S. D. (2010). Rapid inactivation of proteins by rapamycin-induced rerouting to mitochondria. *Dev. Cell* 18, 324–331. doi: 10.1016/j.devcel.2009.12.015

Rstudio Team (2019). *RStudio: Integrated development for R*. Boston, MA: RStudio, Inc.

Sánchez-Rodríguez, C., Shi, Y., Kesten, C., Zhang, D., Sancho-Andrés, G., Ivakov, A., et al. (2018). The cellulose synthases are cargo of the TPLATE adaptor complex. *Mol. Plant* 11, 346–349. doi: 10.1016/j.molp.2017.11.012

Schindelin, J., Arganda-Carreras, I., Frise, E., Kaynig, V., Longair, M., Pietzsch, T., et al. (2012). Fiji: an open-source platform for biological-image analysis. *Nat. Methods* 9, 676–682. doi: 10.1038/nmeth.2019

Schneider, C. A., Rasband, W. S., and Eliceiri, K. W. (2012). NIH image to ImageJ: 25 years of image analysis. *Nat. Methods* 9, 671–675. doi: 10.1038/nmeth.2089

Sorge, E., Demidov, D., Lermontova, I., Houben, A., and Conrad, U. (2021). Engineered degradation of EYFP-tagged CENH3 *via* the 26S proteasome pathway in plants. *PLoS One* 16:e0247015. doi: 10.1371/journal.pone.0247015

Sparkes, I. A., Runions, J., Kearns, A., and Hawes, C. (2006). Rapid, transient expression of fluorescent fusion proteins in tobacco plants and generation of stably transformed plants. *Nat. Protoc.* 1, 2019–2025. doi: 10.1038/nprot.2006.286

Traub, L. M. (2019). A nanobody-based molecular toolkit provides new mechanistic insight into clathrin-coat initiation. *elife* 8:e41768. doi: 10.7554/eLife.41768

Van Damme, D., Coutuer, S., De Rycke, R., Bouget, F. -Y., Inze, D., and Geelen, D. (2006). Somatic cytokinesis and pollen maturation in *Arabidopsis* depend on TPLATE, which has domains similar to coat proteins. *Plant Cell* 18, 3502–3518. doi: 10.1105/tpc.106.040923

Wang, C., Hu, T., Yan, X., Meng, T., Wang, Y., Wang, Q., et al. (2016). Differential regulation of Clathrin and its adaptor proteins during membrane recruitment for endocytosis. *Plant Physiol.* 171, 215–229. doi: 10.1104/pp.15.01716

Wang, P., Pleskot, R., Zang, J., Winkler, J., Wang, J., Yperman, K., et al. (2019). Plant AtEH/Pan1 proteins drive autophagosome formation at ER-PM contact sites with actin and endocytic machinery. *Nat. Commun.* 10:5132. doi: 10.1038/s41467-019-12782-6

Wang, C., Yan, X., Chen, Q., Jiang, N., Fu, W., Ma, B., et al. (2013). Clathrin light chains regulate Clathrin-mediated trafficking, auxin signaling, and development in *Arabidopsis*. *Plant Cell* 25, 499–516. doi: 10.1105/tpc.112.108373

Wang, S., Yoshinari, A., Shimada, T., Hara-Nishimura, I., Mitani-Ueno, N., Feng Ma, J., et al. (2017). Polar localization of the NIP5;1 boric acid channel is maintained by endocytosis and facilitates boron transport in *Arabidopsis* roots. *Plant Cell* 29, 824–842. doi: 10.1105/tpc.16.00825

Winkler, J., Mylle, E., De Meyer, A., Pavie, B., Merchie, J., Grones, P., et al. (2021). Visualizing protein–protein interactions in plants by rapamycin-dependent delocalization. *Plant Cell* doi: 10.1093/plcell/koab004

Yamaoka, S., Shimono, Y., Shirakawa, M., Fukao, Y., Kawase, T., Hatsugai, N., et al. (2013). Identification and dynamics of *Arabidopsis* adaptor protein-2 complex and its involvement in floral organ development. *Plant Cell* 25, 2958–2969. doi: 10.1105/tpc.113.114082

Yeung, B. G., Phan, H. L., and Payne, G. S. (2013). Adaptor complex-independent Clathrin function in yeast. *Mol. Biol. Cell* 10, 3643–3659. doi: 10.1091/mbc.10.11.3643

Yoshinari, A., Fujimoto, M., Ueda, T., Inada, N., Naito, S., and Takano, J. (2016). DRP1-dependent endocytosis is essential for polar localization and boron-induced degradation of the borate transporter BOR1 in *Arabidopsis thaliana*. *Plant Cell Physiol.* 57, 1985–2000. doi: 10.1093/pcp/pcw121

Yoshinari, A., Hosokawa, T., Amano, T., Beier, M. P., Kunieda, T., Shimada, T., et al. (2019). Polar localization of the borate exporter BOR1 requires AP2-dependent endocytosis. *Plant Physiol.* 179, 1569–1580. doi: 10.1104/pp.18.01017

Zhang, Y., Yu, Q., Jiang, N., Yan, X., Wang, C., Wang, Q., et al. (2017). Clathrin regulates blue light-triggered lateral auxin distribution and hypocotyl phototropism in *Arabidopsis*. *Plant Cell Environ.* 40, 165–176. doi: 10.1111/pce.12854

Conflict of Interest: The authors declare that the research was conducted in the absence of any commercial or financial relationships that could be construed as a potential conflict of interest.

Advantages of publishing in Frontiers

OPEN ACCESS
Articles are free to read for greatest visibility and readership

FAST PUBLICATION
Around 90 days from submission to decision

HIGH QUALITY PEER-REVIEW
Rigorous, collaborative, and constructive peer-review

TRANSPARENT PEER-REVIEW
Editors and reviewers acknowledged by name on published articles

Frontiers
Avenue du Tribunal-Fédéral 34
1005 Lausanne | Switzerland

Visit us: www.frontiersin.org
Contact us: frontiersin.org/about/contact

REPRODUCIBILITY OF RESEARCH
Support open data and methods to enhance research reproducibility

DIGITAL PUBLISHING
Articles designed for optimal readership across devices

FOLLOW US
@frontiersin

IMPACT METRICS
Advanced article metrics track visibility across digital media

EXTENSIVE PROMOTION
Marketing and promotion of impactful research

LOOP RESEARCH NETWORK
Our network increases your article's readership